Development of Polymer and Lipid Materials for Enhanced Delivery of Nucleic Acids and Proteins

by

Ahmed Atef Eltoukhy

B.S., Chemical Engineering
Stanford University, 2007

SUBMITTED TO THE DEPARTMENT OF BIOLOGICAL ENGINEERING
IN PARTIAL FULFILLMENT OF THE REQUIREMENTS FOR THE DEGREE OF

DOCTOR OF PHILOSOPHY IN BIOLOGICAL ENGINEERING
AT THE
MASSACHUSETTS INSTITUTE OF TECHNOLOGY

JUNE 2013

Signature of Author: _____
Department of Biological Engineering
May 3, 2013

Certified by: _____
Robert Langer
David H. Koch Institute Professor
Thesis Supervisor

Certified by: _____
Daniel G. Anderson
Samuel A. Goldblith Associate Professor of Chemical Engineering
Thesis Supervisor

Accepted by: _____
Forest M. White
Mitsui Career Development Associate Professor of Biological Engineering
Chair, Biological Engineering Graduate Program Committee

This thesis has been examined by a committee of the Biological Engineering Department as follows:

Thesis Committee Chair: _____

Ram Sasisekharan
Alfred H. Caspary Professor of Biological Engineering

Thesis Supervisor, Committee Member: _____

Robert Langer
David H. Koch Institute Professor

Thesis Supervisor, Committee Member: _____

Daniel G. Anderson
Samuel A. Goldblith Associate Professor of Chemical Engineering

Committee Member: _____

Sangeeta N. Bhatia
John J. and Dorothy Wilson Professor of Health Sciences & Technology and EECS

Development of Polymer and Lipid Materials for Enhanced Delivery of Nucleic Acids and Proteins

By Ahmed Atef Eltoukhy

SUBMITTED TO THE DEPARTMENT OF BIOLOGICAL ENGINEERING
ON MAY 3, 2013 IN PARTIAL FULFILLMENT OF THE REQUIREMENTS
FOR THE DEGREE OF DOCTOR OF PHILOSOPHY IN BIOLOGICAL ENGINEERING

ABSTRACT

The development of synthetic vectors enabling efficient intracellular delivery of macromolecular therapeutics such as nucleic acids and proteins could potentially catalyze the clinical translation of many gene and protein-based therapies. However, progress has been hindered by a lack of safe and effective materials and by insufficient insight into the relationship between key delivery properties and efficacy.

Accordingly, working with a promising class of cationic, degradable gene delivery vectors, poly(β-amino ester)s (PBAEs), we develop novel, hydrophobic PBAE terpolymers that display dramatically increased gene delivery potency and nanoparticle stability. We then develop a technique based on size-exclusion chromatography that enables the isolation of well-defined, monodisperse PBAE polymer fractions with greater transfection activities than the starting polymer. This technique also allows us to elucidate the dependence of gene delivery properties on polymer molecular weight (MW). Subsequently, we examine the cellular uptake and trafficking mechanisms of PBAE/DNA polyplexes, and demonstrate that polyplex internalization and transfection depend on a key endo/lysosomal cholesterol transport protein, Niemann-Pick C1 (Npc1).

Finally, working with cationic lipids termed lipidoids, which have shown exceptional potency for the delivery of RNAi therapeutics, we develop these materials for intracellular delivery of proteins using a simple and novel approach in which nucleic acids serve as a handle for protein encapsulation and delivery. Preliminary *in vivo* experiments suggest the potential application of this approach toward lipidoid-mediated delivery of protein-based vaccines.

Taken together, the work presented here advances the development of polymer and lipid materials for the safe and effective intracellular delivery of DNA and protein therapeutics.

Thesis Supervisors: Robert Langer and Daniel G. Anderson

ACKNOWLEDGEMENTS

First, I would like to express my deepest appreciation for and utmost gratitude to my thesis advisors, Robert Langer and Daniel Anderson. Bob has been an inspiring role model who has graciously encouraged my personal and professional development, and Dan has been an outstanding mentor who has offered invaluable guidance and support at every step of my thesis research. I am truly fortunate to have had the opportunity to interact with them, learn from them, and work in their labs.

I would like to thank the other members of my thesis committee, Ram Sasisekharan and Sangeeta Bhatia. They have provided terrific support and guidance for which I am grateful. I also want to acknowledge the BE department for offering me the opportunity to come to MIT and for providing a stimulating learning environment.

Among the tremendous network of scientists comprising the Langer and Anderson labs, I am fortunate to count many collaborators and friends. Among current labmates, I would particularly like to thank Delai Chen, Gaurav Sahay, Yizhou Dong, Chris Alabi, Omid Veiseh, Jeisa Pelet, Roman Bogorad, Hao Yin, Manos Karagiannis, Rose Kanasty, Omar Khan, James Dahlman, Tim O'Shea, Yi Chen, Patrick Fenton, Beata Chertok, and Janet Zoldan. Among former labmates, I would like to thank Daniel Siegwart, Shan Jiang, Jordan Green, David Nguyen, Avi Schroeder, Seung-Woo Cho, Said Bogatyrev, Hao Cheng, Chris Levins, Kevin Love, Michael Goldberg, João Guerreiro, Fan Yang, Nathan Hwang, Kerry Mahon, and Cheol Am Hong.

I would also like to thank the undergraduate students I have mentored, especially my UROP, Jay Rajan, as well as my 10.29 project team, Danielle Class, Mark Kalinich, and Jefferson Sanchez.

Additionally, I would like to acknowledge my collaborators at Mount Sinai School of Medicine, including Kevin Costa, Kenneth Fish, Irene Turnbull, Amy Rosen Kontorovich, and Satish Rao. It has been a pleasure to work with them.

I am very grateful for the friends who have enlivened and enriched my experience at MIT, particularly those from college who ended up in Boston along with me, and those from among my BE classmates, lab, and the Egyptian community at MIT.

Last but not least, I would like to thank my family. I am deeply indebted to my mom and dad for their unwavering love and support despite the toll my time in Boston has taken on them. I also want to thank my brother, sister-in-law, and two adorable nieces for their encouragement. I am very fortunate to have in my father and in my brother two close examples of successful scientist-entrepreneurs, and I greatly appreciate the guidance and advice they have provided.

TABLE OF CONTENTS

LIST OF FIGURES

LIST OF TABLES

1 INTRODUCTION

The development of synthetic vectors enabling efficient intracellular delivery of macromolecular therapeutics such as nucleic acids and proteins could potentially catalyze the clinical translation of many gene and protein-based therapies. However, progress has been hindered by a lack of safe and effective materials and by insufficient insight into the relationship between key delivery properties and efficacy. For instance, the biodegradable, cationic polymers known as poly(β-aminoester)s (PBAEs) have shown tremendous potential as non-viral gene delivery carriers in numerous studies, yet several key challenges and questions remain unaddressed, such as poor stability of polymer/DNA nanoparticles under physiological conditions, batch-to-batch variability in transfection performance, and the lack of mechanistic knowledge of cellular uptake and trafficking pathways. Similarly, lipid-based nanoparticles (LNPs) incorporating cationic lipid materials termed lipidoids have demonstrated excellent *in vitro* and *in vivo* efficacy for delivery of oligonucleotides such as short interfering RNA (siRNA), but their application toward intracellular delivery of protein-based therapeutics is impeded by the wide range of physicochemical properties characterizing these diverse macromolecules.

Accordingly, the overall objective of this thesis is to develop polymer and lipid-based materials for safe, effective intracellular delivery of gene and protein therapeutics, primarily through the following specific aims:

(1) Development of novel, degradable PBAE polymers with enhanced gene delivery potency and nanoparticle aggregation resistance

(2) Systematic investigation into the gene delivery properties of PBAE polymers, particular with respect to the effects of polymer hydrophobicity and molecular weight, and with respect to the mechanisms employed for cellular internalization and trafficking

(3) Development of lipid-based nanoparticles for efficient intracellular delivery of proteins by way of oligonucleotide conjugation

In light of these aims, Chapter 2 of this thesis offers a broad survey outlining the current clinical prospects for gene therapy, the limitations of viral vectors, the barriers to non-viral delivery, and the most commonly studied synthetic gene carriers. It also details the development of poly(β-amino ester)s as gene delivery materials and presents some of the remaining unresolved challenges and questions for these polymers. Chapter 3 describes the development of novel, degradable PBAE terpolymers demonstrating significantly improved gene delivery potency and nanoparticle stability, and Chapter 4 explores the potential of these polymers for gene transfection of clinically relevant cell types as well as for *in vivo* gene delivery. Chapter 5 details a systematic study of the effect of PBAE molecular weight on gene delivery properties, the results of which elucidate a potential cause of PBAE batch-to-batch variability. Chapter 6 then reveals new mechanistic insights into the dependence of PBAE/DNA polyplex internalization and transfection on a key cholesterol transport protein, Niemann-Pick C1 (Npc1). Subsequently, Chapter 7 describes a simple and novel approach for achieving efficient intracellular protein

delivery with lipid-based nanoparticles via oligonucleotide conjugation. Finally, Chapter 8 provides a conclusion that summarizes the major findings and contributions of this thesis and discusses the future outlook for continued development of these materials.

2 BACKGROUND

2.1 MOTIVATION FOR GENE THERAPY

In a broad sense, gene therapy can be defined as the intentional modulation of gene expression within cells to prevent or treat a pathological process[1]. More narrowly, this modulation of gene expression is accomplished through the introduction of exogenous nucleic acids, such as DNA, messenger RNA (mRNA), small interfering RNA (siRNA), microRNA, or antisense oligonucleotides. In contrast to many small molecule or protein-based drugs, a singular aspect of DNA therapeutics is that for many diseases, especially monogenic disorders defined by inheritance of one mutated gene, the cure – a nucleic acid representing a functional copy of the gene – is plainly manifest. However, because most cells are impermeable to these large, negatively charged macromolecules, a carrier or vector is typically required to mediate effective intracellular delivery.

This fundamental engineering challenge, which is in equal measures both exciting and exasperating, largely explains why within the U.S., gene therapy remains a strictly experimental approach, with no FDA-approved gene therapeutics yet on the market despite nearly 2,000 clinical trials of gene therapy worldwide since 1989 (Figure 2.1). Nevertheless, recent clinical progress, including the approval of the first gene therapeutic for use in Europe, has marked a resurgence of optimism for a field burdened by a tumultuous history[2].

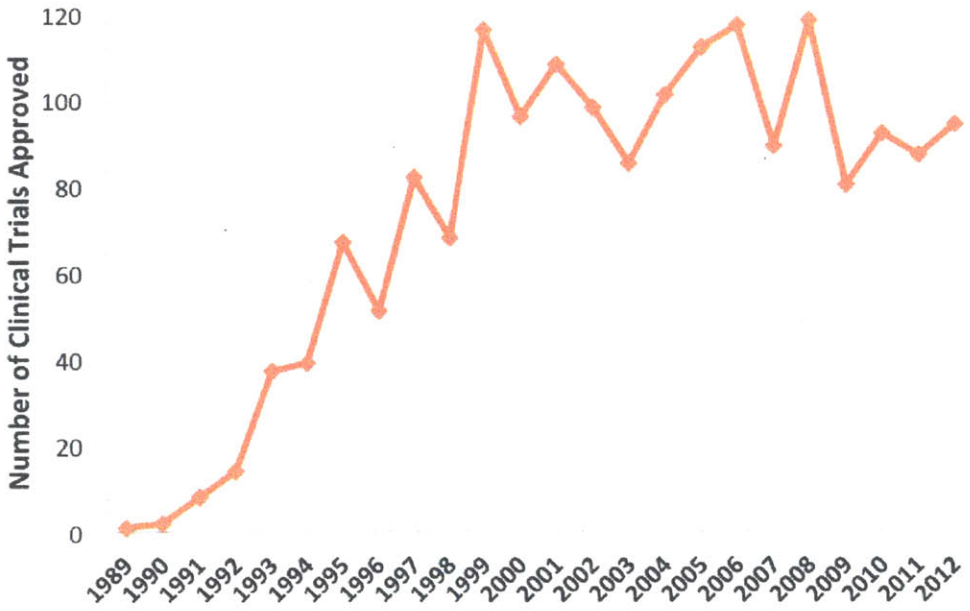

Figure 2.1 Clinical trials of gene therapy approved by year
1,903 clinical trials of gene therapy have been approved worldwide since 1989. Adapted from Ginn et al.[3]

Over the past two decades, gene therapy has been investigated clinically for the treatment or prevention of a wide range of diseases[3] (Figure 2.2). Cancer-related diseases comprise nearly two-thirds of the indications addressed by clinical trials thus far. Gene therapies for cancer treatment generally adhere to one of the following broad strategies: mutation compensation, immunopotentiation, suicide gene therapy, oncolytic virotherapy, and radio- or chemo-sensitization[4, 5]. Controversially, two cancer gene therapeutics have already been approved for use in China, even though similar versions have failed to pass clinical development in the U.S.: Gendicine, a modified adenovirus encoding the human p53 gene, and H101/Oncorine, a recombinant oncolytic adenovirus targeting p53-deficient cancer cells[2, 6].

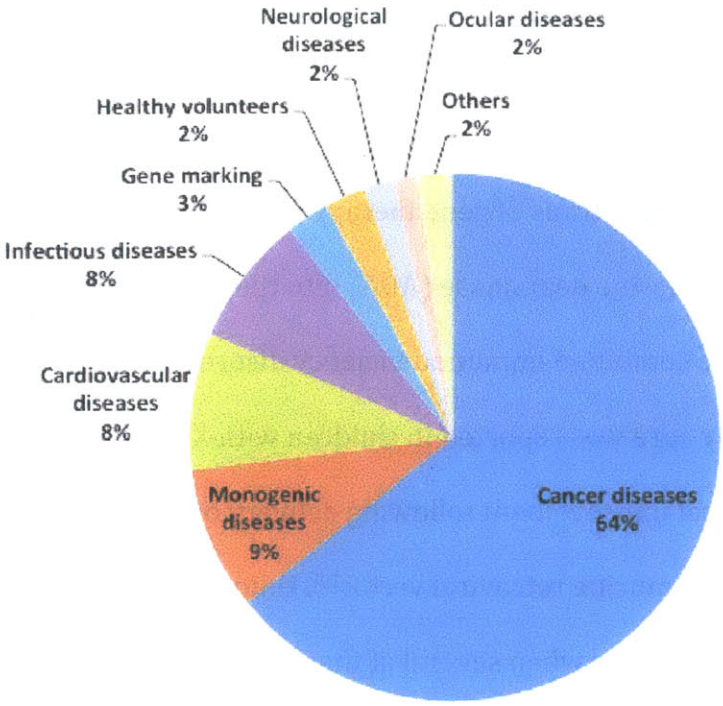

Figure 2.2 Indications addressed by gene therapy clinical trials worldwide since 1989
Adapted from Ginn et al.[3]

Within the U.S., Allovectin-7, a locally administered formulation consisting of a DNA plasmid encoding two immunotherapeutic genes and a cationic lipid delivery reagent, is currently undergoing a Phase III clinical study for treatment of advanced metastatic melanoma[7] (ClinicalTrials.gov ID: NCT00395070). Also undergoing a Phase III clinical trial is ProstAtak, which consists of an adenoviral vector encoding the herpes thymidine kinase gene, for suicide gene therapy of prostate cancer in conjunction with a prodrug and radiation therapy (ClinicalTrials.gov ID: NCT01436968).

Despite the enormous potential of gene therapy to address monogenic diseases, this class of disorders represents only ~9% of gene therapy clinical trials to date (Figure 2.2), which include some major successes along with some tragic failures. One of the earliest human trials of gene therapy in the early 1990s involved the retroviral transfer of adenosine deaminase (ADA) into the T cells of two children with ADA-associated severe combined immunodeficiency disorder (ADA-SCID)[8]. In 2000, the first gene therapy cure was reported in children with X-linked SCID who experienced dramatic clinical improvement following delivery of interleukin-2 receptor gamma chain with a murine retroviral vector[9]. Unfortunately, the trial's success was marred two years later when several of these young patients developed leukemia resulting in one death[10, 11]. Just a few years earlier, the gene therapy field had suffered its first major setback with the death of a Jesse Gelsinger, an 18-year-old clinical trial patient who experienced a severe immune response after receiving adenoviral gene therapy for a mild form of ornithine transcarbamylase (OTC) deficiency[2]. On the basis of preclinical studies, cystic fibrosis, a severe and fatal lung disease caused by mutations in the CFTR gene, appeared to be a promising early candidate for gene therapy, but clinical trials in humans have so far shown a disappointing lack of efficacy[12].

Nevertheless, one recent triumph has been the approval of Glybera in Europe for the treatment of lipoprotein lipase (LPL) deficiency[13]. This orphan metabolic disease results from mutation of the LPL gene and is characterized by elevated levels of blood plasma triglycerides and debilitating bouts of pancreatitis[14]. When administered as a series of intramuscular injections, Glybera, an adeno-associated

viral (AAV) vector encoding an LPL gene construct, has shown efficacy in reducing plasma triglycerides and rates of pancreatitis [15].

Cardiovascular diseases are the targets of approximately 8% of clinical gene therapy studies to date, but clinical trial results have so far been marked by low gene transfer efficacy[16]. A promising exception may be Mydicar, an AAV vector encoding SERCA2a (sarcoplasmic reticulum Ca^{+2}-ATPase), currently under Phase IIb study for congestive heart failure (ClinicalTrials.gov ID: NCT01643330). In a Phase IIa trial, patients treated with the highest dose of Mydicar experienced significant reduction of major cardiovascular events over a 12-month period compared with those receiving placebo[17].

Infectious diseases comprise another 8% of indications that have been addressed for clinical gene therapy trials. One interesting example under Phase I/II study is a cell-based therapy for HIV/AIDS termed SB-728-T, which consists of autologous CD4+ T cells genetically modified with a zinc finger nuclease to resist HIV infection (ClinicalTrials.gov ID: NCT00842634).

Neurological diseases comprise a relatively small proportion of targets of active gene therapy trials. In a Phase II study, patients with Parkinson's disease showed some improvement in motor function following subthalmic infusion of AAV2-GAD, an adeno-associated viral vector encoding glutamic acid decarboxylase (GAD)[18], yet its clinical development is in doubt following the bankruptcy of the trial's corporate sponsor. However, another gene therapeutic for Parkinson's disease, an AAV vector encoding neurturin, is currently undergoing Phase I/II studies[19].

With respect to ocular diseases, recent early-phase clinical trials have raised the prospects for treatment of some forms of inherited blindness, such as Leber's congenital amaurosis (LCA)[20]. In a pair of landmark studies, some patients with LCA caused by mutations in the gene encoding an essential retinal pigment epithelial protein (RPE65) experienced marked improvements in vision following local injection of AAV vectors delivering the RPE65 gene[21, 22]. A follow-up study in three patients showed efficacy after a second administration to the contralateral eye[23].

2.2 LIMITATIONS OF VIRAL VECTORS

As suggested above, the key challenge limiting clinical translation of gene therapeutics is the lack of delivery vectors considered safe and effective. Many of the aforementioned clinical trials have employed modified viruses such as retroviruses, lentiviruses, adenoviruses, and adeno-associated viruses (AAVs) to deliver genes; in fact, nearly 70% of gene therapy clinical trials to date have involved viral vectors[3] (Figure 2.3). Although they can be quite efficient and have advanced the field of gene therapy in significant ways, several limitations have been associated with viral vectors, as described below.

(1) *Carcinogenesis*: Retroviruses and lentiviruses in particular have been associated with a risk of carcinogenesis[24]. The development of leukemia in children receiving retroviral gene therapy for X-linked SCID has been attributed to a combination of insertional mutagenesis caused by viral genome integration, acquired somatic mutations[25], and transgene-specific

effects[26]. Although AAV vectors are generally considered safer due to a very low probability of integration, and have become more widely used in recent years, tumorigenesis has been observed in mice treated with this class of vectors[27], and the long-term cancer risk is still unclear[1].

(2) *Immune responses*: Pre-existing immunity comprises a serious safety concern for certain classes of viral vectors, especially adenoviruses[28]. The death of Jesse Gelsinger within days of receiving adenoviral gene therapy was blamed on a severe innate immune response characterized by dramatically elevated levels of inflammatory cytokines[28]. In contrast, AAVs have not been associated with such severe immune responses, but pre-existing immunity to many AAV serotypes in significant fractions of the human population can greatly diminish their efficacy[29]. Furthermore, adaptive immune responses, both humoral and cell-mediated, can prevent the possibility of repeat dosing and result in the elimination of transduced cells[29].

(3) *Broad tropism*: Some viral serotypes show relatively narrow transduction specificity, or tropism, for particular cells or tissues, but many others have broad tropism[30]. This feature may be undesirable if the transgene is expressed in non-target tissues following systemic delivery.

(4) *Limited DNA packaging capacity*: AAVs have a DNA cargo capacity of <5 kb; retroviruses, lentiviruses, and some adenoviruses have packaging capacities of ~8 kb, which may limit the potential for transduction of long transgenes[31].

(5) *Difficulty of production*: Depending on the viral vector, raising the necessary numbers of vector particles can be challenging, requiring purification procedures that may be difficult and costly to scale up[32].

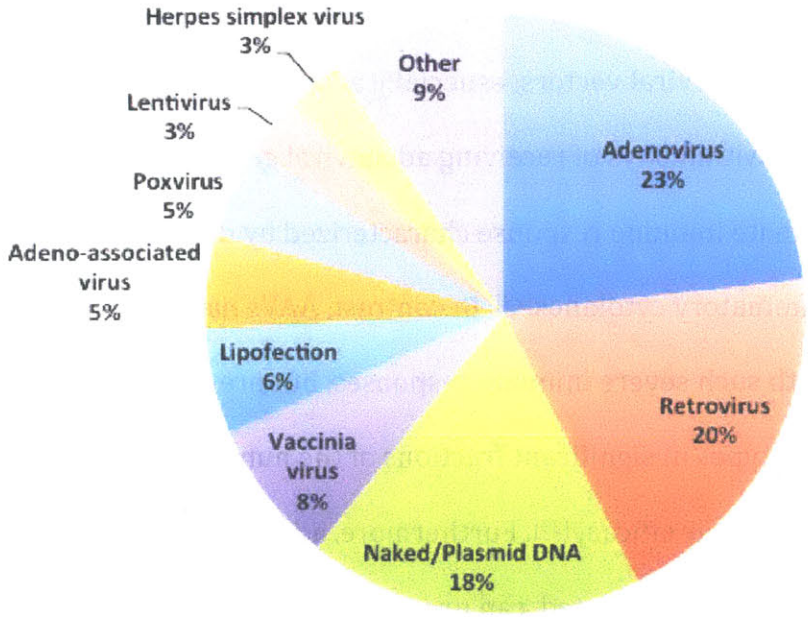

Figure 2.3 Vectors used in gene therapy clinical trials worldwide since 1989
Adapted from Ginn et al.[3]

Non-viral gene therapy has the potential to address many of these limitations, particularly with respect to safety. For DNA-based therapeutics, transgenes are often encoded on plasmids that are episomal and non-integrating, reducing the risk of cancer due to insertional mutagenesis. Moreover, due to the general lack of pre-existing immunity, synthetic vehicles tend to have comparably lower immunogenicity and toxicity. These carriers also have the potential to deliver larger genetic payloads and are typically easier to synthesize.

A number of non-viral gene delivery strategies have been developed so far. These strategies include the injection of naked DNA alone or in combination with

physical methods[33-39], such as gene gun, electroporation, hydrodynamic delivery, sonoporation, magnetofection, and laser irradiation. Because these techniques are generally less applicable to systemic gene delivery in humans, a panoply of synthetic delivery vectors have also been developed including lipids and liposomes[40, 41], polymers (linear and branched polymers, dendrimers, and polysaccharides)[42-50], polymersomes[51], cell-penetrating peptides[52-54], and inorganic nanoparticles[55]. Traditionally, synthetic vectors have been plagued by low delivery efficiency relative to viral vectors[45]. Whereas viruses have been naturally selected to deliver their genomes efficiently to mammalian cells, most synthetic vectors have not been designed to mediate gene delivery past the multiple barriers that confront them, which are detailed in the next section.

2.3 BARRIERS TO SYSTEMIC NON-VIRAL GENE DELIVERY

2.3.1 Extracellular barriers

For systemic delivery of DNA therapeutics, an initial barrier is the poor chemical stability of nucleic acids due to the presence of endonucleases in physiological fluids and the extracellular space. The half-life of plasmid DNA has been estimated to be 10 min. following intravenous injection in mice[56] and 60 min. following intratracheal instillation in mouse lungs[57]. For this reason, entrapment of the DNA within a nanoparticulate carrier is desirable in order to provide protection from nuclease degradation, as well as to improve circulation time.

Polyplexes, for instance, are spherical or toroidal nanoparticulate complexes formed from the condensation of plasmid DNA by cationic polymers[46]. The collapse

of DNA's expanded wormlike chain, representing a loss of entropy, is driven primarily by entropic gain due to the release of counterions upon polymer-DNA binding, which is favored by electrostatic interaction between the cationic polymer and the anionic phosphate backbone[58]. Similarly, mixtures of cationic lipids, neutral lipids, and DNA are able to spontaneously assemble into lipoplexes or liposomes characterized by DNA entrapped within lamellar or inverted hexagonal arrangements of lipid bilayers[59]. An excess of cationic polymer or lipid promotes enhanced DNA binding and the formation of stable complexes with positively charged surfaces; however, at high salt concentrations, electrostatic repulsion between the positively charged complexes is reduced, making them prone to colloidal instability and aggregation within physiological fluids[60]. In particular, aggregation of nanoparticles within the blood, either via colloidal instability or via interaction with blood components such as serum proteins and erythrocytes, can inhibit localization within the desired tissues, induce rapid clearance by circulating macrophages, and even cause embolism within lung capillaries[42].

Selective accumulation of the gene therapeutic at the cell or tissue of interest is another major challenge[61]. Passive targeting can be achieved through modulation of nanoparticle size, charge, shape, or surface chemistry. For instance, systemic gene delivery to liver hepatocytes generally requires particles smaller than ~100-200 nm to traverse the fenestrated endothelium[62], whereas uptake in macrophages can be achieved with positively charged, spherical particles on the order of 500 nm and above[63]. Stabilization of nanoparticles with non-fouling polymers such as polyethylene glycol (PEG) can increase circulation time within the

blood and promote accumulation in tumors with leaky vasculatures, a phenomenon known as the enhanced permeation and retention (EPR) effect[64]. Active targeting of synthetic gene vectors has been attempted using numerous ligands including small molecules, vitamins, carbohydrates, peptides, growth factors, antibodies, and aptamers[62, 65], but unfortunately there have been relatively few clear demonstrations of efficacy.

2.3.2 Cellular internalization

Once the nanoparticulate gene carrier is within the vicinity of the target cell, it may adsorb to the cell surface non-specifically through electrostatic interaction with negatively charged proteoglycans[66]. Internalization and endocytosis of the nanoparticle may then proceed through a variety of mechanisms[67]. Besides phagocytosis for some types of immune cells, these endocytic mechanisms include macropinocytosis, clathrin-dependent endocytosis, caveolae-mediated endocytosis, and a growing number of clathrin- and caveolae-independent pathways such as RhoA-dependent, Arf6-dependent, Cdc42-dependent, and flotillin-dependent endocytosis[68]. For most of the nanoparticles commonly used for non-viral gene delivery, including poly-L-lysine (PLL) and polyethylenimine (PEI)-based polyplexes, as well as various lipoplexes and liposomes, evidence exists for the use of multiple endocytic mechanisms[69-77], not all of which may contribute to successful gene expression[71, 78]. In some cases, an active targeting ligand may allow uptake and endocytosis of the nanoparticle to proceed selectively through one pathway after binding to a specific cell surface receptor[79].

2.3.3 Endosomal escape

Once internalized, the nanoparticle will generally be located within a vesicular structure known as an endosome formed from pinching off an invagination of the membrane[68]. Depending on the endocytic mechanism, cargo within the endosomes may then follow a pathway leading through increasingly acidified compartments toward enzymatic degradation within lysosomes (pH ~4.5), or may get recycled back to the extracellular space[67]. Dissection of these routes has been accomplished primarily via co-localization of the nanoparticles with certain protein markers of endocytic trafficking pathways, such as caveolin-1 (caveolae), Rab5 and EEA1 (early endosomes), Rab7 and ESCRTs (late endosomes), LAMP-1 (lysosomes), and Rab11 (recycling compartments)[80].

Efficient cytosolic localization and gene expression have generally been assumed to depend on an active mechanism for endosomal escape mediated by the gene carrier[46]. For lipoplexes, two mechanisms have been proposed, one involving interaction and fusion of the lipid carrier with endosomal membranes, and the other involving detergent-like destabilization of these membranes[77]. In contrast, polyplexes have been hypothesized to escape via a "proton-sponge" mechanism hinging on the ability of amines in the polymer with suitable pK_a values to buffer acidic endosomes or lysosomes[81, 82]. The polymer's ability to absorb protons presumably results in increased activity of pH-dependent proton pumps, which in turn promotes facilitated diffusion and internalization of chloride ions to maintain electroneutrality[83]. This increase in osmolarity is then thought to cause osmotic swelling of the endosomes or lysosomes leading to rupture. Despite the relative lack

of alternative hypotheses, this mechanism has been controversial, with some reports providing evidence to bolster it[84-86] and others challenging it[87-89].

2.3.4 Cytosolic trafficking and nuclear localization

Microinjection experiments suggest that a key cellular barrier limiting the efficiency of polymeric gene delivery is the transport of DNA from the cytoplasm to the nucleus. Working with a mouse cell line deficient in thymidine kinase (TK), Mario Capecchi reported nearly 30 years ago that if he microinjected plasmid DNA encoding TK directly into the nuclei, 50-100% expressed TK activity, as detected by the incorporation of ^{3}H-thymidine into DNA following autoradiographic analysis[90]. However, in over 1,000 cells receiving cytoplasmic injections of the same plasmid DNA, no TK activity was detected. The inefficiency of transgene expression following cytoplasmic microinjection of DNA relative to nuclear microinjection has since been confirmed by several other groups[91].

The importance of the nuclear barrier is further highlighted in the observation that quiescent or slowly dividing cells with intact nuclei are generally more difficult to transfect than cells that divide rapidly and undergo frequent breakdown of their nuclear envelopes[92]. In one study, transfection efficiency with lipoplexes and polyplexes was found to be cell-cycle dependent: luciferase expression was 30- to 500-fold higher in K-562 and HeLa cells transfected during S or G2 phase compared with cells transfected during G1 phase[93]. This effect was much less pronounced (only a fourfold difference) when the cells were transduced with recombinant adenoviruses.

Both deterministic and stochastic kinetic models of synthetic gene delivery have identified nuclear uptake as a potential rate-limiting step. In a direct comparison of the kinetics of intracellular gene transfer by PEI and by an adenoviral vector in the C3A human hepatocellular carcinoma cell line, one of the main advantages of the adenovirus in its superior gene delivery was its faster rate of nuclear import[94]. Similarly, after running stochastic simulations of synthetic gene delivery using PEI as an example, another group suggested that slow nuclear transport greatly reduced overall delivery because plasmids in the cytoplasm are quickly digested by nucleases[95], with an apparent half-life of 50-90 min[96]. Due to their relatively large size (25-80 nm in diameter), the diffusion coefficient of DNA plasmids in the cytoplasm is estimated to be small, on the order of 10^{-3} or 10^{-4} $\mu m^2/s$, and it has been observed for HeLa cells that DNA longer than 2,000 bp undergoes little or no diffusion in the cell cytoplasm[97]. Even so, polyplexes have been seen to accumulate quickly in the perinuclear region apparently via motor-protein driven transport on microtubules[98].

The nuclear envelope features a double membrane studded with ~3,000-5,000 nuclear pore complexes (NPCs) that serve as conduits between the nuclear and cytoplasmic compartments. Transport through the NPCs is selective, not only due to the small diameter of the pore (~25 nm), but also the presence of hydrophobic Phe-Gly (FG) sequence motifs in nucleoporin proteins lining the channel[99]. Molecules with a molecular weight less than ~40 kDa can enter the nucleus passively, but larger molecules require active transport[100].

Several groups have tried co-opting endogenous mechanisms for nuclear trafficking of proteins by directly attaching a nuclear localization signal (NLS) peptide to plasmid DNA or to the vector; however, these efforts have yielded mixed results likely attributable to confounding variables such as the conjugation method, the site of attachment, and the number of NLS peptides attached, as well as masking of the positively-charged NLS through its association with the negatively-charged DNA backbone[101-103]. An alternative strategy relies on the presence of a so-called DNA nuclear targeting sequence (DTS) within the plasmid to enhance nuclear localization, presumably by binding to newly synthesized transcription factors in the cytoplasm that facilitate shuttling to the nucleus [92, 104]. The evidence in support of such a strategy has also been mixed[105].

2.3.5 Vector unpacking

Vector unpacking is generally assumed to be necessary for DNA release and gene expression, but the extent to which suboptimal dissociation affects gene delivery is not fully clear. For lipoplexes, it has been proposed that fusion of the cationic lipid with endosomal membrane lipids facilitates not only endosomal escape but also DNA release[106, 107]. Polyplexes, meanwhile, have been observed to localize to the nucleus intact where they presumably undergo dissociation[108, 109]. For certain polyplexes, mechanistic studies have implicated slow vector unpacking as an explanation for decreased transfection efficiency[110-112]. A recent report suggests that lipoplex-delivered plasmids are nearly 10-fold more efficiently expressed, on the basis of protein expression per plasmid number in the nucleus,

than polyplex-delivered plasmids, a potential consequence of incomplete polyplex dissociation within the nucleus[113].

2.3.6 Gene expression

For DNA therapeutics, expression of the transgene and production of the protein of interest constitute the final barrier, which has sometimes been neglected despite its significant contribution to the overall transfection efficacy of a gene carrier. Plasmids are routinely used as expression vectors in non-viral gene therapy studies due to the relative ease of construction and amplification. The choice of enhancer/promoter combination has a tremendous impact on both the level and duration of transgene expression. Viral enhancers and promoters derived from cytomegalovirus (CMV), respiratory syncytial virus (RSV), and simian virus 40 (SV40) are frequently used to achieve high-level expression in a wide variety of mammalian cell types and tissues, but this expression is typically short-lived[114]. Constitutive mammalian promoters such as the human polyubiquitin C (UbC) and the elongation factor 1-α (EF1-α) promoters have been observed to result in more persistent expression[115]. Tissue-specific promoters such as the α-fetoprotein enhancer/albumin promoter for expression within the liver[116] offer the possibility of enhanced safety by minimizing off-target transgene expression. Numerous cis-acting sequences including various polyadenylation signals[117], introns[117, 118], and scaffold/matrix attachment regions (S/MAR)[119] have been reported to increase the level and persistence of transgene expression. DNA size and topology have been shown to affect gene expression efficiency, with small, covalently closed circular (ccc) plasmids mediating greater transgene expression than large or linearized

constructs[120]. Highly supercoiled plasmid DNA is often stated to be preferable for transfection over relaxed forms, although there is evidence to contradict this assumption[121].

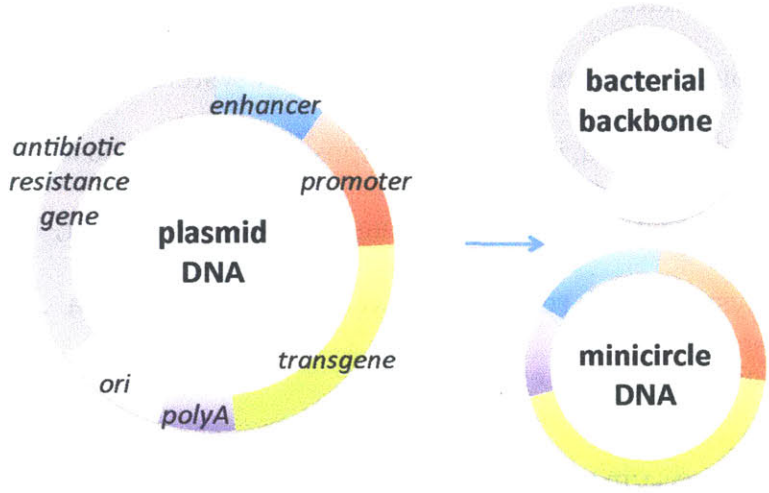

Figure 2.4 Schematic representation of plasmid and minicircle vectors

Recently, compact DNA vectors known as minicircles have been developed that demonstrate superior levels and duration of gene expression relative to full-length DNA plasmids[122-126]. The major distinction between the two constructs is that minicircles lack a bacterial backbone, consisting of an origin of replication and an antibiotic resistance gene, necessary for propagation in bacteria, while retaining only the mammalian expression cassette (Figure 2.4). Like plasmids, minicircles are non-integrating and characterized by transient expression. However, minicircles present at least four key advantages over plasmids: (1) increased potency due to the elimination of features that are unnecessary for therapeutic gene expression; (2) lower risk of TLR9-mediated immunogenicity owing to the reduction of unmethylated CpG motifs[127, 128]; (3) increased gene delivery efficiency due to more

compact DNA cargo; and (4) significantly greater level and potential for duration of gene expression[129]. This last advantage has been hypothesized to result from the absence of the bacterial backbone, which may induce gene silencing through the formation of repressive heterochromatin[130].

In an effort to promote longer-term expression, a number of systems for transgene integration have been developed, including transposition systems based on the recombinases phiC31[131], piggyBac[132], and Sleeping Beauty[133]. However, the safety of these integrating systems with respect to unwanted side effects as a result of transgene insertion has not yet been established[1].

2.4 OVERVIEW OF CURRENT NON-VIRAL VECTORS

To address these formidable barriers, myriad natural and synthetic materials have been explored as non-viral vectors for safe and effective gene delivery. A brief survey of the most commonly studied materials has been provided below.

2.4.1 Lipid-based vectors

Lipid-based vectors are among the most widely used and most clinically advanced non-viral gene carriers. Fraley et al. first showed in 1980 that liposomes composed of the phospholipid phosphatidylserine could entrap and deliver SV40 DNA to CV-1 monkey kidney cells[134]. More efficient transfection was obtained in 1987 by Felgner et al., who demonstrated that the synthetic cationic lipid DOTMA spontaneously formed small, uniform liposomes capable of efficient encapsulation and delivery of DNA to various mammalian cell lines[135]. Cationic lipids such as DOTMA are characterized structurally by three components: a cationic headgroup, a

hydrophobic tail, and a linking group between these domains[41]. DOSPA, DOTAP, DMRIE, and DC-Cholesterol feature particular modifications of these three domains and are examples of cationic lipids that have been applied for liposomal gene delivery[107] (Figure 2.5). Neutral lipids, such as the fusogenic phospholipid DOPE or the membrane component cholesterol, have been included in liposomal formulations as "helper lipids" to enhance transfection activity and nanoparticle stability[40]. Pairs of cationic lipids and helper lipids are widely available as commercial reagents for *in vitro* transfection, with one example being Lipofectamine, a combination of DOSPA and DOPE[41].

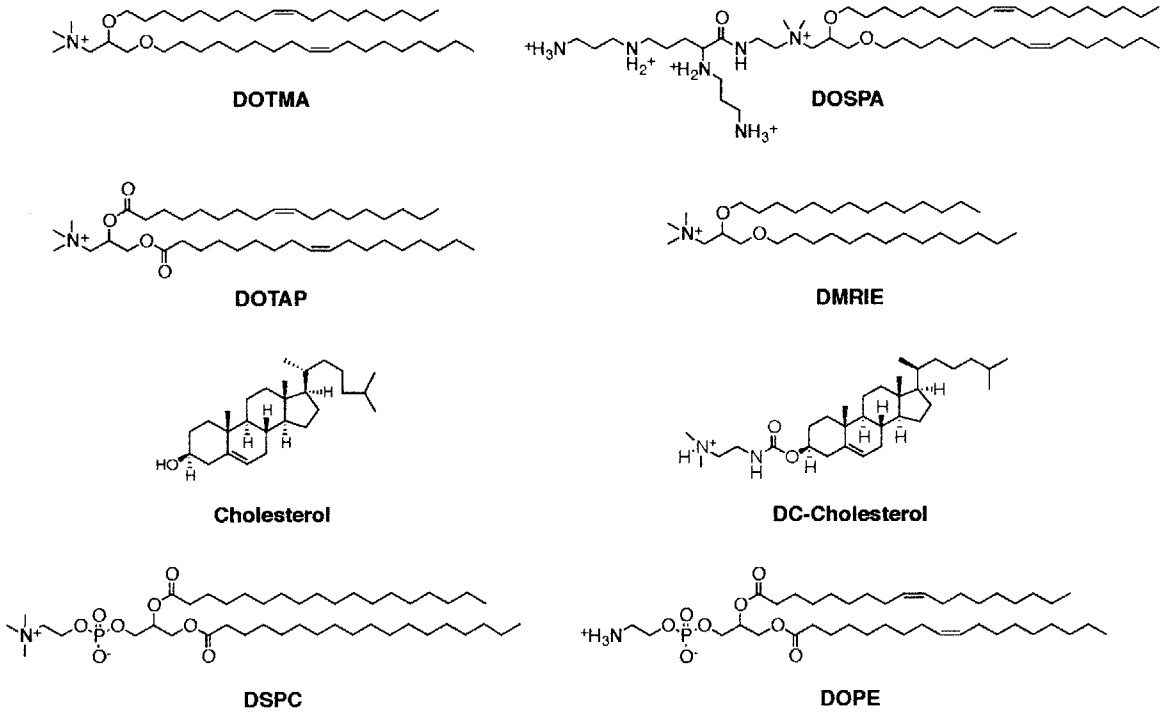

Figure 2.5 Chemical structures of cationic and neutral lipids commonly used in gene delivery studies

Although some traditional liposomes including DC-Chol/DOPE and DMRIE/DOPE have been applied clinically for gene therapy[41], their delivery efficacy has generally been low due to poor stability and rapid clearance, and more recently, lipid formulations have been developed that show greater clinical potential[136]. So-called stable nucleic acid-lipid particles (SNALPs), or lipid-based nanoparticles (LNPs), typically comprise at least four components including a synthetic cationic amino lipid, a phospholipid such as DSPC, a PEG-lipid conjugate, and cholesterol; these components are combined in an organic solvent such as ethanol and then mixed with nucleic acids in an acidic aqueous buffer to form stable nanoparticles[40]. The most promising amino lipid materials, such as DLinDMA-based ionizable lipids[137] and cationic lipid-like molecules termed lipidoids[138, 139] (Figure 2.6), have been developed primarily for LNP-mediated delivery of RNAi therapeutics and are currently under clinical investigation[140, 141]. Interestingly, the pK_a of the ionizable DLinDMA-based lipids has been found to correlate tightly with their hepatic gene silencing activity in mice, with an optimal pK_a range of 6.2-6.5[142].

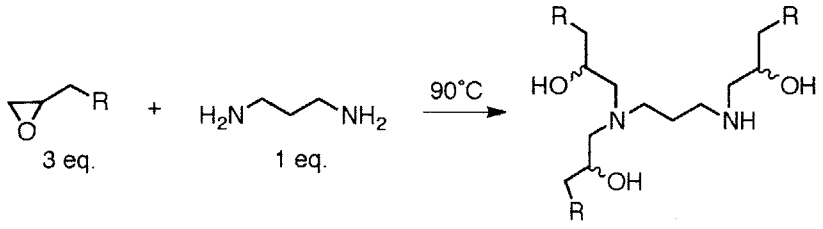

Figure 2.6 Synthesis of epoxide-derived lipidoids
Adapted from Love et al.[139]

In general, although they have been used to achieve systemic DNA delivery to subcutaneous mouse tumor xenografts[143], such LNPs appear to have less potency for delivery of plasmid DNA as compared with siRNA, perhaps a consequence of

poorer relative entrapment of the larger DNA cargo. An additional limitation is that cationic lipids have been observed to stimulate immune or anti-inflammatory responses[144].

2.4.2 Polymeric vectors

The extraordinary chemical diversity of polymers has enabled a plethora of biomaterials applications, most notably within the fields of tissue engineering and the controlled release and delivery of drugs. Selected examples of polymers that have been frequently studied as gene delivery vectors are highlighted below.

2.4.2.1. Poly(L-lysine)

Poly(L-lysine) (PLL) is a homopolypeptide of the basic amino acid lysine, the side chain of which terminates in a primary ε-amine with a pK_a of ~9.3-9.5[145]. Polylysine's capacity to condense DNA has been known since at least the 1960s[146, 147]. Pioneering studies in the late 1980s indicated that PLL conjugated to the asialoorosomucoid glycoprotein could potentially be applied toward non-viral liver-targeted gene delivery[148, 149]. In general, in the absence of a lysosomal disruption agent such as chloroquine, PLL has relatively poor transfection activity, presumably because its amine groups tend to be positively charged at physiological pH and therefore have low capacity for endosomal buffering and lysis[41]. Moreover, unmodified PLL demonstrates fairly significant *in vitro* cytotoxicity[150]. Numerous modified variants of PLL with enhanced gene delivery properties have been reported[145]. One prominent example includes the grafting of histidine's imidazole functionalities (pK_a ~ 6.5) to the side chains of PLL in an effort to increase its

endosomal buffering capacity[151]. Another example is the synthesis of a degradable polyester analog of PLL, poly[α-(4-aminobutyl)-L-glycolic acid] (PAGA), which is characterized by improved transfection activity and reduced cytotoxicity[152].

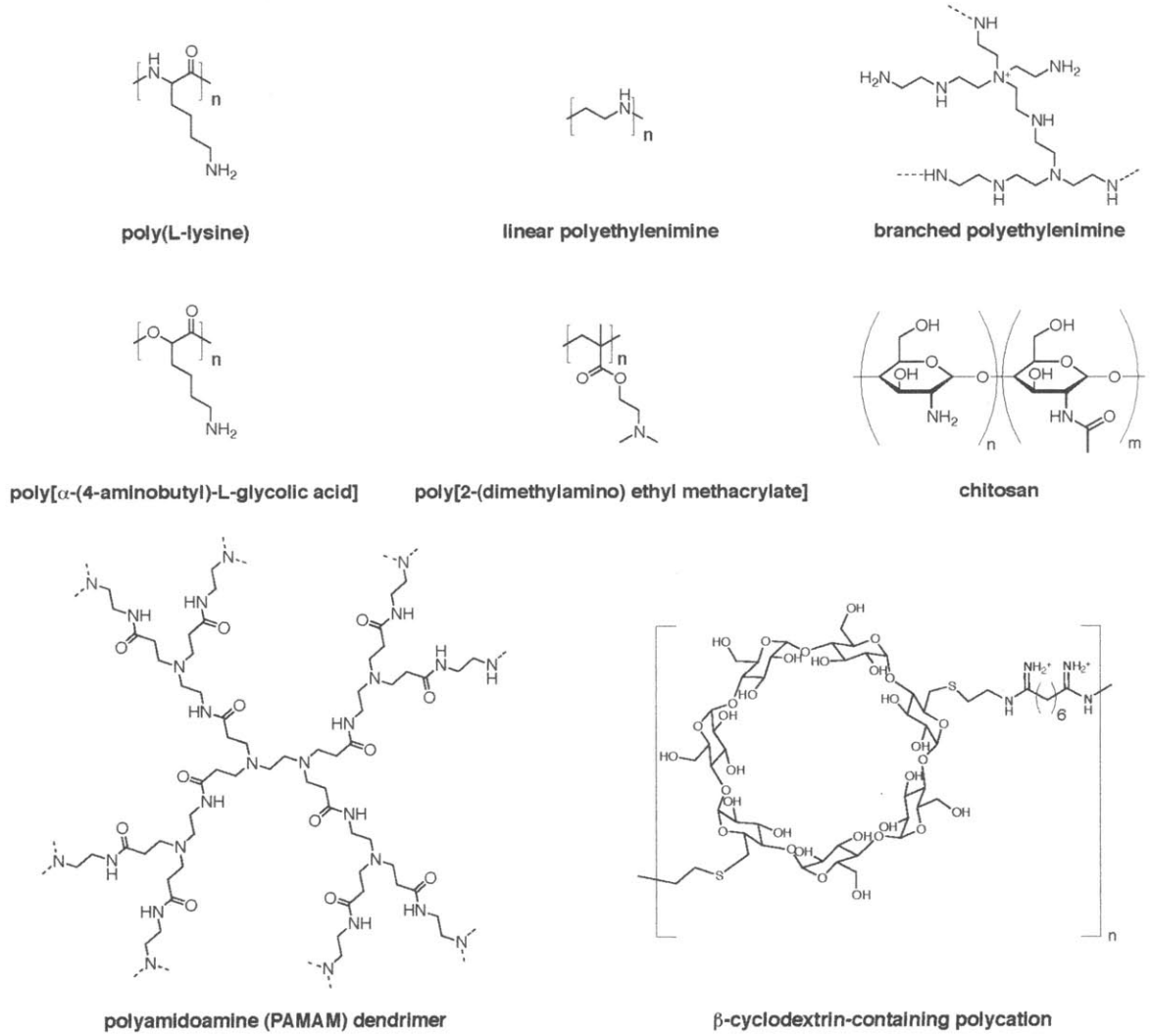

Figure 2.7 Chemical structures of selected polymeric gene vectors

2.4.2.2. Polyethylenimine

Polyethylenimine (PEI) and its variants have become the most widely used polymeric materials for gene delivery. With a nitrogen atom at every third position along the polymer, PEI is capable of an extremely high charge density at reduced pH

values, a characteristic which is postulated to aid in condensation of DNA and endosomal escape[153]. PEI's gene transfection activity *in vitro* was first demonstrated in 1995 by Behr and colleagues[81]. Soon after, it was shown that the transfection efficiency and cytotoxicity of PEI strongly depend on its structural properties, especially with respect to molecular weight[154] (MW) and the linear versus branched forms[155, 156]. In mice, intravenous injection of PEI/DNA polyplexes has been observed to afford gene transfection in the lungs[157-159], perhaps as a result of nanoparticle aggregates accumulating within pulmonary capillaries[160]. Several groups have also reported tumor gene delivery in mice using PEI/DNA polyplexes[161, 162]. In humans, PEI is under clinical study for local gene therapy of bladder cancer (ClinicalTrials.gov ID: NCT00595088) and pancreatic cancer (ClinicalTrials.gov ID: NCT01413087). Nonetheless, because PEI is well known to induce significant cytotoxicity[163, 164], modifications to PEI have been extensively investigated, with prominent examples including block copolymers of PEG and PEI to improve stability and biocompatibility[165, 166], degradable disulfide-crosslinked PEIs to reduce toxicity[167], and alkylated PEI to increase potency[168, 169].

2.4.2.3. Poly[(2-dimethylamino) ethyl methacrylate]

Poly[(2-dimethylamino) ethyl methacrylate] (pDMAEMA) is a water-soluble cationic polymer first investigated for gene delivery by Hennink and coworkers[170, 171]. Effective DNA condensation and gene transfer require relatively high MW (>300 kDa) pDMAEMA[172]. Although these polymers have been evaluated in rodents for systemic *in vivo* gene delivery[173, 174], additional studies are needed to ameliorate aggregation and toxicity issues that have been observed[175].

2.4.2.4. Carbohydrate-based polymers

A number of promising natural and synthetic carbohydrate-based polymers are currently under study for gene delivery applications. One of the oldest chemical methods of transfection, developed in the late 1960s, involves the use of cationic diethylaminoethyl (DEAE)-modified dextran[176]; however, this material is mainly limited to *in vitro* gene transfer for biological studies. A carbohydrate-based material more actively being researched is chitosan, a polysaccharide derivative of chitin composed of cationic glucosamine and *N*-acetyl glucosamine units joined by β(1,4) glycosidic linkages. A relatively biocompatible, biodegradable, and inexpensive material, unmodified chitosan has relatively low transfection activity, but modified versions of chitosan have been synthesized with greater gene delivery potential[177, 178]. Chitosan's mucoadhesive and permeability-enhancing properties have enabled its use for certain oral gene delivery applications[179], such as immunization of mice against peanut antigen-induced anaphylactic responses[180].

Produced from the enzymatic degradation of starch, cyclodextrins (CDs) are cyclic oligosaccharides of glucose linked by α(1-4) glycosidic bonds, with six-, seven-, or eight-membered glucose rings respectively defining the α-, β-, or γ-variants. Cyclodextrin's membrane-permeabilizing properties have been exploited for gene transfection through the synthesis of CD-based polymers and through the grafting of CDs to existing gene delivery materials[181]. Davis and colleagues synthesized novel, linear β-CD-containing polycations and described the effects of a variety of structural modifications on gene transfection activity[182-184]. Although they are typically extremely water soluble, CDs are characterized by a cup-shaped topology

with a hydrophobic internal cavity that can facilitate the inclusion of non-polar guest molecules such as poorly soluble drugs[185]. This unique feature was used to enable direct non-covalent PEGylation of polyplexes formed from β-CD-containing polymers and DNA through the addition of adamantane-PEG conjugates; stable ternary complexes are efficiently formed due to the interaction of adamantane with CD[186]. Targeted versions of these CD-containing polymer systems are currently under clinical investigation for delivery of RNAi therapeutics to solid tumors[187, 188].

2.4.2.5. Dendrimers

Dendrimers are polymers featuring perfectly defined, tree-like molecular architectures in which monomers with branching points radiate symmetrically from a central core[50]. They are synthesized in a stepwise fashion, with each reaction step yielding a new layer and defining an additional "generation" of dendrimer. A chemically diverse set of cationic dendrimers has been studied for gene delivery[49], with the most common based on polyamidoamine (PAMAM). The potential of PAMAM dendrimers for *in vitro* gene delivery was first explored through a series of studies in the mid-1990s[189-191]. Like PEI-based polymers, PAMAM dendrimers have a high density of secondary and tertiary amines and appear to be capable of endosomal buffering and osmotic swelling[85]. PAMAM/DNA complexes have also been observed to accumulate and mediate transgene expression within the mouse lungs following systemic administration[192]. Moreover, they have been used for suicide gene therapy of subcutaneous mouse tumor xenografts via intratumoral injection[193, 194]. As with many cationic vectors, one issue has been toxicity associated with PAMAM's positive charge[50], but a variety of modified PAMAM

dendrimers have recently been developed to improve the efficacy and safety profile of these materials[195].

2.4.3 Cell-penetrating peptides

Within the last two decades, hundreds of natural and synthetic cell-penetrating peptides (CPPs) have been identified and developed, with most falling into two classes, cationic arginine-rich peptides and amphipathic peptides[196]. The former class includes the HIV TAT protein transduction domain (PTD), the *Drosophila* Antennapedia homeodomain-derived penetratin peptide, and the synthetic octoarginine (Arg_8) peptide, whereas the latter class includes the chimeric peptides KALA, MPG, Pep-1, and Transportan (Table 2.1).

	Peptide	Origin	Sequence	Ref.
Cationic	TAT	HIV-1 TAT (47-57) transcriptional activator	YGRKKRRQRRR	[197]
	Penetratin	*Drosophilia* Antennapedia homeodomain	RQIKIWFQNRRMKWKK	[198]
	Arg_8	Chimeric	RRRRRRRR	[199, 200]
	CH_5-TAT-H_5C	Chimeric	CHHHHHRKKRRQRRRRHHHHHC	[201]
Amphipathic	KALA	Chimeric	WEAKLAKALAKALAKHLAKALAKALKACEA	[202]
	MPG	Chimeric	GALFLGFLGAAGSTMGAWSQPKKKRKV	[203]
	Pep-1	Chimeric	KETWWETWWTEWSQPKKKRKV	[204]
	Transportan	Chimeric	GWTLNSAGYLLGKINLKALAALAKKIL	[205]
	PPTG1	Chimeric	GLFKALLKLLKSLWKLLLKA	[206]

Table 2.1 Selected examples of cell-penetrating peptides

Although these peptides have been fused to or non-covalently complexed with nucleic acids to promote cellular internalization, the major limitation for many CPPs is the inability to mediate efficient endosomal escape[207]. For this reason, CPPs

are often either conjugated to traditional non-viral gene vectors such as polyplexes or liposomes[208], or they are otherwise designed with specific functionalities to enhance endosomal escape or overall gene transfection[53, 207]. Examples of peptides intentionally designed to mediate more efficient gene transfer include an endoosmolytic TAT peptide incorporating cysteine and histidine residues[201] (CH_5-TAT-H_5C), an N-terminal stearylated oligoarginine peptide[209], and the chimeric amphipathic peptide PPTG1[206].

2.4.4 Inorganic nanoparticles

Several kinds of inorganic nanoparticles (NPs) have been applied for non-viral gene delivery, most prominently silica, gold, iron oxide, quantum dots, and carbon nanotubes[55]. Technically, inorganic NPs have been used since the 1970s to achieve low levels of *in vitro* gene transfer using the method of calcium phosphate transfection[210]. While calcium phosphate NPs continue to receive some study, more recently attention has shifted to NPs with better prospects for *in vivo* translation.

Each class of inorganic NP presents particular advantages and disadvantages. For instance, silica NPs are considered biodegradable and relatively biocompatible, with surfaces that are easily functionalized, but they present some issues with respect to toxicity[211-213]. Similarly, gold NPs are easily functionalized using thiol moieties, and can enable a number of interesting imaging and treatment modalities such as photothermal cancer therapy, but they lack degradability[214]. Useful as MRI contrast agents and effectors for magnetic hypertherapy, iron oxide NPs are biodegradable and biocompatible, but achieving uniform surface functionalization and NP stabilization is challenging[215]. Quantum dots are extremely small particles

(< 10 nm) that can enable unique fluorescent imaging applications[216], but elements commonly present within their cores, especially cadmium and selenium, are known to induce considerable cytotoxicity[217]. Finally, the unique physical and chemical properties of carbon nanotubes (CNTs), which allow them to be easily functionalized and applied as photoluminescence, Raman, and photoacoustic contrast agents[218], are quite exciting, yet concerns remain regarding their lack of degradability and potential toxicity[219].

In order to bind nucleic acids and mediate transfection, the surfaces of most inorganic NPs need to be suitably functionalized. Silica nanoparticles, for example, have been shown to yield efficient gene delivery when functionalized with various amine groups[220, 221] or with PAMAM dendrimers[221]. Preliminary studies have established that amine-functionalized CNTs are capable of binding and condensing plasmid DNA[222, 223]. Recently, magnetically-enhanced delivery of DNA and RNA was accomplished using novel lipidoid-coated iron oxide NPs[224]. Gold nanoparticles, meanwhile, have been shown to mediate effective gene transfection *in vitro* when conjugated to PEI[225, 226]. In another example, efficient siRNA transfection of stem cells was achieved using gold nanoparticles functionalized with poly(β-amino ester)s, a promising group of cationic polymers which are described at length in the next section.

2.5 DEVELOPMENT OF POLY(BETA-AMINO ESTER)S FOR GENE THERAPY

Poly(β-amino esters) (PBAEs) are a class of polymeric gene vectors characterized by their relative ease of synthesis and their biodegradability. With

their ability to condense plasmid DNA into nanoparticles on the order of 50-200 nm in diameter, PBAEs have demonstrated high gene delivery efficiency to a variety of cell types with low cytotoxicity[227]. In addition to gene transfer, these polymers have been employed for a number of other applications, including hydrophobic drug delivery[228-234], biomaterials for cell encapsulation and tissue engineering[235-238], drug release from polyelectrolyte films[239-242], and the modification of other delivery materials[243, 244]. PBAEs have also been incorporated into poly(lactic-co-glycolic acid) (PLGA) microparticles for the generation of improved non-viral genetic vaccines for cancer[245, 246]. The rapid development of poly(β-amino ester)s, from their initial synthesis and characterization to their extensive preclinical evaluation ten years later, owes at least in part to the powerful approach of combinatorial polymer library synthesis coupled with high-throughput screening and characterization.

2.5.1 Initial synthesis and characterization

Although in the 1980s the synthesis of poly(ester amines) formed from the Michael-type addition of bisfunctional amines to diacrylate esters had been previously reported[247, 248], the suitability of these polymers as gene carriers was first explored in 2000 by Lynn and Langer[249]. The polymer reaction scheme is displayed in Figure 2.8. These polymers were selected for investigation for three reasons. First, it was hypothesized that the incorporation of tertiary amines into the polymer backbone could facilitate electrostatic interactions with DNA as well as buffer the endosomal compartment, allowing for escape of DNA to the cytoplasm[81]. Second, the presence of hydrolysable ester bonds in the backbone offered the

possibility of a less toxic polymer than non-degrading alternatives, assuming that the small-molecule acid degradation products could be cleared rapidly. Third, and perhaps most significantly, the polymers could be synthesized in a one-step reaction from commercially available monomers with a range of structural diversity, thereby allowing the investigation of structure-property relationships and the engineering of polymers with desired functionalities. In this initial study, three such polymers were synthesized from the addition of the bis(secondary amines) N,N′-dimethylethylenediamine, piperazine, or 4,4′-trimethylenedipiperidine to 1,4-butanediol diacrylate, and critical features of the resulting polymers, including the degradation kinetics, cytotoxicity, and DNA binding abilities, were explored.

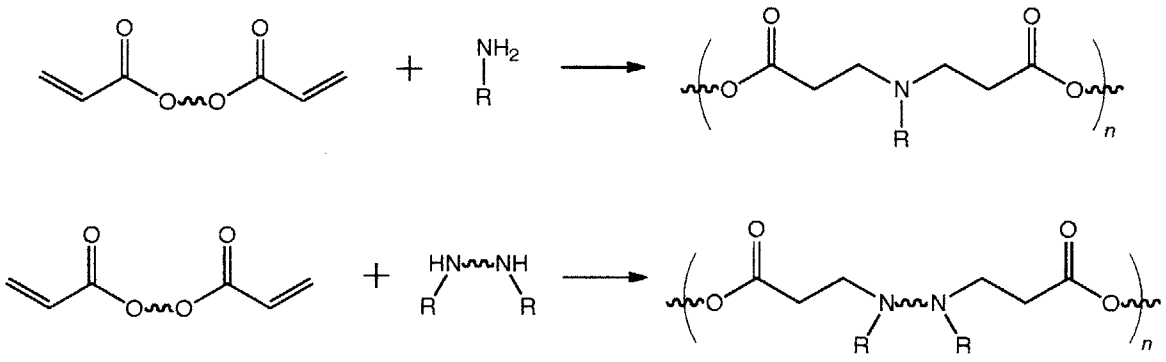

Figure 2.8 Synthesis of poly(β-amino ester)s
Poly(β-amino ester)s are synthesized from either the conjugate addition of a primary amine to a diacrylate monomer (*top*), or from the addition of a bis(secondary amine) to a diacrylate monomer (*bottom*).

Clearly, the degradation kinetics of an ideal gene delivery carrier should reflect a careful balance between a slow rate that inhibits unpacking and clearance and a rapid rate that precludes its functional utility. The degradation profiles of the polymers were assessed in water at 37°C in the presence of salt at two physiologically relevant pH values: (1) pH 5.1, roughly the pH encountered in the

lysosome, and (2) pH 7.4, as is encountered in the cytoplasm. In general, the polymers, which ranged in molecular weight from 5.8 to 31.2 kDa, degraded more rapidly at pH 7.4, with two of the polymers undergoing complete degradation within 5 hours. At the reduced pH, the half-life was approximately 7-8 hours. Though at odds with the well-known phenomenon of acid- (or base-) catalyzed ester hydrolysis, these degradation profiles match those of similar polyesters containing pendant amines; these amines are thought to act as intramolecular nucleophilic catalysts for which reactivity increases with pH[250, 251]. Given that the polymers contained only tertiary amines, which make for poor nucleophiles, Lynn and Langer considered this mechanism unlikely, but a more in-depth mechanistic investigation of the degradation kinetics of such polymers has not yet been performed.

To assess cytotoxicity, the authors used the commonly employed MTT assay. Strikingly, at concentrations as high as 100 μg/mL, the polymers had no effect on the viability of NIH 3T3 cells. In contrast, linear 25 kDa polyethylenimine (PEI) was highly toxic at this concentration, lending support to the hypothesis that the incorporation of degradable functionalities helps to reduce the toxicity of cationic polymers. The polymers also appeared promising in their capacity to bind and condense DNA. An agarose gel retardation assay showed that these polymers could inhibit the migration of plasmid DNA at weight ratios above 10:1 polymer:DNA. More importantly, quasi-electric light scattering revealed that in HEPES buffer at pH 7, complexes formed from the polymers and DNA above a 2:1 weight ratio were in the range of 50-150 nm. The measured ζ-potentials for these complexes were slightly positive at +10-15 mV, and the relative consistency of both particle size and

charge over time at 25°C suggested good particle stability with only a minor degree of particle aggregation. In general, as the polymer:DNA weight ratio increased, the polymer was better able to condense DNA into nanoparticles of smaller size with a more positive ζ-potential. For *in vitro* gene delivery, the slight positive charge on the particles may be desirable with respect to facilitation of cellular uptake via electrostatic interaction with the negatively charged cell surface.

One year later, Lynn and colleagues published a follow-up report in which they synthesized an initial library of 140 structurally diverse poly(β-amino esters) and screened them for DNA binding ability and *in vitro* transfection efficiency[151]. This paper provided a significant proof-of-concept for the combinatorial library approach to the identification of superior gene delivery materials. The library was formed by reacting 7 different diacrylates with each of 20 different amines. The resulting polymers ranged in molecular weight from 2 to 50 kDa, and half of them were sufficiently water-soluble to be included in a high-throughput DNA binding assay. Using an agarose gel slab with 500 lanes, they found that 56 of 70 water-soluble PBAEs could retard plasmid DNA when complexed at a polymer:DNA weight ratio of 20:1.

They then tested whether these PBAEs could mediate delivery and expression of a luciferase-encoding plasmid DNA in COS-7 cells, an immortalized line of African green monkey kidney fibroblasts frequently used in transfection assays. Two of the polymers yielded transfection levels 4 to 8 times that of PEI, with their performance rivaling that of a leading commercially available lipid reagent, Lipofectamine 2000. The short time required for these experiments, two weeks

from library synthesis to identification of "hits," further bolstered the value of this approach.

A more thorough characterization of this initial library revealed additional features of the structure-activity relationship for these polymers[252]. In general, smaller particle sizes below 250 nm and positive ζ-potentials were correlated with higher rates of DNA uptake, as assessed by the degree of internalization of a fluorescently labeled plasmid. Additionally, the authors used a FACS-based assay they developed[253] to measure the local pH environment of the delivered DNA. In this assay, pH values of 5 or less indicate that the polyplexes are unable to avoid eventual trafficking to lysosomes, whereas values closer to neutral pH suggest that the polymeric vector has mediated endosomal escape. The polymer-DNA complexes with the highest transfection efficiency in this library yielded average pH measurements above 6.5, implying that they had been able to buffer the endosome and successfully escape the lysosomal pathway. With regard to cytotoxicity, the majority of the DNA nanoparticles formed from PBAEs in this library appeared to have no impact on cell viability as measured by the MTT assay. Optimization of the synthesis, formulation, and transfection conditions for two members of the library resulted in polyplexes that could yield higher gene transfection efficiency in COS-7 cells than Lipofectamine 2000 and PEI[254].

2.5.2 High-throughput screening and selection

To accelerate the development of these polymeric gene carriers, Daniel Anderson and colleagues in the same group synthesized a large combinatorial library of 2,350 structurally distinct PBAEs from the reaction of 25 diacrylates,

designated by letters, with 94 primary or bis(secondary amine)s, designated by numbers.[255] Because the polymer products were generally viscous and therefore not amenable to automated fluid handling, all polymerization reactions were carried out in DMSO in a 96-well plate format, and the resulting polymer-DMSO solutions were directly processed for downstream characterization and screening. The authors determined that the residual levels of DMSO had no effect on gene delivery efficiency or cytotoxicity. After optimization of transfection conditions, 46 of the polymers, or roughly 2%, were found to transfect COS-7 cells at efficiencies better or equal to that of PEI.

Analysis of the structure-activity relationship for the lead polymers from this first-generation library suggested that the acrylate monomers were almost always hydrophobic, whereas the amine monomers tended to contain an alcohol, imidazole, or secondary diamine. It was also observed that the molecular weight and end-group termination, as governed by the ratio of monomers used during polymerization, dramatically affected transfection efficiency. Consequently, the authors decided to synthesize a more focused, second-generation library of PBAEs with 6 to 12 different molecular weights and chain end-groups – 486 variants in all – to probe the structural space represented by the best performing polymers[256].

In this focused library, the top performing PBAEs converged in chemical structure, lending support to the identification of important structure-function trends. The top nine polymers were synthesized from amino alcohols, which may suggest a key role for pendant hydroxyl functionalities in the side chains. The top three polymers, C32, JJ28, and C28, differed in structure by only one carbon. Formed

from the addition of 5-amino-1-pentanol ("32") to 1,4-butanediol diacrylate ("C") at a molar ratio of 1.2:1, C32, the most effective polymer overall, outperformed PEI and Lipofectamine 2000 in transfection of COS-7 cells. This polymer also formed the tightest complexation with DNA, resulting in 71 nm particles with a ζ-potential of +15 mV in HEPES buffer at pH 7.2. C32 synthesized with a 1.2:1 amine:acrylate ratio was nearly 50-fold more effective than C32 synthesized with a ratio of 1.025:1. This difference in transfection efficiency is likely due to differences in both molecular weight and terminal chain groups.

In another study, the C32 PBAE was used to deliver a suicide gene to prostate tumor xenografts in mice[257]. The prostate tumor xenografts were generated by mixing PC3 or LNCaP human prostate cancer cells with Matrigel and injecting the cells subcutaneously into the flanks of nude (athymic) mice. As a proof-of-concept, two days after intratumoral (i.t.) injection of a luciferase-encoding plasmid complexed with C32 nanoparticles, the local level of luminescence was 26-fold higher than with naked DNA alone and 4-fold higher than could be achieved with *in vivo*-jetPEI, a commercially available linear PEI intended for *in vivo* application. Interestingly, intramuscular injections yielded the opposite results; naked DNA gave the highest expression in healthy muscle, followed by jet-PEI and then C32, suggesting that the PBAE/DNA nanoparticles may be useful for targeting tumors while avoiding the surrounding healthy tissue. Histological analyses of the muscle tissue injected with the PBAE nanoparticles showed no evidence of pathology, and there was no significant difference relative to saline-injected mice with respect to a

number of commonly used toxicity markers for renal function, liver function, and muscle damage.

The researchers then used C32 to deliver a DNA construct encoding the A-chain of the diphtheria toxin (DT-A) to the prostate tumor xenografts. DT-A inhibits protein synthesis and causes apoptosis by catalyzing the transfer of ADP-ribose from NAD to elongation factor 2 (EF-2), which is essential for protein production. Because tight control of DT-A expression is crucial, two levels of gene regulation were used. The construct, which also encodes the Flp site-specific recombinase, must undergo a recombination event by Flp in order to express DT-A. Because Flp transcription is driven by a modified promoter/enhancer of the human prostate specific antigen (PSA) gene, DT-A expression is localized to prostate cells. When a series of i.t. injections of nanoparticles containing C32 and the DT-A construct was performed, the average growth rate of these tumors was suppressed twofold compared with tumors injected with a mock treatment. 40% of the experimentally treated tumors regressed in size. Combined with the data showing that C32 transfected healthy muscle poorly without noticeable toxicity, these experiments provided evidence that PBAEs may be promising carriers for suicide gene delivery for prostate cancer.

2.5.3 End-modification and ligand coating for cell-specific gene delivery

Because the high-throughput screening results highlighted the importance of the terminal functional group, researchers in the Langer lab synthesized and characterized a third-generation library of amine end-capped PBAEs[258-260]. The researchers were motivated by the desire to further expand the limits of the

chemical space imposed by the conjugate addition reaction[261]. To this end, in one version of the library, they developed a synthesis scheme (Figure 2.9) that involved the production of an intermediate acrylate-terminated C32 polymer, which was then end-capped by reaction with each of 37 different amine molecules, including primary monoamines and primary or secondary diamines [259].

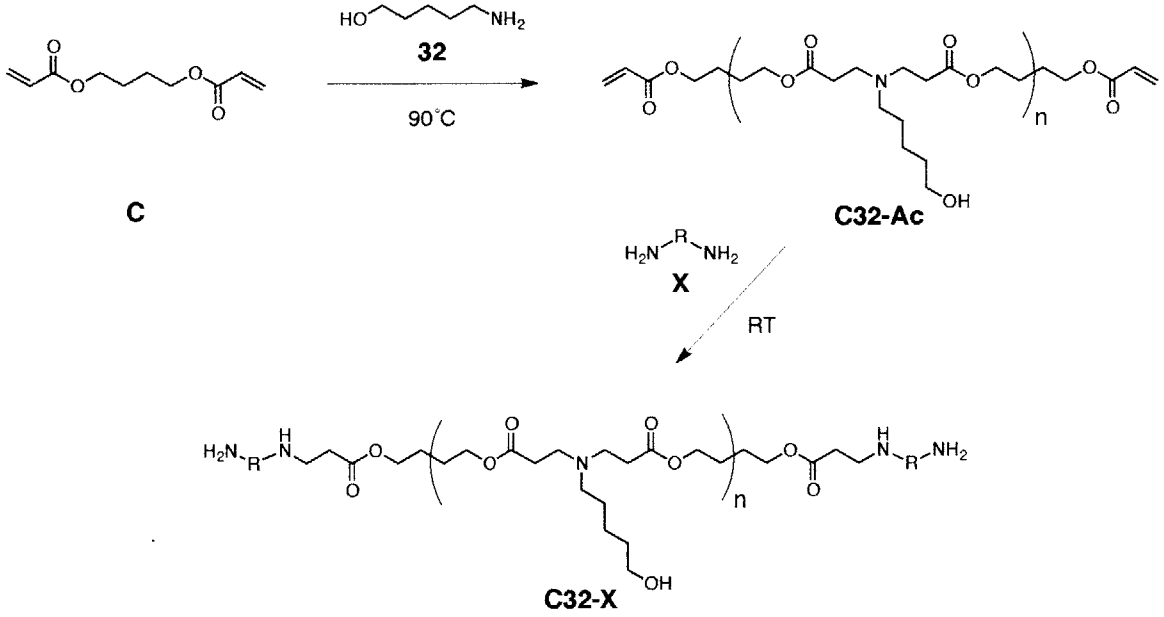

Figure 2.9 Synthesis of amine end-modified PBAEs
5-amino-1-pentanol (32) is added to an excess of 1,4-butanediol diacrylate (C) to yield acrylate-terminated C32, which is then reacted with excess diamine to produce amine end-modified PBAE.

The modification of the end groups had a significant impact on *in vitro* transfection efficiency. Following optimization of the polymer:DNA weight ratio, five of the 37 provided gene delivery performance better or equal to that of the unmodified C32 polymer in COS-7 cells. The most effective polymers were those conjugated with primary diamines, but even among these polymers, single carbon differences in the end-capping group dramatically modulated DNA binding ability and cellular uptake. Characterization of C32-117, a lead end-modified PBAE, relative

to unmodified C32, showed that this polymer was able to complex DNA roughly twice as efficiently, form nanoparticles that were 30% smaller, and mediate a twofold improvement in plasmid cellular uptake[258]. Because the unmodified polymer contained no primary amines, with its chains terminating in alcohol groups, the authors reasoned that the addition of primary amine end-groups increased the polymers' cationic charge, which improved DNA binding and condensation[261]. For the first time, cationic polymers, including C32-117 and two other end-capped PBAEs, were shown to be nearly as effective as adenovirus at transfecting primary human endothelial cells.

The polymer group was also found to alter the specificity of *in vitro* gene transfection in various cell lines[262]. In a report that screened 60 additional end-capped C32 variants for transfection efficiency in five different cell lines, it was observed that in some cases, variants that yielded the maximum transfection efficiency for delivery to one cell line mediated little or no transfection in others. For example, C32-117 was found to yield high levels of transfection in the HeLa human cervical cancer cell line and the HepG2 human hepatocellular carcinoma cell line, but not in the DC2.4 immortalized murine dendritic cell line; in contrast, a different end-modified variant, C32-254, had excellent performance in DC2.4 cells and poor activity in HeLa and HepG2 cells. End-capped PBAEs have demonstrated particularly efficient DNA transfection of cultured stem cells; for this reason, they have been used to genetically modify mesenchymal stem cells and embryonic stem cell-derived cells for the promotion of angiogenesis in a mouse ischemic hindlimb model[263, 264]. Recently, end-modified PBAEs have been used for non-viral gene transfection of

mouse mammary epithelial cells[265], human endothelial cells[266], and human glioblastoma cells[267, 268].

End-modified C32 polymers were also found to have promising *in vivo* gene delivery performance. In transgenic mice bearing ovarian tumors, C32-117 was able to deliver and mediate strong expression of a luciferase gene in the tumors at a level significantly higher than that of unmodified C32 following intraperitoneal administration[258]. A follow-up study demonstrated preclinical safety and efficacy of C32-117 complexed with a DT-A gene construct for suicide gene therapy of three different mouse models of ovarian cancer[269]. Biodistribution data in mice suggested that intraperitoneal administration of PBAE/DNA polyplexes yielded high gene expression in the fat and stomach, whereas intravenous administration resulted in expression concentrated in the lungs, liver, and spleen[259]. Perhaps in an analogous manner to the cell line preferences observed *in vitro*, the polymer end group may play a role in dictating organ-to-organ differences in gene expression.

One of the long-term objectives in the drug delivery field has been the incorporation of targeting functionalities to reduce possible adverse effects of nonspecific delivery and to minimize the total drug dose required. As mentioned earlier, these targeting functionalities include small molecules, peptides, proteins, antibodies, or aptamers that recognize and bind to cell surface markers expressed specifically in the tissue of interest. The integrin-binding arginine-glycine-aspartic acid (RGD) peptide has been well-studied for its ability to enhance tumor-targeted drug delivery due to the overexpression of $\alpha v\beta 3$ and $\alpha v\beta 5$ integrins on the surface of endothelial cells in many malignant tumors[270].

The use of RGD peptides to achieve targeted gene delivery with poly(β-amino ester)s has been explored. In one study, the RGD peptide was chemically conjugated to the side chains of poly(β-amino ester)s via disulfide linkages, which enabled the targeting ligand to be cleaved upon encountering the reducing environment within the cell[271]. In another study, an RGD peptide was linked to a stretch of negatively charged glutamate residues, and the anionic peptide was electrostatically coated to the surface of positively charged PBAE/DNA nanoparticles by mixing at a slightly acidic pH[272]. RGD-coated C32/DNA nanoparticles were found to deliver DNA in a ligand-specific manner to primary human umbilical vein endothelial cells (HUVEC). It has been further reported that PBAE/DNA nanoparticles coated with various peptides can mediate tissue-specific gene expression in mice even in the absence of a particular targeting motif like RGD, although the mechanism at play is unknown[273]. Electrostatically coated targeting ligands may be advantageous to those that are chemically coupled because they may be less likely to alter the chemical and biophysical properties of the polymer that enable efficient delivery[274].

2.5.4 Unsolved challenges

As illustrated above, PBAEs have shown tremendous potential as non-viral vectors for gene therapy. Nonetheless, for this class of polymers, several challenges and questions remain, among them the following three:

(1) *Poor stability under physiological conditions*: Aggregation in the blood poses a serious challenge to the development of many cationic gene delivery polymers for systemic administration. For PBAE/DNA polyplexes, one

indication of poor stability is the rapid growth in particle diameter within minutes of dilution in a high ionic strength buffer. As seen from dynamic light scattering (DLS) measurements in Figure 2.10, at low salt concentration, polyplexes remain relatively stable at either pH 5.2 or pH 7.55; however, at physiological salt concentration (150 mM NaCl), nanoparticles demonstrate a rapid increase in diameter, implicating salt as a major contributor to polyplex aggregation. Another sign of instability has been breathing difficulty and acute toxicity observed in some mice upon intravenous injection of polyplexes, suggesting the possibility of embolism with lung capillaries.

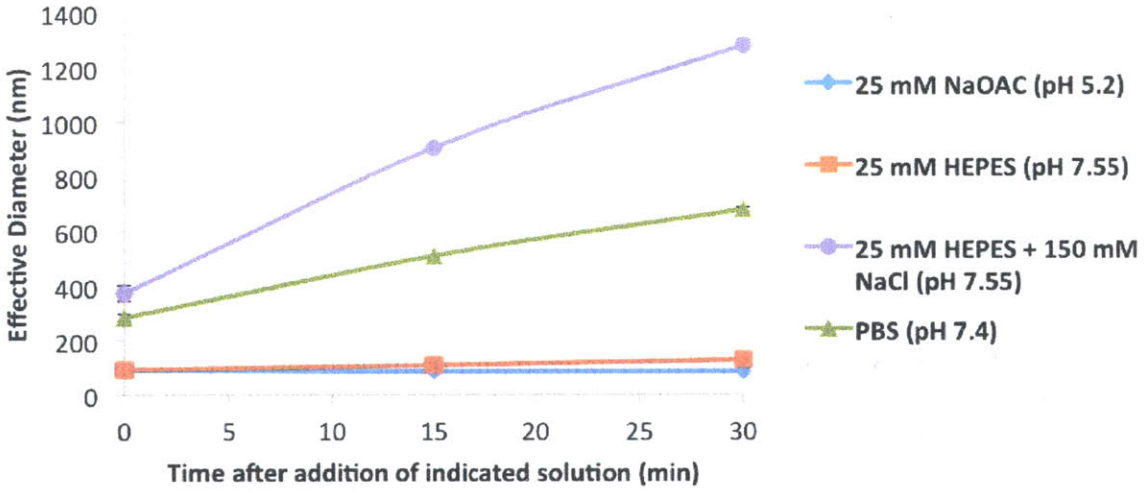

Figure 2.10 Aggregation of PBAE polyplexes under physiological conditions
Polyplexes consisting of the PBAE C32-122 and plasmid DNA were prepared at a 30:1 w/w ratio in 25 mM sodium acetate buffer (NaOAc) at pH 5.2. After a 5 min incubation at RT, the polyplexes were diluted in the indicated buffers and the diameters were measured by dynamic light scattering (DLS).

(2) *Batch-to-batch variability*: Inconsistency in the transfection performance of various batches of PBAE polymers has sometimes been observed, as shown in Figure 2.11. This variation was hypothesized to result at least in part from subtle differences in the molecular weight distributions (MWD) of the

batches. As a result, we were motivated to examine in detail the effect of MW and MWD on the gene delivery properties of amine end-modified PBAEs, a subject which had not yet received systematic investigation.

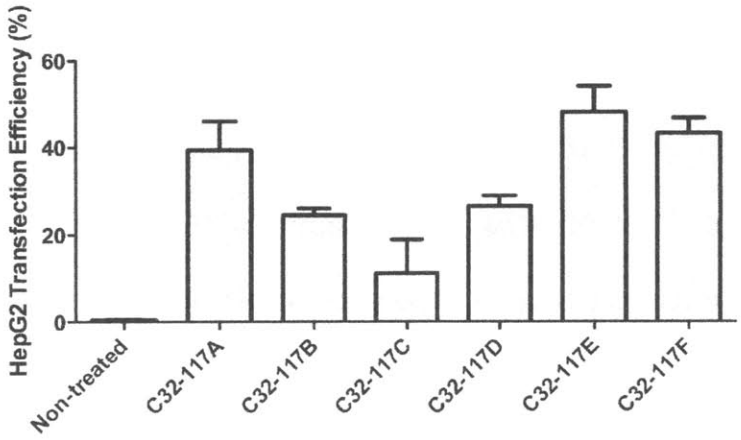

Figure 2.11 PBAE batch-to-batch variability
Different batches of the PBAE C32-117 were complexed with GFP-encoding plasmid DNA and incubated with HepG2 cells. Transfection efficiency was assessed after 24 h by FACS analysis.

(3) *Limited understanding of cellular uptake and trafficking*: The mechanisms by which PBAE polyplexes are internalized and trafficked within cells have not yet been studied. This lack of knowledge represents a hindrance to the rational design of more effective gene carriers.

As suggested in the introduction, the thesis research detailed here aims to make contributions within these areas that deepen our understanding of the gene delivery properties of these polymers and facilitate their continued development as non-viral gene vectors.

2.6 REFERENCES

[1] Kay, M. A. State-of-the-art gene-based therapies: the road ahead. *Nat. Rev. Genet.* **12**, 316 (2011).

[2] Sheridan, C. Gene therapy finds its niche. *Nat Biotechnol* **29**, 121 (2011).

[3] Ginn, S. L., Alexander, I. E., Edelstein, M. L., Abedi, M. R., Wixon, J. Gene therapy clinical trials worldwide to 2012 - an update. *J Gene Med* **15**, 65 (2013).

[4] Buchsbaum, D. J., Miller, C. R., McNally, L. R., Kaliberov, S. A. in Principles of Cancer Biotherapy. (eds. R. K. Oldham, R. O. Dillman) 589 (Springer Netherlands, 2009).

[5] Rocconi, R. P., Numnum, T. M., Stoff-Khalili, M., Makhija, S., Alvarez, R. D., Curiel, D. T. Targeted gene therapy for ovarian cancer. *Curr Gene Ther* **5**, 643 (2005).

[6] Guo, J., Xin, H. Splicing Out the West? *Science* **314**, 1232 (2006).

[7] Bedikian, A. Y., Richards, J., Kharkevitch, D., Atkins, M. B., Whitman, E., Gonzalez, R. A phase 2 study of high-dose Allovectin-7 in patients with advanced metastatic melanoma. *Melanoma Res* **20**, 218 (2010).

[8] Blaese, R. M., Culver, K. W., Miller, A. D., Carter, C. S., Fleisher, T., Clerici, M., Shearer, G., Chang, L., Chiang, Y., Tolstoshev, P., Greenblatt, J. J., Rosenberg, S. A., Klein, H., Berger, M., Mullen, C. A., Ramsey, W. J., Muul, L., Morgan, R. A., Anderson, W. F. T lymphocyte-directed gene therapy for ADA- SCID: initial trial results after 4 years. *Science* **270**, 475 (1995).

[9] Cavazzana-Calvo, M., Hacein-Bey, S., de Saint Basile, G., Gross, F., Yvon, E., Nusbaum, P., Selz, F., Hue, C., Certain, S., Casanova, J. L., Bousso, P., Deist, F. L., Fischer, A. Gene therapy of human severe combined immunodeficiency (SCID)-X1 disease. *Science* **288**, 669 (2000).

[10] Branca, M. A. Gene therapy: cursed or inching towards credibility? *Nat Biotechnol* **23**, 519 (2005).

[11] Hacein-Bey-Abina, S., von Kalle, C., Schmidt, M., Le Deist, F. o., Wulffraat, N., McIntyre, E., Radford, I., Villeval, J.-L., Fraser, C. C., Cavazzana-Calvo, M. A serious adverse event after successful gene therapy for X-linked severe combined immunodeficiency. *New England Journal of Medicine* **348**, 255 (2003).

[12] Tate, S., Elborn, S. Progress towards gene therapy for cystic fibrosis. *Expert Opin Drug Deliv* **2**, 269 (2005).

[13] Moran, N. First gene therapy approved. *Nat Biotech* **30**, 1153 (2012).

[14] Gaudet, D., Méthot, J., Kastelein, J. Gene therapy for lipoprotein lipase deficiency. *Current Opinion in Lipidology* **23**, 310 (2012).

[15] Wierzbicki, A. S., Viljoen, A. Alipogene tiparvovec: gene therapy for lipoprotein lipase deficiency. *Expert Opin Biol Ther* **13**, 7 (2013).

[16] Hedman, M., Hartikainen, J., Yla-Herttuala, S. Progress and prospects: hurdles to cardiovascular gene therapy clinical trials. *Gene Ther* **18**, 743 (2011).

[17] Jessup, M., Greenberg, B., Mancini, D., Cappola, T., Pauly, D. F., Jaski, B., Yaroshinsky, A., Zsebo, K. M., Dittrich, H., Hajjar, R. J. Calcium Upregulation by Percutaneous Administration of Gene Therapy in Cardiac Disease (CUPID): a phase 2 trial of intracoronary gene therapy of sarcoplasmic reticulum Ca2+-ATPase in patients with advanced heart failure. *Circulation* **124**, 304 (2011).

[18] LeWitt, P. A., Rezai, A. R., Leehey, M. A., Ojemann, S. G., Flaherty, A. W., Eskandar, E. N., Kostyk, S. K., Thomas, K., Sarkar, A., Siddiqui, M. S., Tatter, S. B., Schwalb, J. M., Poston, K. L., Henderson, J. M., Kurlan, R. M., Richard, I. H., Van Meter, L., Sapan, C. V., During, M. J., Kaplitt, M. G., Feigin, A. AAV2-GAD gene therapy for advanced Parkinson's disease: a double-blind, sham-surgery controlled, randomised trial. *Lancet Neurol* **10**, 309 (2011).
[19] Bartus, R. T., Baumann, T. L., Brown, L., Kruegel, B. R., Ostrove, J. M., Herzog, C. D. Advancing neurotrophic factors as treatments for age-related neurodegenerative diseases: developing and demonstrating "clinical proof-of-concept" for AAV-neurturin (CERE-120) in Parkinson's disease. *Neurobiol Aging* **34**, 35 (2013).
[20] Colella, P., Cotugno, G., Auricchio, A. Ocular gene therapy: current progress and future prospects. *Trends in Molecular Medicine* **15**, 23 (2009).
[21] Maguire, A. M., Simonelli, F., Pierce, E. A., Pugh, E. N., Mingozzi, F., Bennicelli, J., Banfi, S., Marshall, K. A., Testa, F., Surace, E. M., Rossi, S., Lyubarsky, A., Arruda, V. R., Konkle, B., Stone, E., Sun, J., Jacobs, J., Dell'Osso, L., Hertle, R., Ma, J.-x., Redmond, T. M., Zhu, X., Hauck, B., Zelenaia, O., Shindler, K. S., Maguire, M. G., Wright, J. F., Volpe, N. J., McDonnell, J. W., Auricchio, A., High, K. A., Bennett, J. Safety and Efficacy of Gene Transfer for Leber's Congenital Amaurosis. *New England Journal of Medicine* **358**, 2240 (2008).
[22] Bainbridge, J. W. B., Smith, A. J., Barker, S. S., Robbie, S., Henderson, R., Balaggan, K., Viswanathan, A., Holder, G. E., Stockman, A., Tyler, N., Petersen-Jones, S., Bhattacharya, S. S., Thrasher, A. J., Fitzke, F. W., Carter, B. J., Rubin, G. S., Moore, A. T., Ali, R. R. Effect of Gene Therapy on Visual Function in Leber's Congenital Amaurosis. *New England Journal of Medicine* **358**, 2231 (2008).
[23] Bennett, J., Ashtari, M., Wellman, J., Marshall, K. A., Cyckowski, L. L., Chung, D. C., McCague, S., Pierce, E. A., Chen, Y., Bennicelli, J. L., Zhu, X., Ying, G.-s., Sun, J., Wright, J. F., Auricchio, A., Simonelli, F., Shindler, K. S., Mingozzi, F., High, K. A., Maguire, A. M. AAV2 Gene Therapy Readministration in Three Adults with Congenital Blindness. *Science Translational Medicine* **4**, 120ra15 (2012).
[24] Baum, C., Kustikova, O., Modlich, U., Li, Z., Fehse, B. Mutagenesis and oncogenesis by chromosomal insertion of gene transfer vectors. *Human gene therapy* **17**, 253 (2006).
[25] Howe, S. J., Mansour, M. R., Schwarzwaelder, K., Bartholomae, C., Hubank, M., Kempski, H., Brugman, M. H., Pike-Overzet, K., Chatters, S. J., de Ridder, D., Gilmour, K. C., Adams, S., Thornhill, S. I., Parsley, K. L., Staal, F. J., Gale, R. E., Linch, D. C., Bayford, J., Brown, L., Quaye, M., Kinnon, C., Ancliff, P., Webb, D. K., Schmidt, M., von Kalle, C., Gaspar, H. B., Thrasher, A. J. Insertional mutagenesis combined with acquired somatic mutations causes leukemogenesis following gene therapy of SCID-X1 patients. *J Clin Invest* **118**, 3143 (2008).
[26] Davé, U. P., Jenkins, N. A., Copeland, N. G. Gene Therapy Insertional Mutagenesis Insights. *Science* **303**, 333 (2004).
[27] Valdmanis, P. N., Lisowski, L., Kay, M. A. rAAV-mediated tumorigenesis: still unresolved after an AAV assault. *Mol Ther* **20**, 2014 (2012).
[28] Bessis, N., GarciaCozar, F. J., Boissier, M. C. Immune responses to gene therapy vectors: influence on vector function and effector mechanisms. *Gene Ther* **11 Suppl 1**, S10 (2004).

[29] Zaiss, A. K., Muruve, D. A. Immunity to adeno-associated virus vectors in animals and humans: a continued challenge. *Gene Ther* **15**, 808 (2008).
[30] Waehler, R., Russell, S. J., Curiel, D. T. Engineering targeted viral vectors for gene therapy. *Nature Reviews Genetics* **8**, 573 (2007).
[31] Thomas, C. E., Ehrhardt, A., Kay, M. A. Progress and problems with the use of viral vectors for gene therapy. *Nat Rev Genet* **4**, 346 (2003).
[32] Bouard, D., Alazard-Dany, D., Cosset, F. L. Viral vectors: from virology to transgene expression. *Br J Pharmacol* **157**, 153 (2009).
[33] Mehier-Humbert, S., Guy, R. H. Physical methods for gene transfer: Improving the kinetics of gene delivery into cells. *Advanced Drug Delivery Reviews* **57**, 733 (2005).
[34] Newman, C. M., Bettinger, T. Gene therapy progress and prospects: ultrasound for gene transfer. *Gene Ther* **14**, 465 (2007).
[35] Wells, D. J. Gene therapy progress and prospects: electroporation and other physical methods. *Gene Ther* **11**, 1363 (2004).
[36] Plank, C., Schillinger, U., Scherer, F., Bergemann, C., Remy, J. S., Krotz, F., Anton, M., Lausier, J., Rosenecker, J. The magnetofection method: using magnetic force to enhance gene delivery. *Biol Chem* **384**, 737 (2003).
[37] Zhang, G., Budker, V. G., Ludtke, J. J., Wolff, J. A. Naked DNA gene transfer in mammalian cells. *Methods Mol Biol* **245**, 251 (2004).
[38] Frenkel, V. Ultrasound mediated delivery of drugs and genes to solid tumors. *Advanced Drug Delivery Reviews* **60**, 1193 (2008).
[39] Yao, C. P., Zhang, Z. X., Rahmanzadeh, R., Huettmann, G. Laser-based gene transfection and gene therapy. *Ieee Transactions on Nanobioscience* **7**, 111 (2008).
[40] Li, W., Szoka, F. Lipid-based Nanoparticles for Nucleic Acid Delivery. *Pharmaceutical Research* **24**, 438 (2007).
[41] Mintzer, M. A., Simanek, E. E. Nonviral vectors for gene delivery. *Chem. Rev.* **109**, 259 (2009).
[42] Morille, M., Passirani, C., Vonarbourg, A., Clavreul, A., Benoit, J. P. Progress in developing cationic vectors for non-viral systemic gene therapy against cancer. *Biomaterials* **29**, 3477 (2008).
[43] Wong, S. Y., Pelet, J. M., Putnam, D. Polymer systems for gene delivery--Past, present, and future. *Prog. Polym. Sci.* **32**, 799 (2007).
[44] Park, T. G., Jeong, J. H., Kim, S. W. Current status of polymeric gene delivery systems. *Advanced Drug Delivery Reviews* **58**, 467 (2006).
[45] Putnam, D. Polymers for gene delivery across length scales. *Nature materials* **5**, 439 (2006).
[46] Pack, D. W., Hoffman, A. S., Pun, S., Stayton, P. S. Design and development of polymers for gene delivery. *Nat Rev Drug Discov* **4**, 581 (2005).
[47] Eliyahu, H., Barenholz, Y., Domb, A. J. Polymers for DNA delivery. *Molecules* **10**, 34 (2005).
[48] Thomas, M., Klibanov, A. M. Non-viral gene therapy: polycation-mediated DNA delivery. *Applied Microbiology and Biotechnology* **62**, 27 (2003).
[49] Dufès, C., Uchegbu, I. F., Schätzlein, A. G. Dendrimers in gene delivery. *Advanced Drug Delivery Reviews* **57**, 2177 (2005).

[50] Lee, C. C., MacKay, J. A., Frechet, J. M. J., Szoka, F. C. Designing dendrimers for biological applications. *Nat Biotech* **23**, 1517 (2005).
[51] Discher, D. E., Ahmed, F. Polymersomes. *Annu Rev Biomed Eng* **8**, 323 (2006).
[52] Saranya, N., Moorthi, A., Saravanan, S., Devi, M. P., Selvamurugan, N. Chitosan and its derivatives for gene delivery. *Int. J. Biol. Macromol.* **48**, 234 (2011).
[53] Morris, M. C., Deshayes, S., Heitz, F., Divita, G. Cell-penetrating peptides: from molecular mechanisms to therapeutics. *Biology of the Cell* **100**, 201 (2008).
[54] Martin, M., Rice, K. Peptide-guided gene delivery. *The AAPS Journal* **9**, E18 (2007).
[55] Sokolova, V., Epple, M. Inorganic nanoparticles as carriers of nucleic acids into cells. *Angew Chem Int Ed Engl* **47**, 1382 (2008).
[56] Kawabata, K., Takakura, Y., Hashida, M. The fate of plasmid DNA after intravenous injection in mice: involvement of scavenger receptors in its hepatic uptake. *Pharm Res* **12**, 825 (1995).
[57] Rolland, A., Sullivan, S. M. Pharmaceutical Gene Delivery Systems. (Marcel Dekker, 2003).
[58] Bloomfield, V. A. DNA condensation by multivalent cations. *Biopolymers* **44**, 269 (1997).
[59] Koltover, I., Salditt, T., Rädler, J. O., Safinya, C. R. An Inverted Hexagonal Phase of Cationic Liposome-DNA Complexes Related to DNA Release and Delivery. *Science* **281**, 78 (1998).
[60] Wiethoff, C. M., Middaugh, C. R. Barriers to nonviral gene delivery. *J Pharm Sci* **92**, 203 (2003).
[61] Schaffer, D. V., Lauffenburger, D. A. Targeted synthetic gene delivery vectors. *Curr Opin Mol Ther* **2**, 155 (2000).
[62] Schatzlein, A. G. Targeting of Synthetic Gene Delivery Systems. *J Biomed Biotechnol* **2003**, 149 (2003).
[63] Doshi, N., Mitragotri, S. Designer biomaterials for nanomedicine. *Advanced Functional Materials* **19**, 3843 (2009).
[64] Albanese, A., Tang, P. S., Chan, W. C. The effect of nanoparticle size, shape, and surface chemistry on biological systems. *Annu Rev Biomed Eng* **14**, 1 (2012).
[65] Wagner, E., Culmsee, C., Boeckle, S. Targeting of polyplexes: toward synthetic virus vector systems. *Adv Genet* **53**, 333 (2005).
[66] Mislick, K. A., Baldeschwieler, J. D. Evidence for the role of proteoglycans in cation-mediated gene transfer. *Proceedings of the National Academy of Sciences* **93**, 12349 (1996).
[67] Sahay, G., Alakhova, D. Y., Kabanov, A. V. Endocytosis of nanomedicines. *J Control Release* **145**, 182 (2010).
[68] Doherty, G. J., McMahon, H. T. Mechanisms of endocytosis. *Annu Rev Biochem* **78**, 857 (2009).
[69] Rejman, J., Bragonzi, A., Conese, M. Role of clathrin- and caveolae-mediated endocytosis in gene transfer mediated by lipo- and polyplexes. *Mol Ther* **12**, 468 (2005).
[70] Luhmann, T., Rimann, M., Bittermann, A. G., Hall, H. Cellular uptake and intracellular pathways of PLL-g-PEG-DNA nanoparticles. *Bioconjug Chem* **19**, 1907 (2008).

[71] van der Aa, M. A., Huth, U. S., Hafele, S. Y., Schubert, R., Oosting, R. S., Mastrobattista, E., Hennink, W. E., Peschka-Suss, R., Koning, G. A., Crommelin, D. J. Cellular uptake of cationic polymer-DNA complexes via caveolae plays a pivotal role in gene transfection in COS-7 cells. *Pharm Res* **24**, 1590 (2007).
[72] von Gersdorff, K., Sanders, N. N., Vandenbroucke, R., De Smedt, S. C., Wagner, E., Ogris, M. The internalization route resulting in successful gene expression depends on both cell line and polyethylenimine polyplex type. *Mol Ther* **14**, 745 (2006).
[73] Wong, A. W., Scales, S. J., Reilly, D. E. DNA internalized via caveolae requires microtubule-dependent, Rab7-independent transport to the late endocytic pathway for delivery to the nucleus. *J Biol Chem* **282**, 22953 (2007).
[74] Grosse, S., Aron, Y., Thévenot, G., François, D., Monsigny, M., Fajac, I. Potocytosis and cellular exit of complexes as cellular pathways for gene delivery by polycations. *The Journal of Gene Medicine* **7**, 1275 (2005).
[75] Rejman, J., Conese, M., Hoekstra, D. Gene transfer by means of lipo- and polyplexes: role of clathrin and caveolae-mediated endocytosis. *J Liposome Res* **16**, 237 (2006).
[76] Khalil, I. A., Kogure, K., Futaki, S., Harashima, H. High density of octaarginine stimulates macropinocytosis leading to efficient intracellular trafficking for gene expression. *J Biol Chem* **281**, 3544 (2006).
[77] Elouahabi, A., Ruysschaert, J. M. Formation and intracellular trafficking of lipoplexes and polyplexes. *Molecular Therapy* **11**, 336 (2005).
[78] Goncalves, C., Mennesson, E., Fuchs, R., Gorvel, J. P., Midoux, P., Pichon, C. Macropinocytosis of polyplexes and recycling of plasmid via the clathrin-dependent pathway impair the transfection efficiency of human hepatocarcinoma cells. *Mol Ther* **10**, 373 (2004).
[79] Gottschalk, S., Cristiano, R. J., Smith, L. C., Woo, S. L. Folate receptor mediated DNA delivery into tumor cells: potosomal disruption results in enhanced gene expression. *Gene therapy* **1**, 185 (1994).
[80] Iversen, T.-G., Skotland, T., Sandvig, K. Endocytosis and intracellular transport of nanoparticles: Present knowledge and need for future studies. *Nano Today* **6**, 176 (2011).
[81] Boussif, O., Lezoualc'h, F., Zanta, M. A., Mergny, M. D., Scherman, D., Demeneix, B., Behr, J. P. A versatile vector for gene and oligonucleotide transfer into cells in culture and in vivo: polyethylenimine. *Proc Natl Acad Sci USA* **92**, 7297 (1995).
[82] Behr, J.-P. The proton sponge: a trick to enter cells the viruses did not exploit. *CHIMIA International Journal for Chemistry* **51**, 1 (1997).
[83] Nguyen, D. N., Green, J. J., Chan, J. M., Langer, R., Anderson, D. G. Polymeric Materials for Gene Delivery and DNA Vaccination. *Advanced Materials* **21**, 847 (2009).
[84] Bieber, T., Meissner, W., Kostin, S., Niemann, A., Elsasser, H. P. Intracellular route and transcriptional competence of polyethylenimine-DNA complexes. *J Control Release* **82**, 441 (2002).

[85] Sonawane, N. D., Szoka, F. C., Verkman, A. S. Chloride Accumulation and Swelling in Endosomes Enhances DNA Transfer by Polyamine-DNA Polyplexes. *Journal of Biological Chemistry* **278**, 44826 (2003).
[86] Akinc, A., Thomas, M., Klibanov, A. M., Langer, R. Exploring polyethylenimine-mediated DNA transfection and the proton sponge hypothesis. *The Journal of Gene Medicine* **7**, 657 (2004).
[87] Godbey, W. T., Barry, M. A., Saggau, P., Wu, K. K., Mikos, A. G. Poly(ethylenimine)-mediated transfection: A new paradigm for gene delivery. *Journal of Biomedical Materials Research* **51**, 321 (2000).
[88] Kichler, A., Leborgne, C., Coeytaux, E., Danos, O. Polyethylenimine-mediated gene delivery: a mechanistic study. *J Gene Med* **3**, 135 (2001).
[89] Benjaminsen, R. V., Mattebjerg, M. A., Henriksen, J. R., Moghimi, S. M., Andresen, T. L. The Possible "Proton Sponge" Effect of Polyethylenimine (PEI) Does Not Include Change in Lysosomal pH. *Molecular Therapy* **21**, 149 (2012).
[90] Capecchi, M. R. High efficiency transformation by direct microinjection of DNA into cultured mammalian cells. *Cell* **22**, 479 (1980).
[91] Zabner, J., Fasbender, A. J., Moninger, T., Poellinger, K. A., Welsh, M. J. Cellular and molecular barriers to gene transfer by a cationic lipid. *J Biol Chem* **270**, 18997 (1995).
[92] Miller, A. M., Dean, D. A. Tissue-specific and transcription factor-mediated nuclear entry of DNA. *Advanced Drug Delivery Reviews* **61**, 603 (2009).
[93] Brunner, S., Sauer, T., Carotta, S., Cotten, M., Saltik, M., Wagner, E. Cell cycle dependence of gene transfer by lipoplex, polyplex and recombinant adenovirus. *Gene Ther* **7**, 401 (2000).
[94] Varga, C., Tedford, N., Thomas, M., Klibanov, A., Griffith, L., Lauffenburger, D. Quantitative comparison of polyethylenimine formulations and adenoviral vectors in terms of intracellular gene delivery processes. *Gene Ther* **12**, 1023 (2005).
[95] Dinh, A., Pangarkar, C., Theofanous, T., Mitragotri, S. Understanding Intracellular Transport Processes Pertinent to Synthetic Gene Delivery via Stochastic Simulations and Sensitivity Analyses. *Biophysical Journal* **92**, 831 (2007).
[96] Lechardeur, D., Sohn, K. J., Haardt, M., Joshi, P. B., Monck, M., Graham, R. W., Beatty, B., Squire, J., O'Brodovich, H., Lukacs, G. L. Metabolic instability of plasmid DNA in the cytosol: a potential barrier to gene transfer. *Gene Ther* **6**, 482 (1999).
[97] Lukacs, G. L., Haggie, P., Seksek, O., Lechardeur, D., Freedman, N., Verkman, A. S. Size-dependent DNA mobility in cytoplasm and nucleus. *J Biol Chem* **275**, 1625 (2000).
[98] Suh, J., Wirtz, D., Hanes, J. Efficient active transport of gene nanocarriers to the cell nucleus. *Proceedings of the National Academy of Sciences* **100**, 3878 (2003).
[99] van der Aa, M., Mastrobattista, E., Oosting, R., Hennink, W., Koning, G., Crommelin, D. The Nuclear Pore Complex: The Gateway to Successful Nonviral Gene Delivery. *Pharm Res* **23**, 447 (2006).
[100] Lechardeur, D., Lukacs, G. L. Nucleocytoplasmic transport of plasmid DNA: a perilous journey from the cytoplasm to the nucleus. *Hum Gene Ther* **17**, 882 (2006).
[101] Brandén, L. J., Mohamed, A. J., Smith, C. I. A peptide nucleic acid-nuclear localization signal fusion that mediates nuclear transport of DNA. *Nat Biotechnol* **17**, 784 (1999).

[102] Escriou, V., Carrière, M., Scherman, D., Wils, P. NLS bioconjugates for targeting therapeutic genes to the nucleus. *Advanced Drug Delivery Reviews* **55**, 295 (2003).
[103] van Der Aa, M., Koning, G., D'oliveira, C., Oosting, R., Wilschut, K., Hennink, W., Crommelin, D. An NLS peptide covalently linked to linear DNA does not enhance transfection efficiency of cationic polymer based gene delivery systems. *J. Gene Med.* **7**, 208 (2005).
[104] Wilson, G. L., Dean, B. S., Wang, G., Dean, D. Nuclear import of plasmid DNA in digitonin-permeabilized cells requires both cytoplasmic factors and specific DNA sequences. *J Biol Chem* **274**, 22025 (1999).
[105] Gaal, E. B., Oosting, R., Eijk, R., Bakowska, M., Feyen, D., Kok, R., Hennink, W., Crommelin, D. A., Mastrobattista, E. DNA Nuclear Targeting Sequences for Non-Viral Gene Delivery. *Pharmaceutical Research* **28**, 1707 (2011).
[106] Xu, Y., Szoka, F. C., Jr. Mechanism of DNA release from cationic liposome/DNA complexes used in cell transfection. *Biochemistry* **35**, 5616 (1996).
[107] Wasungu, L., Hoekstra, D. Cationic lipids, lipoplexes and intracellular delivery of genes. *Journal of Controlled Release* **116**, 255 (2006).
[108] Godbey, W. T., Wu, K. K., Mikos, A. G. Tracking the intracellular path of poly(ethylenimine)/DNA complexes for gene delivery. *Proc Natl Acad Sci U S A* **96**, 5177 (1999).
[109] Breunig, M., Lungwitz, U., Liebl, R., Fontanari, C., Klar, J., Kurtz, A., Blunk, T., Goepferich, A. Gene delivery with low molecular weight linear polyethylenimines. *J. Gene Med.* **7**, 1287 (2005).
[110] Schaffer, D. V., Fidelman, N. A., Dan, N., Lauffenburger, D. A. Vector unpacking as a potential barrier for receptor-mediated polyplex gene delivery. *Biotechnol. Bioeng.* **67**, 598 (2000).
[111] Ho, Y. P., Chen, H. H., Leong, K. W., Wang, T. H. Evaluating the intracellular stability and unpacking of DNA nanocomplexes by quantum dots-FRET. *Journal of Controlled Release* **116**, 83 (2006).
[112] Chen, H. H., Ho, Y. P., Jiang, X., Mao, H. Q., Wang, T. H., Leong, K. W. Quantitative comparison of intracellular unpacking kinetics of polyplexes by a model constructed from quantum dot-FRET. *Mol Ther* **16**, 324 (2008).
[113] Cohen, R. N., Aa, M. A. v. d., Macaraeg, N., Lee, A. P., Jr, F. C. S. Quantification of plasmid DNA copies in the nucleus after lipoplex and polyplex transfection. *Journal of Controlled Release* **135**, 166 (2009).
[114] Gill, D., Pringle, I., Hyde, S. Progress and Prospects: The design and production of plasmid vectors. *Gene Ther.* **16**, 165 (2009).
[115] Gill, D. R., Smyth, S. E., Goddard, C. A., Pringle, I. A., Higgins, C. F., Colledge, W. H., Hyde, S. C. Increased persistence of lung gene expression using plasmids containing the ubiquitin C or elongation factor 1alpha promoter. *Gene Ther* **8**, 1539 (2001).
[116] Wooddell, C. I., Reppen, T., Wolff, J. A., Herweijer, H. Sustained liver-specific transgene expression from the albumin promoter in mice following hydrodynamic plasmid DNA delivery. *J Gene Med* **10**, 551 (2008).
[117] Miao, C. H., Ohashi, K., Patijn, G. A., Meuse, L., Ye, X., Thompson, A. R., Kay, M. A. Inclusion of the hepatic locus control region, an intron, and untranslated region

increases and stabilizes hepatic factor IX gene expression in vivo but not in vitro. *Mol Ther* **1**, 522 (2000).
[118] Chapman, B. S., Thayer, R. M., Vincent, K. A., Haigwood, N. L. Effect of intron A from human cytomegalovirus (Towne) immediate-early gene on heterologous expression in mammalian cells. *Nucleic Acids Res* **19**, 3979 (1991).
[119] Argyros, O., Wong, S. P., Niceta, M., Waddington, S. N., Howe, S. J., Coutelle, C., Miller, A. D., Harbottle, R. P. Persistent episomal transgene expression in liver following delivery of a scaffold/matrix attachment region containing non-viral vector. *Gene Ther* **15**, 1593 (2008).
[120] Kreiss, P., Mailhe, P., Scherman, D., Pitard, B., Cameron, B. a., Rangara, R., Aguerre-Charriol, O., Airiau, M., Crouzet, J. l. Plasmid DNA size does not affect the physicochemical properties of lipoplexes but modulates gene transfer efficiency. *Nucleic Acids Research* **27**, 3792 (1999).
[121] Bergan, D., Galbraith, T., Sloane, D. L. Gene transfer in vitro and in vivo by cationic lipids is not significantly affected by levels of supercoiling of a reporter plasmid. *Pharm Res* **17**, 967 (2000).
[122] Darquet, A. M., Cameron, B., Wils, P., Scherman, D., Crouzet, J. A new DNA vehicle for nonviral gene delivery: supercoiled minicircle. *Gene Ther* **4**, 1341 (1997).
[123] Darquet, A. M., Rangara, R., Kreiss, P., Schwartz, B., Naimi, S., Delaère, P., Crouzet, J., Scherman, D. Minicircle: an improved DNA molecule for in vitro and in vivo gene transfer. *Gene Ther* **6**, 209 (1999).
[124] Chen, Z. Y., He, C. Y., Ehrhardt, A., Kay, M. A. Minicircle DNA vectors devoid of bacterial DNA result in persistent and high-level transgene expression in vivo. *Mol Ther* **8**, 495 (2003).
[125] Chen, Z. Y., He, C. Y., Kay, M. A. Improved production and purification of minicircle DNA vector free of plasmid bacterial sequences and capable of persistent transgene expression in vivo. *Hum Gene Ther* **16**, 126 (2005).
[126] Kay, M. A., He, C. Y., Chen, Z. Y. A robust system for production of minicircle DNA vectors. *Nat Biotechnol* **28**, 1287 (2010).
[127] Bauer, S., Kirschning, C. J., Häcker, H., Redecke, V., Hausmann, S., Akira, S., Wagner, H., Lipford, G. B. Human TLR9 confers responsiveness to bacterial DNA via species-specific CpG motif recognition. *Proceedings of the National Academy of Sciences* **98**, 9237 (2001).
[128] Hyde, S. C., Pringle, I. A., Abdullah, S., Lawton, A. E., Davies, L. A., Varathalingam, A., Nunez-Alonso, G., Green, A. M., Bazzani, R. P., Sumner-Jones, S. G., Chan, M., Li, H., Yew, N. S., Cheng, S. H., Boyd, A. C., Davies, J. C., Griesenbach, U., Porteous, D. J., Sheppard, D. N., Munkonge, F. M., Alton, E. W., Gill, D. R. CpG-free plasmids confer reduced inflammation and sustained pulmonary gene expression. *Nat Biotechnol* **26**, 549 (2008).
[129] Mayrhofer, P., Schleef, M., Jechlinger, W. Use of minicircle plasmids for gene therapy. *Methods Mol Biol* **542**, 87 (2009).
[130] Chen, Z. Y., Riu, E., He, C. Y., Xu, H., Kay, M. A. Silencing of episomal transgene expression in liver by plasmid bacterial backbone DNA is independent of CpG methylation. *Mol Ther* **16**, 548 (2008).
[131] Ehrhardt, A., Xu, H., Huang, Z., Engler, J. A., Kay, M. A. A direct comparison of two nonviral gene therapy vectors for somatic integration: in vivo evaluation of the

bacteriophage integrase phiC31 and the Sleeping Beauty transposase. *Mol Ther* **11**, 695 (2005).
[132] Wu, S. C., Meir, Y. J., Coates, C. J., Handler, A. M., Pelczar, P., Moisyadi, S., Kaminski, J. M. piggyBac is a flexible and highly active transposon as compared to sleeping beauty, Tol2, and Mos1 in mammalian cells. *Proc Natl Acad Sci U S A* **103**, 15008 (2006).
[133] Aronovich, E. L., McIvor, R. S., Hackett, P. B. The Sleeping Beauty transposon system: a non-viral vector for gene therapy. *Hum Mol Genet* **20**, R14 (2011).
[134] Fraley, R., Subramani, S., Berg, P., Papahadjopoulos, D. Introduction of liposome-encapsulated SV40 DNA into cells. *J Biol Chem* **255**, 10431 (1980).
[135] Felgner, P. L., Gadek, T. R., Holm, M., Roman, R., Chan, H. W., Wenz, M., Northrop, J. P., Ringold, G. M., Danielsen, M. Lipofection: a highly efficient, lipid-mediated DNA-transfection procedure. *Proc Natl Acad Sci U S A* **84**, 7413 (1987).
[136] Whitehead, K. A., Langer, R., Anderson, D. G. Knocking down barriers: advances in siRNA delivery. *Nat Rev Drug Discov* **8**, 129 (2009).
[137] Semple, S. C., Akinc, A., Chen, J., Sandhu, A. P., Mui, B. L., Cho, C. K., Sah, D. W., Stebbing, D., Crosley, E. J., Yaworski, E., Hafez, I. M., Dorkin, J. R., Qin, J., Lam, K., Rajeev, K. G., Wong, K. F., Jeffs, L. B., Nechev, L., Eisenhardt, M. L., Jayaraman, M., Kazem, M., Maier, M. A., Srinivasulu, M., Weinstein, M. J., Chen, Q., Alvarez, R., Barros, S. A., De, S., Klimuk, S. K., Borland, T., Kosovrasti, V., Cantley, W. L., Tam, Y. K., Manoharan, M., Ciufolini, M. A., Tracy, M. A., de Fougerolles, A., MacLachlan, I., Cullis, P. R., Madden, T. D., Hope, M. J. Rational design of cationic lipids for siRNA delivery. *Nat Biotechnol* **28**, 172 (2010).
[138] Akinc, A., Zumbuehl, A., Goldberg, M., Leshchiner, E. S., Busini, V., Hossain, N., Bacallado, S. A., Nguyen, D. N., Fuller, J., Alvarez, R., Borodovsky, A., Borland, T., Constien, R., de Fougerolles, A., Dorkin, J. R., Narayanannair Jayaprakash, K., Jayaraman, M., John, M., Koteliansky, V., Manoharan, M., Nechev, L., Qin, J., Racie, T., Raitcheva, D., Rajeev, K. G., Sah, D. W., Soutschek, J., Toudjarska, I., Vornlocher, H. P., Zimmermann, T. S., Langer, R., Anderson, D. G. A combinatorial library of lipid-like materials for delivery of RNAi therapeutics. *Nat Biotechnol* **26**, 561 (2008).
[139] Love, K. T., Mahon, K. P., Levins, C. G., Whitehead, K. A., Querbes, W., Dorkin, J. R., Qin, J., Cantley, W., Qin, L. L., Racie, T., Frank-Kamenetsky, M., Yip, K. N., Alvarez, R., Sah, D. W., de Fougerolles, A., Fitzgerald, K., Koteliansky, V., Akinc, A., Langer, R., Anderson, D. G. Lipid-like materials for low-dose, in vivo gene silencing. *Proceedings of the National Academy of Sciences* **107**, 1864 (2010).
[140] DeVincenzo, J., Lambkin-Williams, R., Wilkinson, T., Cehelsky, J., Nochur, S., Walsh, E., Meyers, R., Gollob, J., Vaishnaw, A. A randomized, double-blind, placebo-controlled study of an RNAi-based therapy directed against respiratory syncytial virus. *Proc Natl Acad Sci U S A* **107**, 8800 (2010).
[141] Tabernero, J., Shapiro, G. I., Lorusso, P. M., Cervantes, A., Schwartz, G. K., Weiss, G. J., Paz-Ares, L., Cho, D. C., Infante, J. R., Alsina, M., Gounder, M. M., Falzone, R., Harrop, J., White, A. C., Toudjarska, I., Bumcrot, D., Meyers, R. E., Hinkle, G., Svrzikapa, N., Hutabarat, R. M., Clausen, V. A., Cehelsky, J., Nochur, S. V., Gamba-Vitalo, C., Vaishnaw, A. K., Sah, D. W., Gollob, J. A., Burris, H. A., 3rd. First-in-Humans Trial of an RNA Interference Therapeutic Targeting VEGF and KSP in Cancer Patients with Liver Involvement. *Cancer Discov* (2013).

[142] Jayaraman, M., Ansell, S. M., Mui, B. L., Tam, Y. K., Chen, J., Du, X., Butler, D., Eltepu, L., Matsuda, S., Narayanannair, J. K., Rajeev, K. G., Hafez, I. M., Akinc, A., Maier, M. A., Tracy, M. A., Cullis, P. R., Madden, T. D., Manoharan, M., Hope, M. J. Maximizing the Potency of siRNA Lipid Nanoparticles for Hepatic Gene Silencing In Vivo. *Angewandte Chemie International Edition* **51**, 8529 (2012).
[143] Ambegia, E., Ansell, S., Cullis, P., Heyes, J., Palmer, L., MacLachlan, I. Stabilized plasmid-lipid particles containing PEG-diacylglycerols exhibit extended circulation lifetimes and tumor selective gene expression. *Biochim Biophys Acta* **1669**, 155 (2005).
[144] Lonez, C., Vandenbranden, M., Ruysschaert, J. M. Cationic liposomal lipids: from gene carriers to cell signaling. *Prog Lipid Res* **47**, 340 (2008).
[145] Kim, S. W. Polylysine Copolymers for Gene Delivery. *Cold Spring Harbor Protocols* **2012**, pdb.ip068619 (2012).
[146] Olins, D. E., Olins, A. L., von Hippel, P. H. Model nucleoprotein complexes: Studies on the interaction of cationic homopolypeptides with DNA. *Journal of Molecular Biology* **24**, 157 (1967).
[147] Laemmli, U. K. Characterization of DNA condensates induced by poly(ethylene oxide) and polylysine. *Proceedings of the National Academy of Sciences* **72**, 4288 (1975).
[148] Wu, G. Y., Wu, C. H. Receptor-mediated in vitro gene transformation by a soluble DNA carrier system. *J Biol Chem* **262**, 4429 (1987).
[149] Wu, G. Y., Wu, C. H. Receptor-mediated gene delivery and expression in vivo. *J Biol Chem* **263**, 14621 (1988).
[150] Choi, Y. H., Liu, F., Kim, J.-S., Choi, Y. K., Jong Sang, P., Kim, S. W. Polyethylene glycol-grafted poly-l-lysine as polymeric gene carrier. *Journal of Controlled Release* **54**, 39 (1998).
[151] Lynn, D., Anderson, D., Putnam, D., Langer, R. Accelerated Discovery of Synthetic Transfection Vectors: Parallel Synthesis and Screening of a Degradable Polymer Library. *J. Am. Chem. Soc.* **123**, 8155 (2001).
[152] Lim, Y.-b., Kim, C.-h., Kim, K., Kim, S. W., Park, J.-s. Development of a safe gene delivery system using biodegradable polymer, poly [a-(4-aminobutyl)-L-glycolic acid]. *J. Am. Chem. Soc* **122**, 6524 (2000).
[153] Lungwitz, U., Breunig, M., Blunk, T., Göpferich, A. Polyethylenimine-based non-viral gene delivery systems. *European Journal of Pharmaceutics and Biopharmaceutics* **60**, 247 (2005).
[154] Godbey, W. T., Wu, K. K., Mikos, A. G. Size matters: molecular weight affects the efficiency of poly(ethylenimine) as a gene delivery vehicle. *J Biomed Mater Res* **45**, 268 (1999).
[155] Wightman, L., Kircheis, R., Rossler, V., Carotta, S., Ruzicka, R., Kursa, M., Wagner, E. Different behavior of branched and linear polyethylenimine for gene delivery in vitro and in vivo. *J Gene Med* **3**, 362 (2001).
[156] Fischer, D., Bieber, T., Li, Y., Elsässer, H. P., Kissel, T. A novel non-viral vector for DNA delivery based on low molecular weight, branched polyethylenimine: effect of molecular weight on transfection efficiency and cytotoxicity. *Pharm Res* **16**, 1273 (1999).

[157] Goula, D., Benoist, C., Mantero, S., Merlo, G., Levi, G., Demeneix, B. A. Polyethylenimine-based intravenous delivery of transgenes to mouse lung. *Gene Ther* **5**, 1291 (1998).
[158] Bragonzi, A., Boletta, A., Biffi, A., Muggia, A., Sersale, G., Cheng, S. H., Bordignon, C., Assael, B. M., Conese, M. Comparison between cationic polymers and lipids in mediating systemic gene delivery to the lungs. *Gene Ther* **6**, 1995 (1999).
[159] Zou, S.-M., Erbacher, P., Remy, J.-S., Behr, J.-P. Systemic linear polyethylenimine (L-PEI)-mediated gene delivery in the mouse. *The Journal of Gene Medicine* **2**, 128 (2000).
[160] Kircheis, R., Wightman, L., Wagner, E. Design and gene delivery activity of modified polyethylenimines. *Advanced Drug Delivery Reviews* **53**, 341 (2001).
[161] Kircheis, R., Schuller, S., Brunner, S., Ogris, M., Heider, K. H., Zauner, W., Wagner, E. Polycation-based DNA complexes for tumor-targeted gene delivery in vivo. *J Gene Med* **1**, 111 (1999).
[162] Coll, J. L., Chollet, P., Brambilla, E., Desplanques, D., Behr, J. P., Favrot, M. In vivo delivery to tumors of DNA complexed with linear polyethylenimine. *Hum Gene Ther* **10**, 1659 (1999).
[163] Godbey, W. T., Wu, K. K., Mikos, A. G. Poly(ethylenimine)-mediated gene delivery affects endothelial cell function and viability. *Biomaterials* **22**, 471 (2001).
[164] Lv, H., Zhang, S., Wang, B., Cui, S., Yan, J. Toxicity of cationic lipids and cationic polymers in gene delivery. *J Control Release* **114**, 100 (2006).
[165] Nguyen, H. K., Lemieux, P., Vinogradov, S. V., Gebhart, C. L., Guerin, N., Paradis, G., Bronich, T. K., Alakhov, V. Y., Kabanov, A. V. Evaluation of polyether-polyethyleneimine graft copolymers as gene transfer agents. *Gene Ther* **7**, 126 (2000).
[166] Petersen, H., Fechner, P. M., Martin, A. L., Kunath, K., Stolnik, S., Roberts, C. J., Fischer, D., Davies, M. C., Kissel, T. Polyethylenimine-graft-poly(ethylene glycol) copolymers: influence of copolymer block structure on DNA complexation and biological activities as gene delivery system. *Bioconjug Chem* **13**, 845 (2002).
[167] Breunig, M., Lungwitz, U., Liebl, R., Goepferich, A. Breaking up the correlation between efficacy and toxicity for nonviral gene delivery. *Proc Natl Acad Sci USA* **104**, 14454 (2007).
[168] Thomas, M., Klibanov, A. M. Enhancing polyethylenimine's delivery of plasmid DNA into mammalian cells. *Proc Natl Acad Sci U S A* **99**, 14640 (2002).
[169] Fortune, J. A., Novobrantseva, T. I., Klibanov, A. M. Highly effective gene transfection in vivo by alkylated polyethylenimine. *J Drug Deliv* **2011**, 204058 (2011).
[170] Cherng, J.-Y., van de Wetering, P., Talsma, H., Crommelin, D. J., Hennink, W. E. Effect of size and serum proteins on transfection efficiency of poly ((2-dimethylamino) ethyl methacrylate)-plasmid nanoparticles. *Pharmaceutical Research* **13**, 1038 (1996).
[171] van de Wetering, P., Cherng, J.-Y., Talsma, H., Hennink, W. E. Relation between transfection efficiency and cytotoxicity of poly (2-(dimethylamino) ethyl methacrylate)/plasmid complexes. *Journal of Controlled Release* **49**, 59 (1997).

[172] van de Wetering, P., Cherng, J. Y., Talsma, H., Crommelin, D. J., Hennink, W. E. 2-(Dimethylamino)ethyl methacrylate based (co)polymers as gene transfer agents. *J Control Release* **53**, 145 (1998).
[173] van de Wetering, P., Schuurmans-Nieuwenbroek, N. M., Hennink, W. E., Storm, G. Comparative transfection studies of human ovarian carcinoma cells in vitro, ex vivo and in vivo with poly(2-(dimethylamino)ethyl methacrylate)-based polyplexes. *J Gene Med* **1**, 156 (1999).
[174] Verbaan, F., van Dam, I., Takakura, Y., Hashida, M., Hennink, W., Storm, G., Oussoren, C. Intravenous fate of poly(2-(dimethylamino)ethyl methacrylate)-based polyplexes. *Eur J Pharm Sci* **20**, 419 (2003).
[175] Misra, A. Challenges in Delivery of Therapeutic Genomics and Proteomics. (Elsevier Science, 2010).
[176] Schenborn, E., Goiffon, V. in Transcription Factor Protocols, Vol. 130. (ed. M. Tymms) 147 (Humana Press, 2000).
[177] Kim, T.-H., Jiang, H.-L., Jere, D., Park, I.-K., Cho, M.-H., Nah, J.-W., Choi, Y.-J., Akaike, T., Cho, C.-S. Chemical modification of chitosan as a gene carrier in vitro and in vivo. *Progress in Polymer Science* **32**, 726 (2007).
[178] Mao, S., Sun, W., Kissel, T. Chitosan-based formulations for delivery of DNA and siRNA. *Adv. Drug Deliv. Rev.* **62**, 12 (2010).
[179] Bowman, K., Leong, K. W. Chitosan nanoparticles for oral drug and gene delivery. *Int J Nanomedicine* **1**, 117 (2006).
[180] Roy, K., Mao, H. Q., Huang, S. K., Leong, K. W. Oral gene delivery with chitosan--DNA nanoparticles generates immunologic protection in a murine model of peanut allergy. *Nat Med* **5**, 387 (1999).
[181] Mellet, C. O., Fernández, J. M. G., Benito, J. M. Cyclodextrin-based gene delivery systems. *Chemical Society Reviews* **40**, 1586 (2011).
[182] Gonzalez, H., Hwang, S. J., Davis, M. New class of polymers for the delivery of macromolecular therapeutics. *Bioconjugate Chemistry* **10**, 1068 (1999).
[183] Reineke, T. M., Davis, M. E. Structural effects of carbohydrate-containing polycations on gene delivery. 1. Carbohydrate size and its distance from charge centers. *Bioconjugate Chemistry* **14**, 247 (2003).
[184] Reineke, T. M., Davis, M. E. Structural effects of carbohydrate-containing polycations on gene delivery. 2. Charge center type. *Bioconjugate Chemistry* **14**, 255 (2003).
[185] Davis, M. E., Brewster, M. E. Cyclodextrin-based pharmaceutics: past, present and future. *Nature Reviews Drug Discovery* **3**, 1023 (2004).
[186] Pun, S. H., Davis, M. E. Development of a nonviral gene delivery vehicle for systemic application. *Bioconjugate Chemistry* **13**, 630 (2002).
[187] Davis, M. E. The first targeted delivery of siRNA in humans via a self-assembling, cyclodextrin polymer-based nanoparticle: from concept to clinic. *Molecular pharmaceutics* **6**, 659 (2009).
[188] Davis, M. E., Zuckerman, J. E., Choi, C. H. J., Seligson, D., Tolcher, A., Alabi, C. A., Yen, Y., Heidel, J. D., Ribas, A. Evidence of RNAi in humans from systemically administered siRNA via targeted nanoparticles. *Nature* **464**, 1067 (2010).
[189] Haensler, J., Szoka, F. C., Jr. Polyamidoamine cascade polymers mediate efficient transfection of cells in culture. *Bioconjug Chem* **4**, 372 (1993).

[190] Tang, M. X., Redemann, C. T., Szoka, F. C. In Vitro Gene Delivery by Degraded Polyamidoamine Dendrimers. *Bioconjugate Chemistry* **7**, 703 (1996).
[191] Kukowska-Latallo, J. F., Bielinska, A. U., Johnson, J., Spindler, R., Tomalia, D. A., Baker, J. R., Jr. Efficient transfer of genetic material into mammalian cells using Starburst polyamidoamine dendrimers. *Proc Natl Acad Sci U S A* **93**, 4897 (1996).
[192] Kukowska-Latallo, J. F., Raczka, E., Quintana, A., Chen, C., Rymaszewski, M., Baker, J. R., Jr. Intravascular and endobronchial DNA delivery to murine lung tissue using a novel, nonviral vector. *Hum Gene Ther* **11**, 1385 (2000).
[193] Maruyama-Tabata, H., Harada, Y., Matsumura, T., Satoh, E., Cui, F., Iwai, M., Kita, M., Hibi, S., Imanishi, J., Sawada, T., Mazda, O. Effective suicide gene therapy in vivo by EBV-based plasmid vector coupled with polyamidoamine dendrimer. *Gene Ther* **7**, 53 (2000).
[194] Nakanishi, H., Mazda, O., Satoh, E., Asada, H., Morioka, H., Kishida, T., Nakao, M., Mizutani, Y., Kawauchi, A., Kita, M., Imanishi, J., Miki, T. Nonviral genetic transfer of Fas ligand induced significant growth suppression and apoptotic tumor cell death in prostate cancer in vivo. *Gene Ther* **10**, 434 (2003).
[195] Xu, Q., Wang, C. H., Pack, D. W. Polymeric carriers for gene delivery: chitosan and poly(amidoamine) dendrimers. *Curr Pharm Des* **16**, 2350 (2010).
[196] Heitz, F., Morris, M. C., Divita, G. Twenty years of cell-penetrating peptides: from molecular mechanisms to therapeutics. *Br J Pharmacol* **157**, 195 (2009).
[197] Vivès, E., Brodin, P., Lebleu, B. A truncated HIV-1 Tat protein basic domain rapidly translocates through the plasma membrane and accumulates in the cell nucleus. *J Biol Chem* **272**, 16010 (1997).
[198] Derossi, D., Joliot, A. H., Chassaing, G., Prochiantz, A. The third helix of the Antennapedia homeodomain translocates through biological membranes. *J Biol Chem* **269**, 10444 (1994).
[199] Wender, P. A., Mitchell, D. J., Pattabiraman, K., Pelkey, E. T., Steinman, L., Rothbard, J. B. The design, synthesis, and evaluation of molecules that enable or enhance cellular uptake: peptoid molecular transporters. *Proc Natl Acad Sci U S A* **97**, 13003 (2000).
[200] Futaki, S., Suzuki, T., Ohashi, W., Yagami, T., Tanaka, S., Ueda, K., Sugiura, Y. Arginine-rich peptides. An abundant source of membrane-permeable peptides having potential as carriers for intracellular protein delivery. *J Biol Chem* **276**, 5836 (2001).
[201] Lo, S. L., Wang, S. An endosomolytic Tat peptide produced by incorporation of histidine and cysteine residues as a nonviral vector for DNA transfection. *Biomaterials* **29**, 2408 (2008).
[202] Wyman, T. B., Nicol, F., Zelphati, O., Scaria, P., Plank, C., Szoka, F. C. Design, synthesis, and characterization of a cationic peptide that binds to nucleic acids and permeabilizes bilayers. *Biochemistry* **36**, 3008 (1997).
[203] Morris, M., Vidal, P., Chaloin, L., Heitz, F., Divita, G. A new peptide vector for efficient delivery of oligonucleotides into mammalian cells. *Nucleic Acids Research* **25**, 2730 (1997).
[204] Morris, M. C., Depollier, J., Mery, J., Heitz, F., Divita, G. A peptide carrier for the delivery of biologically active proteins into mammalian cells. *Nat Biotechnol* **19**, 1173 (2001).

[205] Pooga, M., Hällbrink, M., Zorko, M. Cell penetration by transportan. *The FASEB journal* **12**, 67 (1998).
[206] Rittner, K., Benavente, A., Bompard-Sorlet, A., Heitz, F., Divita, G., Brasseur, R., Jacobs, E. New basic membrane-destabilizing peptides for plasmid-based gene delivery in vitro and in vivo. *Mol Ther* **5**, 104 (2002).
[207] Mäe, M., Andaloussi, S. E., Lehto, T., Langel, Ü. Chemically modified cell-penetrating peptides for the delivery of nucleic acids. *Expert opinion on drug delivery* **6**, 1195 (2009).
[208] Koren, E., Torchilin, V. P. Cell-penetrating peptides: breaking through to the other side. *Trends in Molecular Medicine* (2012).
[209] Futaki, S., Ohashi, W., Suzuki, T., Niwa, M., Tanaka, S., Ueda, K., Harashima, H., Sugiura, Y. Stearylated arginine-rich peptides: a new class of transfection systems. *Bioconjugate Chemistry* **12**, 1005 (2001).
[210] Graham, F., Van der Eb, A. A new technique for the assay of infectivity of human adenovirus 5 DNA. *Virology* **52**, 456 (1973).
[211] Slowing, I. I., Vivero-Escoto, J. L., Wu, C.-W., Lin, V. S. Y. Mesoporous silica nanoparticles as controlled release drug delivery and gene transfection carriers. *Advanced Drug Delivery Reviews* **60**, 1278 (2008).
[212] Lin, W., Huang, Y.-w., Zhou, X.-D., Ma, Y. In vitro toxicity of silica nanoparticles in human lung cancer cells. *Toxicology and applied pharmacology* **217**, 252 (2006).
[213] Xie, G., Sun, J., Zhong, G., Shi, L., Zhang, D. Biodistribution and toxicity of intravenously administered silica nanoparticles in mice. *Archives of toxicology* **84**, 183 (2010).
[214] Boisselier, E., Astruc, D. Gold nanoparticles in nanomedicine: preparations, imaging, diagnostics, therapies and toxicity. *Chemical Society Reviews* **38**, 1759 (2009).
[215] Laurent, S., Forge, D., Port, M., Roch, A., Robic, C., Vander Elst, L., Muller, R. N. Magnetic iron oxide nanoparticles: synthesis, stabilization, vectorization, physicochemical characterizations, and biological applications. *Chemical reviews* **108**, 2064 (2008).
[216] Michalet, X., Pinaud, F. F., Bentolila, L. A., Tsay, J. M., Doose, S., Li, J. J., Sundaresan, G., Wu, A. M., Gambhir, S. S., Weiss, S. Quantum Dots for Live Cells, in Vivo Imaging, and Diagnostics. *Science* **307**, 538 (2005).
[217] Derfus, A. M., Chan, W. C., Bhatia, S. N. Probing the cytotoxicity of semiconductor quantum dots. *Nano letters* **4**, 11 (2004).
[218] Liu, Z., Tabakman, S., Welsher, K., Dai, H. Carbon nanotubes in biology and medicine: In vitro and in vivo detection, imaging and drug delivery. *Nano Res.* **2**, 85 (2009).
[219] Firme III, C. P., Bandaru, P. R. Toxicity issues in the application of carbon nanotubes to biological systems. *Nanomedicine: Nanotechnology, Biology and Medicine* **6**, 245 (2010).
[220] Kneuer, C., Sameti, M., Bakowsky, U., Schiestel, T., Schirra, H., Schmidt, H., Lehr, C.-M. A nonviral DNA delivery system based on surface modified silica-nanoparticles can efficiently transfect cells in vitro. *Bioconjugate Chemistry* **11**, 926 (2000).

[221] Bharali, D. J., Klejbor, I., Stachowiak, E. K., Dutta, P., Roy, I., Kaur, N., Bergey, E. J., Prasad, P. N., Stachowiak, M. K. Organically modified silica nanoparticles: a nonviral vector for in vivo gene delivery and expression in the brain. *Proceedings of the National Academy of Sciences of the United States of America* **102**, 11539 (2005).
[222] Pantarotto, D., Singh, R., McCarthy, D., Erhardt, M., Briand, J. Ä., Prato, M., Kostarelos, K., Bianco, A. Functionalized Carbon Nanotubes for Plasmid DNA Gene Delivery. *Angewandte Chemie International Edition* **43**, 5242 (2004).
[223] Singh, R., Pantarotto, D., McCarthy, D., Chaloin, O., Hoebeke, J., Partidos, C. D., Briand, J.-P., Prato, M., Bianco, A., Kostarelos, K. Binding and condensation of plasmid DNA onto functionalized carbon nanotubes: toward the construction of nanotube-based gene delivery vectors. *Journal of the American Chemical Society* **127**, 4388 (2005).
[224] Jiang, S., Eltoukhy, A. A., Love, K. T., Anderson, D. G. Lipidoid-coated Iron Oxide Nanoparticles for Efficient DNA and siRNA delivery. *Nano letters* (2013).
[225] Thomas, M., Klibanov, A. M. Conjugation to gold nanoparticles enhances polyethylenimine's transfer of plasmid DNA into mammalian cells. *Proceedings of the National Academy of Sciences* **100**, 9138 (2003).
[226] Ow Sullivan, M. M., Green, J. J., Przybycien, T. M. Development of a novel gene delivery scaffold utilizing colloidal gold-polyethylenimine conjugates for DNA condensation. *Gene Ther* **10**, 1882 (2003).
[227] Luten, J., van Nostrum, C. F., De Smedt, S. C., Hennink, W. E. Biodegradable polymers as non-viral carriers for plasmid DNA delivery. *J Control Release* **126**, 97 (2008).
[228] Potineni, A., Lynn, D. M., Langer, R., Amiji, M. M. Poly(ethylene oxide)-modified poly(beta-amino ester) nanoparticles as a pH-sensitive biodegradable system for paclitaxel delivery. *J Control Release* **86**, 223 (2003).
[229] Shenoy, D., Little, S., Langer, R., Amiji, M. Poly(ethylene oxide)-modified poly(beta-amino ester) nanoparticles as a pH-sensitive system for tumor-targeted delivery of hydrophobic drugs: part 2. In vivo distribution and tumor localization studies. *Pharm Res* **22**, 2107 (2005).
[230] Shenoy, D., Little, S., Langer, R., Amiji, M. Poly(ethylene oxide)-modified poly(beta-amino ester) nanoparticles as a pH-sensitive system for tumor-targeted delivery of hydrophobic drugs. 1. In vitro evaluations. *Mol Pharm* **2**, 357 (2005).
[231] Devalapally, H., Shenoy, D., Little, S., Langer, R., Amiji, M. Poly(ethylene oxide)-modified poly(beta-amino ester) nanoparticles as a pH-sensitive system for tumor-targeted delivery of hydrophobic drugs: part 3. Therapeutic efficacy and safety studies in ovarian cancer xenograft model. *Cancer Chemother Pharmacol* **59**, 477 (2007).
[232] Ko, J., Park, K., Kim, Y. S., Kim, M. S., Han, J. K., Kim, K., Park, R. W., Kim, I. S., Song, H. K., Lee, D. S., Kwon, I. C. Tumoral acidic extracellular pH targeting of pH-responsive MPEG-poly(beta-amino ester) block copolymer micelles for cancer therapy. *J Control Release* **123**, 109 (2007).
[233] Min, K. H., Kim, J. H., Bae, S. M., Shin, H., Kim, M. S., Park, S., Lee, H., Park, R. W., Kim, I. S., Kim, K., Kwon, I. C., Jeong, S. Y., Lee, D. S. Tumoral acidic pH-responsive MPEG-poly(beta-amino ester) polymeric micelles for cancer targeting therapy. *J Control Release* **144**, 259 (2010).

[234] Shen, Y., Tang, H., Zhan, Y., Van Kirk, E. A., Murdoch, W. J. Degradable poly(beta-amino ester) nanoparticles for cancer cytoplasmic drug delivery. *Nanomedicine* **5**, 192 (2009).
[235] Nguyen, M. K., Lee, D. S. Injectable biodegradable hydrogels. *Macromol Biosci* **10**, 563 (2010).
[236] Anderson, D. G., Tweedie, C. A., Hossain, N., Navarro, S. M., Brey, D. M., Van Vliet, K. J., Langer, R., Burdick, J. A. A combinatorial library of photocrosslinkable and degradable materials. *Advanced Materials* **18**, 2614 (2006).
[237] Brey, D. M., Erickson, I., Burdick, J. A. Influence of macromer molecular weight and chemistry on poly(beta-amino ester) network properties and initial cell interactions. *J Biomed Mater Res A* **85**, 731 (2008).
[238] Hawkins, A. M., Milbrandt, T. A., Puleo, D. A., Hilt, J. Z. Synthesis and analysis of degradation, mechanical and toxicity properties of poly(β-amino ester) degradable hydrogels. *Acta biomaterialia* (2011).
[239] Wood, K. C., Boedicker, J. Q., Lynn, D. M., Hammond, P. T. Tunable drug release from hydrolytically degradable layer-by-layer thin films. *Langmuir* **21**, 1603 (2005).
[240] Zhang, J., Fredin, N. J., Janz, J. F., Sun, B., Lynn, D. M. Structure/property relationships in erodible multilayered films: influence of polycation structure on erosion profiles and the release of anionic polyelectrolytes. *Langmuir* **22**, 239 (2006).
[241] Zhang, J., Montanez, S. I., Jewell, C. M., Lynn, D. M. Multilayered films fabricated from plasmid DNA and a side-chain functionalized poly(beta-amino ester): surface-type erosion and sequential release of multiple plasmid constructs from surfaces. *Langmuir* **23**, 11139 (2007).
[242] Su, X., Kim, B. S., Kim, S. R., Hammond, P. T., Irvine, D. J. Layer-by-layer-assembled multilayer films for transcutaneous drug and vaccine delivery. *ACS Nano* **3**, 3719 (2009).
[243] Cherng, J. Y., Lee, Y. P., Lin, C. H., Chang, K. H., Chang, W. Y., Shau, M. D. The characteristics and transfection efficiency of PEI modified by biodegradable poly(beta-amino ester). *J Mater Sci Mater Med* **21**, 1543 (2010).
[244] Lee, J. S., Green, J. J., Love, K. T., Sunshine, J., Langer, R., Anderson, D. G. Gold, poly(beta-amino ester) nanoparticles for small interfering RNA delivery. *Nano Lett* **9**, 2402 (2009).
[245] Little, S., Lynn, D., Ge, Q., Anderson, D., Puram, S. V., Chen, J., Eisen, H. N., Langer, R. Poly-beta amino ester-containing microparticles enhance the activity of nonviral genetic vaccines. *Proc Natl Acad Sci USA* **101**, 9534 (2004).
[246] Little, S. R., Lynn, D. M., Puram, S. V., Langer, R. Formulation and characterization of poly (β amino ester) microparticles for genetic vaccine .... *Journal of Controlled Release* (2005).
[247] Kargina, O. V., Mishustina, L. A., Kiselev, V. Y., Kabanov, V. A. Self-Splitted Water-Soluble Ionogenic Polymers. *Vysokomol. Soedin. Ser. A* **28**, 1139 (1986).
[248] Rao, W., Smith, D. J. Poly(Butanediol Spermate): A Hydrolytically Labile Polyester-Based Nitric Oxide Carrier. *Journal of Bioactive and Compatible Polymers* **14**, 54 (1999).

[249] Lynn, D. M., Langer, R. Degradable Poly ([beta]-amino esters): Synthesis, Characterization, and Self-Assembly with Plasmid DNA. *J. Am. Chem. Soc* **122**, 10761 (2000).
[250] Lim, Y. B., Choi, Y. H., Park, J. S. A self-destroying polycationic polymer: Biodegradable poly(4-hydroxy-L-proline ester). *Journal of the American Chemical Society* **121**, 5633 (1999).
[251] Lim, Y.-b., Kim, C.-h., Kim, K., Kim, S. W., Park, J.-s. Development of a Safe Gene Delivery System Using Biodegradable Polymer, Poly[Œ±-(4-aminobutyl)-l-glycolic acid]. *Journal of the American Chemical Society* **122**, 6524 (2000).
[252] Akinc, A., Lynn, D., Anderson, D., Langer, R. Parallel Synthesis and Biophysical Characterization of a Degradable Polymer Library for Gene Delivery. *J. Am. Chem. Soc.* **125**, 5316 (2003).
[253] Akinc, A., Langer, R. Measuring the pH environment of DNA delivered using nonviral vectors: Implications for lysosomal trafficking. *Biotechnol. Bioeng.* **78**, 503 (2002).
[254] Akinc, A., Anderson, D., Lynn, D., Langer, R. Synthesis of Poly(β-amino ester)s Optimized for Highly Effective Gene Delivery. *Bioconjugate Chem.* **14**, 979 (2003).
[255] Anderson, D. G., Lynn, D. M., Langer, R. Semi-Automated Synthesis and Screening of a Large Library of Degradable Cationic Polymers for Gene Delivery. *Angew. Chem. Int. Ed.* **42**, 3153 (2003).
[256] Anderson, D., Akinc, A., Hossain, N., Langer, R. Structure/property studies of polymeric gene delivery using a library of poly(beta-amino esters). *Mol Ther* **11**, 426 (2005).
[257] Anderson, D. G., Peng, W., Akinc, A., Hossain, N., Kohn, A., Padera, R., Langer, R., Sawicki, J. A. A polymer library approach to suicide gene therapy for cancer. *Proc. Natl. Acad. Sci. USA* **101**, 16028 (2004).
[258] Green, J. J., Zugates, G. T., Tedford, N. C., Huang, Y., Griffith, L. G., Lauffenburger, D. A., Sawicki, J. A., Langer, R., Anderson, D. G. Combinatorial modification of degradable polymers enables transfection of human cells comparable to adenovirus. *Adv. Mater.* **19**, 2836 (2007).
[259] Zugates, G., Peng, W., Zumbuehl, A., Jhunjhunwala, S., Huang, Y., Langer, R., Sawicki, J., Anderson, D. Rapid Optimization of Gene Delivery by Parallel End-modification of Poly(β-amino ester)s. *Mol Ther* **15**, 1306 (2007).
[260] Zugates, G., Tedford, N., Zumbuehl, A., Jhunjhunwala, S., Kang, C., Griffith, L., Lauffenburger, D., Langer, R., Anderson, D. Gene Delivery Properties of End-Modified Poly(β-amino ester)s. *Bioconjugate Chem.* **18**, 1887 (2007).
[261] Green, J. J., Langer, R., Anderson, D. G. A Combinatorial Polymer Library Approach Yields Insight into Nonviral Gene Delivery. *Acc Chem Res* **41**, 749 (2008).
[262] Sunshine, J., Green, J. J., Mahon, K. P., Yang, F., Eltoukhy, A. A., Nguyen, D. N., Langer, R., Anderson, D. G. Small-Molecule End-Groups of Linear Polymer Determine Cell-type Gene-Delivery Efficacy. *Adv. Mater.* **21**, 4947 (2009).
[263] Yang, F., Green, J. J., Dinio, T., Keung, L., Cho, S. W., Park, H., Langer, R., Anderson, D. G. Gene delivery to human adult and embryonic cell-derived stem cells using biodegradable nanoparticulate polymeric vectors. *Gene Ther* **16**, 533 (2009).
[264] Yang, F., Cho, S. W., Son, S. M., Bogatyrev, S. R., Singh, D., Green, J., Mei, Y., Park, S., Bhang, S. H., Kim, B. S., Langer, R., Anderson, D. Genetic engineering of

human stem cells for enhanced angiogenesis using biodegradable polymeric nanoparticles. *Proc. Natl. Acad. Sci. USA* **107**, 3317 (2010).
[265] Bhise, N. S., Gray, R. S., Sunshine, J. C., Htet, S., Ewald, A. J., Green, J. J. The relationship between terminal functionalization and molecular weight of a gene delivery polymer and transfection efficacy in mammary epithelial 2-D cultures and 3-D organotypic cultures. *Biomaterials* **31**, 8088 (2010).
[266] Shmueli, R. B., Sunshine, J. C., Xu, Z., Duh, E. J., Green, J. J. Gene delivery nanoparticles specific for human microvasculature and macrovasculature. *Nanomedicine: Nanotechnology, Biology and Medicine* **8**, 1200 (2012).
[267] Tzeng, S. Y., Guerrero-Cazares, H., Martinez, E. E., Sunshine, J. C., Quinones-Hinojosa, A., Green, J. J. Non-viral gene delivery nanoparticles based on poly(beta-amino esters) for treatment of glioblastoma. *Biomaterials* **32**, 5402 (2011).
[268] Tzeng, S. Y., Green, J. J. Subtle Changes to Polymer Structure and Degradation Mechanism Enable Highly Effective Nanoparticles for siRNA and DNA Delivery to Human Brain Cancer. *Advanced Healthcare Materials* **2**, 468 (2013).
[269] Huang, Y. H., Zugates, G. T., Peng, W., Holtz, D., Dunton, C., Green, J. J., Hossain, N., Chernick, M. R., Padera, R. F., Jr., Langer, R., Anderson, D. G., Sawicki, J. A. Nanoparticle-delivered suicide gene therapy effectively reduces ovarian tumor burden in mice. *Cancer Res* **69**, 6184 (2009).
[270] Ruoslahti, E., Bhatia, S. N., Sailor, M. J. Targeting of drugs and nanoparticles to tumors. *The Journal of Cell Biology* **188**, 759 (2010).
[271] Zugates, G., Anderson, D., Little, S., Lawhorn, I., Langer, R. Synthesis of Poly(β-amino ester)s with Thiol-Reactive Side Chains for DNA Delivery. *J. Am. Chem. Soc.* **128**, 12726 (2006).
[272] Green, J. J., Chiu, E., Leshchiner, E. S., Shi, J., Langer, R., Anderson, D. G. Electrostatic ligand coatings of nanoparticles enable ligand-specific gene delivery to human primary cells. *Nano Lett* **7**, 874 (2007).
[273] Harris, T. J., Green, J. J., Fung, P. W., Langer, R., Anderson, D. G., Bhatia, S. N. Tissue-specific gene delivery via nanoparticle coating. *Biomaterials* **31**, 998 (2010).
[274] Shmueli, R. B., Anderson, D. G., Green, J. J. Electrostatic surface modifications to improve gene delivery. *Expert opinion on drug delivery* **7**, 535 (2010).

3 DEVELOPMENT OF DEGRADABLE HYDROPHOBIC POLY(BETA-AMINO ESTER) TERPOLYMERS FOR ENHANCED GENE DELIVERY POTENCY AND NANOPARTICLE STABILITY*

3.1 INTRODUCTION

Gene therapy is a promising treatment strategy for a variety of inherited and acquired diseases, but safe and efficient delivery remains a challenge. Though gene therapy mediated by viral vectors has recently made great clinical progress, limitations associated with their use persist, such as the possibility of adverse immune reactions, the difficulty of repeat dosing, and small DNA loading capacities.[1, 2] Non-viral vectors, meanwhile, continue to suffer from generally low DNA delivery efficiency.[3] Nonetheless, the diversity of synthetic materials offers potential for the identification and incorporation of functional motifs that confer not only efficient gene transfection, but also formulation stability and biocompatibility.[4]

Poly(β-amino ester)s (PBAEs) are a class of cationic gene delivery polymers that have been studied pre-clinically for applications including local cancer therapy and the genetic modification of stem cells for treatment of ischemia[5, 6]. Synthesis is relatively simple and versatile, and is based on the Michael-type conjugate addition

* This chapter has been published as Eltoukhy, A. A., Chen, D., Alabi, C. A., Langer, R., Anderson, D. G. Degradable terpolymers with alkyl side chains demonstrate enhanced gene delivery and nanoparticle stability. *Adv. Mater.* **25**, 1487 (2013).

of a primary or secondary amine to a diacrylate. Using this approach, combinatorial library synthesis and high-throughput screening methods have been developed to identify polymers that deliver DNA with high efficiency and low cytotoxicity[7-9]. Through these experiments, structural features associated with highly active gene delivery polymers have emerged, such as the presence of hydroxyl groups in the side chains and the conjugation of certain primary amines to the chain ends[10-13]. In addition to high transfection efficiency, the degradability of the polyester backbone offers the possibility of reduced toxicity and rapid clearance, a feature that distinguishes PBAEs from polyethylenimine (PEI), the most widely used gene delivery polymer[14].

Cationic polymers can form polymer-DNA polyplexes that may aggregate under physiological conditions[15, 16]. This potential aggregation in the blood represents a serious barrier to the systemic delivery of nucleic acids, since large aggregates can in some cases lead to embolism or otherwise may be quickly cleared by the reticuloendothelial system[16, 17]. Colloidal stability is a complex phenomenon influenced by many factors including concentration, surface charge, pH, ionic strength, and the presence of serum proteins, but a common approach to improve formulation stability is to introduce a polymer shield comprising polyethyleneglycol (PEG), poloxamers, or other non-fouling polymers[18]. Although attachment of PEG can be covalent or non-covalent, the latter may be preferable to avoid potential issues resulting from direct PEGylation of gene delivery polymers, such as impaired DNA condensation and decreased uptake[19, 20]. For nanoparticles with sufficiently hydrophobic surfaces, one simple non-covalent approach entails coating the

particles with PEGylated phospholipid conjugates[21]. Therefore, we hypothesized that the inclusion of long, linear alkanes in PBAE side chains might facilitate non-covalent, hydrophobic interaction with PEG-lipid conjugates, resulting in stable particle formulations upon nanoprecipitation with DNA at high concentration. Because the modification of cationic polymers with hydrophobic groups has been reported to increase the physical encapsulation of nucleic acids, promote cellular adsorption, and reduce the positive surface charge associated with cytotoxicity and aggregation, we further hypothesized that hydrophobic PBAE terpolymers might deliver DNA more efficiently than PBAEs lacking alkyl side chains and might condense DNA into polyplexes with greater aggregation resistance[22-24].

3.2 Materials and Methods

3.2.1 Materials

Diacrylate and amine monomers, as well as end-capping reagents, were purchased from Sigma-Aldrich (St. Louis, MO, USA), Alfa Aesar (Ward Hill, MA, USA), TCI America (Portland, OR, USA), and Monomer-Polymer & Dajac Labs (Trevose, PA, USA). $(PEO)_4$-*bis*-amine ("122") was acquired from Molecular Biosciences (Boulder, CO, USA). All reagents were used without further purification. Plasmid DNA encoding green fluorescent protein (gWiz-GFP) was purchased from Aldevron (Fargo, ND, USA). PEG-lipid conjugate (1,2-distearoyl-*sn*-glycero-3-phosphoethanolamine-N-[methoxy(polyethylene glycol)-5000], or 18:0 PEG5000 PE) was obtained from Avanti Polar Lipids (Alabaster, AL, USA). Slide-A-Lyzer MINI dialysis devices (20 kDa MWCO, 0.1ml) were purchased from Pierce Biotechnology

(Rockford, IL, USA). HeLa cells (ATCC, Manassas, VA, USA) were cultured in DMEM (Invitrogen, Carlsbad, CA, USA) supplemented with 10% fetal bovine serum (Invitrogen).

3.2.2 Polymer synthesis

The monomers were dissolved in DMSO (Sigma-Aldrich) to a concentration of 200 mg ml^{-1}. Alkylamines generally required heating to 60°C to enable complete dissolution. Library scale reactions were performed in glass shell vials (1 mL) with polyethylene snap caps (Waters, Milford, MA, USA) in a 96-well reaction block (Symyx, Santa Clara, CA, USA). To each vial equipped with stir bar, diacrylate monomer, hydrophobic amine monomer, and hydrophilic amine monomer were added such that their molar ratio was 1.2:0.3:0.7 and the total mass of monomers was 100 mg. After heating and stirring at 90°C for 48 h, the reactions were allowed to cool to RT, and to each vial, end-capping amine (0.2 mmol in 0.5 mL DMSO) was added. The reactions were stirred at 40°C for 24 h, divided into aliquots, and then stored frozen at -20°C. Top-performing polymers were resynthesized by scaling up the reactions tenfold.

3.2.3 Analytical Gel Permeation Chromatography (GPC)

GPC was performed using a Waters system equipped with a 2400 differential refractometer, 515 pump, and 717-plus autosampler. The flow rate was 1 ml min^{-1} and the mobile phase was tetrahydrofuran (THF). The Styragel columns (Waters) and detector were thermostated at 35ºC. Linear polystyrene standards were used for calibration.

3.2.4 Preparative GPC/HPLC

DD24-C12-122 was subjected to GPC using a Phenogel 5μm MXL gel filtration column (300 mm x 7.8 mm, Phenomenex, P/No. 00H-3087-KO) with THF as the mobile phase at a flow rate of 1 ml min^{-1}. The separation was performed on a 1200 Series Agilent HPLC system equipped with a UV diode array detector and a 1260 Infinity analytical scale fraction collector. The column compartment was kept at 40°C during fractionation. Based on the absorption of the polymer at 260 nm (**Fig. S2**), polymer was collected between 5.2 and 7.7 min. The fractionated polymer was transferred to a tared vial and dried until further analysis.

3.2.5 NMR

The HPLC-purified DD24-C12-122 polymer, along with the monomers and end-capping reagent, was characterized on a Varian mercury spectrometer by ^{1}H-NMR spectroscopy (500 MHz, DMSO-d_6).

3.2.6 Transfection experiments

One day before transfection, 12,500 HeLa cells (100 μl) were seeded into each well of a 96-well polystyrene tissue culture plate. In a typical example, for a 150 ng/well DNA dose, gWiz-GFP plasmid DNA (5 mg ml^{-1}) was diluted to 15 μg ml^{-1} in 25 mM sodium acetate (NaOAc) buffer at pH 5.2. Polymers (100 mg ml^{-1}) were thawed immediately prior to transfection and diluted in NaOAc buffer to a concentration of 300 μg ml^{-1} (20:1 w/w polymer:DNA). To form DNA-polymer nanoparticles, polymer solution (25 μl) was added to DNA (25 μl) in a half-area 96-well plate, mixed by repeated pipetting using a multichannel pipette, and allowed to

incubate for 10 min at room temperature. Polymer-DNA complexes (30 μl) were then gently mixed with fresh medium (195 μl) pre-warmed to 37°C. Conditioned medium was removed using a 12-channel aspirating wand and replaced with the complexes diluted in medium (150 μl). Following a 4-h incubation, complexes were removed with the aid of a multi-channel aspiration wand and replaced with fresh medium (100 μl). Lipofectamine 2000 (Invitrogen) was used according to the protocol provided by the vendor.

3.2.7 Fluorescence-activated cell sorting (FACS)

GFP expression was assessed 48 h after transfection. After aspirating conditioned medium, cells were washed with PBS and detached with 0.25% trypsin-EDTA (25 μl, Invitrogen). FACS running buffer (50 μl), consisting of 98% PBS and 2% FBS, was added to each well. Cells were mixed thoroughly and then transferred to a 96-well round-bottom plate. GFP expression was measured using FACS on a BD LSR II (Becton Dickinson, San Jose, CA, USA). To determine the viabilities of treated cells relative to non-treated control cells, propidium iodide stain (Invitrogen) was added to the FACS buffer (1:200 v/v). The relative viability was calculated as the ratio of live treated cells per well to the mean number of live non-treated cells per well. 2D gating was used to separate increased auto-fluorescence signals from increased GFP signals to more accurately count positively expressing cells. Gating and analysis were performed using FlowJo v8.8 software (TreeStar, Ashland, OR, USA).

3.2.8 *Dye exclusion assay*

A working solution of PicoGreen was prepared by diluting 80 μl of stock solution in 15.92 ml NaOAc buffer. In each well of a 96-well plate, 50 μl of polymer at 0.6, 1.2, or 2.4 mg ml^{-1} in NaOAc buffer was added to 50 μL of DNA at 0.06 mg ml^{-1} in NaOAc buffer. After 5 min, 100 μl of PicoGreen working solution was added to the complexes. After an additional 5 min incubation, 30 μl was transferred to 200 μl of 10% serum-containing medium in a black 96-well assay plate. The fluorescence was then measured on a Tecan Infinite M1000 plate reader using the FITC filter set (excitation 485 nm, emission 535 nm). The reduction in relative fluorescence (RF), or the relative encapsulation efficiency, was calculated using the relationship $(F_{DNA}-F_{sample})/(F_{DNA}-F_{blank})$, where F_{sample} is the fluorescence of the polymer–DNA–PicoGreen sample, F_{DNA} is the fluorescence of DNA–PicoGreen (no polymer), and F_{blank} is the fluorescence of a sample with no polymer or DNA (only PicoGreen).

3.2.9 *Gel electrophoresis*

Polyplexes were formed by repeatedly mixing 25 μl of polymer (0.04, 0.2, or 0.8 mg ml^{-1} in NaoAc buffer) with 25 μl of plasmid DNA (0.04 mg ml^{-1} gWiz-GFP in NaOAc buffer). After 10 min incubation at RT, 10 μl of each sample (~200 ng total DNA) was loaded into each lane of a pre-cast 0.8% agarose E-gel (Invitrogen) stained with ethidium bromide. Control lanes were loaded with 200 ng of free control pDNA and ~5 μl of TrackIt 1 Kb Plus DNA ladder (Invitrogen). The gel was run using the E-gel electrophoresis system (Invitrogen) for 30 min at RT, and the bands were visualized with a gel imager.

3.2.10 Particle formulation with PEG-lipid at high DNA concentration

Polymer in DMSO (100 mg ml^{-1}) and 18:0 PEG5000 PE in ethanol (10 mg ml^{-1}) were co-dissolved in acetonitrile to yield final concentrations of 8 mg ml^{-1} and 10 mol%, respectively. gWiz-GFP pDNA (5 mg ml^{-1}) was diluted to 0.4 mg ml^{-1} in 25 mM NaOAc buffer. The polymer and PEG-lipid in acetonitrile (25 µl) was then added to DNA (25 µl) and mixed by repeated pipetting. After incubation for 10 min, the formulations were diluted in PBS (50 µl) and dialyzed against PBS (3 l) for 3 h at RT.

3.2.11 Dynamic light scattering (DLS) measurements

Particle sizes and ζ potentials were measured using a ZetaPALS DLS detector (Brookhaven Instruments Corp., Holtsville, NY, USA, 15-mW laser, incident beam 676 nm). Correlation functions were collected at a scattering angle of 90°, and particle sizes were obtained from the MAS option of BIC's particle sizing software (v. 2.30) using the viscosity and refractive index of water at 25°C. Particle sizes are expressed as effective diameters (z-average or hydrodynamic diameters) calculated using the Stokes-Einstein relationship from the diffusion coefficient obtained by cumulant analysis. Average electrophoretic mobilities were measured at 25°C using BIC PALS ζ-potential analysis software, and ζ-potentials were calculated using the Smoluchowski model for aqueous suspensions. For polyplex sizing, particles were prepared in NaOAc buffer as for DNA transfection, except volumes were scaled up by a factor of five. Once formed in NaOAc buffer, complexes were diluted fourfold in either additional NaOAc buffer or PBS and then sized at the indicated times. For DLS measurements of particles prepared by nanoprecipitation, particles (either freshly prepared or dialyzed) were diluted 100-fold in NaOAc buffer or PBS as indicated.

3.3 Results and Discussion

3.3.1 PBAE terpolymer library synthesis and screening

In this study, we synthesized random PBAE terpolymers by step-growth polymerization of three starting monomers: a diacrylate, a hydrophobic alkylamine, and a comparatively hydrophilic amine. Previous work has shown the importance of terminal amine groups[11, 12]. Therefore, we used a two-step reaction scheme involving co-polymerization of the amine monomers with excess diacrylate to yield acrylate-terminated base polymer, followed by reaction with excess diamine to produce amine end-modified PBAE terpolymer (Figure 3.1a). Because it is not easily predicted which PBAEs would benefit from the inclusion of alkyl side chains, we used combinatorial library synthesis and screening as a tool to accelerate their development. Our initial library (Figure 3.1b) consisted of 80 amine-end modified PBAE terpolymers synthesized using 8 diacrylates, 10 hydrophilic amines, one hydrophobic amine (dodecylamine), and one end-capping diamine ("122"). Based on pilot studies, we chose a monomer molar feed ratio of 1.2:0.7:0.3 diacrylate:hydrophilic amine:hydrophobic amine for the polymerization, and the reactions were carried out in DMSO. Under these conditions, eight of the 80 polymers precipitated out of reaction, while the remaining library members were soluble.

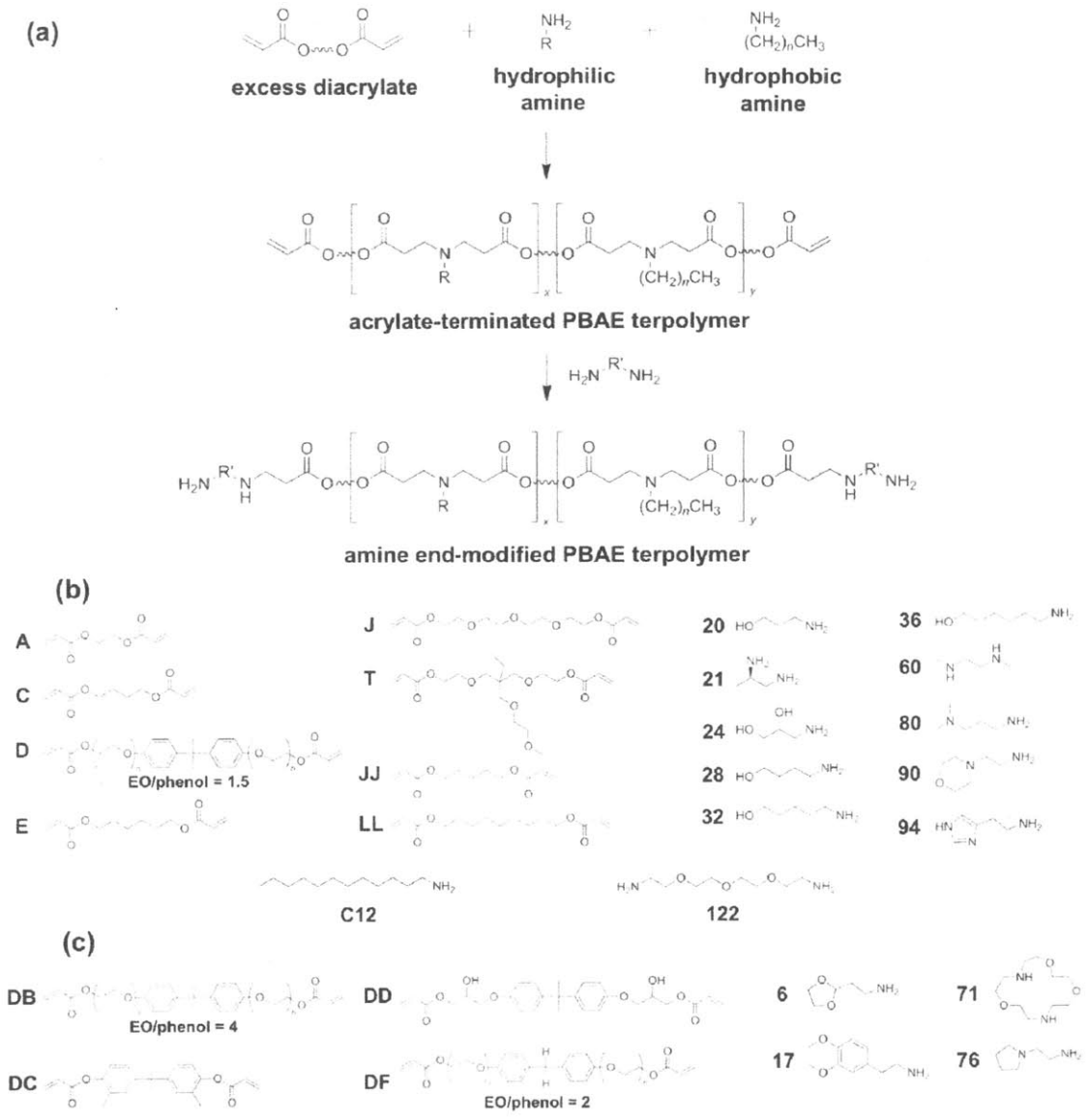

Figure 3.1 Synthetic scheme and monomers for a library of hydrophobic, amine end-modfied PBAE terpolymers
a) Two-step synthesis of hydrophobic, amine end-modified poly(β-amino ester) (PBAE) terpolymers. **b)** Structures of diacrylates (A-LL), hydrophilic amines (20-94), hydrophobic amine (C12), and end-capping diamine (122) used for the synthesis of the initial screening library. **c)** Additional monomers used to synthesize the second screening library. ("EO" = ethylene oxide.)

Using these 72 polymers, we formed complexes with GFP-encoding plasmid DNA and incubated them with cultured HeLa cells in serum-containing growth medium for 4 h. As a screen for transfection efficiency, we performed fluorescence-

activated cell sorting (FACS) 48 h later to quantify the proportion of cells expressing GFP.

As shown in the heat map (Figure 3.2a), the top five PBAE terpolymers transfected over 70% of HeLa cells, and four of these five, D90-C12-122, D60-C12-122, D21-C12-122, and D24-C12-122, shared a common diacrylate structure based on bisphenol A ethoxylate ("D"). The top two polymers from this screen outperformed one of the best previously identified PBAEs lacking alkyl side chains, C32-122, and rivaled the commercially available lipid reagent Lipofectamine 2000 in transfection efficiency (Figure 3.2b).

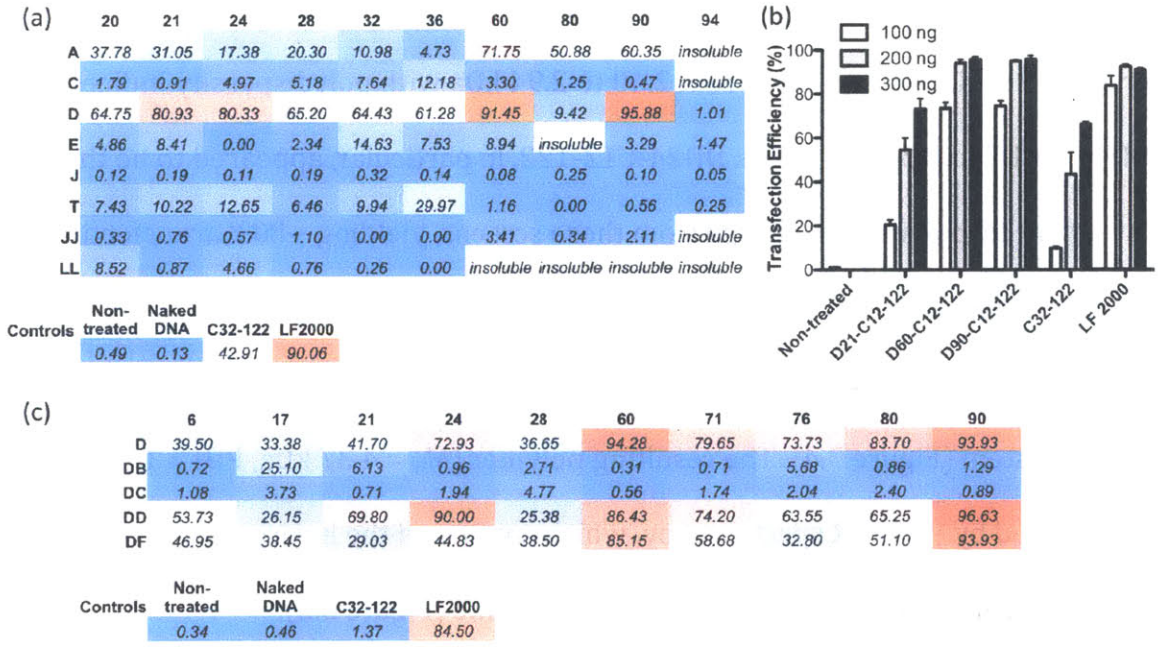

Figure 3.2 Development of hydrophobic PBAE terpolymers with high DNA transfection potency
a) Heat map of DNA transfection efficiencies of HeLa cells with the initial terpolymer library (300 ng DNA/well; 20:1 polymer:DNA w/w), as determined by FACS analysis. **b)** Transfection of HeLa cells with lead polymers from the initial library. **c)** Heat map of HeLa transfection efficiencies with the second, focused library (150 ng DNA/well).

To investigate the structural space surrounding these polymers, we synthesized a second library of hydrophobic PBAE terpolymers focused on bisphenol diacrylate monomers (Figure 3.1c). When we screened this set of polymers for transfection efficiency at half the DNA dose used in the first library, five polymers emerged in addition to D60-C12-122 and D90-C12-122 that transfected HeLa cells with greater than 85% efficiency (Figure 3.2c). After re-synthesizing these polymers on a larger scale, and transfecting cells at reduced DNA doses, we observed that these five polymers, based on DD24, DD90, DD60, DF90, and DF60, exhibited transfection potencies in HeLa cells superior to Lipofectamine 2000 (Figure 3.3a-b). These polymers were generally short, ranging in weight-average molecular weight (M_w) from 2.40 to 2.94 kDa with polydispersity indices (PDI) from 1.7 to 2.3 (Table 3.1). DD24-C12-122, in particular, appeared to be the most potent terpolymer to emerge from these screens, yielding ~80% transfection efficiency at the 50 ng dose without producing significant toxicity (Figure 3.3c). This polymer was purified by preparative gel permeation chromatography (GPC) using an HPLC system (Figure 3.4). The resulting polymer (M_w = 4.37 kDa, PDI = 1.43) was characterized by ^{1}H-NMR spectroscopy, which confirmed the incorporation of the hydrophobic amine as well as the end-capping amine (Figure 3.5).

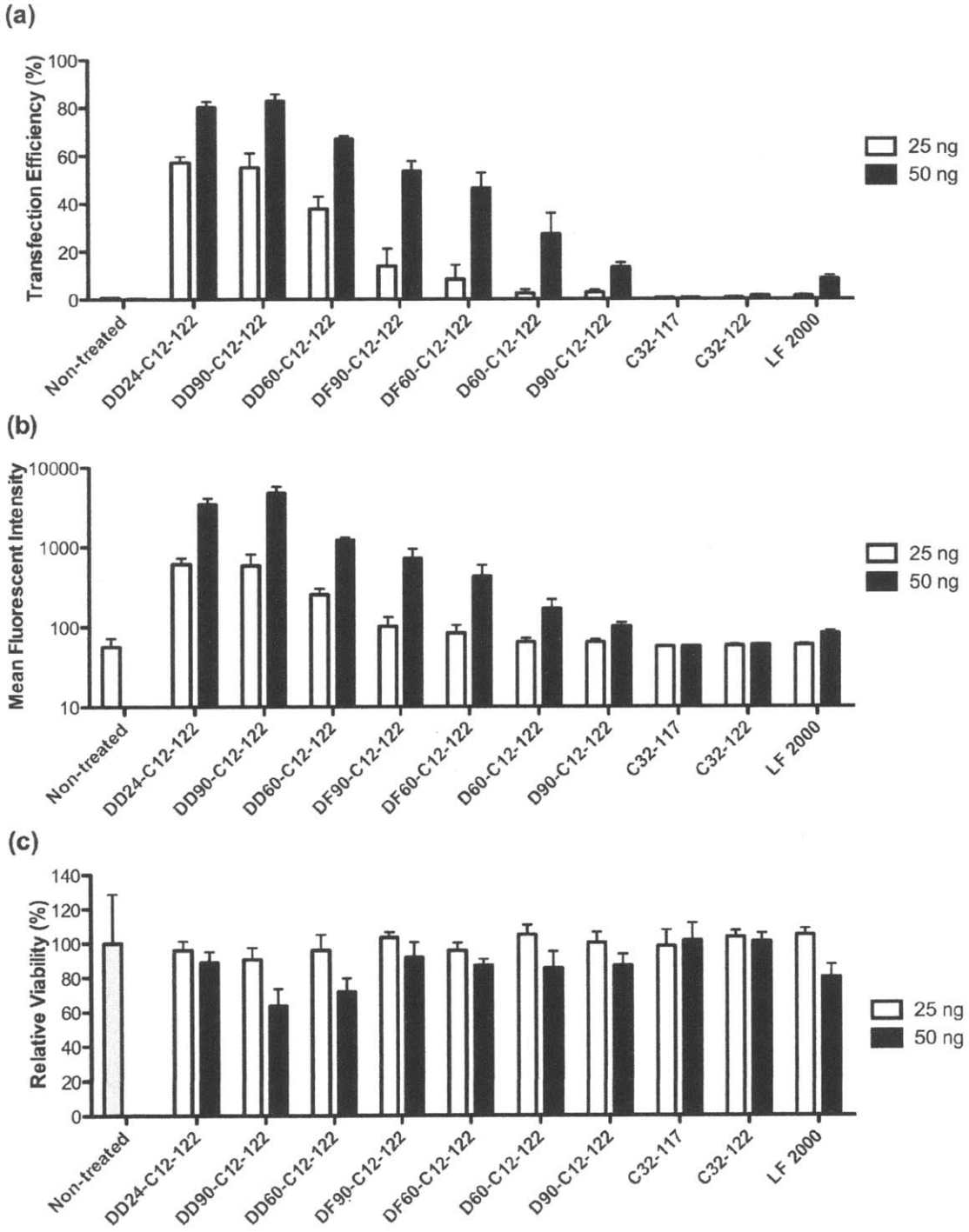

Figure 3.3 Transfection performance of lead PBAE terpolymers at reduced DNA doses in HeLa cells

a) DNA transfection efficiencies, **b)** geometric mean fluorescent intensities, and **c)** relative viabilities of HeLa cells after treatment with the top PBAE terpolymers at reduced DNA doses.

Polymer	M_w (Da)	M_n (Da)	PDI
D60-C12-122	2400	1167	2.057
D90-C12-122	2689	1356	1.983
DD24-C12-122	2891	1622	1.782
DD60-C12-122	2375	1381	1.712
DD90-C12-122	2811	1553	1.810
DF60-C12-122	2713	1176	2.307
DF90-C12-122	2939	1315	2.235

Table 3.1 MW of top-performing PBAE terpolymers
GPC analysis of top-performing PBAE terpolymers. M_w = weight-average molecular weight, M_n = number-average molecular weight, PDI = polydispersity index = M_w/M_n.

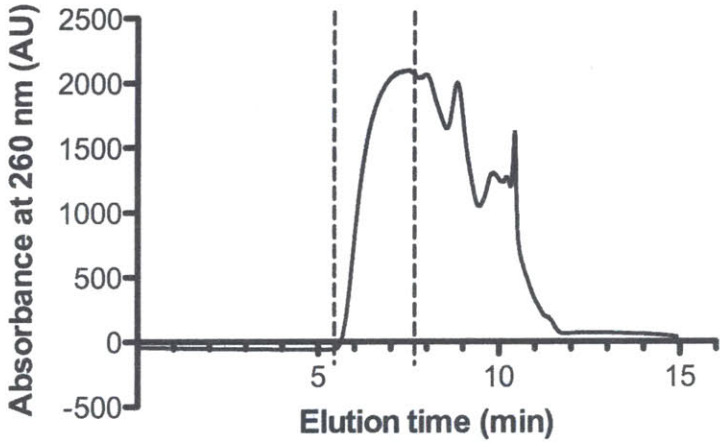

Figure 3.4 HPLC/SEC purification of DD24-C12-122
An example chromatogram showing the elution of DD24-C12-122 polymer from the GPC column. Using a preparative HPLC system, eluted polymer was collected between 5.2 and 7.7 min.

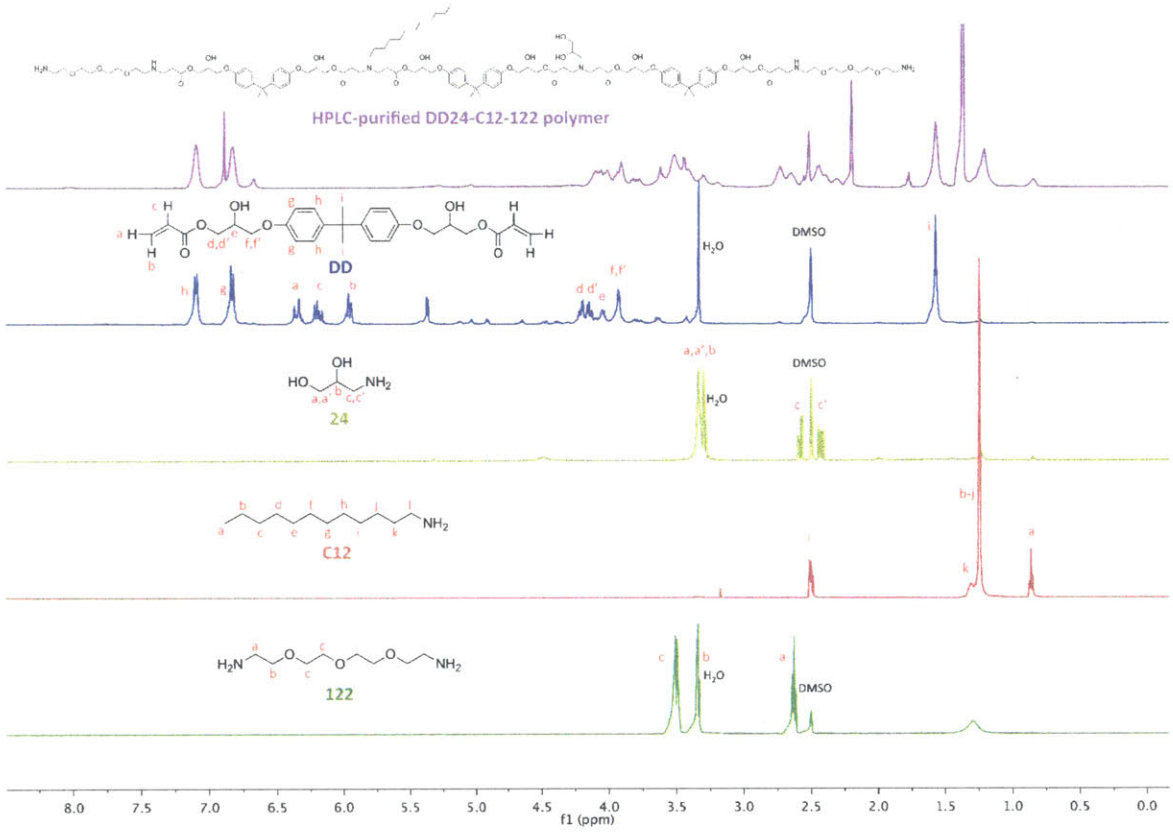

Figure 3.5 ^{1}H NMR spectra of DD24-12-122 and monomers
^{1}H NMR spectrum (500 MHz, DMSO-d_6) of HPLC-purified DD24-C12-122 polymer (top), compared with the spectra for the monomers (DD, 24, C12) and the end-capping reagent (122). The structure of a representative DD24-C12-122 oligomer is shown. The disappearance of the acrylate peaks (a-c for monomer DD) in the polymer spectrum suggests that amine end-capped polymer was successfully formed from acrylate-terminated base polymer.

3.3.2 Effect of alkyl side chain content on PBAE polyplex stability and transfection

When we used dynamic light scattering (DLS) measurements to compare the stabilities of D60-C12-122, D90-C12-122, and C32-122 polyplexes formed at low DNA concentration, we observed that all three polymers formed stable, sub-100 nm complexes with plasmid DNA under conditions of reduced pH and low ionic strength (Figure 3.6a). However, when the polyplexes were diluted in phosphate-buffered saline (PBS) at physiological pH and ionic strength, only the complexes formed from

the PBAE terpolymers remained stable, with effective diameters below 100 nm (Figure 3.6b).

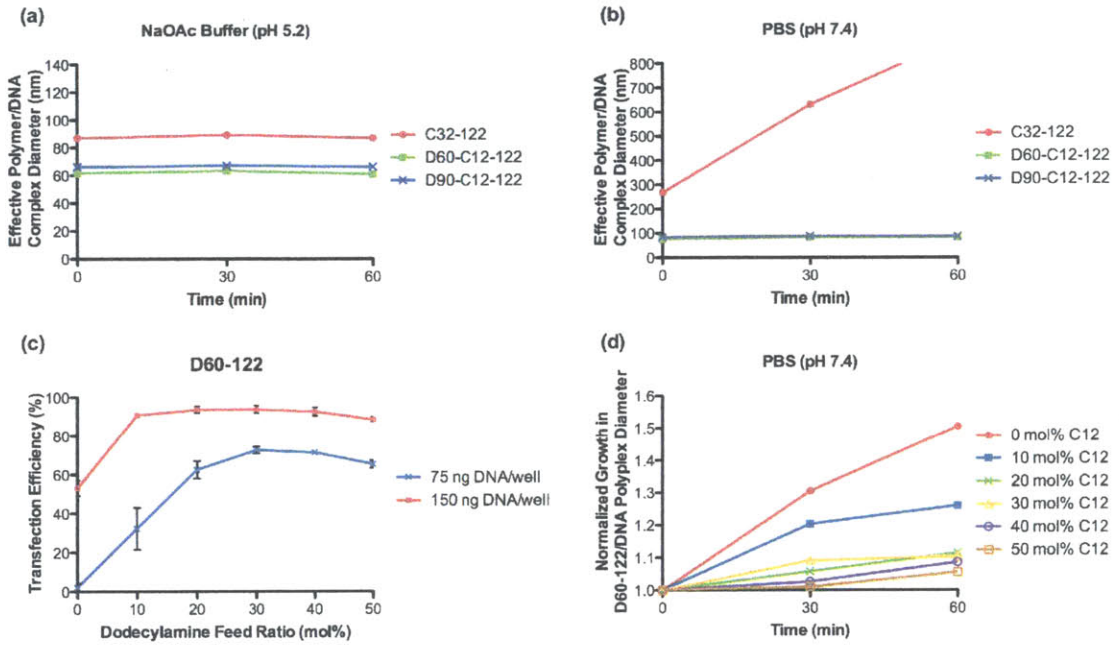

Figure 3.6 Effect of alkyl side chain content on PBAE polyplex stability and transfection
a-b) Stabilities of polyplexes formed from C32-122, D60-C12-122, and D90-C12-122 after self-assembly in sodium acetate (NaOAc) buffer at pH 5.2 or after dilution in phosphate-buffered saline (PBS) at pH 7.4. Polyplexes were formed at low DNA concentration (0.03 mg ml^{-1}) with a polymer:DNA w/w ratio of 20:1. **c)** HeLa transfection efficiencies and **d)** polyplex stabilities of D60-122 polymers synthesized with varying dodecylamine molar feed ratios.

To examine the effect of alkyl side chain content on PBAE terpolymer transfection efficiency and complex stability in greater depth, we synthesized D60-C12-122 using a range of molar feed ratios for which the dodecylamine (C12) feed varied from 0 to 50 mol% of the total amine feed, while the diacrylate:amine ratio was kept constant at 1.2:1.0. An increase in the alkylamine feed ratio up to 30 mol% C12 generally corresponded to an increase in transfection potency in HeLa cells, with a rough plateau in efficiency between 30 and 50 mol% C12 (Figure 3.6c).

Interestingly, the alkylamine feed ratio also appeared to correlate positively with polyplex stability in PBS (Figure 3.6d). One hour after dilution in PBS, polyplexes formed from D60-122 polymer lacking alkyl side chains grew 50% in diameter, in contrast to <10% growth for those formed from D60-122 terpolymers synthesized with C12 feed ratios at or above 20 mol%.

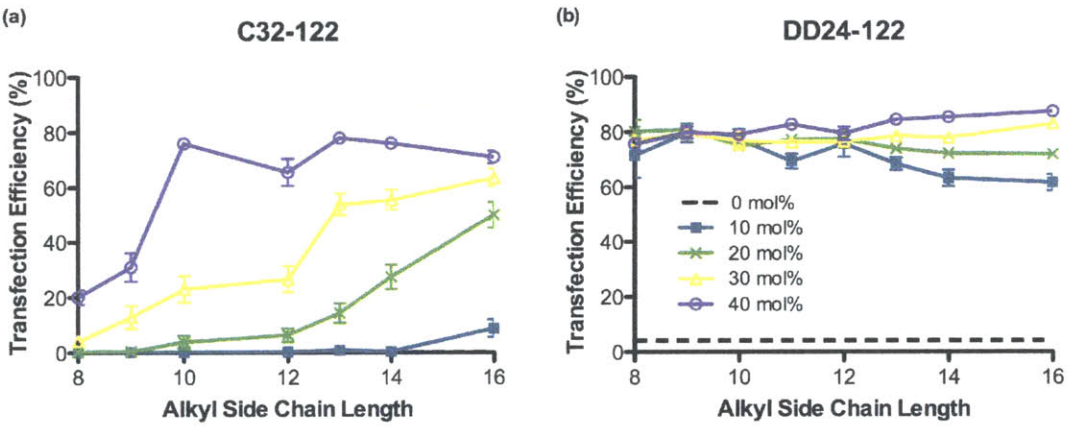

Figure 3.7 Effect of alkyl side chain length and content on PBAE transfection efficiency
HeLa transfection efficiencies of C32-122 **(a)** and DD24-122 **(b)** polymers (100 ng DNA/well) synthesized with varying chain lengths and molar feed ratios of alkylamine. At these doses, C32-122 and DD24-122 synthesized with 0 mol% alkylamine yielded transfection efficiencies of 0.2% and 4.2%, respectively.

To determine how the alkyl side chain length affects the gene delivery efficiency of PBAE terpolymers, we synthesized C32-122 and DD24-122 using alkylamines ranging from 8 to 16 carbons in length. We also varied the alkylamine molar feed from 0 to 40 mol% of the total amine feed, with the diacrylate:amine molar ratio fixed at 1.2:1.0. We observed a positive association between the alkyl side chain length of C32-122 terpolymers and transfection efficiency of HeLa cells (Figure 3.7a). As was true for D60-122, there was also a positive correlation between alkylamine feed ratio and transfection activity of the C32-122 terpolymers.

At this DNA dose, though, varying the alkyl side chain length and content of DD24-122 terpolymers did not yield much variation in observed transfection efficiencies of HeLa cells (Figure 3.7b). Nonetheless, for both C32-122 and DD24-122, the best-performing hydrophobic terpolymers produced a marked enhancement in transfection activity relative to the polymers synthesized without alkylamine (C32-122: 0.22% vs. 78.1%; DD24-122: 4.2% vs. 87.5%).

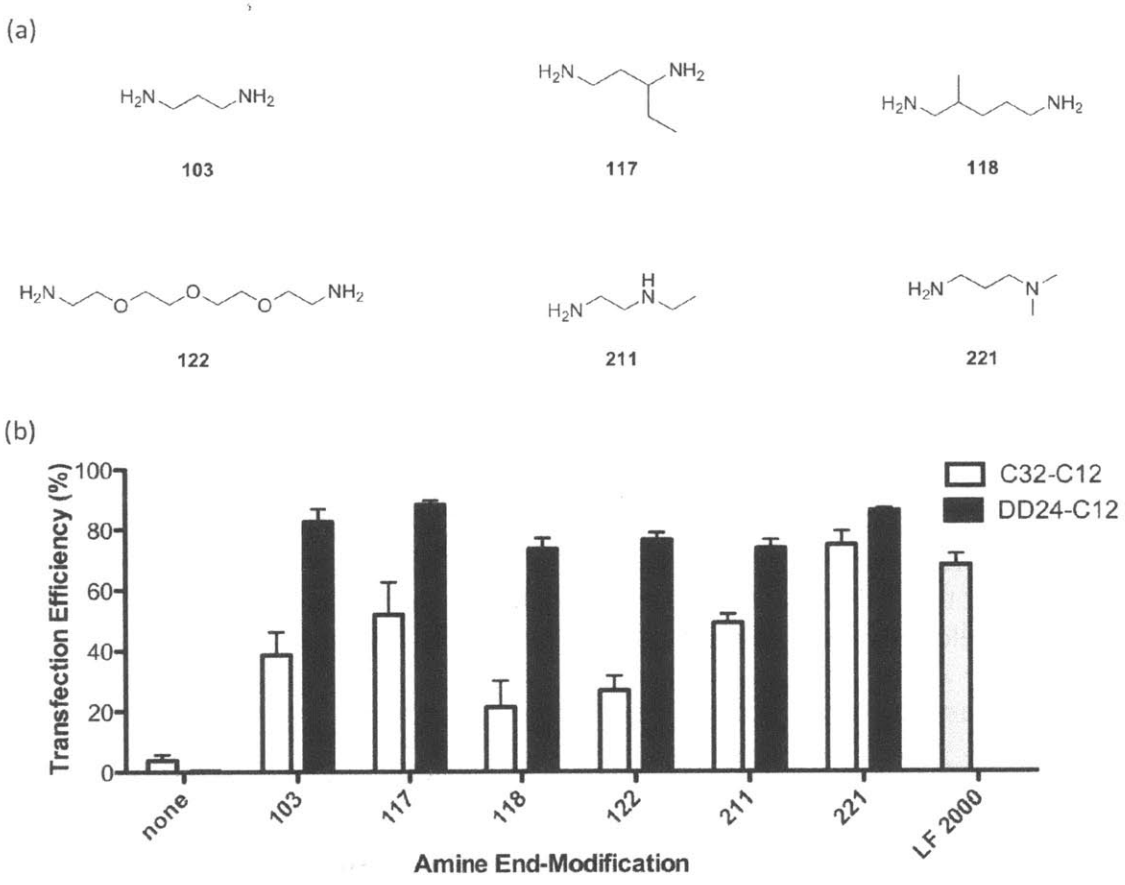

Figure 3.8 Effect of amine end-modification of PBAE terpolymer transfection efficiency

a) Structures of diamine end-capping molecules. **b)** Effect of amine end-modification on DNA transfection efficiency of HeLa cells with C32 and DD24 terpolymers. Terpolymers were synthesized using a monomer molar feed ratio of 1.2:0.3:0.7 diacrylate:hydrophobic amine:hydrophilic amine. "None" refers to terpolymers synthesized using an excess of amine monomers (1.0:0.36:0.84 diacrylate:hydrophobic amine:hydrophilic amine) and no end-modification.

Because polymer terminal group modification has been previously shown to affect transfection efficiency[11, 12], we also synthesized C32-C12 and DD24-C12 polymers with end-capping diamines other than 122 (Figure 3.8a). For the C32 terpolymers, amine end-modification dramatically influenced transfection efficiency, but for the DD24 terpolymers, there was less variation at this dose (Figure 3.8b). We expect that at lower DNA doses, we would observe greater variation in transfection activity as a result of changes to the alkylamine feed ratio and terminal groups of DD24 terpolymers.

Due to their low molecular weights and high polydispersities, the polymers resulting from the step-growth polymerization of the three starting monomers likely represent a mixture of three species: copolymers of the diacrylate and the hydrophilic amine, copolymers of the diacrylate and the hydrophobic amine, and finally terpolymers incorporating all three monomers. To elucidate which species is responsible for the observed enhancements in transfection potency and nanoparticle stability, and whether there might be a synergistic interaction between the relatively hydrophilic and hydrophobic copolymer species, we prepared four PBAE variants containing the DD diacrylate: one synthesized with only the hydrophilic 24 amine (DD24-122, DD:24 = 1.2:1.0 mol/mol, M_w = 2.48 kDa); another synthesized with only the hydrophobic C12 amine (DDC12-122, DD:C12 = 1.2:1.0, M_w = 5.38 kDa); a third synthesized with 70 mol% of the hydrophilic amine and 30% of the hydrophobic amine (DD24-C12-122, DD:24:C12 = 1.2:0.7:0.3, M_w = 3.03 kDa); and a fourth comprising a 70%:30% v/v mixture of DD24-122 to DDC12-122 (M_w = 3.44 kDa). To avoid polymer crosslinking that was observed at high molar ratios of

the C12 amine, these end-capping reactions were performed at room temperature rather than at 40°C.

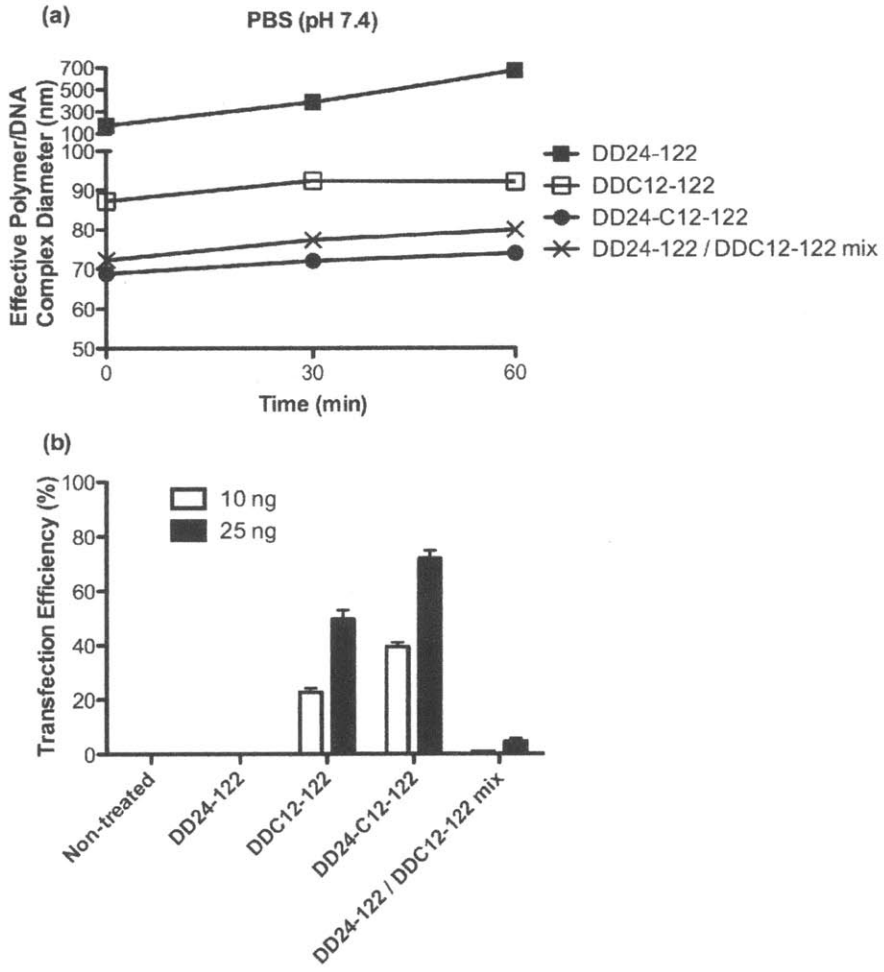

Figure 3.9 Identification of polymer species responsible for polyplex stability and transfection potency
Comparison of **(a)** polyplex stabilities in PBS and **(b)** DNA transfection efficiencies of HeLa cells for a DD diacrylate-based PBAE synthesized with only the hydrophilic 24 amine (DD24-122, DD:24 = 1.2:1.0 mol/mol); a PBAE synthesized with only the hydrophobic C12 amine (DDC12-122, DD:C12 = 1.2:1.0); a PBAE synthesized with 70 mol% of the hydrophilic amine and 30% of the hydrophobic amine (DD24-C12-122, DD:24:C12 = 1.2:0.7:0.3); and a 70%:30% v/v mix of DD24-122 and DDC12-122.

When we examined polyplex stabilities in PBS, only the relatively hydrophilic DD24-122 was unstable, whereas DDC12-122, DD24-C12-122, and the polymer

mixture all resisted aggregation (Figure 3.9a). When we compared their transfection efficiencies, the polymer synthesized using all three monomers (DD24-C12-122) was significantly more potent than the mixture of the DD24-122 and DDC12-122 polymers, as well as the hydrophobic DDC12-122 polymer alone (Figure 3.9b). These data suggest that although a synergistic effect between the hydrophilic and hydrophobic polymers may contribute to polyplex stability, the presence of terpolymer species incorporating both the hydrophilic and hydrophobic amines is most likely responsible for the enhanced potency of the alkane-containing PBAEs.

3.3.3 Effect of alkyl side chain content on DNA binding and encapsulation efficiency

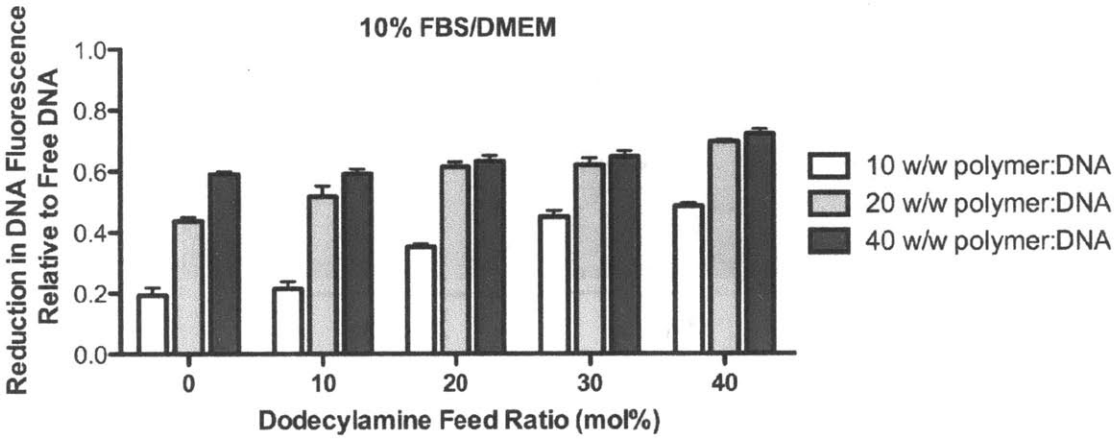

Figure 3.10 Relative encapsulation efficiencies of C32-C12-122 terpolymers of varying hydrophobicity
PicoGreen assay on polymer-DNA polyplexes formed from C32-C12-122 terpolymers of varying dodecylamine feed ratio. The complexes were formed in NaOAc buffer (pH 5.2), and then diluted in 10% serum-containing medium containing the fluorescent DNA-binding dye PicoGreen.

While some studies suggest that hydrophobic modification of polymers decreases binding and encapsulation of nucleic acids (cite ZZZ), several others report the opposite trend (cite ZZZ). We observed that C32-C12-122 terpolymer

hydrophobicity was associated with increasing encapsulation of plasmid DNA upon complexation, as reflected in the results of a PicoGreen dye exclusion assay performed in 10% serum-containing media (Figure 3.10). Strictly speaking, it should be noted that the dye exclusion assay measures the degree of protection afforded to DNA by the polymer from intercalation of the fluorescent stain (i.e. encapsulation), and not necessarily the polymer-DNA binding/complexation efficiency, because PicoGreen could label both free DNA in solution as well as any accessible polymer-bound DNA (e.g., on the nanoparticle surface).

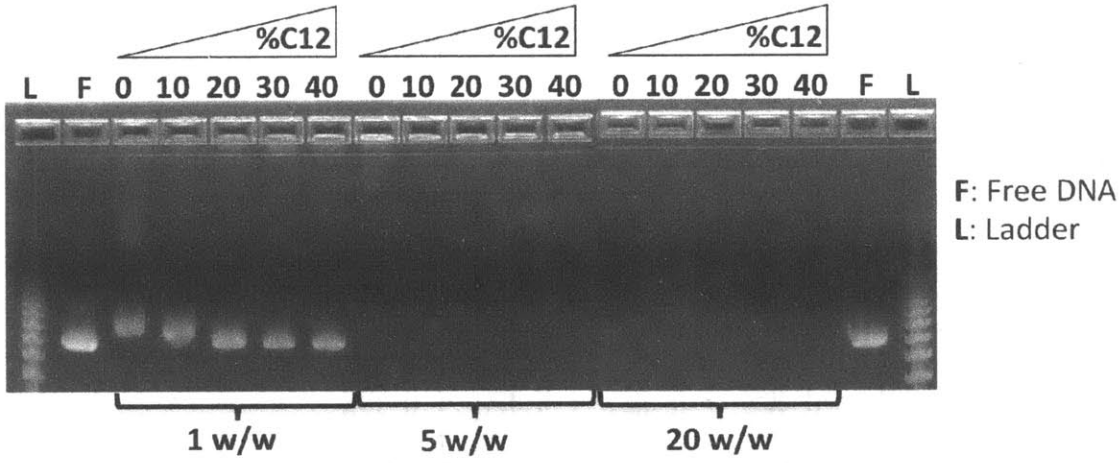

Figure 3.11 Relative DNA binding efficiencies of C32-C12-122 terpolymers of varying hydrophobicity
Polymer-DNA polyplexes were formed in NaOAc buffer (pH 5.2) from C32-C12-122 terpolymers of varying dodecylamine feed ratio and then electrophoresed on a 0.8% agarose gel.

To assess the relative DNA binding efficiencies of these C32-C12-122 hydrophobic terpolymers, we used a gel retardation assay by forming polyplexes with DNA at various weight ratios and then visualizing the relative quantity of free DNA remaining by agarose gel electrophoresis. At polymer:DNA weight ratios of 5:1 or higher, which are most commonly used for transfection, we could not detect free

DNA from any of complexes formed from the C32-C12-122 variants (Figure 3.11). However, at a lower weight ratio of 1:1, it was observed that as the terpolymer alkyl side chain content increased, the relative amount of retarded, polymer-bound plasmid DNA at the top of the gel generally increased, and that of free DNA decreased (Figure 3.11). Therefore, taking the results from the PicoGreen and the gel retardation assays together, increasing hydrophobicity of C32 terpolymers was correlated with increasing efficiency of DNA binding and encapsulation.

3.3.4 Formulation of terpolymer/DNA nanoparticles with PEG-lipid conjugates

Finally, to test our hypothesis that the incorporation of hydrophobic side chains in PBAEs can facilitate their interaction with PEG-lipid conjugates, we used a nanoprecipitation approach to formulate particles comprised of polymer and DNA in the presence or absence of PEG-lipid. Working with C32-122 and D60-122-based polymers, we dissolved either the copolymers lacking alkyl side chains (C:32 = 1.2:1.0 mol/mol; D:60 = 1.2:1.0) or the terpolymer variants (C:32:C12 = 1.2:0.7:0.3; D:60:C12 = 1.2:0.7:0.3) in acetonitrile with or without PEG-lipid and mixed them with DNA at high concentration in sodium acetate buffer at pH 5.2. To remove the organic solvent, we then dialyzed the formulations against PBS for 3 h. Comparing particle sizes before and after dialysis, we found that only the formulations employing both the terpolymers and the PEG-lipid conjugate gave rise to well-defined and stable nanoparticles (Figure 3.12a). At this high DNA concentration, D60-122, for instance, produced large particles ~1 μm in size whether or not PEG-lipid was present. In contrast, when PEG-lipid was present, the terpolymer version, D60-C12-122, produced particles that remained stable after dialysis at ~250 nm in

size; in the absence of PEG-lipid, the particles grew to >700 nm in diameter after dialysis, a size which seemed poorly defined given the large variation between replicate measurements.

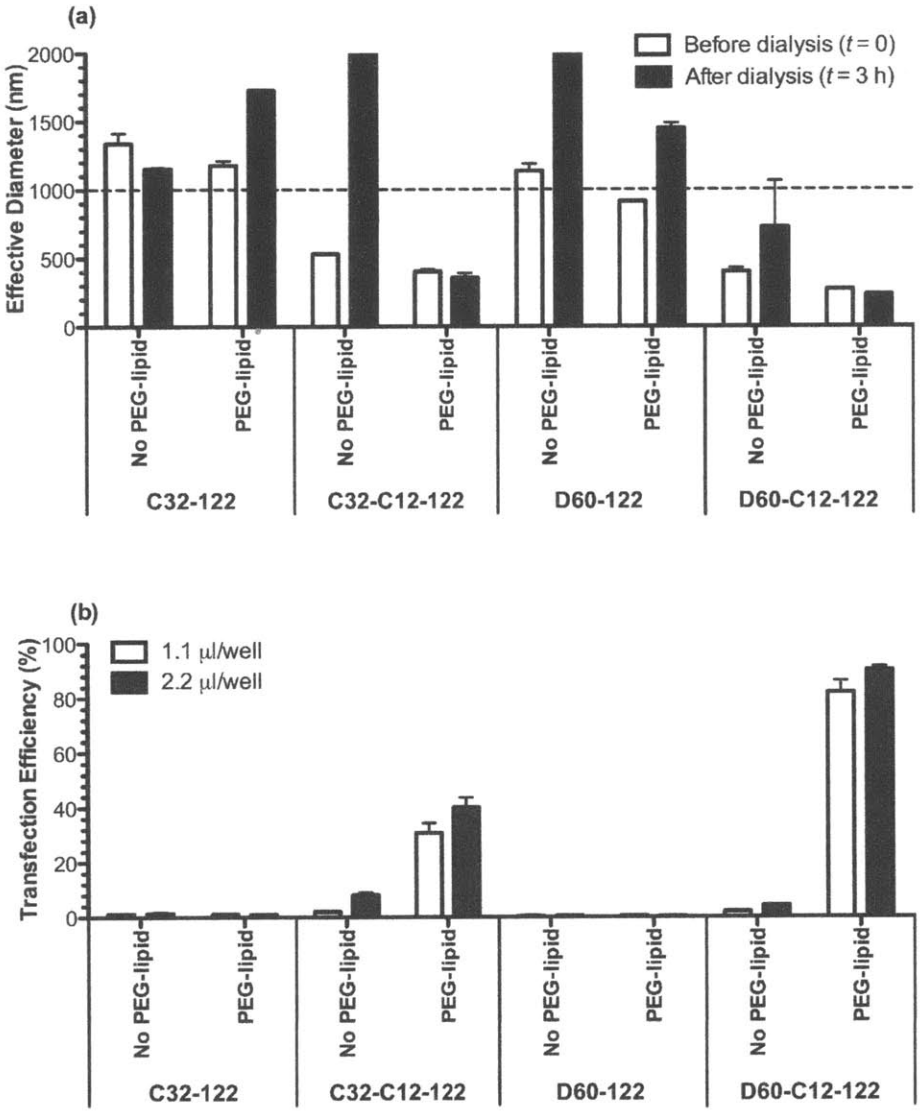

Figure 3.12 Effects of PBAE alkyl side chains (C12) and the presence of PEG-lipid conjugate on nanoparticle formulation stability and transfection efficiency at high DNA concentration

a) Particle sizes before and after dialysis against PBS. **b)** Transfection efficiencies of HeLa cells using equal doses of each formulation (approximately 75 ng and 150 ng of DNA/well).

When we then transfected HeLa cells using identical volumes of formulation per well, corresponding to approximately 75 ng and 150 ng of DNA, we found that only the terpolymer formulations including PEG-lipid yielded significant transfection (Figure 3.12b). Further support for non-covalent interaction of the PEG-lipid conjugate was provided by ζ-potential measurements, which showed a reduction in ζ-potential upon inclusion of PEG-lipid for particles formed from hydrophobic C32-122 terpolymers, but not for particles formed from regular C32-122 (Table 3.2). Taken together, these data suggest that at high DNA concentration, PBAE terpolymers incorporating alkyl side chains, but not polymers lacking them, are capable of interacting with PEG-lipid conjugates and DNA to form stable nanoparticles, and that these particles retain the ability to mediate gene delivery.

	No PEG-lipid (mV)	PEG-lipid (mV)
C32-122 (0 mol% C12)	27.0 ± 4.1	27.2 ± 3.3
C32-C12-122 (20 mol% C12)	37.2 ± 5.1	11.1 ± 1.9
C32-C12-122 (40 mol% C12)	46.5 ± 2.1	12.9 ± 2.5

Table 3.2 ζ-potential measurements of nanoparticles formed from C32-122 terpolymers of varying hydrophobicity
Formulations were prepared by nanoprecipitation of DNA with the polymers (20:1 w/w polymer:DNA) in the presence or absence of PEG-lipid conjugate (10 mol%). Freshly prepared nanoparticles were diluted 100-fold in NaOAc buffer (pH 5.2) prior to measurement (mean ± SD, n = 3).

Due to the commercial availability of functionalized PEG-lipid conjugates, the capacity of the hydrophobic PBAE terpolymers to support formulation with PEG-lipid represents a straightforward non-covalent method for attaching targeting ligands such as peptides to the polymer/DNA nanoparticles. Although the particles produced using a combination of PBAE terpolymers and PEG-lipid were rather large

here, with effective diameters of ~250-350 nm, there is likely significant potential for optimization of particle size through variation of the PBAE alkyl side chain length and content, the ratio of PBAE:DNA:PEG-lipid, the lengths of the lipid tails and PEG polymer in the PEG-lipid conjugate, and the use of additional excipients such as cholesterol or poloxamers. Furthermore, increasing the mixing rate with the aid of a microfluidic mixing device should enable the formulation of smaller nanoparticles[25].

3.4 CONCLUSIONS

In summary, we employed parallel synthesis and screening as a tool to accelerate the development of degradable alkane-containing PBAE terpolymers for gene delivery, guided by our hypothesis that they might provide superior transfection potency and particle stability over polymers lacking hydrophobic side chains. The top-performing PBAE terpolymers exhibited transfection potencies in HeLa cells significantly higher than that of Lipofectamine 2000. Transfection efficiency was generally positively correlated with increasing hydrophobicity, as defined by either increasing the feed ratio of alkylamine monomer or increasing its chain length. Increasing the hydrophobic content of the polymers also appeared to be associated with greater polyplex stability at low DNA concentration. At high DNA concentrations under conditions of physiological pH and ionic strength, these hydrophobic PBAE terpolymers were better able to facilitate interaction with PEG-lipid and DNA to yield stable, well-defined nanoparticles capable of transfecting cultured cells *in vitro*. This simple yet powerful approach to improving the

transfection potency and formulation stability of degradable cationic polymers may facilitate the development of multifunctional, nanoparticulate gene delivery systems suitable for *in vivo* application.

3.5 REFERENCES

[1] Sheridan, C. Gene therapy finds its niche. *Nat. Biotechnol.* **29**, 459 (2011).

[2] Kay, M. A. State-of-the-art gene-based therapies: the road ahead. *Nat. Rev. Genet.* **12**, 316 (2011).

[3] Al-Dosari, M. S., Gao, X. Nonviral gene delivery: principle, limitations, and recent progress. *AAPS J.* **11**, 671 (2009).

[4] Mintzer, M. A., Simanek, E. E. Nonviral vectors for gene delivery. *Chem. Rev.* **109**, 259 (2009).

[5] Anderson, D. G., Peng, W., Akinc, A., Hossain, N., Kohn, A., Padera, R., Langer, R., Sawicki, J. A. A polymer library approach to suicide gene therapy for cancer. *Proc. Natl. Acad. Sci. USA* **101**, 16028 (2004).

[6] Yang, F., Cho, S. W., Son, S. M., Bogatyrev, S. R., Singh, D., Green, J., Mei, Y., Park, S., Bhang, S. H., Kim, B. S., Langer, R., Anderson, D. Genetic engineering of human stem cells for enhanced angiogenesis using biodegradable polymeric nanoparticles. *Proc. Natl. Acad. Sci. USA* **107**, 3317 (2010).

[7] Lynn, D., Anderson, D., Putnam, D., Langer, R. Accelerated Discovery of Synthetic Transfection Vectors: Parallel Synthesis and Screening of a Degradable Polymer Library. *J. Am. Chem. Soc.* **123**, 8155 (2001).

[8] Akinc, A., Lynn, D., Anderson, D., Langer, R. Parallel Synthesis and Biophysical Characterization of a Degradable Polymer Library for Gene Delivery. *J. Am. Chem. Soc.* **125**, 5316 (2003).

[9] Anderson, D. G., Lynn, D. M., Langer, R. Semi-Automated Synthesis and Screening of a Large Library of Degradable Cationic Polymers for Gene Delivery. *Angew. Chem. Int. Ed.* **42**, 3153 (2003).

[10] Anderson, D. G., Akinc, A., Hossain, N., Langer, R. Structure/property studies of polymeric gene delivery using a library of poly(beta-amino esters). *Mol. Ther.* **11**, 426 (2005).

[11] Zugates, G. T., Peng, W., Zumbuehl, A., Jhunjhunwala, S., Huang, Y. H., Langer, R., Sawicki, J. A., Anderson, D. G. Rapid optimization of gene delivery by parallel end-modification of poly(beta-amino ester)s. *Mol. Ther.* **15**, 1306 (2007).

[12] Green, J. J., Zugates, G. T., Tedford, N. C., Huang, Y., Griffith, L. G., Lauffenburger, D. A., Sawicki, J. A., Langer, R., Anderson, D. G. Combinatorial modification of degradable polymers enables transfection of human cells comparable to adenovirus. *Adv. Mater.* **19**, 2836 (2007).

[13] Sunshine, J., Green, J. J., Mahon, K. P., Yang, F., Eltoukhy, A. A., Nguyen, D. N., Langer, R., Anderson, D. G. Small-Molecule End-Groups of Linear Polymer Determine Cell-type Gene-Delivery Efficacy. *Adv. Mater.* **21**, 4947 (2009).
[14] Lynn, D. M., Langer, R. Degradable Poly ([beta]-amino esters): Synthesis, Characterization, and Self-Assembly with Plasmid DNA. *J. Am. Chem. Soc* **122**, 10761 (2000).
[15] Neu, M., Fischer, D., Kissel, T. Recent advances in rational gene transfer vector design based on poly(ethylene imine) and its derivatives. *J. Gene Med.* **7**, 992 (2005).
[16] Morille, M., Passirani, C., Vonarbourg, A., Clavreul, A., Benoit, J.-P. Progress in developing cationic vectors for non-viral systemic gene therapy against cancer. *Biomaterials* **29**, 3477 (2008).
[17] Wong, S. Y., Pelet, J. M., Putnam, D. Polymer systems for gene delivery--Past, present, and future. *Prog. Polym. Sci.* **32**, 799 (2007).
[18] Wu, L., Zhang, J., Watanabe, W. Physical and chemical stability of drug nanoparticles. *Adv. Drug. Deliv. Rev.* **63**, 456 (2011).
[19] Ogris, M., Steinlein, P., Carotta, S., Brunner, S., Wagner, E. DNA/polyethylenimine transfection particles: Influence of ligands, polymer size, and PEGylation on internalization and gene expression. *AAPS J.* **3**, 43 (2001).
[20] Millili, P. G., Selekman, J. A., Blocker, K. M., Johnson, D. A., Naik, U. P., Sullivan, M. O. Structural and functional consequences of poly(ethylene glycol) inclusion on DNA condensation for gene delivery. *Microsc. Res. Tech.* **73**, 866 (2010).
[21] Jokerst, J. V., Lobovkina, T., Zare, R. N., Gambhir, S. S. Nanoparticle PEGylation for imaging and therapy. *Nanomedicine* **6**, 715 (2011).
[22] Liu, Z., Zhang, Z., Zhou, C., Jiao, Y. Hydrophobic modifications of cationic polymers for gene delivery. *Prog. Polym. Sci.* **35**, 1144 (2010).
[23] Schroeder, A., Dahlman, J. E., Sahay, G., Love, K. T., Jiang, S., Eltoukhy, A. A., Levins, C. G., Wang, Y., Anderson, D. G. Alkane-modified short polyethyleneimine for siRNA delivery. *J. Controlled Release* **160**, 172 (2012).
[24] Zhou, J., Liu, J., Cheng, C. J., Patel, T. R., Weller, C. E., Piepmeier, J. M., Jiang, Z., Saltzman, W. M. Biodegradable poly(amine-co-ester) terpolymers for targeted gene delivery. *Nat. Mater.* **11**, 82 (2012).
[25] Chen, D., Love, K. T., Chen, Y., Eltoukhy, A. A., Kastrup, C., Sahay, G., Jeon, A., Dong, Y., Whitehead, K. A., Anderson, D. G. Rapid Discovery of Potent siRNA-Containing Lipid Nanoparticles Enabled by Controlled Microfluidic Formulation. *J. Am. Chem. Soc.* **134**, 6948 (2012).

4 DEVELOPMENT OF DEGRADABLE HYDROPHOBIC PBAE TERPOLYMERS FOR CELL-SPECIFIC GENE DELIVERY

4.1 INTRODUCTION

As presented in Chapter 3, the initial development of the hydrophobic PBAE terploymers proceeded through library synthesis and screening in HeLa cells, a cervical cancer cell line. Although this cell line has been commonly used in *in vitro* assays due to its potential relevance to cancer biology and its ease of culture, efficient gene transfection of HeLa cells is readily achieved through a variety of means. In this chapter, we focus on the development of these degradable hydrophobic PBAE terpolymers for gene transfection of difficult-to-transfect primary cells with greater clinical relevance.

We identify terpolymers such as DD24-C12-122 and LL24-C12-122 that mediate gene transfection of primary human umbilical vein endothelial cells (HUVECs), mesenchymal stem cells, and primary neonatal rat cardiomyocytes with greater efficacy than that of a widely used commercial reagent. We explore the chemical space surrounding these polymers by synthesizing a small library of structurally related terpolymers, characterizing their biophysical properties, and screening them for gene delivery to HeLa cells, HUVECs, and rat cortical neurons. Finally, we present preliminary experiments exploring the potential of these polymers for systemic gene delivery *in vivo*.

4.2 MATERIALS AND METHODS

4.2.1 Materials

Diacrylate and amine monomers, as well as end-capping reagents, were purchased from Sigma-Aldrich (St. Louis, MO, USA), Alfa Aesar (Ward Hill, MA, USA), TCI America (Portland, OR, USA), and Monomer-Polymer & Dajac Labs (Trevose, PA, USA). $(PEO)_4$-*bis*-amine ("122") was acquired from Molecular Biosciences (Boulder, CO, USA). All reagents were used without further purification. Plasmids encoding green fluorescent protein (gWiz-GFP) and firefly luciferase (gWiz-Luc) were purchased from Aldevron (Fargo, ND, USA). PEG-lipid conjugates were obtained from Avanti Polar Lipids (Alabaster, AL, USA). HeLa cells (ATCC, Manassas, VA, USA) were cultured in DMEM (Invitrogen, Carlsbad, CA, USA) supplemented with 10% fetal bovine serum (Invitrogen). Primary human umbilical vein endothelial cells (HUVECs) were obtained from Lonza (Walkersville, MD, USA) and cultured according to the vendor's protocols. Primary porcine mesenchymal stem cells (pMSCs), primary neonatal rat cardiomyocytes (NRCMs), and primary rat cortical neurons were isolated and cultured according to standard protocols.

4.2.2 Polymer synthesis

The monomers were dissolved in DMSO (Sigma-Aldrich) to a concentration of 200 mg ml^{-1}. Dodecylamine required heating to ~60°C to enable complete dissolution. Library scale reactions were performed in glass shell vials (1 mL) with polyethylene snap caps (Waters, Milford, MA, USA) in a 96-well reaction block (Symyx, Santa Clara, CA, USA). To each vial equipped with stir bar, diacrylate

monomer, hydrophobic amine monomer, and hydrophilic amine monomer were added such that their molar ratio was 1.2:0.3:0.7 and the total mass of monomers was 100 mg. After heating and stirring at 90°C for 48 h, the reactions were allowed to cool to RT, and to each vial, end-capping amine (0.2 mmol in 0.5 mL DMSO) was added. The reactions were stirred at 40°C for 24 h, divided into aliquots, and then stored frozen at -20°C. Top-performing polymers were resynthesized by scaling up the reactions tenfold.

4.2.3 Analytical Gel Permeation Chromatography (GPC)

GPC was performed using a Waters system equipped with a 2400 differential refractometer, 515 pump, and 717-plus autosampler. The flow rate was 1 ml min^{-1} and the mobile phase was tetrahydrofuran (THF). The Styragel columns (Waters) and detector were thermostated at 35ºC. Linear polystyrene standards were used for calibration.

4.2.4 Transfection experiments

One to three days before transfection, cells (100 μl) were seeded into each well of a 96-well polystyrene tissue culture plate, clear bottom for GFP transfections and white bottom for luciferase transfections (HeLa: 12,500 per well 1 d prior; HUVEC: 9,000 per well 1 d prior; pMSCs: 4,500 2-3 d prior). In a typical example, for a 150 ng/well DNA dose, plasmid DNA (5 mg ml^{-1}) was diluted to 15 μg ml^{-1} in 25 mM sodium acetate (NaOAc) buffer at pH 5.2. Polymers (100 mg ml^{-1}) were thawed immediately prior to transfection and diluted in NaOAc buffer to a concentration of 300 μg ml^{-1} (20:1 w/w polymer:DNA). To avoid precipitation within the pipet tip,

hydrophobic PBAE terpolymers were diluted by first adding polymer and then adding aqueous buffer; maximum solubility for these poylmers was typically on the order of 5 mg ml^{-1} in NaOAc buffer.

To form DNA-polymer nanoparticles, polymer solution (25 μl) was added to DNA (25 μl) in a half-area 96-well plate, mixed by repeated pipetting using a multichannel pipette, and allowed to incubate for 10 min at room temperature. Polymer-DNA complexes (30 μl) were then gently mixed with fresh medium (195 μl) pre-warmed to 37°C. Conditioned medium was removed using a 12-channel aspirating wand and replaced with the complexes diluted in medium (150 μl). Following a 4-h incubation, complexes were removed with the aid of a multi-channel aspiration wand and replaced with fresh medium (100 μl). Lipofectamine 2000 (Invitrogen) was used according to the protocol provided by the vendor.

4.2.5 GFP expression analysis

After aspirating conditioned medium, cells were washed with PBS and detached using 25 μl per well of 0.25% trypsin-EDTA (Invitrogen). 50 μl of FACS running buffer, consisting of 98% PBS, 2% FBS, and 1:200 v/v propidium iodide solution (Invitrogen), was added to each well. Cells were mixed thoroughly and then transferred to a 96-well round-bottom plate. GFP expression was measured using FACS on a BD LSR II (Becton Dickinson, San Jose, CA, USA). Propidium iodide (PI) staining was used to exclude dead cells from the analysis. PI staining was also used to determine the viabilities of treated cells relative to non-treated control cells, where the relative viability was calculated as the ratio of live (unstained) treated

cells per well to the mean number of live non-treated cells per well. 2D gating was used to separate increased auto-fluorescence signals from increased GFP signals to more accurately count positively expressing cells. Gating and analysis were performed using FlowJo v8.8 software (TreeStar, Ashland, OR, USA).

4.2.6 Luciferase expression analysis

Luciferase expression was analyzed using a Bright-Glo assay kit (Promega, Madison, WI, USA). Briefly, Bright-Glo solution (100 µl) was added to each well of the 96-well plate containing medium and cells. Luminescence was measured using a Tecan Infinite M1000 plate reader.

4.2.7 Dynamic light scattering (DLS) measurements

Particle sizes were measured using a ZetaPALS DLS detector (Brookhaven Instruments Corp., Holtsville, NY, USA, 15-mW laser, incident beam 676 nm). Correlation functions were collected at a scattering angle of 90°, and particle sizes were obtained from the MAS option of BIC's particle sizing software (v. 2.30) using the viscosity and refractive index of water at 25°C. Particle sizes are expressed as effective diameters (z-average or hydrodynamic diameters) calculated using the Stokes-Einstein relationship from the diffusion coefficient obtained by cumulant analysis. Particles were prepared in NaOAc buffer as for DNA transfection, except volumes were scaled up by a factor of five. Once formed in NaOAc buffer, complexes were diluted fourfold in additional NaOAc buffer, 1X PBS, or 10% serum-containing media as indicated.

4.2.8 *Dye exclusion assay*

A working solution of PicoGreen was prepared by diluting 80 μl of stock solution in 15.92 ml NaOAc buffer. In each well of a 96-well plate, 50 μl of polymer at 1.2 mg ml^{-1} in NaOAc buffer was added to 50 μL of DNA at 0.06 mg ml^{-1} in NaOAc buffer. After 5 min, 100 μl of PicoGreen working solution was added to the complexes. After an additional 5 min incubation, 30 μl was transferred to 200 μl of 10% serum-containing medium in a black 96-well assay plate. The fluorescence was then measured on a Tecan Infinite M1000 plate reader using the FITC filter set (excitation 485 nm, emission 535 nm). The reduction in relative fluorescence (RF), or the relative encapsulation efficiency, was calculated using the relationship $(F_{DNA}-F_{sample})/(F_{DNA}-F_{blank})$, where F_{sample} is the fluorescence of the polymer–DNA–PicoGreen sample, F_{DNA} is the fluorescence of DNA–PicoGreen (no polymer), and F_{blank} is the fluorescence of a sample with no polymer or DNA (only PicoGreen).

4.2.9 *Nanoparticle formulation at high DNA concentration*

Hydrophobic PBAE terpolymer in DMSO (100 mg ml^{-1}) and various PEG-lipids in ethanol as indicated (10 mg ml^{-1}) were co-dissolved in acetonitrile to yield final concentrations of 8 mg ml^{-1} and either 3 mol% or 10 mol%, respectively. gWiz-GFP pDNA (5 mg ml^{-1}) was diluted to 0.4 mg ml^{-1} in 25 mM NaOAc buffer. The polymer and PEG-lipid in acetonitrile was then added to DNA and mixed by repeated pipetting. After incubation for 10 min, the formulations were diluted in PBS (1:1 v/v) and dialyzed against PBS (3 l) for 3 h at RT using a Pierce Slide-A-Lyzer MINI dialysis devices (20 kDa MWCO, 0.1ml; Pierce, Rockford, IL, USA) for

small volume formulations and a Pierce Slide-A-Lyzer G2 cassette (20K MWCO, 3 ml) for large volume formulations.

4.2.10 In vivo transfection experiments

In vivo transfection experiments were performed using 6-8 wk old, male BALB/c mice (Charles River, Wilmington, MA). All mouse experiments were done in accordance with protocols approved by MIT's Committee on Animal Care (CAC). As described above, D60-C12-122 and D90-C12-122 were formulated with 16:0 PEG 5000 PE and gWiz-Luc using a 20:1 w/w ratio of polymer:DNA and a PEG-lipid concentration of 10 mol%. After overnight dialysis at 4°C, the nanoparticle formulation was removed from G2 dialysis cassette. Due to wide variability in measurements of total DNA concentration using the PicoGreen assay in combination with a particle disruption agent such as heparin, the DNA concentration was calculated based on volume change as a result of dialysis, and the formulations were accordingly diluted to 0.1 mg ml^{-1} in sterile PBS and stored at 4°C until administration. Using a 28-gauge 0.5-inch insulin syringe, 200 µl (~1 mg/kg dose) was injected into the peritoneal cavity of a mouse (IP) or into the tail-vein (IV).

For C32-122/DNA complexes, polymer diluted in 25 mM NaOAc buffer (60 µl, 12 mg ml^{-1}) was added to gWiz-Luc DNA (60 ul , 0.4 mg ml^{-1}) diluted in 25 mM NaOAc buffer to yield a 30:1 w/w polymer:DNA ratio. After a 5-minute incubation at RT, 120 µl of a 20% w/v solution of glucose in PBS was added to the polymer–DNA mixture. Of the resulting 240 µl volume, 200 µl was injected immediately into the peritoneal cavity of a mouse.

4.2.11 *Whole-animal bioluminescence imaging*

Bioluminescence imaging was performed using an IVIS imaging system (Xenogen, Alameda, CA) on whole mice at 6 h, 24 h, and 72 h after injection of luciferase-encoding DNA nanoparticles. To capture the peak of luminescence emission, a series of images were taken five min. apart for 30 min. on each treatment group of isoflurane-anesthetized mice following IP injection of Xenolight RediJect D-luciferin (150 mg/kg; Caliper Life Sciences, Waltham, MA). Xenogen Living Image v. 4.2 acquisition and analysis software was used to quantify luciferase expression from the optical images.

4.3 Results and Discussion

4.3.1 *PBAE terpolymer transfection of HUVECs, pMSCs, and NRCMs*

To assess the potential of the hydrophobic PBAE terpolymers for transfection of endothelial cells, we re-screened our initial library of ~72 terpolymers (Figure 3.1a-b) for DNA transfection of primary human umbilical vein endothelial cells (HUVECs). The polymers were complexed with GFP-encoding DNA at a 20:1 w/w ratio and the resulting particles were incubated with HUVECs at a DNA dose of 100 ng per well for 4 hours. GFP expression and transfection efficiency were analyzed by FACS measurements after two days.

The results of this screen in HUVECs (Figure 4.1) differed strikingly from those of our initial one in HeLa cells (Figure 3.2). As with the results in HeLa cells, the structure of the diacrylate monomer appeared to influence transfection efficacy to a greater extent than that of the amine monomer; in the HeLa screen, the top-

performing terpolymers were those formed from the bisphenol-containing diacrylate monomer "D", but in HUVECs, there was a preference for the terpolymers formed from long straight-chain alkyl diacrylates such as "JJ" and "LL." Four terpolymers, including LL24-C12-122, LL28-C12-122, LL32-C12-122, and LL36-C12-122 mediated gene transfection efficiencies of ~30% or more in HUVECs, which at this dose represented significantly higher potency than that of Lipofectamine 2000 (~10% efficiency). These terpolymers also significantly outperformed C32-122, one of the top PBAE copolymers lacking alkyl side chains.

	20	21	24	28	32	36	60	80	90	94
A	0.51	0.71	0.54	0.53	0.57	0.60	0.53	0.69	0.43	insoluble
C	1.26	3.77	0.82	0.88	8.16	14.88	0.63	0.49	1.35	insoluble
D	0.72	0.89	1.06	0.69	0.84	0.76	6.88	16.53	4.32	1.78
E	3.87	4.40	3.13	10.50	9.26	14.95	1.56	insoluble	3.01	5.32
J	0.57	0.48	0.62	0.54	0.43	0.37	0.43	0.45	0.50	0.50
T	0.62	0.51	0.58	0.46	0.47	0.74	1.97	1.24	1.10	0.67
JJ	6.48	23.45	15.18	18.98	21.73	23.05	0.65	1.12	13.15	insoluble
LL	0.83	0.72	29.58	30.75	34.33	42.13	insoluble	insoluble	insoluble	insoluble

	Non-treated	Naked DNA	C32-122	LF2000
Controls	0.80	0.63	0.99	9.58

Figure 4.1 Screening the initial PBAE terpolymer library for gene transfection of HUVECs.
Heat map of DNA transfection efficiencies in HUVECs with the initial PBAE terpolymer library (100 ng DNA/well; 20:1 polymer:DNA w/w), as determined by FACS analysis.

When the results of the two screens were plotted side-by-side or in a scatter plot, no significant overlap was observed between the polymers that performed best in HeLa cells and those that performed best in HUVECS (Figure 4.2). Besides the difference in the DNA doses that were used for the screens, we hypothesized that one factor contributing to the apparent lack of correlation could be the difference in the transfection media between the two cell types. While the HeLa growth medium

consisted of 10% fetal bovine serum (FBS), the HUVEC growth medium contained only 2% FBS.

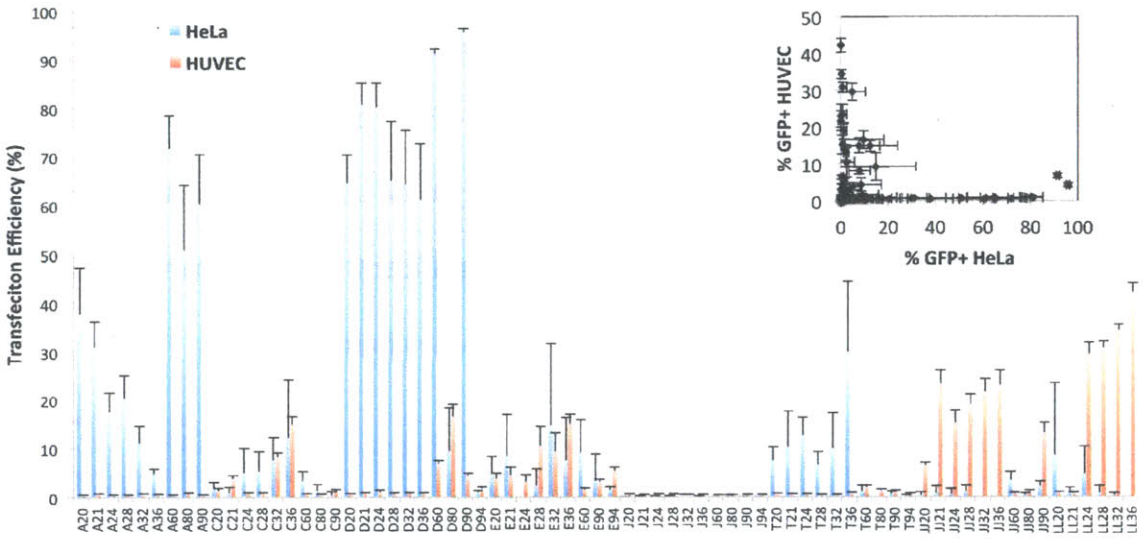

Figure 4.2 Comparison of PBAE terpolymer library screen results in HeLa cells and HUVECs
The results of the PBAE terpolymer library screens in the two cell types plotted side-by-side. *Inset:* correlation between gene transfection efficiencies of HUVEC and HeLa cells by hydrophobic PBAE terpolymers represented in the initial library.

To examine the effect of serum content on PBAE-mediated gene transfection of HUVECs, we performed a side-by-side transfection of these cells in 2% FBS-containing growth medium or 10% FBS/DMEM, i.e. regular HeLa medium (Figure 4.3). As a control, HeLa cells were transfected in parallel with the same polyplexes in 10% FBS/DMEM medium. The transfections were performed using the top nine PBAE terpolymers identified in the HeLa cell screen as well as the top nine terpolymers identified in the HUVEC screen. Interestingly, no significant difference was observed with regard to the effect of growth medium on PBAE-mediated HUVEC gene transfection. As expected, in this side-by-side transfection, HeLa cells

proved more amenable to DNA transfection than HUVECs, and in general the same trends were observed with regard to the influence of diacrylate structure on PBAE-mediated cell-type specificity.

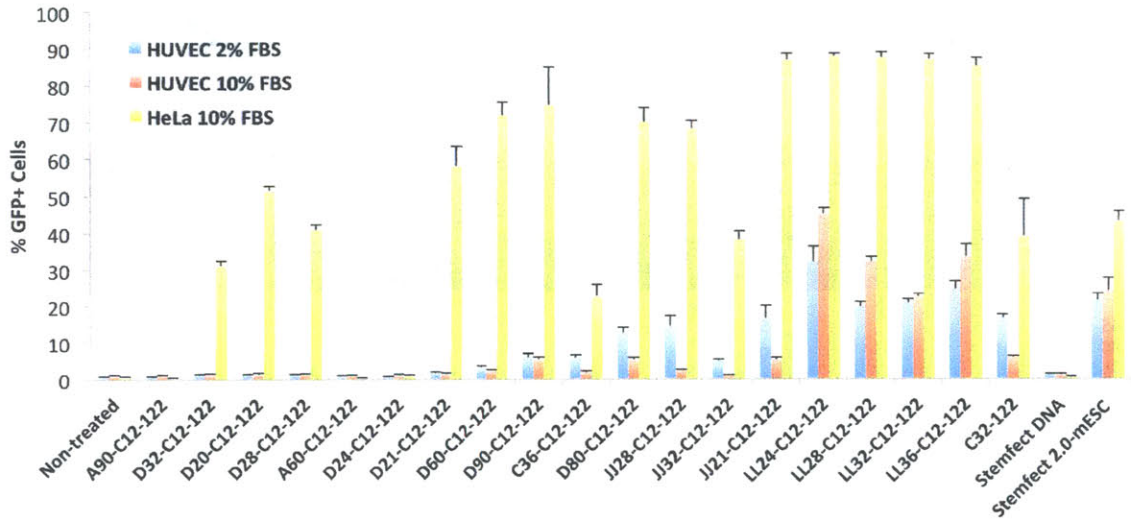

Figure 4.3 Influence of growth medium on PBAE-mediated transfection of HUVECs and HeLa cells
Side-by-side GFP transfection of HUVECs with top-performing PBAE terpolymers in 2% FBS-containing growth medium or 10% FBS/DMEM, and of HeLa in 10% FBS/DMEM. A90-D90 (left to right) and C36 to LL36 represent the top nine PBAE terpolymers identified in the HeLa cell screen and the top nine terpolymers identified in the HUVEC screen, respectively.

Contrary to our expectations based on the initial screening results, some of the LL-containing terpolymers, in particular LL24-C12-122, mediated highly potent gene transfection in HeLa cells. This result was previously missed due to the higher dose used in the initial screens (300 ng/well vs. 100 ng/well); at this high dose, significant cytotoxicity was observed with the LL-containing polymers, but at reduced doses, both viability and transfection were dramatically improved. Moreover, a few of the polymers that had performed well in HeLa in the initial

screen, such as A60 and D24, performed quite poorly in this particular experiment, a difference that may likely be attributed not only to the reduced DNA dose but also to potential degradation of the polymers since their synthesis (~3 months).

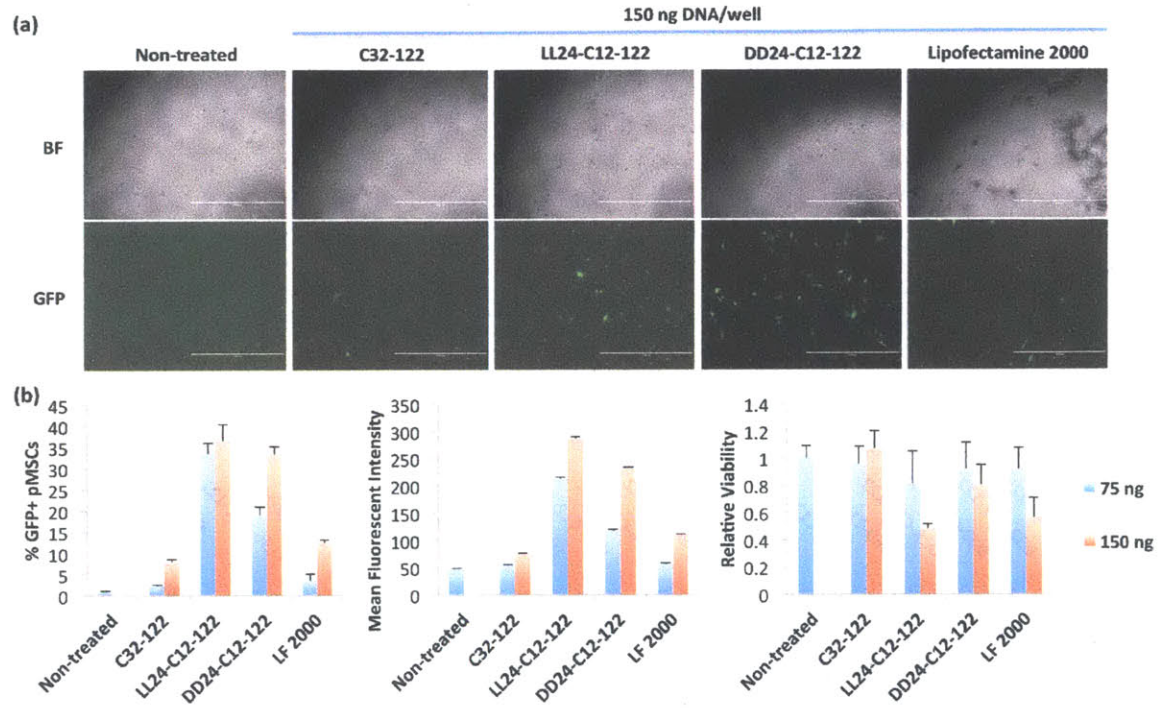

Figure 4.4 Transfection of porcine mesenchymal stem cells by hydrophobic PBAE terpolymers

Porcine mesenchymal stem cells (pMSCs) were transfected with a GFP-encoding plasmid using various PBAEs and Lipofectamine 2000 (LF 2000). FACS analysis was used two days later to quantify GFP expression efficiency *(left)*, geometric mean GFP fluorescent intensity *(middle)*, and relative viability *(right)*.

We next assessed the potential for the top-performing terpolymers to emerge from these screens to deliver genes to primary mesenchymal stem cells (pMSCs). Working with porcine MSCs, we transfected cells with a GFP plasmid using C32-122, LL24-C12-122, DD-24-C12-122, or Lipofectamine 2000, and compared the resulting transfection efficacies by microscopy and FACS analysis. At the low doses applied, LL24-C12-122 and DD24-C12-122 mediated significantly greater GFP transfection in the pMSCS than was achieved with C32-122 or Lipofectamine 2000

(Figure 4.4). For instance, at the 75 ng dose, FACS analysis showed that LL24-C12-122 yielded a pMSC gene transfection efficiency of ~35%, in comparison with ~3% efficiency for Lipofectamine 2000. GFP expression in the LL24-C12-122-treated cells was ~4-fold that of the Lipofectamine-treated cells. At this dose, there was a small but non-significant reduction in relative viability for the LL24-C12-122-treated cells.

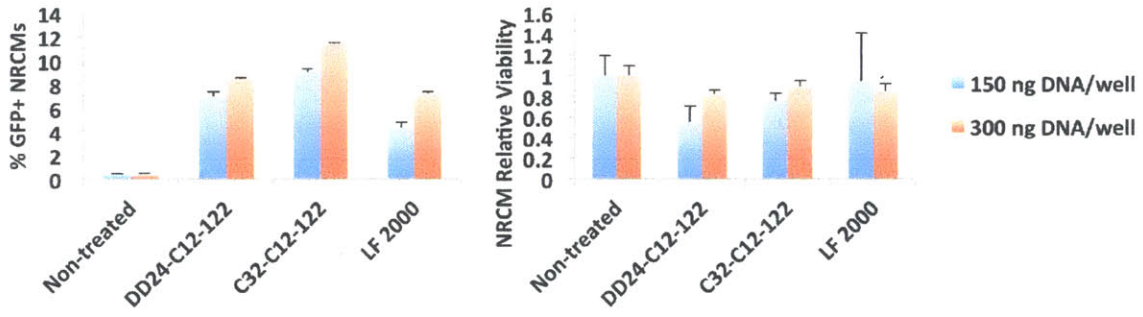

Figure 4.5 Transfection of neonatal rat cardiomyocytes by hydrophobic PBAE terpolymers
Neonatal rat cardiomyocytes (NRCMs) were transfected with a GFP-encoding plasmid using DD24-C12-122, C32-C12-122, and Lipofectamine 2000 (LF 2000). FACS analysis was used two days later to quantify GFP expression efficiency *(left)* and relative cell viability *(right)*.

We also evaluated the potential of hydrophobic PBAE terpolymers for efficient DNA transfection of cardiac tissue. We performed a screen of a subset of these polymers for transfection of primary neonatal rat cardiomyocytes (NRCMs). NRCMs are notoriously difficult to transfect, and as expected, many of the PBAEs that were screened, including the top performing polymers lacking alkyl side chains such as C32-103, C32-117, and C32-122, showed minimal transfection (<2% efficiency; data not shown). Nonetheless, a handful of hydrophobic PBAE terpolymers, including DD24-C12-122 and C32-C12-122, showed modest but

significant improvements in transfection potency over Lipofectamine 2000; for example, C32-C12-122 achieved a transfection efficiency of nearly 12% compared with ~7% for Lipofectamine 2000 (Figure 4.5).

4.3.2 Combinatorial library of PBAE terpolymers centered on DD24-C12-122 and LL24-C12-122

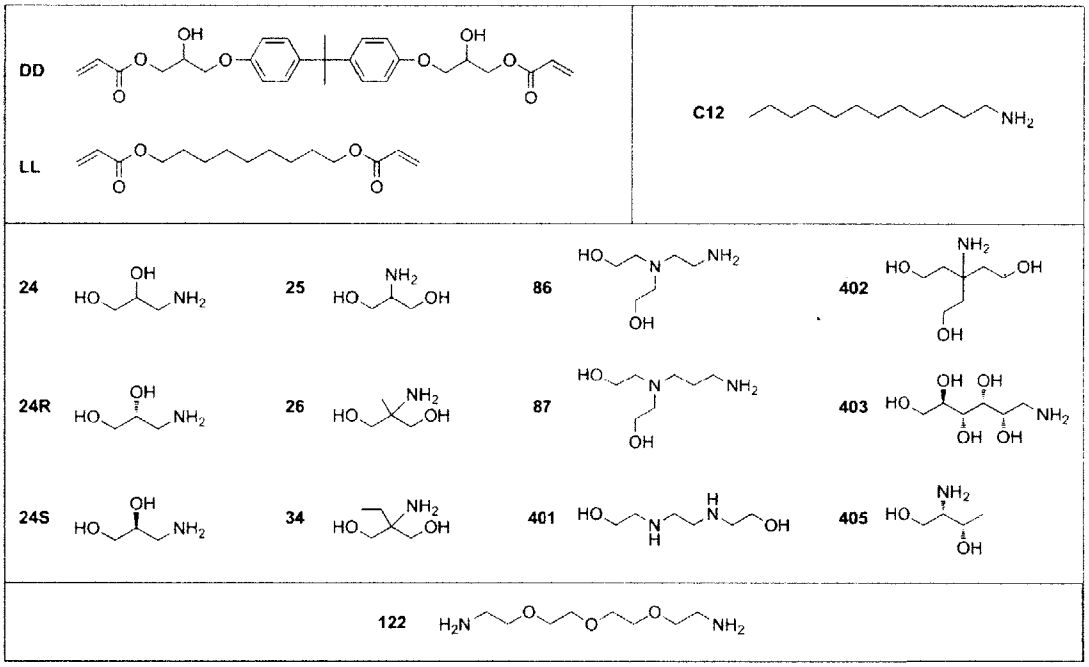

Figure 4.6 Combinatorial library of 24 PBAE terpolymers centered on DD24-C12-122 and LL24-122
Structure of diacrylate monomers (DD, LL), hydrophobic amine (C12), hydrophilic amines (24-405), and end-capping diamine (122) used for the synthesis of the small combinatorial library of PBAE terpolymers surrounding the chemical space of DD24-C12-122 and LL24-C12-122. The diacrylate:hydrophobic amine:hydrophilic amine molar ratio was 1.2:0.3:0.7.

Given the high potencies observed using DD24-C12-122 and LL24-C12-122 in multiple cell types, and the fact that they share a common hydrophilic amine monomer ("24"), we explored the chemical space surrounding these terpolymers by synthesizing and characterizing a small library of polymers built using the same

diacrylate, hydrophobic amine, and end-capping amine reagents, but varying in their hydrophilic amine monomers. Based on the structure of the "24" amine, 3-amino-1,2-propanediol, which notably features two hydroxyl groups, for the combinatorial library we selected nine other hydrophilic amine monomers also possessing multiple hydroxyl groups (Figure 4.6). Because the 24 monomer is a racemic mixture, we also included the purified enantiomers, 24R and 24S, within the library to determine whether polymer tacticity might influence its gene delivery properties.

After synthesizing this small library of 24 terpolymers, we then applied GPC, DLS, and a PicoGreen dye exclusion assay to rigorously characterize the biophysical properties of these polymers and the nanoparticles resulting from their complexation with DNA. As expected, GPC analysis showed that most of these polymers were quite short, with M_w ranging from 1.33 kDa for LL26 to 3.5 kDa for DD24 (Figure 4.7a). (For brevity, the PBAE terpolymers in this library will be referred to by only their diacrylate and hydrophilic amine monomers, since they share the same hydrophobic amine monomer and end-capping reagent.) With respect to the DD24 and LL24 terpolymers varying in tacticity, DD24R and DD24S showed no significant difference in MWD, although these polymers were slightly shorter than the polymer constructed from the racemic 24 monomer. The LL24 stereochemical variants showed minimal variation in MWD.

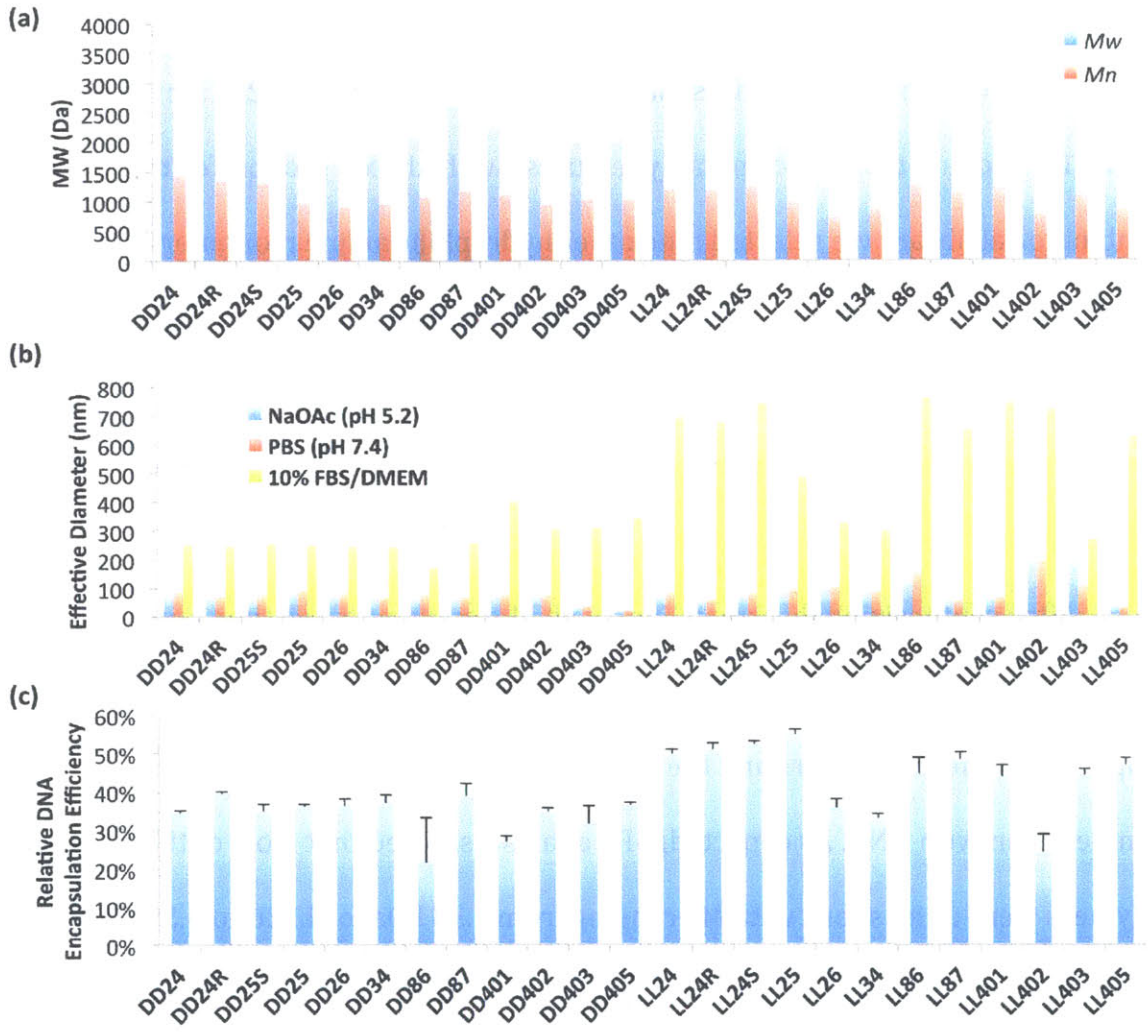

Figure 4.7 Biophysical properties of the DD24- and LL24-focused combinatorial library
(a) M_w and M_n of the terpolymers as determined by GPC analysis. **(b)** Particle diameters of the terpolymer/pDNA complexes formed in NaOAc buffer (pH 5.2) and then further diluted and measured by DLS as indicated. **(c)** Relative pDNA encapsulation efficiencies of the terpolymers as determined by a PicoGreen dye exclusion assay. Polyplexes were formed at a 20:1 w/w polymer:DNA ratio.

With respect to nanoparticle size, DLS measurements showed that most of these polymers were capable of forming sub-100 nm complexes with DNA in NaOAc at pH 5.2, with some swelling immediately after dilution in PBS at pH 7.4 (Figure 4.7b). However, the measured particle sizes in 10% FBS/DMEM media tended to be

more variable and generally quite large, reflecting some degree of aggregation. Most of the DD-containing polymers, with the exception of DD401, formed particles that remained sub-300 nm in serum-containing medium, whereas only LL26, LL34, and LL403 formed similarly tight particles in medium. The remainder of the LL-containing polymers grew in size to 600 nm or larger upon dilution in serum-containing medium. There was little variation in the nanoparticle sizes under these three conditions for the DD24 and LL24 polymers varying in tacticity.

Finally, we measured the relative DNA encapsulation efficiency at 20:1 polymer:DNA w/w ratio using a PicoGreen DNA-binding dye exclusion assay. In general, most of the DD-containing polymers were able to encapsulate ~35% of the DNA. However, DD86 was characterized by a lower encapsulation efficiency of only ~20%. Several of the LL-containing polymers, including LL24, LL25, LL86, and LL87, were characterized by relatively high DNA encapsulation efficiencies approaching 50%. The stereochemical variants of DD24 and LL24 did not show significant variation in DNA encapsulation efficiency.

When we transfected HeLa cells with these polymers, 21 of the 24 polymers in the library outperformed Lipofectamine 2000 (LF 2000) at a DNA dose of 50 ng per well (Figure 4.8). LL86, LL401, LL25, DD403, and DD87 in particular, showed excellent transfection activities along with the original library members DD24 and LL24. Polymer tacticity did not appear to affect transfection activity to a significant extent. One of the polymers that had the lowest DNA encapsulation efficiencies, DD86, also had the poorest DNA transfection activity in HeLa cells.

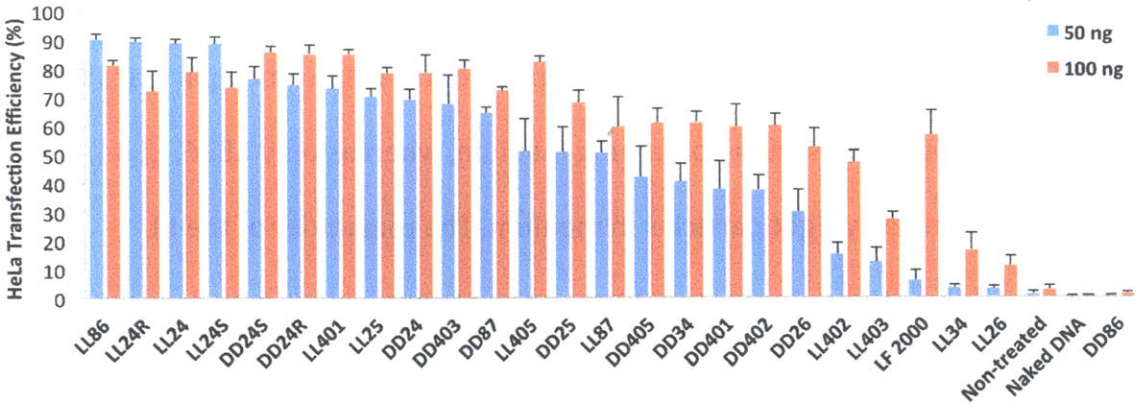

Figure 4.8 HeLa transfection efficiencies of the DD24- and LL24-focused combinatorial library
Transfection efficiencies in HeLa cells using the 24 members of the terpolymer library at a polymer:DNA w/w ratio of 20:1. Efficiencies were determined by FACS analysis of GFP expression two days after transfection of GFP-encoding pDNA.

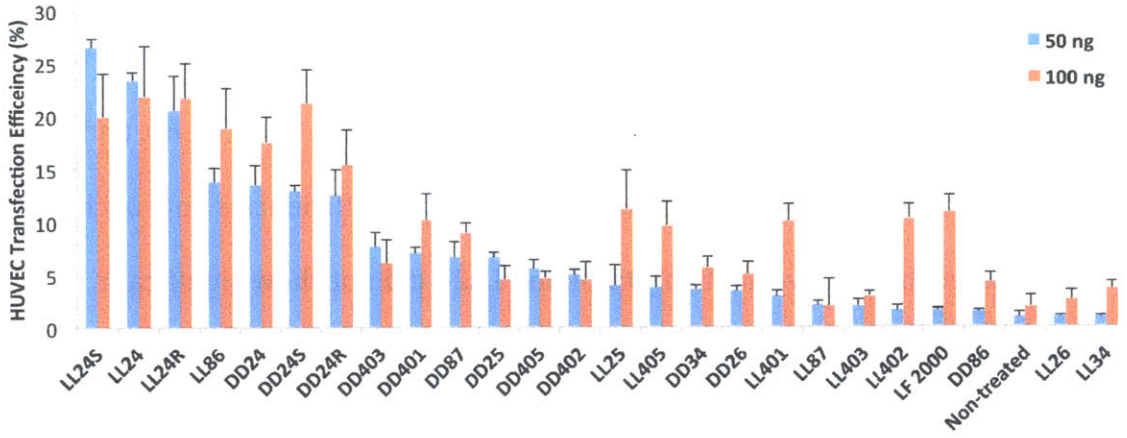

Figure 4.9 HUVEC transfection efficiencies of the DD24- and LL24-focused combinatorial library
Transfection efficiencies in HUVECs using the 24 members of the terpolymer library at a polymer:DNA w/w ratio of 20:1. Efficiencies were determined by FACS analysis of GFP expression two days after transfection of GFP-encoding pDNA.

In analogous fashion, we screened the polymers for DNA transfection efficiency in HUVECs, and we found that LL86, DD403, DD401, and DD87 displayed potent transfection activity along with the variants of DD24 and LL24. Notably, LL86, DD403, and DD87 were also among those polymers that performed best in

HeLa cells. At the other end of the performance spectrum, DD86, LL26, and LL34 again showed the three poorest transfection potencies, as they had in HeLa cells. As with HeLa cells, 21 of the 24 polymers displayed transfection efficiencies rivaling or outperforming LF 2000. These common trends suggest possible structural convergence with respect to optimal transfection activity.

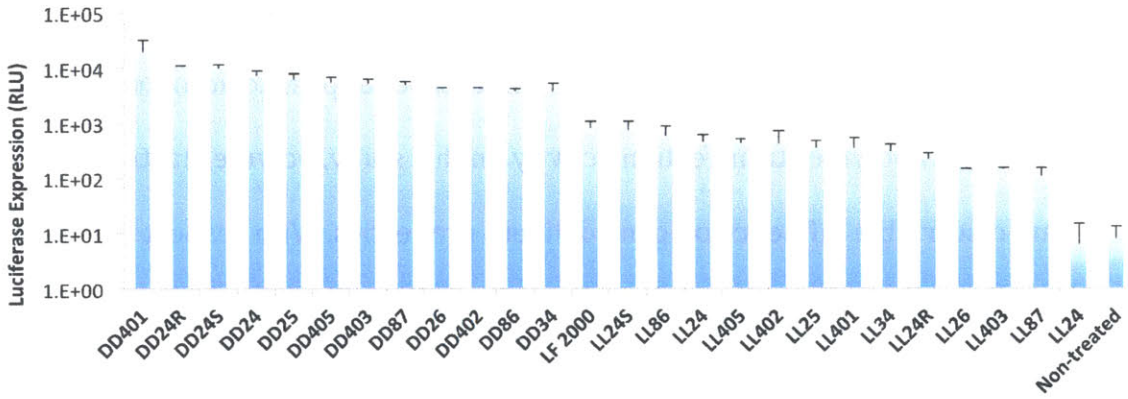

Figure 4.10 Rat cortical neuron transfection activities of the DD24- and LL24-focused combinatorial library
Transfection activities in rat cortical neurons using the 24 members of the terpolymer library at a polymer:DNA w/w ratio of 20:1. Relative luciferase expression was measured using a plate reader two days after transfection of luciferase-encoding pDNA.

Nonetheless, when we then screened the polymers for transfection of primary rat cortical neurons, we obtained very different results (Figure 4.10). In contrast to the previous experiments using GFP DNA and FACS analysis, this experiment was performed by complexing the polymers with luciferase-encoding DNA, incubating the nanoparticles with the cells for 4 hours, and then assaying for luminescence after two days. In this experiment, we observed that the structure of the diacrylate significantly influenced the measured transfection efficacy. All DD-

containing polymers, including DD86, demonstrated significantly enhanced transfection activity relative to LF 2000, whereas the LL-containing polymers displayed activity that was equivalent or worse. Surprisingly, only LL24 failed to mediate significant luciferase expression.

Taken together, these screening results suggest weak correlations between the measured polymer and nanoparticle properties and DNA transfection activity. Although there was some correlation between polymer DNA encapsulation efficiency and transfection activity, structural differences appear to account for most of the variation in polymer transfection activity. In this study, polymer tacticity showed no discernible influence on gene delivery properties. With respect to cell-type specificity, HeLa and HUVECs generally appeared to share common preferences with regard to gene delivery polymer structure. The intriguing preliminary experiment that suggests very different structural preferences in rat cortical neurons warrants further study to corroborate the observations and elucidate a mechanism.

4.3.3 PBAE terpolymer/DNA formulation development and in vivo transfection

The *in vitro* results described so far in this chapter have been performed using simple polyplexes, which tend to be relatively unstable at high concentrations under physiological conditions (as covered in detail in the Chapter 3). Ultimately, clinical application will require the development of stable formulations displaying excellent *in vivo* biocompatibility without compromising gene delivery efficacy. Toward this end, we explored the development of PBAE terpolymer nanoparticle formulations suitable for *in vivo* use. Using the nanoprecipitation approach

described previously, we co-dissolved D60-C12-122 (1.2:0.7:0.3 molar ratio of D:60:C12) with various PEG-lipid conjugates in acetonitrile and then pipet-mixed them with GFP-encoding plasmid DNA in sodium acetate buffer (pH 5.2). The PEG-lipid conjugates varied in the structure of the lipid tail (phosphoethanolamine/PE vs. ceramide; carbon chain length/saturation) as well as the PEG chain lengths (3 kDa or 5 kDa), and we used two molar ratios of the PEG-lipid conjugate to the polymer content (3% or 10%). The polymer:DNA weight ratio was held fixed at 20:1. Once prepared, the formulations were dialyzed against PBS for 3 h, and their transfection activities were compared in HeLa cells at a DNA dose of approximately 75 ng per well.

The results of this experiment demonstrate that the identity of the PEG-lipid conjugate strongly influences the stability of the nanoparticle formulations and their corresponding transfection efficacies (Figure 4.11). When the terpolymer/DNA nanoparticles are prepared without PEG-lipid, HeLa transfection efficiency was ~20%. In contrast, transfection efficiency was ~75% or higher with some of the formulation prepared with PEG-lipid conjugates, particularly C18:0 PEG PE (5 kDa PEG, 3 mol%), C16:0 PEG PE (5 kDa, 10 mol%), and C8 PEG ceramide (5 kDa, 10 mol%). Other formulations containing PEG-lipid conjugates did not improve transfection efficacy over the simple polyplexes, such as those containing C14:0 PEG PE (3 or 5 kDa, 3 mol%) and C16 PEG ceramide (5 kDa, 3 mol%).

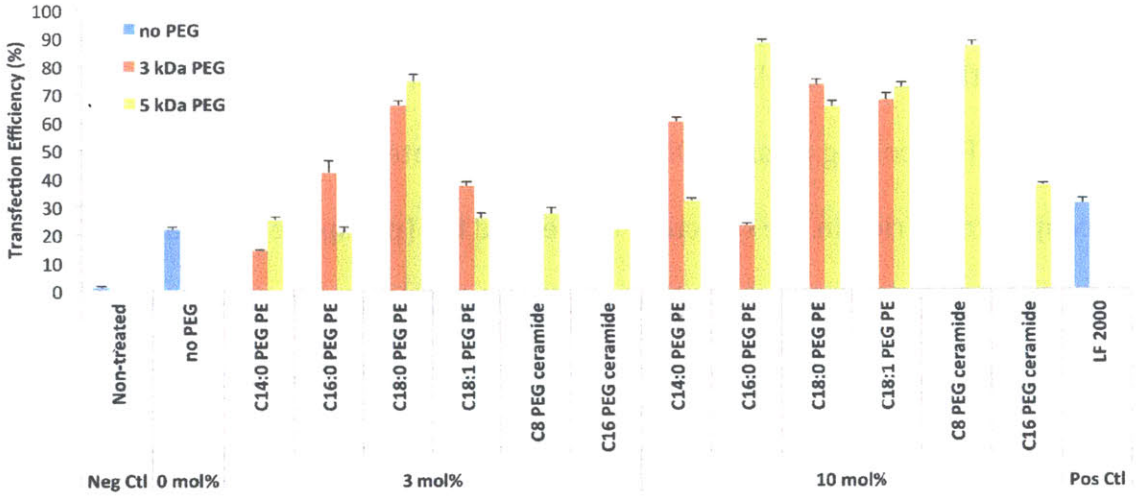

Figure 4.11 HeLa transfection efficiencies of D60-C12-122/DNA nanoparticle formulations containing various PEG-lipid conjugates
D60-C12-122 nanoparticle formulations containing various PEG-lipid conjugates were prepared by nanoprecipitation with GFP-encoding plasmid DNA and used to transfect HeLa cells 3 h after dialysis against PBS. FACS analysis was used after two days to quantify the proportion of cells expressing GFP.

In general, for the PEG-lipid conjugates containing phosphoethanolamine (PE), longer lipid tails, longer PEG, and a higher molar ratio of the PEG-lipid conjugate improved transfection efficacy. The observed trends make sense given that these factors should in principle promote nanoparticle stability and aggregation resistance during the dialysis against PBS. Nonetheless, for the PEG ceramide conjugates, while higher molar ratio improved performance, the conjugate with the shorter lipid tails (C8) was superior to that with the longer tails (C16). With the exception of one PEG ceramide formulation (C8, 5 kDa, 10 mol%), the PEG ceramide formulations were generally less efficacious than their PEG PE counterparts. Taken together, these data highlight the significance of certain structural features of PEG-lipid conjugates contributing to improved polymer/DNA nanoparticle stability and transfection activity.

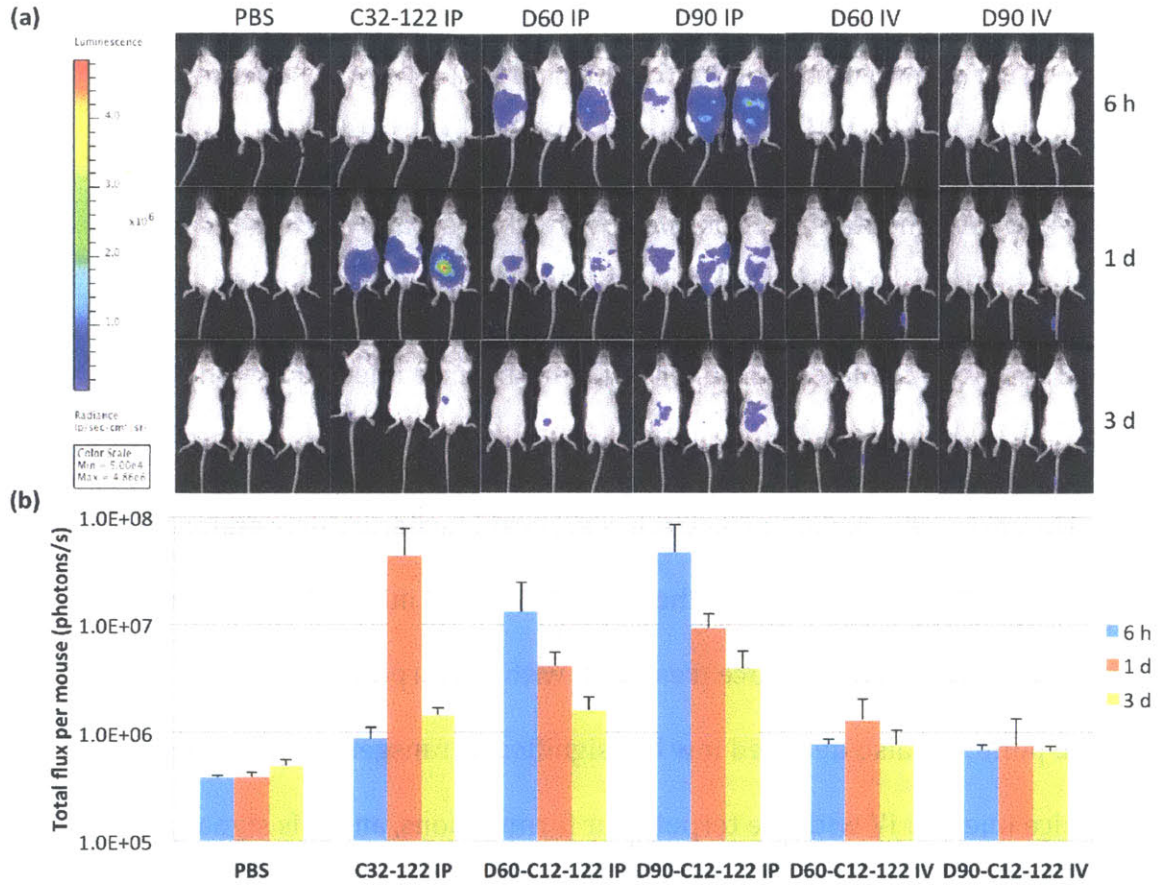

Figure 4.12 Intraperitoneal and intravenous gene delivery in mice using D60-C12-122 and D90-C12-122 terpolymers
(a) Whole-animal optical images of luciferase expression in BALB/c mice 6 hours, 1 day, and 3 days after injection of D60-C12-122 and D90-C12-122 formulations and C32-122 polyplexes. Radiance (photons/sec/cm^2/sr) is indicated in the color scale bar at left. **(b)** Quantification of whole-body luciferase expression (total flux/mouse) at various times after treatment as indicated (mean ± SD, n = 3 mice per group).

Using the results of this experiment, we then prepared D60-C12-122 and D90-C12-122 nanoparticle formulations with luciferase-encoding plasmid DNA and C16:0 PEG 5 kDa PE (20:1 w/w polymer:DNA; 10 mol% PEG-lipid). After dialysis against PBS for 3 h and storage overnight at 4°C, the formulations were administered to BALB/c mice via intraperitoneal (IP) or intravenous (IV) injections at approximately a 1 mg/kg DNA dose. We also administered freshly prepared C32-

122 polyplexes IP as a positive control. Whole-animal bioluminescence was assayed for each group at three time points (6 h, 1 d, and 3 d) following injection. We observed that the kinetics of expression varied for each of the treatment groups (Figure 4.12). At 6 h after injection, we observed moderately strong luciferase expression in the abdominal cavities of mice injected IP with the D60 and D90 formulations, with no detectable expression in the mice injected IV with these formulations or in the mice injected IP with the C32-122 polyplexes.

However, one day after injection, significant luciferase expression in the abdominal cavity was observed in the C32-122 treated mice, while luciferase expression decreased in the mice treated IP with the terpolymer formulations. At this time point, we also detected low but significant transgene expression in the tails of the mice injected IV with the terpolymer formulations, and this signal persisted at the 3 d time point. Meanwhile, at this 3 d time point, luciferase expression significantly decreased in all of the IP-injected animals, with the most durable expression observed in the mice treated with the D90 terpolymer formulations. These preliminary *in vivo* data suggest that the terpolymer formulations are capable of mediating significant transgene expression after IP or IV injection that persists for at least three days. Further experiments will be necessary to characterize the pharmacokinetics of expression in greater detail and to optimize the formulations and dosing for maximal *in vivo* transfection efficacy.

4.4 CONCLUSIONS

Through a series of screens, PBAE terpolymers were identified that mediated superior gene delivery to various difficult-to-transfect cell types relative to a popular commercially available lipid reagent, Lipofectamine 2000, and to one of the top-performing PBAE copolymers lacking alkyl side chains, C32-122. PBAE terpolymers, including DD24-C12-122 and LL24-C12-122, demonstrated excellent transfection potency in HUVECs, porcine MSCs, and neonatal rat cardiomyocytes. Synthesis and screening of a small library of terpolymers surrounding the chemical space of DD24-C12-122 and LL24-C122 identified polymers with high transfection efficacy in HeLa cells, HUVECs, and rat cortical neurons. While there was some correlation between polymer DNA encapsulation efficiency and transfection activity, structural differences appeared to account for most of the variation in polymer transfection activity. Finally, formulation development with the terpolymer D60-C12-122 suggested that the identity of the PEG-lipid conjugate strongly affects the stability of the nanoparticle formulations and their corresponding transfection efficacies. Following IP or IV administration, terpolymer formulations yielded observable transgene expression in mice that persisted for at least three days.

5 EFFECT OF MOLECULAR WEIGHT OF AMINE END-MODIFIED POLY(BETA-AMINO ESTER)S ON GENE DELIVERY EFFICIENCY AND TOXICITY†

5.1 INTRODUCTION

Gene therapy is a promising treatment strategy for many inherited disorders including cystic fibrosis, severe combined immunodeficiency, and hemophilia, in addition to cancer and infectious diseases such as AIDS. Despite recent clinical progress[1], concerns with the use of viral vectors, including immunogenicity, small DNA cargo capacity, and difficulty of large-scale production, have led to continued interest in the development of synthetic carriers[2]. A diverse collection of materials has been studied for potential as synthetic gene delivery agents, including lipids, polymers, polysaccharides, polypeptides, dendrimers, and inorganic nanoparticles[3]. However, sub-optimal delivery efficiency *in vivo* relative to viral vectors has inhibited their widespread clinical use[4, 5]. Though viruses have been naturally selected to efficiently navigate the multiple intra- and extra-cellular barriers to successful gene transfer, the flexibility of polymer chemistries offers great potential to identify and incorporate functionalities that confer not only

† This chapter has been published as Eltoukhy, A. A., Siegwart, D. J., Alabi, C. A., Rajan, J. S., Langer, R., Anderson, D. G. Effect of molecular weight of amine end-modified poly(β-amino ester)s on gene delivery efficiency and toxicity. *Biomaterials* **33**, 3594 (2012).

effective gene transfection, but also superior biocompatibility, enhanced formulation stability, and low toxicity[6, 7].

Toward this end, a more comprehensive understanding of the structure-property relationship for gene delivery polymers is critical to the elucidation of design principles for future generations of synthetic gene vectors. The molecular weight (MW) and molecular weight distribution (MWD) of cationic polymers are among the factors known to dramatically affect their gene delivery performance. For example, it was reported that higher MW poly(2-(dimethylamino)ethyl methacrylate (PDMAEMA), (M_w > 300 kDa) yielded greater *in vitro* gene transfection than polymers with lower MW (M_w < 60 kDa)[8]. This trend was confirmed more recently by another group, which found that transfection activity increased with the M_w of PDMAEMA up to at least 915 kDa[9]. Similarly, for various other polymeric carriers including trehalose-based glycopolymers[10], four-branched star vectors[11], and quaternized celluloses[12], higher MW was correlated with increasing gene delivery activity for the range of molecular weights examined. For poly(L-lysine) (PLL), however, polymers of intermediate length (M_w = 54 kDa) produced optimal gene transfection relative to longer (M_w = 225 kDa) or shorter (M_w < 22.4 kDa) variants[13], a phenomenon that has been attributed to an optimal rate of vector unpacking[14].

For polyethylenimine (PEI), there are a variety of studies on the relationship between polymer MW and DNA transfection activity. Using branched PEIs ranging in MW from 0.6 to 70 kDa, one group found that higher MW variants mediated significantly greater *in vitro* DNA transfection, which they speculated might owe to a

greater capacity for endosomal escape [15]. In contrast, another group reported that *in vitro* transfection activity decreased with increasing MW for three branched PEIs ranging in M_w from 1.8 to 70 kDa [16]. Likewise, in a comparison between a low MW PEI (M_w = 11.9 kDa) with low degrees of branching and a high MW, highly branched PEI (M_w = 1,616 kDa), it was observed the low MW variant had much greater transfection potency and lower toxicity[17]. In another study, 25 kDa branched PEI was fractionated by size, and a particular fraction with M_w of roughly 4-10 kDa displayed optimal performance relative to higher or lower MW fractions[18]. Finally, with linear PEIs ranging in M_w from 1.0-9.0 kDa, it was observed that at low N:P ratios, transfection generally increased with MW, but that at higher N:P ratios, polymers of intermediate length were superior[19].

Poly(β-amino esters) (PBAEs) are a promising class of polymeric gene vectors characterized by their ease of synthesis and biodegradability[20-24]. With their capacity to condense plasmid DNA (pDNA) into nanoparticles on the order of 50-200 nm in diameter, PBAEs have yielded high gene delivery efficiency to a variety of cell types with low toxicity[25, 26]. The use of combinatorial polymer library synthesis coupled with high-throughput screening and characterization has revealed structural motifs associated with highly active gene delivery polymers; in particular, the presence of hydroxyl groups in the side chains and the conjugation of certain primary amines to the chain ends dramatically modulate the efficiency of DNA transfection in different cell types[27-30]. Amine end-capped PBAEs, especially those based on poly(5-amino-1-pentanol-co-1,4-butanediol diacrylate) (C32), have demonstrated potential for a number of clinically relevant applications, including

suicide gene therapy for ovarian cancer[31], genetic modification of stem cells for treatment of ischemia[32], and gene transfer to glioblastoma cells[33]. However, the impact of chain length on nucleic acid delivery has not yet been systematically examined for this important group of degradable gene delivery polymers.

In this chapter, we applied two strategies to obtain amine end-modified PBAEs with variation in MW: modulation of monomer stoichiometry and preparative size exclusion chromatography (SEC). Using the first approach, we observed that polymers of intermediate MW mediated optimal DNA transfection activity. For these polymers, we did not observe a significant correlation between polymer MW and toxicity. Optimal performance was associated with higher DNA encapsulation efficiency and smaller nanoparticle size, but not with nanoparticle ζ-potential. However, using preparative SEC to obtain more monodisperse polymer fractions from a polydisperse starting polymer, we found that the transfection efficiencies of size-fractionated, well-defined PBAEs generally increased with MW. In addition, this approach allowed us to isolate polymer fractions that were more potent than the starting material, which indicates the potentially broad applicability of this separation technique for gene delivery polymers synthesized by step-growth polymerization.

5.2 Materials and Methods

5.2.1 Materials

1,4-butanediol diacrylate ("C") and 5-amino-1-pentanol ("32") were purchased from Alfa Aesar (Ward Hill, MA, USA). 1,3-diaminopropane ("103"), 1,3-

pentanediamine ("117"), and 2-methyl-1,5-pentanediamine ("118") were obtained from Sigma-Aldrich (St. Louis, MO, USA). $(PEO)_4$-*bis*-amine ("122") was acquired from Molecular Biosciences (Boulder, CO, USA). All reagents were used without further purification. Plasmid DNA encoding green fluorescent protein (gWiz-GFP) was purchased from Aldevron (Fargo, ND, USA). HeLa cells (ATCC, Manassas, VA, USA) were cultured in DMEM (Invitrogen, Carlsbad, CA, USA) supplemented with 10% fetal bovine serum (Invitrogen). Quant-IT PicoGreen dsDNA reagent was purchased from Invitrogen.

5.2.2 Polymer synthesis

Acrylate-terminated C32 poly(β-amino ester) was synthesized in ~5 g batches by reacting 1,4-butanediol diacrylate ("C") and 5-amino-1-pentanol ("32") in bulk at 70°C for 48 h with stirring. To obtain MW variants, 15 monomer molar ratios between 1:1 and 1.3:1 C:32 were chosen for polymerization: 1.0, 1.025, 1.04, 1.05, 1.06, 1.075, 1.1, 1.125, 1.15, 1.175, 1.2, 1.225, 1.25, 1.25, 1.275, and 1.3:1 (C:32). After cooling, 1 g of each batch was end-capped with 2 mmol of each of 4 different amines (103, 117, 118, and 122) by reaction in anhydrous tetrahydrofuran (THF) overnight at RT at a concentration of 100 mg/mL. The following day, the 60 resulting C32 variants were purified by precipitation in anhydrous hexanes (1:3 v/v THF:hexanes) and dried under vacuum for 24 h. Polymers were then dissolved at 100 mg/mL in dimethyl sulfoxide (DMSO) and stored at -20°C until use.

In a typical example, for the 1.1:1 C:32 molar ratio, 3.394 g C (17.12 mmol) was added to 1.605 g 32 (15.55 mmol) in a 20 mL glass vial equipped with stir bar

and sealed with a screw cap. It was heated in a reaction block at 70°C for 48 h with stirring. For end-modification of this polymer with the 103 amine, the 5 g batch of C32-Ac was cooled and then dissolved in 10 mL of anhydrous THF; of this solution, 2 mL was transferred to a 20 mL glass vial containing 8 mL of 103 amine at 0.25 M in THF (2 mmol). After stirring overnight at RT, the polymer was isolated by precipitation into hexanes and was then analyzed by SEC.

5.2.3 Analytical size exclusion chromatography (SEC)

Analytical SEC was performed using a Waters system (Milford, MA) equipped with a 2400 differential refractometer, 515 pump, and 717-plus autosampler. The flow rate was 1 mL/min and the mobile phase was THF. The Styragel columns (Waters) and detector were thermostated at 35ºC. Linear polystyrene standards were used for calibration.

5.2.4 in vitro GFP plasmid DNA transfection

One day before transfection, 15,000 HeLa cells in 100 μL of medium were seeded into each well of a 96-well polystyrene tissue culture plate. In a typical example, for a 600 ng/well DNA dose, pDNA was diluted to 0.06 mg/mL in 25 mM sodium acetate (NaOAc) buffer at pH 5.2. Polymers were thawed immediately prior to transfection and diluted in NaOAc buffer to a concentration 20, 30, or 40 times that of the DNA concentration, depending on the desired polymer:DNA w/w ratio. To form DNA-polymer nanoparticles, 25 μL of polymer solution was added to 25 μL of DNA in a half-area 96-well plate, mixed by repeated pipetting using a

multichannel pipette, and allowed to incubate for 5 min at RT. 30 μL of polymer-DNA complexes were then gently mixed with 195 μL of fresh medium warmed to 37°C. Conditioned medium was removed using a 12-channel aspirating wand and replaced with 150 μL of the complexes diluted in medium. Following a 4 h incubation, complexes were removed with the aid of a multi-channel aspiration wand and replaced with 100 μL of fresh medium. GFP expression was assessed 48 h after transfection by fluorescence-activated cell sorting (FACS).

5.2.5 FACS analysis

After aspirating conditioned medium, cells were washed with PBS and detached using 25 μL per well of 0.25% trypsin-EDTA (Invitrogen). 50 μL of FACS running buffer, consisting of 98% PBS, 2% FBS, and 1:200 v/v propidium iodide solution (Invitrogen), was added to each well. Cells were mixed thoroughly and then transferred to a 96-well round-bottom plate. GFP expression was measured using FACS on a BD LSR II (Becton Dickinson, San Jose, CA, USA). Propidium iodide (PI) staining was used to exclude dead cells from the analysis. PI staining was also used to determine the viabilities of treated cells relative to non-treated control cells, where the relative viability was calculated as the ratio of live (unstained) treated cells per well to the mean number of live non-treated cells per well. 2D gating was used to separate increased auto-fluorescence signals from increased GFP signals to more accurately count positively expressing cells. Gating and analysis were performed using FlowJo v8.8 software (TreeStar, Ashland, OR, USA).

5.2.6 *Dynamic light scattering (DLS) measurements*

To form complexes using the same concentrations and conditions that were optimal for transfection (40 w/w polymer:DNA), 150 μL of polymer at 2.4 mg/mL in NaOAc buffer was mixed with 150 μL of plasmid DNA (gWiz-GFP) at 0.06 mg/mL in NaOAc buffer. After incubation for 5 min at RT, 1.2 mL of 10% serum-containing medium was added to the mixture, which was then immediately subjected to DLS measurements using a ZetaPALS DLS detector (Brookhaven Instruments Corp., Holtsville, NY, USA, 15-mW laser, incident beam 676 nm). To ensure that all measurements represented the same time point of analysis, the size and ζ-potential data were obtained independently. Correlation functions were collected at a scattering angle of 90°, and particle sizes were calculated using the MAS option of BICs particle sizing software (v. 2.30) using the viscosity and refractive index of water at 25°C. Particle sizes are expressed as effective diameters assuming a log-normal distribution. Electrophoretic mobilities were measured at 25°C using BIC Phase Analysis Light Scattering (PALS) ζ-potential software, and ζ-potentials were calculated using the Smoluchowski model for aqueous suspensions.

5.2.7 *Dye exclusion assay*

The dye exclusion assay to determine polymer-DNA encapsulation efficiency was performed as described previously[29]. Briefly, a working solution of PicoGreen was prepared by diluting 80 μL of stock solution in 15.92 mL NaOAc buffer. In each well of a 96-well plate, 50 μL of polymer at 2.4 mg/mL in NaOAc buffer was added to

50 μL of DNA at 0.06 mg/mL in NaOAc buffer. After 5 min, 100 μL of PicoGreen working solution was added to the complexes. After an additional 5 min incubation, 30 μL was transferred to 200 μL of 10% serum-containing medium in a black 96-well assay plate. The fluorescence was then measured on a Tecan Infinite M1000 plate reader using the FITC filter set (excitation 485 nm, emission 535 nm). The reduction in relative fluorescence (RF), or the relative encapsulation efficiency, was calculated using the relationship $(F_{DNA} - F_{sample})/(F_{DNA} - F_{blank})$, where F_{sample} is the fluorescence of the polymer–DNA–PicoGreen sample, F_{DNA} is the fluorescence of DNA–PicoGreen (no polymer), and F_{blank} is the fluorescence of a sample with no polymer or DNA (only PicoGreen).

5.2.8 Preparative SEC

Polymers were fractionated based on size with a Phenogel 5μm MXL gel filtration column (300 mm x 7.8 mm, Phenomenex, P/No. 00H-3087-KO) using THF as the mobile phase at a flow rate of 1 mL/min. The separation was done on a 1200 Series Agilent HPLC system equipped with a UV diode array detector and a 1260 Infinity analytical scale fraction collector. The column compartment was kept at 40°C during fractionation. Polymer fractions were collected at 0.2 min intervals based on the absorption of the polymer at 254 nm. The fractions were transferred into tared vials, dried, weighed, and then dissolved to 100 mg/mL in DMSO. They were stored at -20°C until further use.

5.3 Results and Discussion

5.3.1 Synthesis and analytical SEC of stoichiometric PBAE variants

One straightforward method for molecular weight control of polymers synthesized by step-growth addition is to vary the stoichiometric ratio of the starting monomers. According to the Carothers relationship, the weight-average molecular weight M_w depends on the molar ratio of reactants r, the fractional monomer conversion p, and the molecular weight of the polymer repeat unit M_0 as follows: $M_w = M_0(1+p)(1+r)/(1-2pr+r)$. In this report, the PBAE C32 was synthesized using a range of 15 monomer molar feed ratios between 1:1 and 1.3:1 "C" (1,4-butanediol diacrylate) to "32" (5-amino-1-pentanol); these acrylate-terminated C32 polymers (C32-Ac) were then end-capped with each of four different amine molecules (Figure 5.1). These end-capping amines, denoted 103, 117, 118, and 122, were selected because they improved transfection performance relative to unmodified C32 polymer[28].

(A)

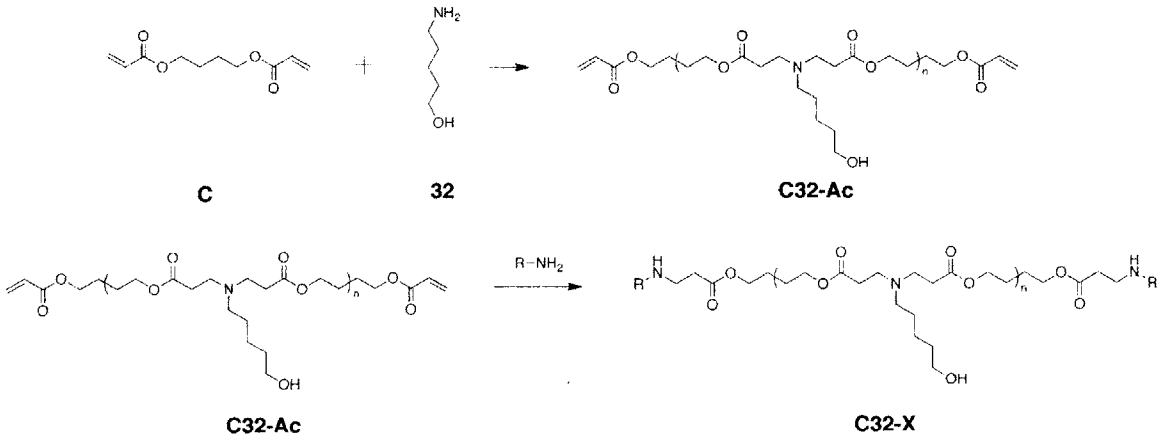

(B)

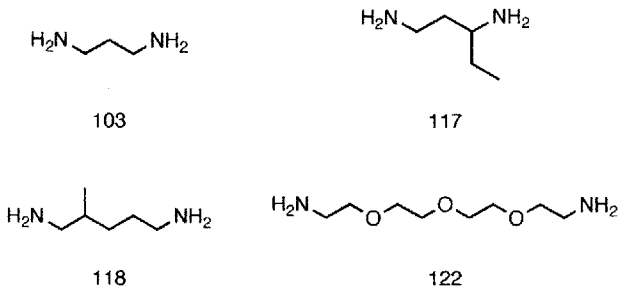

Figure 5.1 Synthesis scheme for end-modified poly(β-amino ester)s.
(A) 5-amino-1-pentanol (32) is added to an excess of 1,4-butanediol diacrylate (C) to yield acrylate-terminated C32, which is then reacted with excess amine to produce end-modified PBAE. **(B)** Structures of diamine molecules used for amine end-capping.

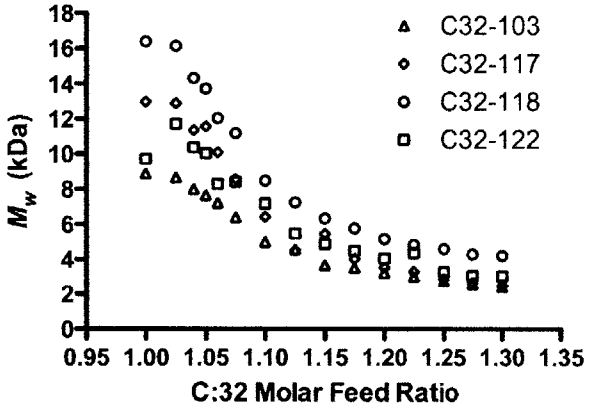

Figure 5.2 Relationship between M_w and C:32 monomer molar feed ratio for amine end-modified PBAEs

As expected, SEC analysis revealed that the molecular weight of these end-modified PBAEs decreased as the feed ratios deviated from stoichiometric unity (Figure 5.2). The polymers ranged in Mw from a maximum of 16.4 kDa for C32-118 synthesized at a feed ratio of 1:1 C:32 to a minimum of 2.4 kDa for C32-103

synthesized at 1.3:1 C:32. Because the end-modified polymers were synthesized from the same 15 batches of intermediate C32-Ac polymer, the differences in MW observed between end-modified PBAEs at the same monomer feed ratio may reflect a limited extent of polymer cross-linking or degradation.

5.3.2 Plasmid DNA transfection and cytotoxicity

To investigate the relationship between the molecular weight of end-modified PBAEs and *in vitro* transfection activity, we formed complexes using the synthesized polymers and GFP-encoding plasmid DNA (pDNA), and then incubated these nanoparticles with cultured HeLa cells in serum-containing growth medium for 4 h. Two days after transfection, we used fluorescence activated cell sorting (FACS) to quantify the proportion of HeLa cells expressing GFP.

When the transfection efficiencies of the various end-modified PBAEs were correlated with M_w, we observed that for a given weight ratio of polymer:DNA, polymers of intermediate length (M_w ~ 5-8 kDa) generally outperformed polymers with higher or lower M_w (Figure 5.3). For example, at a polymer:DNA w/w ratio of 40:1 (equivalent to N:P ratio of ~44:1), C32-122 with M_w = 5.5 kDa (synthesized at a C:32 molar feed ratio of 1.125:1) successfully transfected ~80% of HeLa cells, in contrast to ~26% for the highest MW variant (M_w = 11.7 kDa) and ~49% for the lowest MW variant (M_w = 3.0 kDa). At a lower polymer:DNA w/w ratio of 30:1 (N:P ~ 33), this trend of optimal transfection activity for polymers of intermediate MW persisted. However, at a w/w ratio of 20:1 or below (N:P ~ 22), none of the MW variants yielded significant transfection.

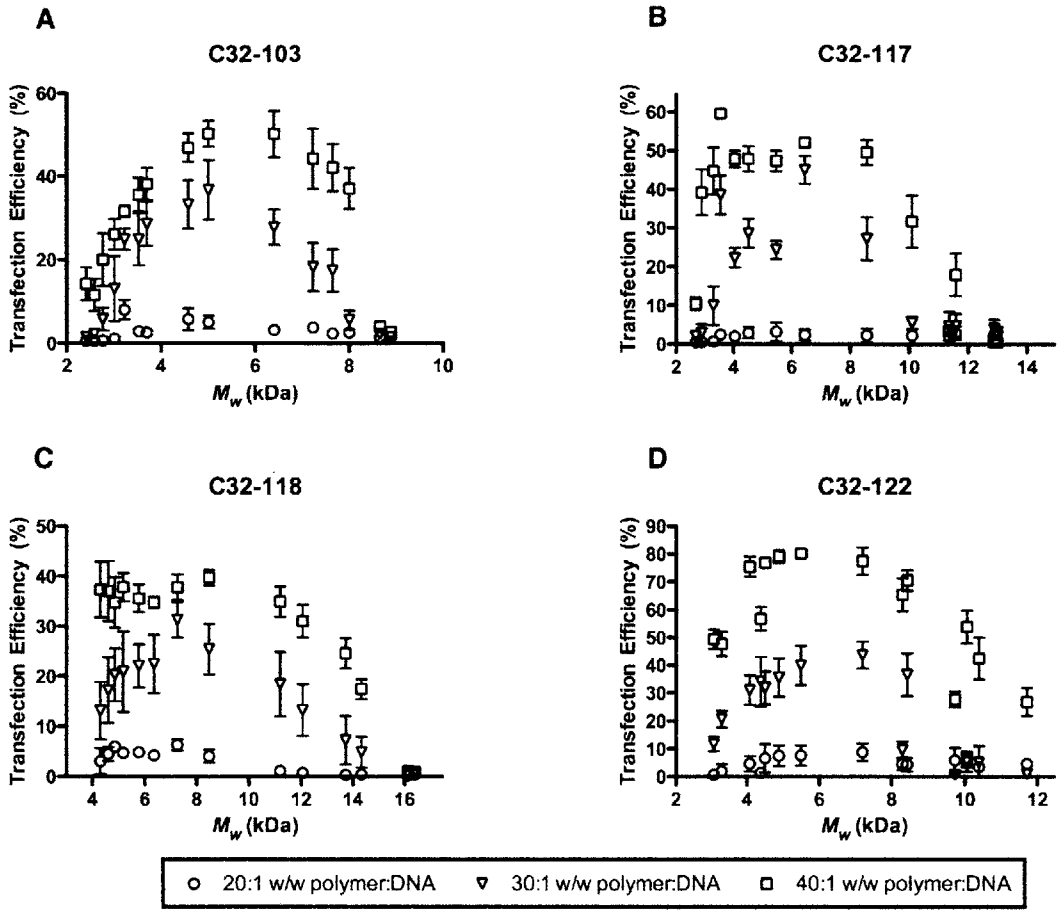

Figure 5.3 Correlation between polymer M_w and gene transfection efficiency in HeLa cells for PBAE stoichiometric variants
Correlation between PBAE M_w and DNA transfection efficiency (mean ± SD, n = 4) in HeLa cells for the stoichiometric variants of C32-103 **(A)**, C32-117 **(B)**, C32-118 **(C)**, and C32-122 **(D)**. The DNA dose is fixed at 600 ng per well of a 96-well plate and transfection was assessed by FACS 48 h.

Because of the frequent reports of a correlation between toxicity and polymer MW for many polymers, including PEI, we examined this relationship by staining transfected cells with propidium iodide immediately prior to FACS. When the viabilities of transfected cells relative to non-treated control cells were plotted against polymer M_w at the highest polymer:DNA w/w ratio used (40:1), we did not observe any significant association between the length of end-modified PBAEs and

their toxicity during transfection (Figure 5.4). Although there was some toxicity associated with C32-103 and C32-117, for each of these polymers, it did not increase with increasing MW. Importantly, for the most effective end-modified PBAE, C32-122, the relative viabilities of transfected cells were not significantly reduced. These results suggest that PBAEs have low toxicity over a wide range of MW, and therefore show promise as non-toxic transfection materials.

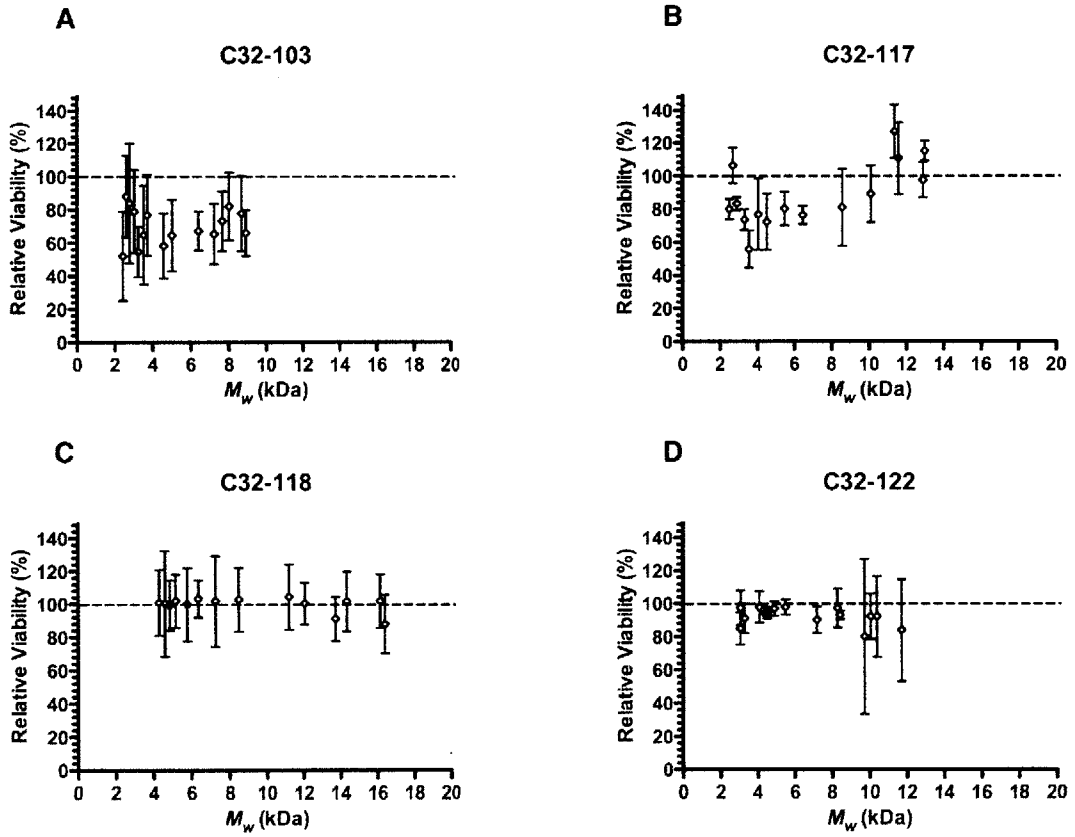

Figure 5.4 Correlation between polymer M_w and relative viability of HeLa cells following DNA transfection with PBAE stoichiometric variants
Correlation between polymer M_w and the relative viability (mean ± SD, n = 4) of HeLa cells following DNA transfection with the stoichiometric variants of C32-103 **(A)**, C32-117 **(B)**, C32-118 **(C)**, and C32-122 **(D)** at a polymer:DNA w/w ratio of 40:1. The DNA dose is held constant at 600 ng per well of a 96-well plate.

5.3.3 *Biophysical characterization of polymer/DNA nanoparticles*

For various other polymeric gene delivery systems, the relationship between MW and gene delivery has been associated with variation in nanoparticle size and charge. To assess the hypothesis that the dependence of transfection efficiency on the MW of end-modified PBAEs reflects biophysical characteristics of the polymer/DNA nanoparticles, we used dynamic light scattering (DLS) to measure the sizes and ζ-potentials of complexes formed from our stoichiometric variants. Polymers and plasmid DNA were mixed at the optimal weight ratio for transfection, 40:1 w/w polymer:DNA (N:P ~ 44:1). To replicate transfection conditions, complexes were prepared by repeated pipetting in 25 mM sodium acetate buffer at pH 5.2, incubated for 5 min at room temperature to allow for self-assembly, and then subjected to DLS immediately following dilution in 10% serum-containing medium.

We observed that for three of the four end-modified PBAEs, C32-118, C32-122, and to a limited extent, C32-103, polymer/DNA nanoparticle diameters were relatively uniform with respect to M_w up to ~6-8 kDa, but above this threshold, particle size increased with increasing M_w (Figure 5.5). The most effective end-modified PBAEs generally yielded nanoparticles less than 200 nm in size. In contrast to all of the other polymers tested, for C32-117, there was no clear association between polymer length and nanoparticle size, with all polymer variants resulting in complexes between 150-200 nm in diameter. Although for a given end-modified PBAE, smaller nanoparticles generally mediated more efficient transfection (Figure

5.6), the smallest complexes were never the most effective, which suggests the significance of factors other than particle size.

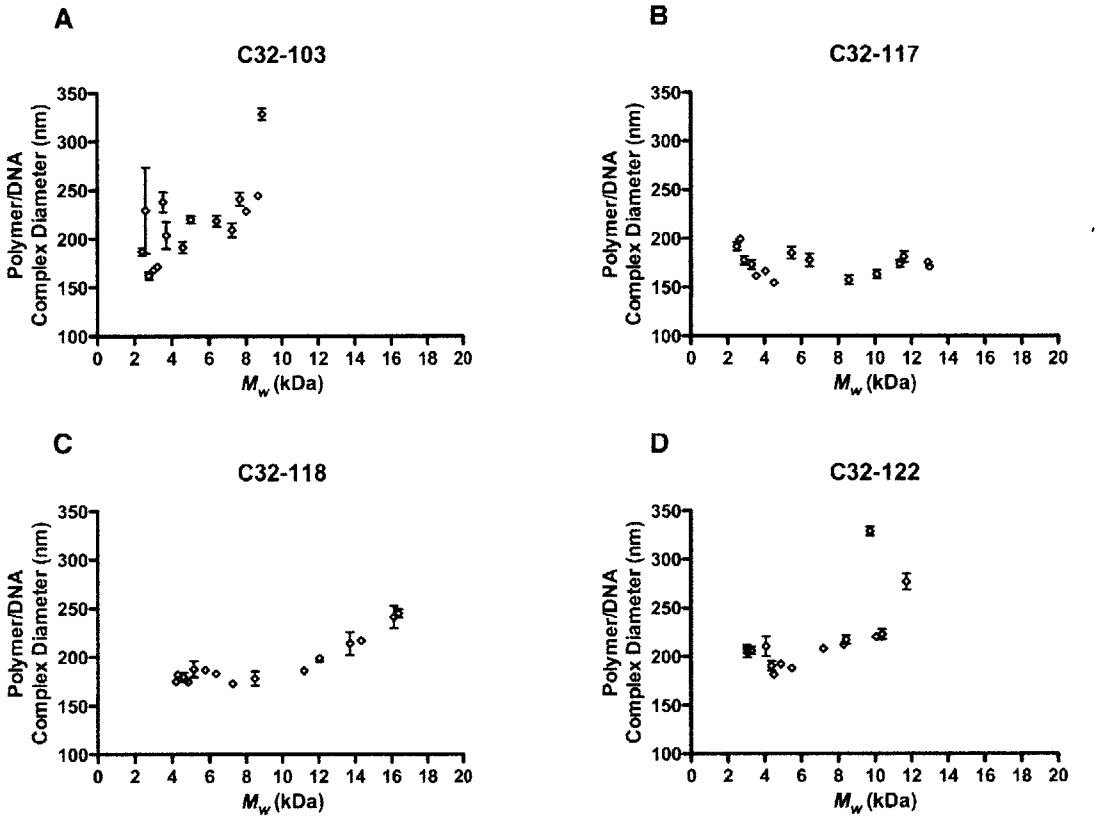

Figure 5.5 Correlation between polymer M_w and polyplex diameter for PBAE stoichiometric variants

Correlation between polymer M_w and diameter (mean ± SD, n = 3) of complexes formed from DNA and stoichiometric variants of C32-103 **(A)**, C32-117 **(B)**, C32-118 **(C)**, and C32-122 **(D)** at a polymer:DNA w/w ratio of 40:1. Polyplexes were formed in sodium acetate buffer at pH 5.2 and then diluted in serum-containing medium immediately prior to measurement.

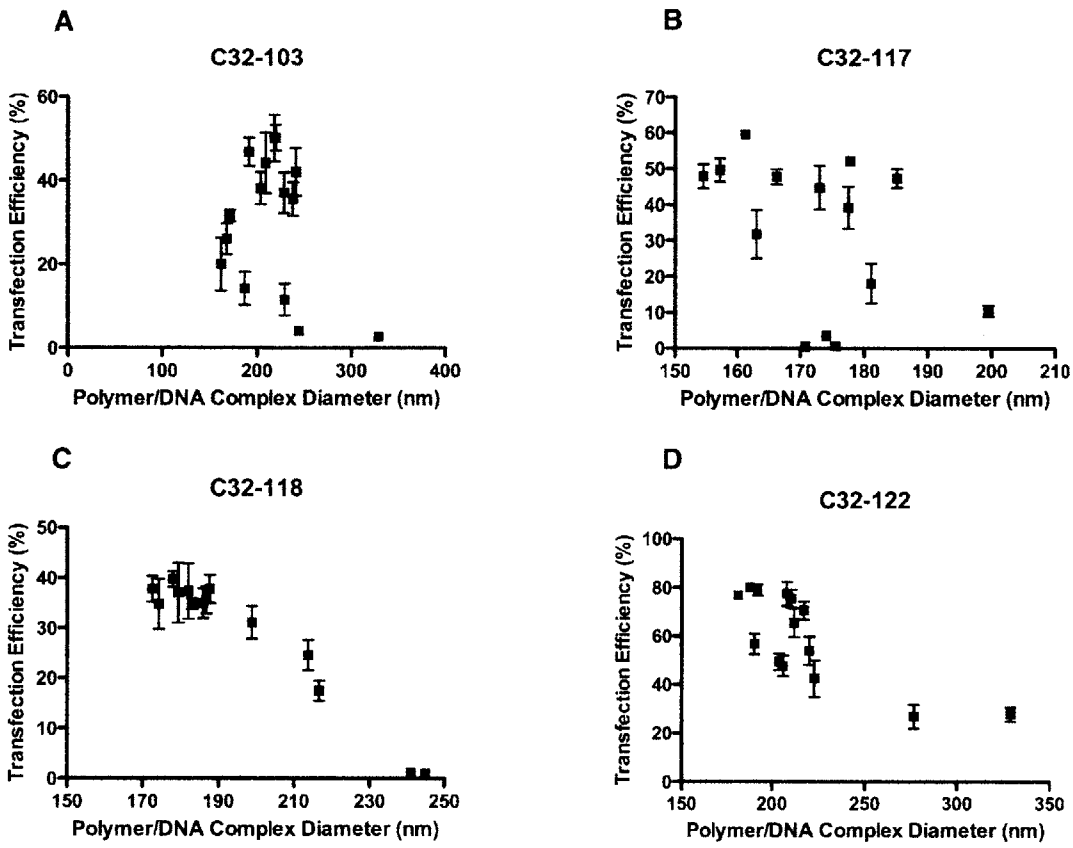

Figure 5.6 Correlation between gene transfection efficiency and polyplex diameter for PBAE stoichiometric variants.
Correlation between transfection efficiency (mean ± SD, n = 4) in HeLa cells and the mean diameters of complexes formed from DNA and stoichiometric variants of C32-103 (A), C32-117 (B), C32-118 (C), and C32-122 (D) at a polymer:DNA w/w ratio of 40:1. Polyplexes were formed in sodium acetate buffer at pH 5.2 and then diluted in serum-containing medium immediately prior to measurement.

Because we wanted a direct comparison with our *in vitro* transfection results, we chose to perform DLS analysis, including the charge measurements, with complexes that were diluted in serum-containing medium. Under these conditions, we observed no significant variation in the nanoparticle ζ-potential, with most polymers producing complexes that were near-neutral in serum-containing medium regardless of MW (Figure 5.7).

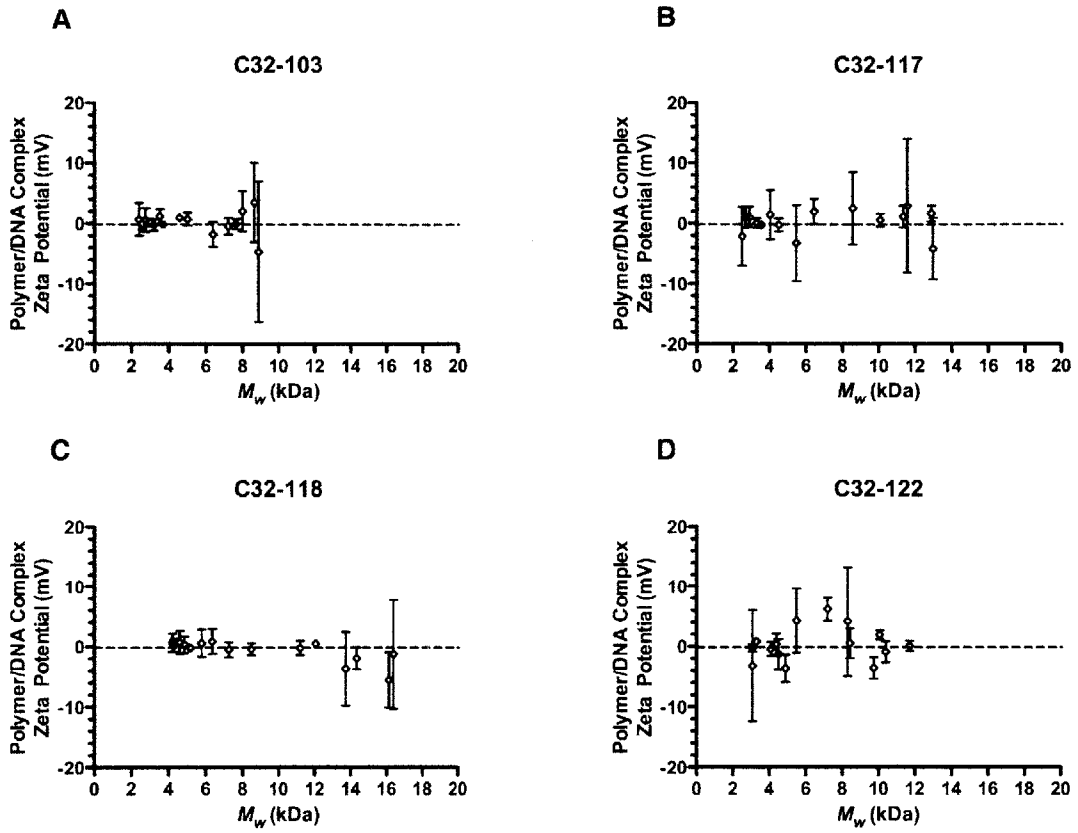

Figure 5.7 Correlation between polymer M_w and ζ-potential for PBAE stoichiometric variants
Correlation between polymer M_w and ζ-potential (mean ± SD, n = 3) of complexes formed from DNA and stoichiometric variants of C32-103 **(A)**, C32-117 **(B)**, C32-118 **(C)**, and C32-122 **(D)** at a polymer:DNA w/w ratio of 40:1. Polyplexes were formed in sodium acetate buffer at pH 5.2 and then diluted in serum-containing medium immediately prior to measurement.

We speculated that either the lack of a buffering agent or the presence of negatively-charged serum proteins could generate spurious data or otherwise mask an underlying trend. However, when we conducted charge measurements of C32-122/DNA nanoparticles in 25 mM sodium acetate buffer at pH 5.2, all particles were similarly characterized by near-neutral ζ-potentials within a narrow range of -1 to +1 mV (Figure 5.8). Therefore, for these end-modified PBAEs, the superior

transfection activity of polymers of intermediate length depends to a certain degree on smaller nanoparticle size, but is independent of nanoparticle charge.

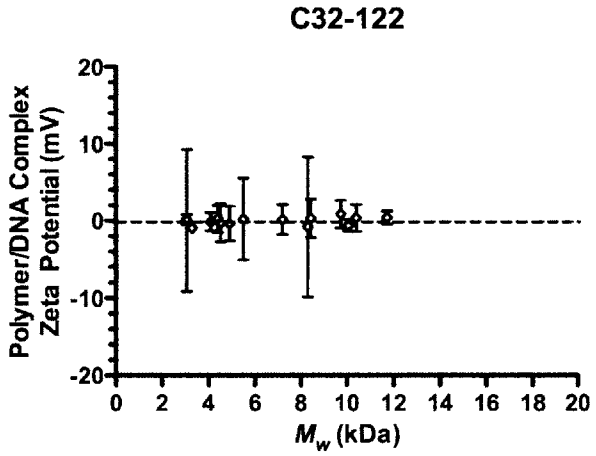

Figure 5.8 Correlation between polymer M_w and ζ-potential for C32-122 stoichiometric variants in sodium acetate buffer
Correlation between polymer M_w and ζ-potential (mean ± SD, n = 3) of complexes formed from DNA and stoichiometric variants of C32-122 at a polymer:DNA w/w ratio of 40:1. Polyplexes were formed and measured in sodium acetate buffer at pH 5.2.

5.3.4 Relative DNA binding efficiency

To assess whether the presence of an optimal polymer MW for transfection reflects enhanced condensation and loading of free plasmid DNA into nanoparticles, we quantified the DNA encapsulation efficiencies of these end-modified PBAE variants by measuring the reduction in relative fluorescence due to the protection of entrapped DNA from intercalation by the PicoGreen dye[34]. Using the same conditions as those for transfection as well as for the DLS measurements above, we found that for at least two of the four end-modified PBAEs, C32-103 and C32-117, polymers of intermediate MW entrapped plasmid DNA with greater efficiency than

higher or lower MW variants (Figure 5.9). For these polymers, the variants with the greatest gene delivery activity in HeLa cells also encapsulated DNA the most efficiently (Figure 5.10). For C32-118 and C32-122, however, encapsulation efficiency generally decreased with polymer MW, and the variants most effective at transfection did not coincide with those that entrapped DNA with the highest efficiency.

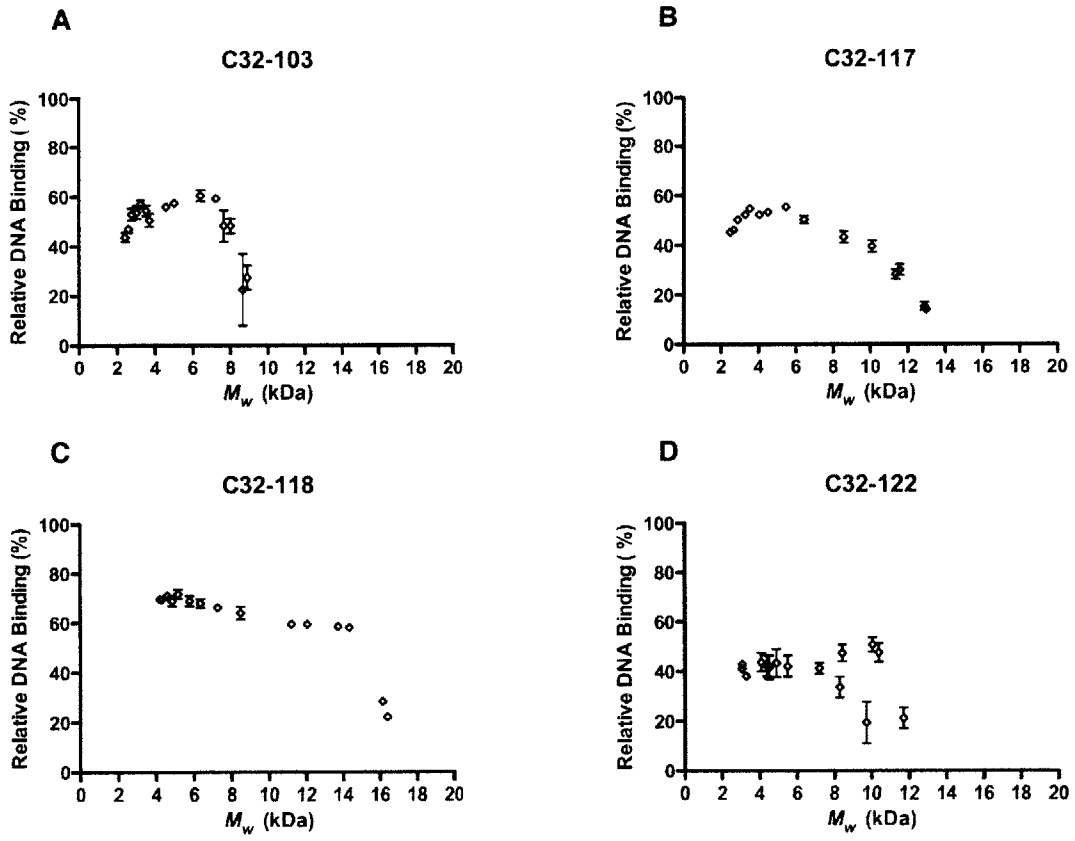

Figure 5.9 Correlation between polymer M_w and relative DNA binding for PBAE stoichiometric variants

Correlation between polymer M_w and relative DNA binding efficiency (mean ± SD, n = 3) of stoichiometric variants of C32-103 (A), C32-117 (B), C32-118 (C), and C32-122 (D) at a polymer:DNA w/w ratio of 40:1.

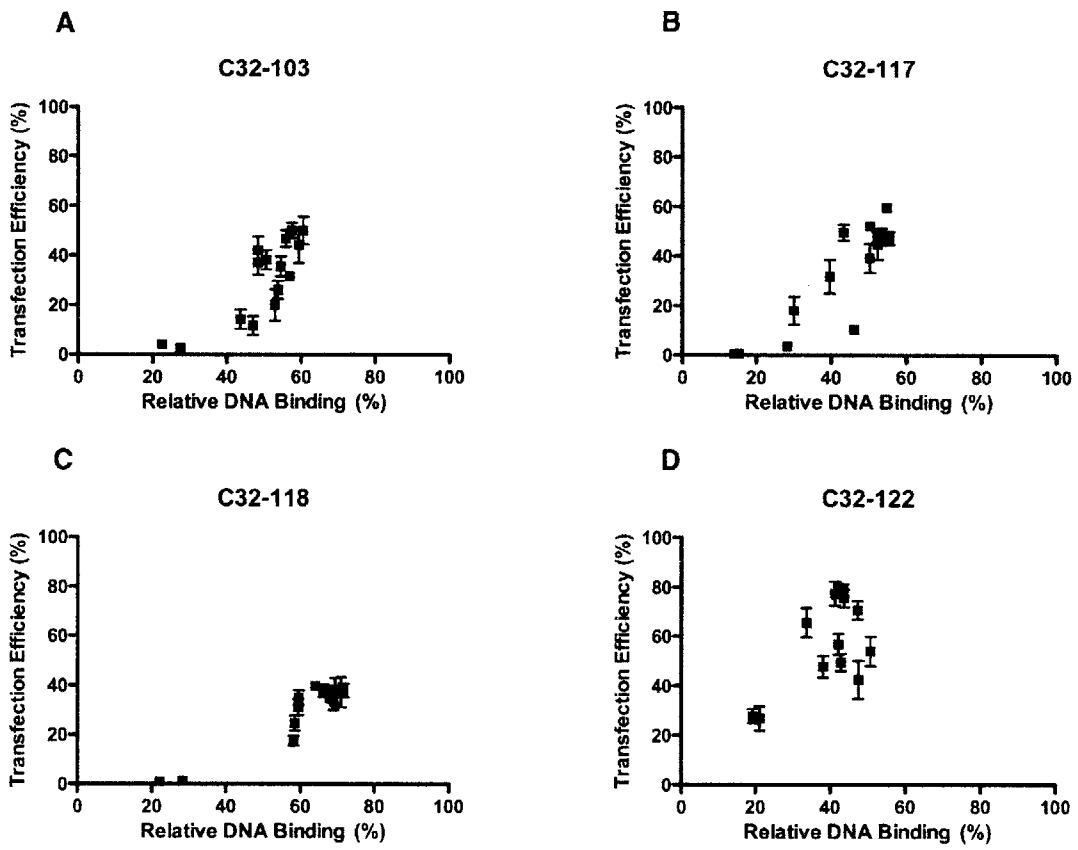

Figure 5.10 Correlation between gene transfection efficiency and relative DNA binding for PBAE stoichiometric variants
Correlation between transfection efficiency (mean ± SD, n = 4) in HeLa cells and relative DNA binding efficiency of stoichiometric variants of C32-103 **(A)**, C32-117 **(B)**, C32-118 **(C)**, and C32-122 **(D)** at a polymer:DNA w/w ratio of 40:1.

From these data, we hypothesize that at least for C32-103 and C32-117, the relatively high DNA entrapment efficiencies of polymers of intermediate MW contribute to their enhanced transfection. Though useful in establishing trends when comparing variants of a particular end-modified polymer, the encapsulation efficiency values obtained from this dye exclusion assay in general appeared to have limited predictive power with respect to transfection activity; for instance, C32-122 variants loaded DNA the least efficiently relative to other end-capped C32 polymers, but actually transfected HeLa cells the most efficiently. These results suggest that

for a given gene delivery polymer, DNA complexation efficiency is one important factor among others, including chemical composition and nanoparticle size, responsible for the variation in transfection activity due to polymer MW.

5.3.5 Preparative SEC

Although they vary in MW, the stoichiometric PBAE variants synthesized above through step-growth polymerization are characterized by broad MWDs. Besides their high polydispersity indices (PDIs), variation of the diacrylate:amine ratio in the polymerization reaction could alter the degree to which polymers are amine end-capped. To obtain polymers varying in MW, but characterized by a narrower MWD, we re-synthesized a particular feed ratio variant of C32-122 (C:32 = 1.1:1; M_w = 6.69 kDa, PDI = 1.50) and subjected it to preparative SEC using an HPLC system with an automated liquid fraction collector (Figure 5.11).

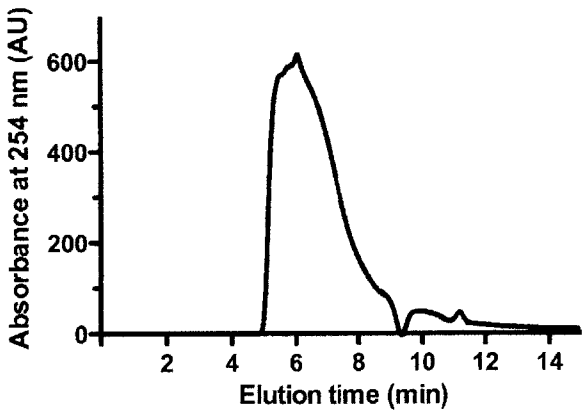

Figure 5.11 Chromatogram of C32-122 eluting from the HPLC/SEC column
An example chromatogram showing the elution of C32-122 polymer from the SEC column. Polymer fractions were collected at 0.2 min intervals between 5 and 9 min.

Analytical SEC of ~13 of the 20 fractions collected (representing ~75% of the total polymer mass loaded) revealed that M_w decreased smoothly with elution time (Figure 5.12**A**). Furthermore, this method allowed for the isolation of fractions with lower PDI (<1.2) than the crude polymer (Figure 5.12**B**).

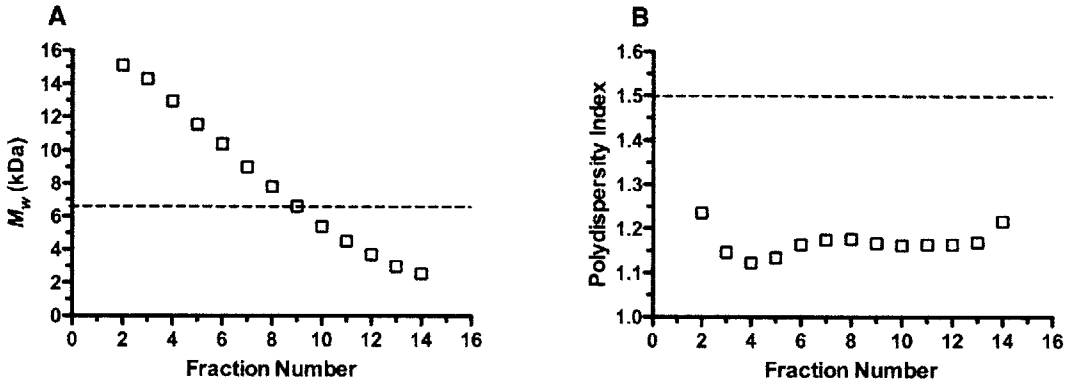

Figure 5.12 Preparative HPLC/SEC on C32-122
The M_w **(A)** and polydispersity indices **(B)** of various successive C32-122 polymer fractions collected by preparative SEC. The dashed lines represent the values for the crude, unfractionated polymer (M_w = 6.66 kDa, PDI = 1.50).

We performed a pDNA transfection experiment using these fractionated C32-122 polymers and assessed the overall transfection efficiency in HeLa cells after 48 h. When polymer length was correlated with transfection efficiency at high DNA doses and polymer:DNA w/w ratio, we observed that transfection efficiency generally increased with polymer M_w (Figure 5.13). At a lower DNA dose, or at a lower polymer:DNA w/w ratio, we found that some high MW fractions exhibited dramatically greater potency than fractions with low MW. These high MW fractions were also more potent than the crude, unfractionated polymer. For example, at a DNA dose of 150 ng per well with a polymer:DNA w/w ratio of 40:1, C32-122 with a

M_w of 12.9 kDa transfected ~62% of cells, in contrast to <10% for polymers below 5 kDa, and ~39% for the crude polymer.

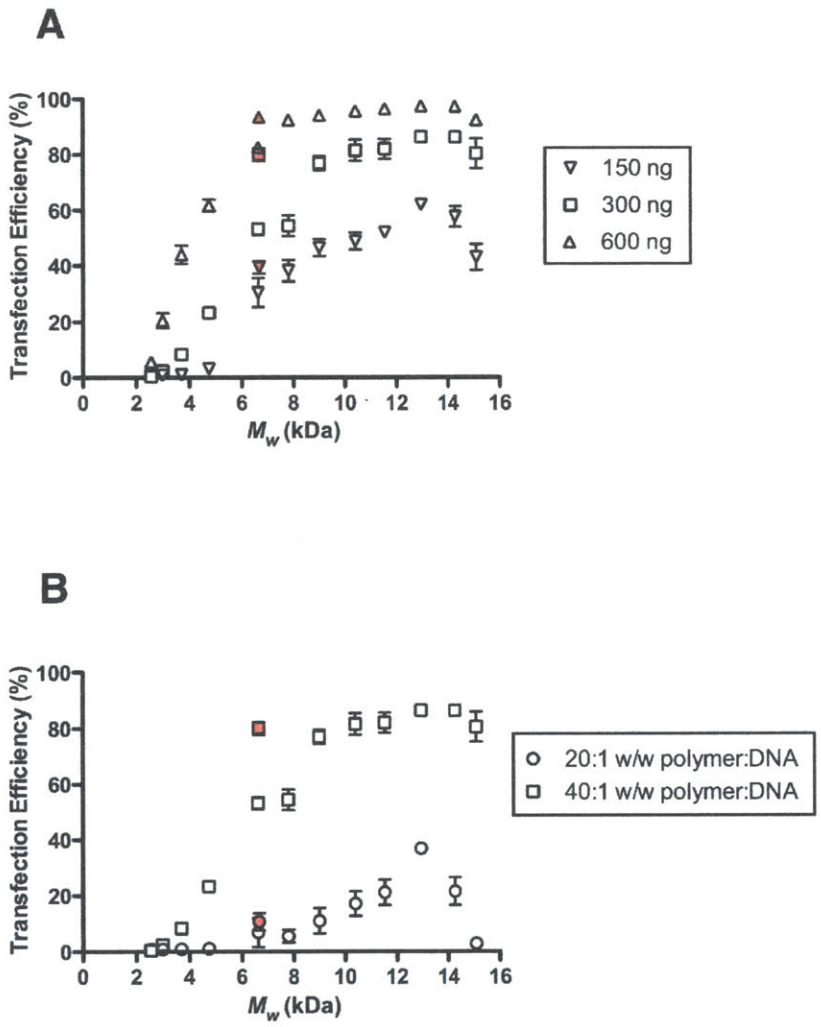

Figure 5.13 Correlation between gene transfection efficiency and M_w of C32-122 polymer fractions isolated by SEC

Correlation between DNA transfection efficiency (mean ± SD, n = 4) in HeLa cells and M_w of C32-122 polymer fractions isolated by SEC. In the left plot **(A)**, the DNA dose per well of a 96-well plate is varied as indicated as the polymer:DNA w/w ratio is held at 40:1. In the right plot **(B)**, the polymer:DNA w/w ratio is varied as the DNA dose is held at 300 ng/well. The filled symbols represent the activity of the crude polymer sample (mean ± SD, n = 4).

These transfection data underscore the importance of using freshly synthesized materials when working with degradable gene-delivery polymers, since the MW threshold for optimal performance can be rather narrow, and the consequence of a small degree of degradation accordingly steep. Furthermore, the isolation of monodisperse polymers improved consistency of physical properties across the samples, and enhanced delivery at higher MW.

When we conducted DLS measurements of the DNA nanoparticles formed using these size-fractionated polymers in serum-containing media, we did not observe significant variation in particle diameter; however, the variation in relative DNA binding efficiency among the size-fractionated polymers appeared to correlate to a certain extent with the observed transfection activities (Figure 5.14).

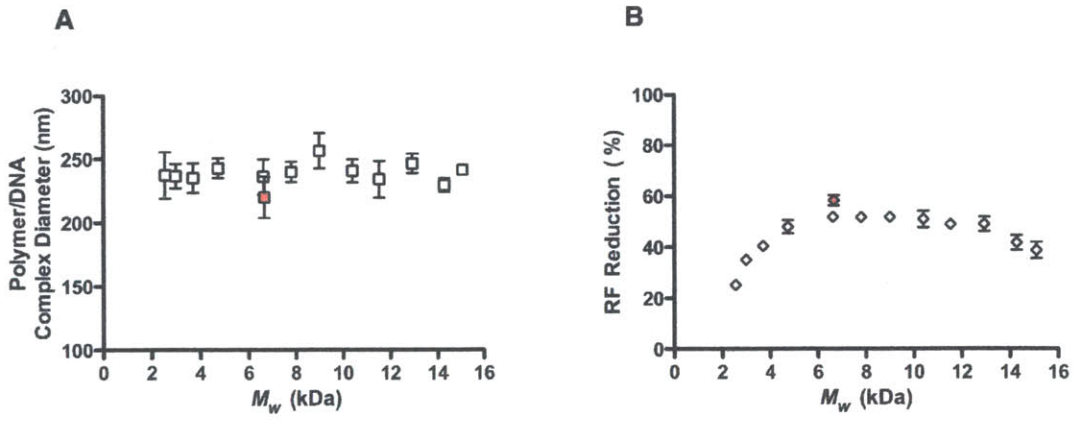

Figure 5.14 Correlation between nanoparticle biophysical properties and polymer M_w for C32-122 SEC fractions
Effective diameters **(A)** and relative DNA binding efficiencies **(B)** of nanoparticles formed from size-fractionated C32-122 at a polymer:DNA w/w ratio of 40:1 in serum-containing medium. The filled symbols represent the values for the crude polymer.

In contrast to our data with the polymer feed ratio variants, we did observe an association between polymer MW and relative cell viability following transfection, which was most prominent at the highest dose and polymer:DNA weight ratio tested (Figure 5.15). Given that under these conditions some polymer fractions transfected nearly 100% of cells, the transfection and viability data taken together imply that a careful selection of polymer MW, DNA dose, and weight ratio (in addition to other known variables such as cell density) could permit highly efficient gene delivery with low cytotoxicity.

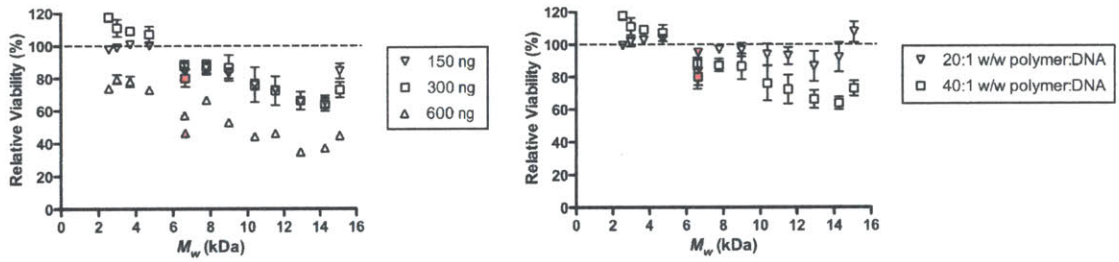

Figure 5.15 Correlation between M_w of C32-122 SEC fractions and relative viability following gene transfection in HeLa cells
Correlation between M_w of C32-122 polymer fractions isolated by SEC and the relative viability (mean ± SD, n = 4) of HeLa cells 48 h after transfection. In the left plot (A), the DNA dose per well of a 96-well plate is varied as indicated as the polymer:DNA w/w ratio is held at 40:1. In the right plot (B), the polymer:DNA w/w ratio is varied as the DNA dose is held at 300 ng/well. The filled symbols represent the activity of the crude polymer sample.

As suggested above, we hypothesize that the observed differences in trends between the C32-122 feed ratio variants and the size-fractionated C32-122 polymer likely result from the high polydispersity indices of the feed ratio variants as well as possible heterogeneity in the extent of amine end-modification. For researchers

working with gene delivery polymers synthesized by step-growth polymerization, our data highlight the potentially broad utility of preparative SEC for the isolation of well-defined, monodisperse fractions with higher transfection potency than the starting material. We expect that this approach should also help to reduce variability between batches of polymers.

Because both data sets suggested a role for DNA complexation efficiency in modulating the relationship between polymer MW and transfection activity, we hypothesize that the best gene delivery polymers owe their performance at least in part to an optimal balance of the rates of complex formation during particle assembly and unpacking within the cell. Additional studies are required to address this hypothesis in greater detail.

5.4 Conclusions

Working with amine end-modified PBAEs, a promising class of degradable gene delivery polymers, we investigated the effect of polymer MW on the transfection activity, toxicity, and biophysical properties of the resulting polymer-DNA nanoparticles. Using variation of monomer stoichiometry, we observed that polymers of intermediate length mediated optimal DNA transfection in HeLa cells. Characterization of these feed ratio variants suggested that optimal performance was related to higher polymer-DNA complexation efficiency and smaller nanoparticle size, but not to nanoparticle charge. In contrast, using preparative SEC to obtain well-defined, monodisperse polymer fractions, we observed that the

transfection activities of size-fractionated PBAEs generally increased with MW, a trend that was weakly associated with more efficient DNA binding. Our ability to isolate polymer fractions with higher transfection potency than the starting material indicates the potentially broad utility of this approach. These results further our understanding of the influence of polymer MWD on nucleic acid delivery, a critical aspect of the structure-property relationship for gene delivery materials.

5.5 REFERENCES

[1] Sheridan, C. Gene therapy finds its niche. *Nat. Biotechnol.* **29**, 459 (2011).

[2] Thomas, C. E., Ehrhardt, A., Kay, M. A. Progress and problems with the use of viral vectors for gene therapy. *Nat Rev Genet* **4**, 346 (2003).

[3] Mintzer, M. A., Simanek, E. E. Nonviral vectors for gene delivery. *Chem. Rev.* **109**, 259 (2009).

[4] Glover, D. J., Lipps, H. J., Jans, D. A. Towards safe, non-viral therapeutic gene expression in humans. *Nat Rev Genet* **6**, 299 (2005).

[5] Edelstein, M. in J Gene Med, Vol. 2011 (Wiley, 2011).

[6] Pack, D. W., Hoffman, A. S., Pun, S., Stayton, P. S. Design and development of polymers for gene delivery. *Nat Rev Drug Discov* **4**, 581 (2005).

[7] Wong, S. Y., Pelet, J. M., Putnam, D. Polymer systems for gene delivery--Past, present, and future. *Prog. Polym. Sci.* **32**, 799 (2007).

[8] van de Wetering, P., Cherng, J. Y., Talsma, H., Crommelin, D. J., Hennink, W. E. 2-(Dimethylamino)ethyl methacrylate based (co)polymers as gene transfer agents. *J Control Release* **53**, 145 (1998).

[9] Layman, J. M., Ramirez, S. M., Green, M. D., Long, T. E. Influence of polycation molecular weight on poly(2-dimethylaminoethyl methacrylate)-mediated DNA delivery in vitro. *Biomacromolecules* **10**, 1244 (2009).

[10] Srinivasachari, S., Liu, Y., Prevette, L. E., Reineke, T. M. Effects of trehalose click polymer length on pDNA complex stability and delivery efficacy. *Biomaterials* **28**, 2885 (2007).

[11] Nemoto, Y., Borovkov, A., Zhou, Y.-M., Takewa, Y., Tatsumi, E., Nakayama, Y. Impact of molecular weight in four-branched star vectors with narrow molecular weight distribution on gene delivery efficiency. *Bioconjug Chem* **20**, 2293 (2009).

[12] Song, Y., Wang, H., Zeng, X., Sun, Y., Zhang, X., Zhou, J., Zhang, L. Effect of molecular weight and degree of substitution of quaternized cellulose on the efficiency of gene transfection. *Bioconjug Chem* **21**, 1271 (2010).

[13] Wolfert, M. A., Dash, P. R., Nazarova, O., Oupicky, D., Seymour, L. W., Smart, S., Strohalm, J., Ulbrich, K. Polyelectrolyte vectors for gene delivery: influence of cationic polymer on biophysical properties of complexes formed with DNA. *Bioconjug Chem* **10**, 993 (1999).
[14] Schaffer, D. V., Fidelman, N. A., Dan, N., Lauffenburger, D. A. Vector unpacking as a potential barrier for receptor-mediated polyplex gene delivery. *Biotechnol. Bioeng.* **67**, 598 (2000).
[15] Godbey, W. T., Wu, K. K., Mikos, A. G. Size matters: molecular weight affects the efficiency of poly(ethylenimine) as a gene delivery vehicle. *J Biomed Mater Res* **45**, 268 (1999).
[16] Morimoto, K., Nishikawa, M., Kawakami, S., Nakano, T., Hattori, Y., Fumoto, S., Yamashita, F., Hashida, M. Molecular weight-dependent gene transfection activity of unmodified and galactosylated polyethyleneimine on hepatoma cells and mouse liver. *Mol Ther* **7**, 254 (2003).
[17] Fischer, D., Bieber, T., Li, Y., Elsässer, H. P., Kissel, T. A novel non-viral vector for DNA delivery based on low molecular weight, branched polyethylenimine: effect of molecular weight on transfection efficiency and cytotoxicity. *Pharm Res* **16**, 1273 (1999).
[18] Werth, S., Urban-Klein, B., Dai, L., Höbel, S., Grzelinski, M., Bakowsky, U., Czubayko, F., Aigner, A. A low molecular weight fraction of polyethylenimine (PEI) displays increased transfection efficiency of DNA and siRNA in fresh or lyophilized complexes. *Journal of Controlled Release* **112**, 257 (2006).
[19] Breunig, M., Lungwitz, U., Liebl, R., Fontanari, C., Klar, J., Kurtz, A., Blunk, T., Goepferich, A. Gene delivery with low molecular weight linear polyethylenimines. *J. Gene Med.* **7**, 1287 (2005).
[20] Lynn, D. M., Langer, R. Degradable Poly ([beta]-amino esters): Synthesis, Characterization, and Self-Assembly with Plasmid DNA. *J. Am. Chem. Soc* **122**, 10761 (2000).
[21] Lynn, D., Anderson, D., Putnam, D., Langer, R. Accelerated Discovery of Synthetic Transfection Vectors: Parallel Synthesis and Screening of a Degradable Polymer Library. *J. Am. Chem. Soc.* **123**, 8155 (2001).
[22] Akinc, A., Lynn, D., Anderson, D., Langer, R. Parallel Synthesis and Biophysical Characterization of a Degradable Polymer Library for Gene Delivery. *J. Am. Chem. Soc.* **125**, 5316 (2003).
[23] Anderson, D. G., Lynn, D. M., Langer, R. Semi-Automated Synthesis and Screening of a Large Library of Degradable Cationic Polymers for Gene Delivery. *Angew. Chem. Int. Ed.* **42**, 3153 (2003).
[24] Anderson, D. G., Peng, W., Akinc, A., Hossain, N., Kohn, A., Padera, R., Langer, R., Sawicki, J. A. A polymer library approach to suicide gene therapy for cancer. *Proc. Natl. Acad. Sci. USA* **101**, 16028 (2004).
[25] Luten, J., van Nostrum, C. F., De Smedt, S. C., Hennink, W. E. Biodegradable polymers as non-viral carriers for plasmid DNA delivery. *J Control Release* **126**, 97 (2008).
[26] Green, J. J., Langer, R., Anderson, D. G. A Combinatorial Polymer Library Approach Yields Insight into Nonviral Gene Delivery. *Acc Chem Res* **41**, 749 (2008).

[27] Anderson, D., Akinc, A., Hossain, N., Langer, R. Structure/property studies of polymeric gene delivery using a library of poly(beta-amino esters). *Mol Ther* **11**, 426 (2005).
[28] Zugates, G., Peng, W., Zumbuehl, A., Jhunjhunwala, S., Huang, Y., Langer, R., Sawicki, J., Anderson, D. Rapid Optimization of Gene Delivery by Parallel End-modification of Poly(β-amino ester)s. *Mol Ther* **15**, 1306 (2007).
[29] Green, J. J., Zugates, G. T., Tedford, N. C., Huang, Y., Griffith, L. G., Lauffenburger, D. A., Sawicki, J. A., Langer, R., Anderson, D. G. Combinatorial modification of degradable polymers enables transfection of human cells comparable to adenovirus. *Adv. Mater.* **19**, 2836 (2007).
[30] Sunshine, J., Green, J. J., Mahon, K. P., Yang, F., Eltoukhy, A. A., Nguyen, D. N., Langer, R., Anderson, D. G. Small-Molecule End-Groups of Linear Polymer Determine Cell-type Gene-Delivery Efficacy. *Adv. Mater.* **21**, 4947 (2009).
[31] Huang, Y. H., Zugates, G. T., Peng, W., Holtz, D., Dunton, C., Green, J. J., Hossain, N., Chernick, M. R., Padera, R. F., Jr., Langer, R., Anderson, D. G., Sawicki, J. A. Nanoparticle-delivered suicide gene therapy effectively reduces ovarian tumor burden in mice. *Cancer Res* **69**, 6184 (2009).
[32] Yang, F., Cho, S. W., Son, S. M., Bogatyrev, S. R., Singh, D., Green, J., Mei, Y., Park, S., Bhang, S. H., Kim, B. S., Langer, R., Anderson, D. Genetic engineering of human stem cells for enhanced angiogenesis using biodegradable polymeric nanoparticles. *Proc. Natl. Acad. Sci. USA* **107**, 3317 (2010).
[33] Tzeng, S. Y., Guerrero-Cazares, H., Martinez, E. E., Sunshine, J. C., Quinones-Hinojosa, A., Green, J. J. Non-viral gene delivery nanoparticles based on poly(beta-amino esters) for treatment of glioblastoma. *Biomaterials* **32**, 5402 (2011).
[34] Welz, C., Fahr, A. Spectroscopic Methods for Characterization oF Nonviral Gene Delivery Systems from a Pharmaceutical Point of View. *Applied Spectroscopy Reviews* **36**, 333 (2001).

6 THE CHOLESTEROL TRANSPORTER NIEMANN PICK C1 PLAYS A CRITICAL ROLE IN DNA INTERNALIZATION AND TRANSFECTION BY POLY(BETA-AMINO ESTER)S

6.1 INTRODUCTION

The tremendous medical promise of gene therapy remains largely unfulfilled due to the lack of safe and effective delivery vehicles[1]. Though regarded as efficient gene carriers, viral vectors also carry serious safety risks including insertional mutagenesis and adverse immune responses[2]. Non-viral gene vectors offer the possibility of improved safety, but have generally failed to attain satisfactory delivery efficacy in clinical testing[3, 4]. Unfortunately, the rational design of synthetic carriers is at present extremely challenging because of the limited mechanistic understanding of the numerous hurdles involved in gene delivery[5].

Cellular uptake constitutes an early step for which there is an increasingly refined picture of the endocytic pathways available for use by nanoparticles[6]. For most cells types other than phagocytes, these endocytic mechanisms include macropinocytosis, clathrin-dependent endocytosis, caveolae-mediated endocytosis, and a growing number of clathrin- and caveolae-independent pathways such as RhoA-dependent, Arf6-dependent, Cdc42-dependent, and flotillin-dependent endocytosis[7]. A handful of nanocarriers appear to rely predominantly on a single pathway. Certain kinds of poly(lactic-co-glycolic acid)(PLGA) nanoparticles, for instance, were reported to be internalized by vascular smooth muscle cells via

clathrin-dependent endocytosis[8-10], whereas DOXIL® and Abraxane® nanoparticles enter tumor cells via caveolae-mediated endocytosis[11, 12]. Macropinocytosis, meanwhile, appeared to be the major pathway used for entry in HeLa cells by siRNA-containing cationic lipid-based nanoparticles (LNPs) formulated with PEG[13]. Nonetheless, for most of the nanoparticles commonly used for non-viral gene delivery, including poly-L-lysine (PLL) and polyethylenimine (PEI)-based polyplexes, as well as various lipoplexes and liposomes, evidence exists for the use of multiple endocytic mechanisms[14-21].

Poly(beta-amino ester)s (PBAEs) are biodegradable cationic polymers that have demonstrated effective gene delivery in a variety of *in vitro* and *in vivo* contexts, including suicide gene therapy of several animal models of cancer[22-24] as well as genetic modification of stem cells for treatment of ischemia[25]. These polymers have consistently shown superior performance and less toxicity in several difficult-to-transfect cell types[26-28] compared to commercially available transfection reagents such as Lipofectamine 2000 (LF 2000). The versatility of the polymerization chemistry[29] has allowed a broad set of structures to be synthesized and screened in a high-throughput manner[30-34], allowing systematic investigation of key parameters affecting gene delivery potency such as polymer molecular weight distribution[35], hydrophobicity of the side chains[36], and amine end-group structure[37-40]. However, the endocytic mechanisms used by PBAEs for internalization have not yet been studied.

In this chapter, we explore the uptake of PBAE/DNA nanoparticles through complementary approaches including pharmacological inhibition and marker co-

localization studies. We observe that PBAE/DNA nanoparticles appear to enter immortalized mouse embryonic fibroblast (MEF) cells through multiple pathways, with an apparent requirement for normal cholesterol trafficking. We show that PBAE polyplex transfection efficacy is dramatically reduced in MEFs deficient in a late endosomal and lysosomal cholesterol transport protein, Niemann-Pick C1 (Npc1), mutations of which are associated with a fatal disease characterized by abnormal lysosomal accumulation of cholesterol[41].

Highlighting the role of this protein in endocytic uptake and cellular trafficking, Npc1-deficient cells were recently identified to inhibit endosomal escape and cellular entry of Ebola virus[42-44]; in contrast, retention and efficacy of lipid-based nanoparticles for siRNA delivery were greatly enhanced in *Npc1-/-* cells (Sahay et al., forthcoming). Here, we find that Npc1 knockout in MEFs greatly inhibits PBAE-mediated DNA internalization, with a slight decrease in DNA uptake mediated by PEI and no apparent effect on DNA uptake mediated by LF 2000. We show that retention of various endocytic markers is altered in Npc1-deficient MEFs, with over 20-fold reduction in uptake of cholera toxin B, two-fold reduction in uptake of transferrin, and ~50%-increase in uptake of dextran. PBAE/DNA polyplexes showed the greatest extent of co-localization with cholera toxin B, suggesting the involvement of shared uptake pathways that are altered in cells lacking Npc1. These studies provide further evidence that Npc1 plays a key role in regulating endocytic mechanisms affecting internalization and efficacy of nanoparticles.

6.2 MATERIALS AND METHODS

6.2.1 Materials

1,4-butanediol diacrylate and 5-amino-1-pentanol were purchased from Alfa Aesar (Ward Hill, MA, USA). Dodecylamine was purchased from Sigma-Aldrich (St. Louis, MO, USA). $(PEO)_4$-*bis*-amine ("122") was acquired from Molecular Biosciences (Boulder, CO, USA). All chemical reagents were used without further purification. Plasmids encoding green fluorescent protein (gWiz-GFP) and firefly luciferase (gWiz-Luc) were purchased from Aldevron (Fargo, ND, USA). jetPEI (Polyplus Transfection, Illkirch, France) and Lipofectamine 2000 were purchased from VWR (Radnor, PA, USA) and Invitrogen (Carlsbad, CA, USA), respectively. Transferrin, cholera toxin B, and 10,000 MW dextran, each labeled with AlexaFluor 647, were purchased from Invitrogen. Cytochalasin D, dynasore hydrate, chlorpromazine hydrochloride, filipin III, genistein, methyl-β-cyclodextrin, 5-(N-ethyl-N-isopropyl)amiloride (EIPA), and U18666A were obtained from Sigma-Aldrich. Immortalized mouse embryonic fibroblast (MEF) cell lineswere cultured in DMEM (Invitrogen) supplemented with 10% fetal bovine serum (Invitrogen).

6.2.2 Polymer synthesis

To synthesize C32-122, acrylate-terminated C32 poly(β-amino ester) was first prepared in a 5 g batch by reacting 1,4-butanediol diacrylate ("C") and 5-amino-1-pentanol ("32") (1.2:1.0 diacrylate:amine molar ratio) without solvent at 90°C for 24 h with stirring. After cooling to RT and dissolving the polymer in 10 mL of

anhydrous THF, it was added to a vial containing 10 mmol of $(PEO)_4$-*bis*-amine (10 mmol in 40 mL anhydrous THF). Following overnight stirring at RT, the amine end-modified polymer was purified by precipitation in anhydrous diethyl ether (1:3 v/v THF:ether) and dried under vacuum for 24 h. C32-122 was then dissolved at 100 mg/mL in dimethyl sulfoxide (DMSO) and stored at -20°C with desiccant until use.

For synthesis of C32-122 terpolymers containing C12 alkyl side chains, dodecylamine, 5-amino-1-pentanol, and 1,4-butanediol diacrylate were sequentially added to a vial equipped with stir bar such that the total mass of monomers was 200 mg, the diacrylate:amine monomer molar ratio was 1.2:1.0, and the molar ratios of the amines C12:32 varied as indicated (0% C12 = 0:1 C12:32, 10% = 0.1:0.9, 20% = 0.2:0.8, etc.). After heating and stirring at 90°C for 48 h, the reactions were allowed to cool to RT, then dissolved in 1 mL of DMSO, to which a solution of $(PEO)_4$-*bis*-amine (0.8 mmol in 1 mL DMSO) was added. The reactions were stirred at RT overnight and then stored frozen with desiccant at -20°C.

6.2.3 DNA transfection experiments

One day before transfection, cells (100 μl) were seeded into each well of a 96-well polystyrene tissue culture plate (HeLa: 12,500 per well; MEFs: 9,000 per well). For studies using the pharmacological inhibitors, conditioned medium was removed 1 hour prior to transfection and replaced with fresh, pre-warmed medium containing the indicated concentration of pharmacological inhibitor. For GFP transfection experiments, gWiz-GFP (5 mg ml^{-1}) was diluted to 160 μg ml^{-1} in 25 mM sodium acetate (NaOAc) buffer at pH 5.2; for DNA uptake experiments, gWiz-Luc

was labeled with Cy3 or Cy5 using the LabelIt kit (Mirus, Madison, WI, USA) following the manufacturer's instructions, and was diluted in NaOAc buffer as above. PBAEs (100 mg ml^{-1}) were thawed immediately prior to transfection and diluted in NaOAc buffer to a concentration of 3.2 mg ml^{-1} (20:1 w/w polymer:DNA). To form DNA-polymer nanoparticles, polymer solution (200 μl) was added to the diluted DNA (200 μl), mixed by repeated pipetting, and allowed to incubate for 10 min at RT. Depending on the dose, polymer-DNA complexes were diluted in NaOAc as needed, and then were gently mixed in a deep 96-well plate with pre-warmed fresh medium (360 μl). For inhibition experiments, this medium was prepared with the indicated concentration of pharmacological inhibitor, whereas for co-localization experiments, labeled transferrin, cholera toxin B, or dextran were present. Conditioned medium was removed using a 12-channel aspirating wand and replaced with the complexes diluted in medium (100 μl). jetPEI and Lipofectamine 2000 were used according to the manufacturers' protocols.

For GFP transfection experiments, following a 3-h incubation at 37°C, complexes were removed with the aid of a multi-channel aspiration wand and replaced with fresh medium (100 μl), and the cells were analyzed for GFP expression by fluorescence-activated cell sorting (FACS) after 24 h at 37°C. For DNA uptake experiments, cells were washed three times at the indicated time point and prepared for analysis by either confocal microscopy or FACS.

6.2.4 FACS analysis

After aspirating conditioned medium and washing cells three times with PBS, cells were detached using 25 µl per well of 0.25% trypsin-EDTA (Invitrogen). Following a 5 min incubation at 37°C, fresh medium (50 µl) was added to the cells, which were mixed thoroughly and then transferred to a 96-well round-bottom plate. Cells were then pelleted, re-suspended in fixation buffer (4% v/v formaldehyde in PBS), incubated for 10 min at RT, pelleted again, and finally re-suspended in ice-cold FACS running buffer (2% v/v FBS in PBS) containing 1:200 v/v propidium iodide (Invitrogen). The cells were kept at 4°C until FACS analysis using a BD LSR II (Becton Dickinson, San Jose, CA, USA). Except for experiments with Cy3-labeled DNA, propidium iodide (PI) staining was used to exclude dead cells from the analysis. PI staining was also used to determine the viabilities of treated cells relative to non-treated control cells, where the relative viability was calculated as the ratio of live (unstained) treated cells per well to the mean number of live non-treated cells per well. For GFP expression analysis, 2D gating was used to separate increased auto-fluorescence signals from increased GFP signals to more accurately count positively expressing cells. Gating and analysis were performed using FlowJo v8.8 software (TreeStar, Ashland, OR, USA). Geometric mean fluorescent intensities of transfected cells were normalized to those of the corresponding non-transfected control cells.

6.3 Results and Discussion

6.3.1 Pharmacological inhibition studies

One approach toward identification of the endocytic mechanisms utilized by nanomaterials involves the use of pharmacologic inhibitors known to interfere with certain uptake pathways. However, this approach has concomitant disadvantages including a lack of pathway selectivity and the induction of toxicity at excessive doses. With these caveats in mind, we screened a set of such inhibitors for their potential to reduce cellular internalization of labeled DNA by C32-122, one of the top-performing amine end-modified poly(β-amino ester) (PBAE) polymers[35]. The inhibitors we initially tested and the pathways these molecules are thought to inhibit are provided in Table 6.1.

Inhibitor	Pathway	Concentrations (μM)
Cytochalasin D	Actin-dependent pathways	10, 1, 0.5, 0.05
Dynasore	Clathrin & caveolar (dynamin-dependent)	100, 10, 1.0, 0.1
Chlorpromazine	Clathrin-mediated	100, 10, 1.0, 0.1
Filipin	Caveolar	100, 10, 1.0, 0.1
5-(N-ethyl-N-isopropyl)amiloride (EIPA)	Macropinocytosis	100, 10, 1.0, 0.1
U18666A	Cholesterol synthesis/trafficking	100, 10, 1.0, 0.1

Table 6.1 Pharmacologic inhibitors tested in the initial screen
The set of pharmacologic inhibitors included in the initial screen along with the pathways they target and the concentrations tested.

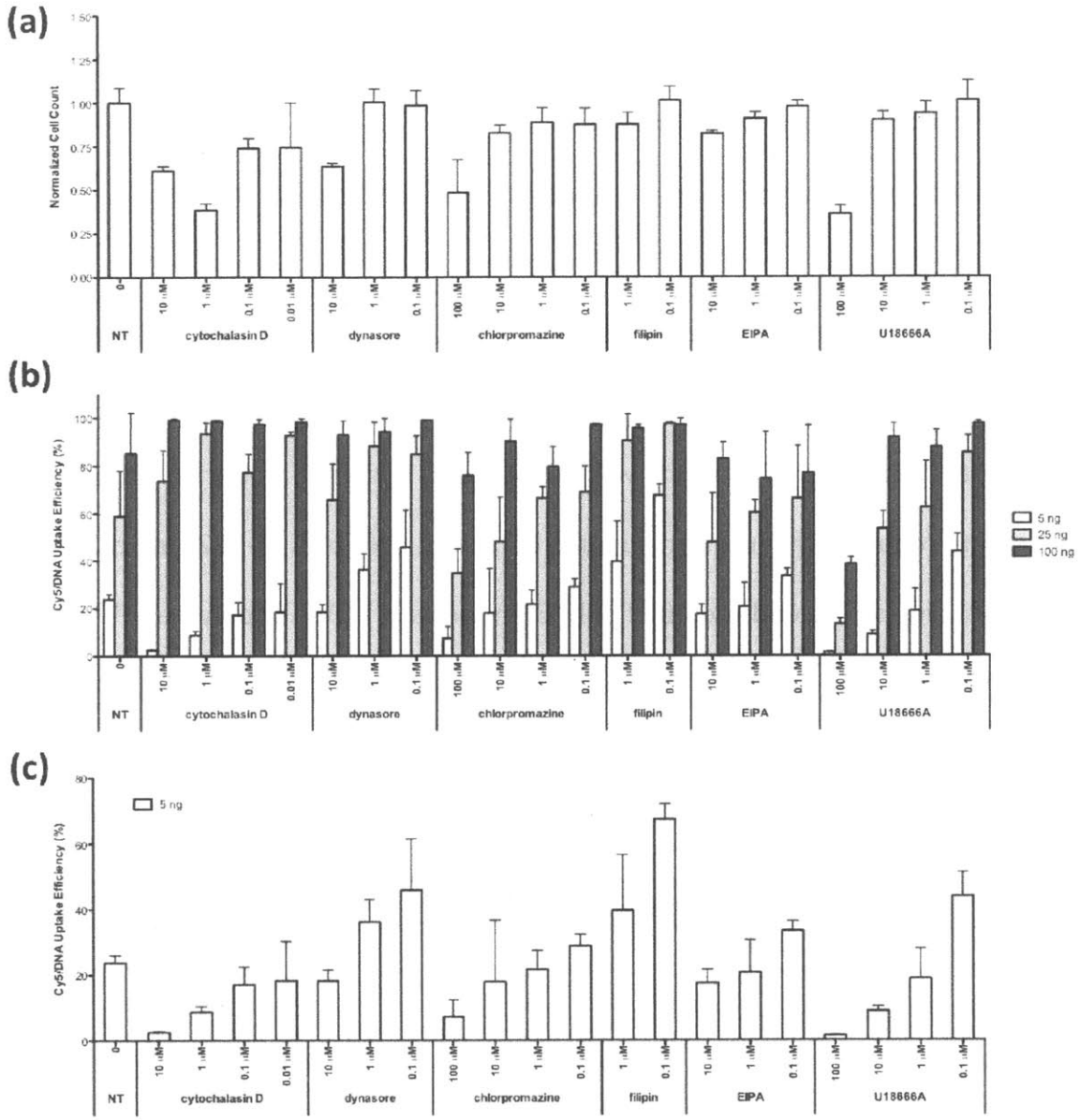

Figure 6.1 Screen for small molecule-mediated inhibition of C32-122-mediated DNA uptake in MEFs

MEFs were transfected with various doses of C32-122 polyplexes containing Cy5-labeled DNA in the presence of the indicated concentrations of endocytic pathway inhibitors. MEFs were pre-treated with the inhibitors 1 h prior to transfection. After 3 h, the cells were washed, fixed, stained with propidium iodide, and analyzed by FACS to determine **(a)** cell viability of control cells treated with inhibitors (mean ± SD, $n = 3$), and **(b)** DNA uptake efficiency (mean ± SD, $n = 3$) at various doses. DNA uptake efficiencies plotted only for the 5 ng DNA/well dose.

In the initial screen, immortalized mouse embryonic fibroblasts (MEFs) were pre-treated with these inhibitors for 1 h, then transfected with various doses of C32-122 polyplexes containing Cy5-labeled DNA in the presence of these inhibitors. After 3 h, the cells were washed, fixed, stained with propidium iodide to label dead cells, and analyzed by FACS to quantify relative cell viability and DNA internalization efficiency (Figure 6.1). To avoid the possibility of confounding effects, we omitted certain inhibitor treatments that at high concentrations resulted in a major reduction in cell viability. It is interesting to note that with some of the inhibitors, at lower concentrations of the drug and higher concentrations of the DNA polyplexes, uptake appears to be elevated, suggesting that the cells may compensate for incomplete suppression by promoting alternate endocytic pathways[45-48]. In many cases, this effect was not actually statistically significant due to the large standard deviations observed for the cells transfected in the absence of inhibitors.

The clearest trends with respect to the effect of each inhibitor on C32-122 polyplex uptake are observed at the 5 ng DNA dose (Figure 6.1c). Dose-dependent decreases in uptake efficiency are seen for cells treated with cytochalasin D, dynasore, chlorpromazine, and U18666A. However, a one-way analysis of variance (ANOVA) test indicates that the only treatments that caused statistically significant decreases in uptake are cytochalasin D (10 μM) and U18666A (100 μM).

To follow-up on this screen, we repeated the pharmacologic inhibition experiment using each inhibitor at a concentration just below the threshold for toxicity and performed high-throughput (HT) confocal microscopy on the treated MEFs. We included two other inhibitors of caveolae-mediated endocytosis, genistein

and methyl-β-cyclodextrin. To test the hypothesis that a component in serum might interact with the PBAE polyplexes and contribute to internalization, we also transfected cells in the absence of serum. The microscopy results were analyzed for DNA uptake and quantified as presented in Figure 6.2.

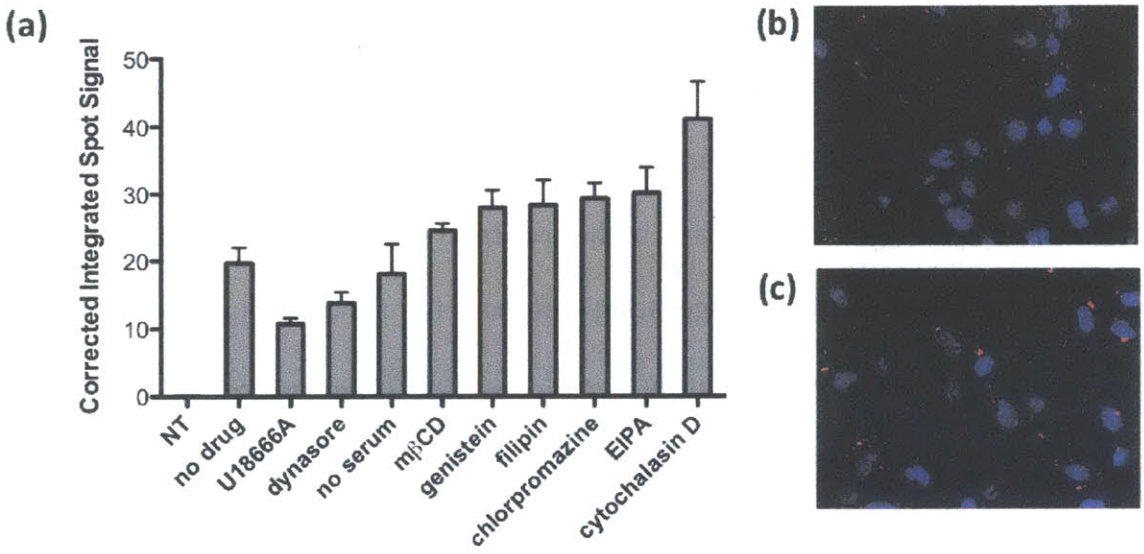

Figure 6.2 C32-122-mediated DNA uptake in MEFs in the presence of various endocytic pathway inhibitors
MEFs were transfected with C32-122 polyplexes containing Cy3-labeled DNA (red) in the presence of various endocytic pathway inhibitors (5 μM U18666A, 50 μM dynasore, 1 mM methyl-β-cyclodextrin, 10 μM genistein, 5 μM filipin, 5 μM chlorpromazine, 10 μM EIPA, and 10 μM cytochalasin D). MEFs were pre-treated with the inhibitors 1 h prior to transfection. After 3 h, the cells were washed, fixed, treated with the nuclear stain Hoescht (blue), and analyzed by high-throughput confocal microscopy to quantify **(a)** DNA uptake (mean ± SD, n = 3). Representative images showing DNA uptake in MEFs **(b)** in the absence of an inhibitor and **(c)** in the presence of U18666A.

In accordance with the initial screening data, we found that U18666A significantly inhibited C32-122-mediated DNA uptake, as seen in the representative microscopy images (Figure 6.2b-c). In contrast, treatment with dynasore yielded a significant decrease in DNA uptake, and surprisingly, cytochalasin D treatment at

this dose caused a significant increase in transfection. As suggested previously, it is possible that the cells may overcome pharmacologic inhibition of one pathway by upregulating alternate pathways through which the polyplexes enter.

The fact that none of the commonly used inhibitors of clathrin-dependent endocytosis (chlorpromazine), caveolae-mediated endocytosis (filipin), and macropinocytosis (EIPA) were effective suggests that PBAE polyplexes may use multiple pathways to enter MEFs. This hypothesis is supported by the statistically significant but inconsistent inhibition observed using cytochalasin D and dynasore, which suppress a broad set of actin- and dynamin-dependent pathways, respectively. Nonetheless, we observed clear and consistent inhibitory effects with U18666A, which prompted us to perform further investigations of the dependence of cholesterol regulation on PBAE-mediated gene delivery.

To determine if U18666A inhibits overall gene transfection by PBAEs, we transfected MEFs with various doses of C32-122 polyplexes containing GFP-encoding plasmid DNA in the presence of the inhibitor and assessed GFP expression efficiency by FACS at 24 h. As was observed with DNA uptake efficiency, U18666A significantly inhibited gene transfection at nearly all DNA doses tested (Figure 6.3). U18666A is an amphipathic steroid with multiple actions, inhibiting both the synthesis of cholesterol[49-52] and its trafficking from late endosomes and lysosomes to the plasma membrane and the endoplasmic reticulum[53-55]. As a result of the latter action, it has also been widely studied as a means of inducing a model of Niemann-Pick type C1 disease[56-58] and may in fact directly interact with and inhibit the sterol sensing site of the Npc1 protein[57, 59, 60].

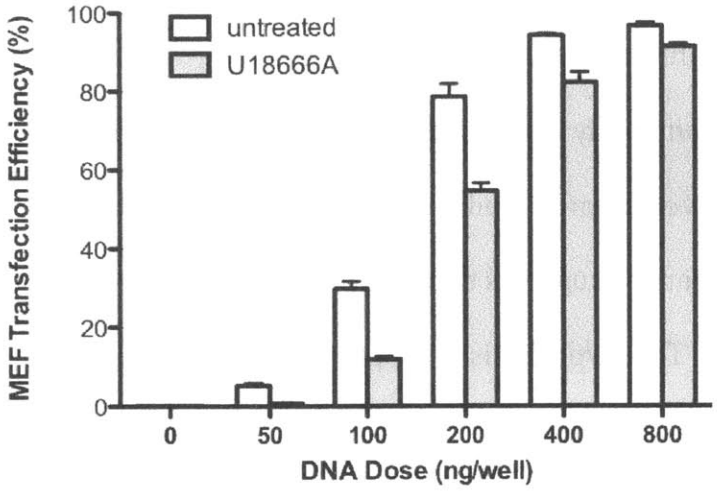

Figure 6.3 U18666A inhibits C32-122-mediated DNA transfection of MEFs
MEFs were pre-treated for 1 h with 5 μM U18666A prior to transfection with the indicated doses of C32-122 polyplexes containing GFP-encoding plasmid DNA in the presence of the inhibitor. After 24 h, GFP expression efficiency was analyzed by FACS (mean ± SD, n = 4).

6.3.2 Studies with cell lines varying in Npc1 expression

To ascertain whether the Npc1 protein plays a role in inhibition of C32-122-mediated DNA transfection, we compared gene transfection efficiencies in *Npc1+/+* and *Npc1-/-* MEF cell lines (Figure 6.4). Fluorescence microscopy one day after transfection with C32-122 polyplexes containing GFP-encoding plasmid DNA showed that GFP expression was dramatically lower in *Npc1-/-* MEFs relative to wild-type cells for the same DNA dose (Figure 6.4a). When FACS analysis was used to compare the dose-response profiles of the two cell lines, we observed that the ED50 concentration was approximately threefold greater for the Npc1 KO cells than that for the wild-type cells (Figure 6.4b). Even more strikingly, GFP expression levels of positively transfected cells were reduced over tenfold in Npc1 KO cells

(Figure 6.4c). These data indicate that the Npc1 protein plays a crucial role in gene transfection by C32-122.

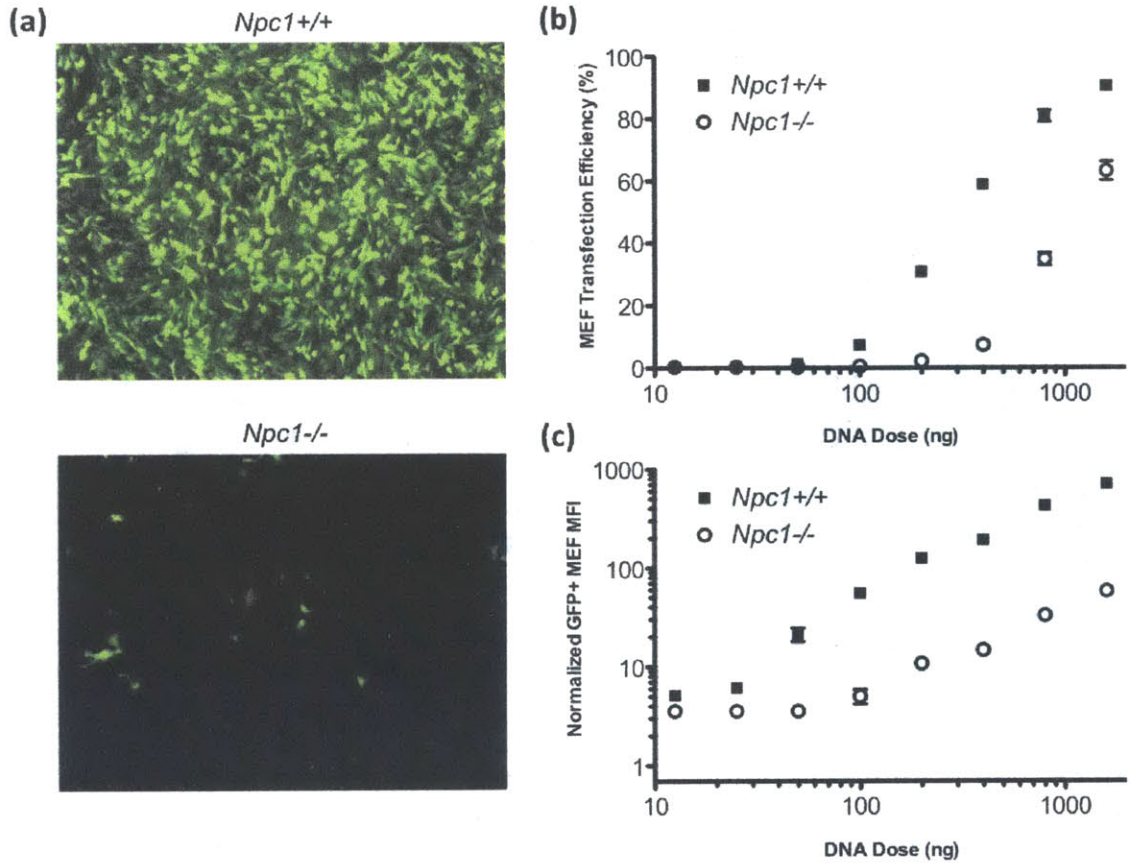

Figure 6.4 Npc1 knockout inhibits C32-122-mediated DNA transfection of MEFs
Npc1+/+ and *Npc1-/-* MEFs were incubated for 3 h with various doses of C32-122 polyplexes containing GFP-encoding plasmid DNA, and GFP expression was assessed by fluorescence microscopy and FACS after 24 h. **(a)** Representative images showing decreased GFP expression in *Npc1-/-* MEFs relative to wild-type MEFs, and FACS analysis of **(b)** GFP expression efficiency and **(c)** normalized geometric mean fluorescent intensity (MFI) of GFP-expressing cells (mean ± SD, n = 4).

Inhibition of PBAE-mediated gene transfection in Npc1-deficient cells could be the result of multiple factors, such as reduced cellular internalization or reduced endosomal escape. To determine whether Npc1 knockout reduces DNA uptake by

C32-122, HT confocal microscopy was used to compare the fluorescent intensity levels of *Npc1+/+* and *Npc1-/-* MEFs treated with polyplexes incorporating Cy3-labeled DNA (Figure 6.5). We observed that Npc1 deficiency was associated with significantly decreased uptake across a range of DNA doses tested.

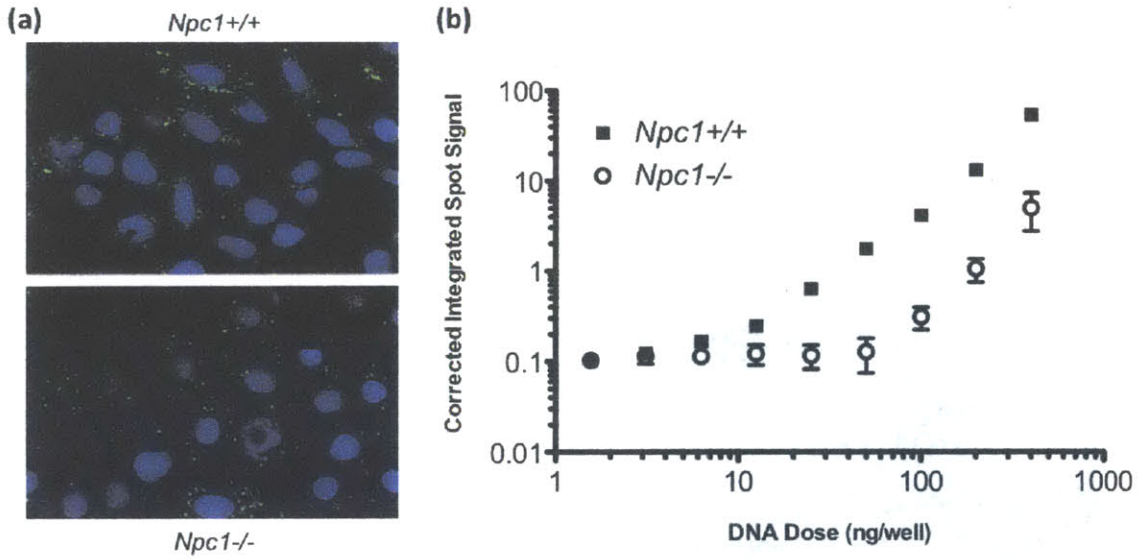

Figure 6.5 Npc1 knockout inhibits C32-122-mediated internalization of DNA in MEFs
Npc1+/+ and *Npc1-/-* MEFs were transfected with various doses of C32-122 polyplexes containing Cy3-labeled plasmid DNA (green). After 3 h, the cells were washed, fixed, treated with the nuclear stain Hoescht (blue), and analyzed by HT confocal microscopy. **(a)** Representative images showing inhibition of uptake in *Npc1-/-* MEFs, and **(b)** quantification of DNA uptake (mean ± SD, $n = 3$).

Characterization of Cy5-labeled DNA internalization by FACS analysis confirmed that Npc1 knockout significantly reduced both the efficiency and the fluorescent intensity of MEFs transfected using C32-122 (Figure 6.6a). To determine whether Npc1 deficiency also affected DNA internalization mediated by other transfection reagents, we conducted analogous experiments with polyethylenimine (PEI) and Lipofectamine 2000 (LF 2000). For LF 2000, Npc1 knockout had no

significant impact on labeled DNA uptake efficiency or on the fluorescent intensity of transfected cells (Figure 6.6c). In contrast, for PEI, Npc1 knockout was associated with a reduction in fluorescent intensity of positively transfected cells but had little effect on uptake efficiency (Figure 6.6b). Comparing the uptake efficiency results, we hypothesize that Npc1 deficiency significantly affects certain early endocytic mechanisms by which PBAE polyplexes are internalized, but not those upon which PEI and LF 2000 rely. Based on the overall uptake results, we further speculate that Npc1 knockout is associated with a later downstream blockage of uptake – perhaps a defect in endosomal escape – that prohibits accumulation of DNA delivered by PBAEs and PEI, but not by LF 2000.

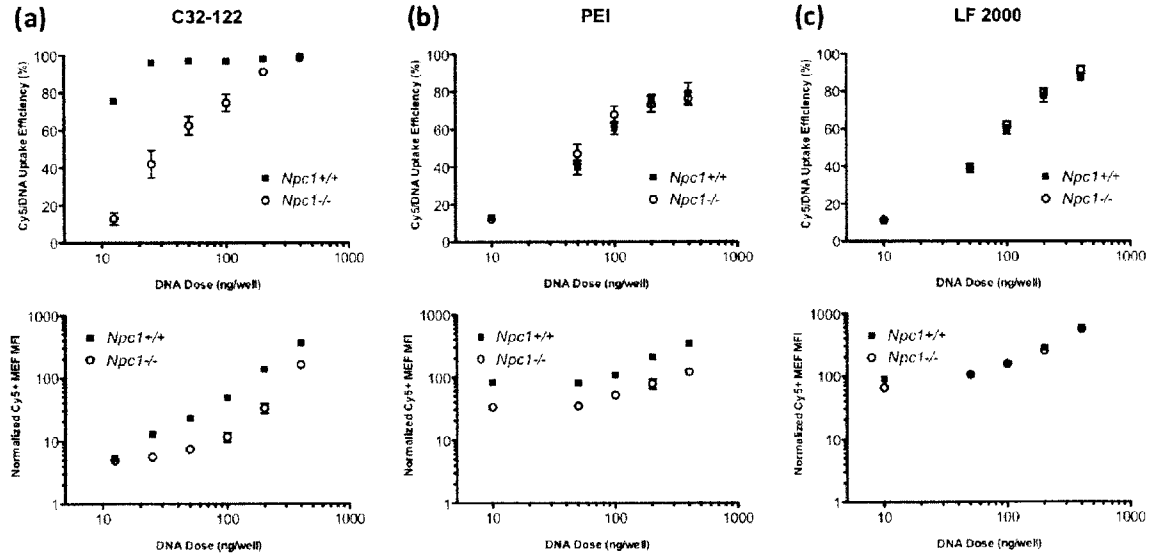

Figure 6.6 Effects of Npc1 knockout on internalization of DNA in MEFs following transfection with C32-122, PEI, and Lipofectamine 2000
Npc1+/+ and *Npc1-/-* MEFs were incubated with various doses Cy5-labeled plasmid DNA (green) complexed with **(a)** C32-122, **(b)** polyethylenimine (PEI), or **(c)** Lipofectamine 2000 (LF2000). After 3 h, the cells were washed, fixed, and analyzed by FACS to determine DNA uptake efficiency (*top*, mean ± SD, $n = 4$) and normalized geometric mean fluorescent intensity (MFI) of Cy5-positive cells (*bottom*, mean ± SD, $n = 4$).

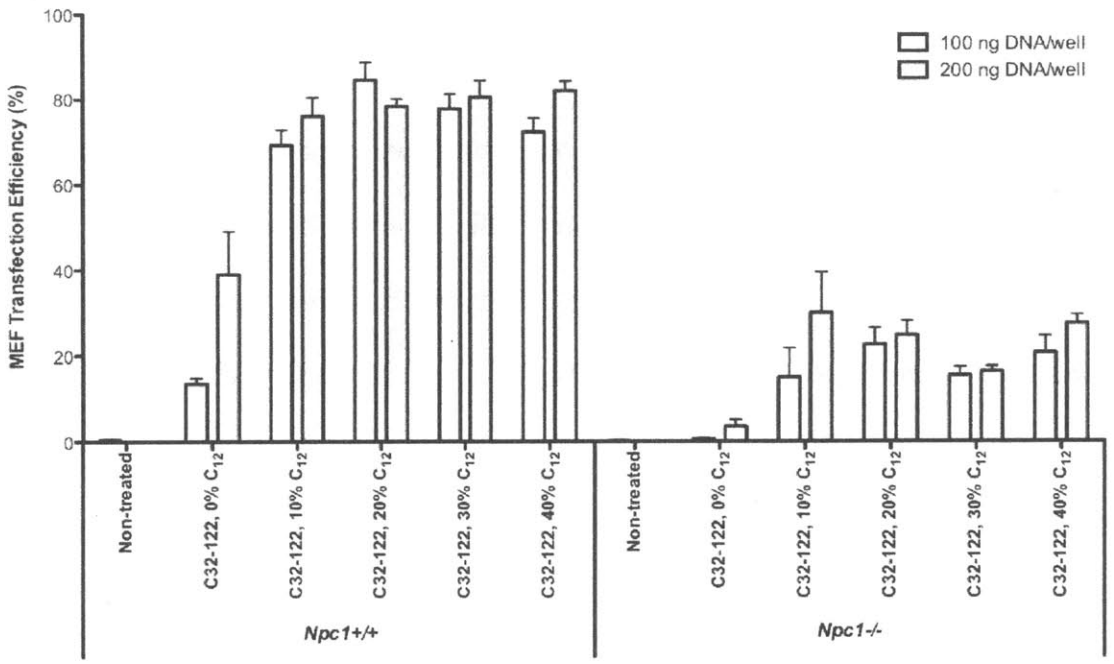

Figure 6.7 Increasing C32-122 terpolymer hydrophobicity improves gene transfection potency in *Npc1-/-* MEFs but does not rescue inhibition
Npc1+/+ and *Npc1-/-* MEFs were incubated for 3 h with the indicated doses of the C32-122 terpolymer variants complexed with GFP-encoding plasmid DNA. GFP expression efficiency (mean ± SD, $n = 4$) was assessed by FACS after 24 h.

Due to the differences in behavior observed for the three materials, we hypothesized that modifying certain chemical properties of the material might alleviate the impact of Npc1 deficiency on gene transfection. We have previously reported that hydrophobic PBAE terpolymers incorporating alkyl side chains demonstrate enhanced gene delivery efficacy and nanoparticle stability[61]. Therefore, we synthesized C32-122 terpolymers of varying hydrophobicity and compared transfection efficacy in wild-type and Npc1 knockout MEFs (Figure 6.7). Although increasing C32-122 terpolymer hydrophobicity was associated with improved gene delivery in both *Npc1+/+* and *Npc1-/-* MEFs, it did not rescue the

inhibitory effect of Npc1 knockout on PBAE gene transfection efficiency. We speculate that the enhancement in gene delivery observed as a result of increasing polymer hydrophobicity likely owes more to a biophysical property of the polyplex such as increased DNA binding efficiency (cf. Figure 3.10, Figure 3.11) than to alteration of the cellular internalization mechanism.

To further elucidate the effects of Npc1, we examined C32-122/DNA uptake and transfection in Chinese hamster ovary (CHO) epithelial cell lines varying in Npc1 expression (Figure 6.8). These cell lines included wild-type CHO cells, Npc1-deficient CHO cells (Null), CHO cells expressing Npc1 with a missense mutation in the sterol-sensing domain (SSD) resulting in defective cholesterol trafficking[62] (P692S), and wild-type CHO cells stably overexpressing human Npc1[63] (hNpc1). As was observed with the immortalized MEFs, Npc1 deficiency in CHO cells inhibited both DNA uptake and transfection mediated by C32-122. In the P692S CHO cells, uptake and transfection were inhibited to a nearly identical extent as the null cells, confirming the specific dependence on Npc1's cholesterol-trafficking function for PBAE-mediated gene delivery. Surprisingly, we observed increased C32-122-mediated DNA uptake and transfection in the CHO cells stably overexpressing human Npc1 (Figure 6.8). These cells have been reported to have a 1.5-fold increase in total cellular cholesterol and a 2.9-fold increase in cholesterol at the plasma membrane[63]. We hypothesize that increased cholesterol localization at the plasma membrane may enhance the activities of certain endocytic mechanisms used by PBAE/DNA nanoparticles. These observations raise the possibility of modulating key cellular factors to improve non-viral gene delivery.

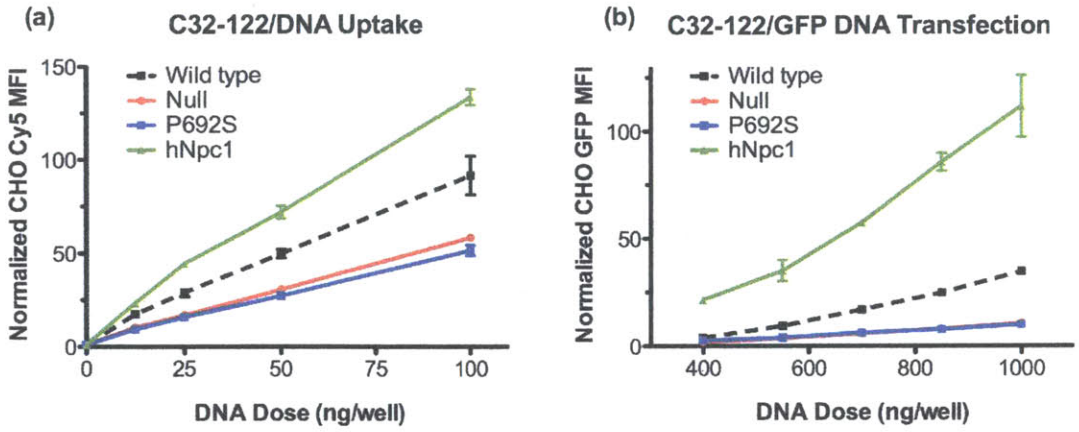

Figure 6.8 C32-122-mediated DNA uptake and transfection in CHO cell lines varying in Npc1 expression

CHO cells varying in Npc1 expression were incubated for 3 h with the indicated doses of **(a)** Cy5-labeled plasmid DNA or **(b)** GFP-encoding plasmid DNA complexed with C32-122 polymer. FACS analysis was used to assess the **(a)** Cy5 geometric mean fluorescent intensities (MFI) of treated cells relative to non-treated cells immediately after washing, or **(b)** the GFP geometric MFI of treated cells relative to non-treated cells after 24 h (mean ± SD, $n = 4$).

To examine the hypothesis that Npc1 deficiency affects endocytic processes that contribute to PBAE polyplex entry, we assessed the relative uptake of various known markers of endocytic pathways in *Npc1+/+* and *Npc1-/-* MEFs. These markers included fluorescently labeled transferrin, cholera toxin B, and 10,000 MW dextran, which are thought to undergo internalization via clathrin-dependent endocytosis, caveolin-mediated endocytosis, and macropinocytosis, respectively. After a 3 h incubation with the cell lines and multiple washes, we observed dramatically reduced uptake of cholera toxin B in the Npc1-deficient cells (Figure 6.9). Furthermore, transferrin uptake appeared to be slightly decreased and dextran uptake slightly increased.

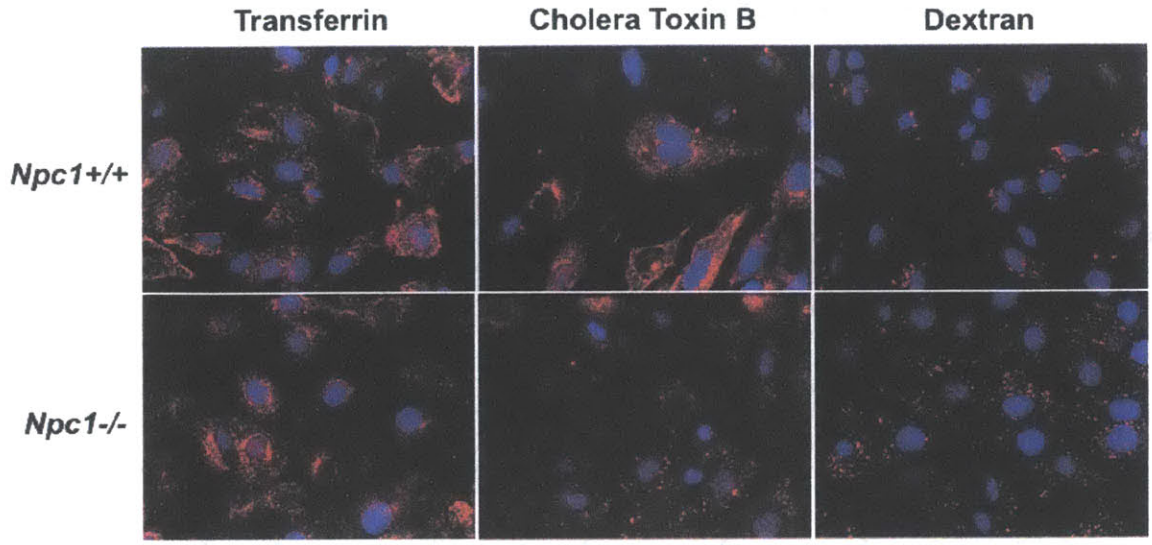

Figure 6.9 Confocal microscopy analysis of relative endocytic pathway activities in *Npc1+/+* and *Npc1-/-* MEFs
MEFs were incubated for 3 h with media containing various AF647-labeled (red) markers: 50 μg/ml transferrin *(left)*, 55 ng/ml cholera toxin B *(middle)*, or 100 μg/ml 10,000 MW dextran *(right)*, traditional markers of clathrin-dependent, endocytosis, caveolae-mediated endocytosis, and macropinocytosis, respectively. After 3 h, the cells were washed, fixed, treated with the nuclear stain Hoescht (blue), and analyzed by HT confocal microscopy.

Quantification of these microscopy results by FACS analysis corroborated these trends (Figure 6.10). Comparing Npc1-deficient cells to wild-type cells, cholera toxin B internalization was reduced ~20-30-fold; transferrin uptake was reduced about twofold; and dextran uptake was increased by ~50%. These results demonstrate in a quantitative manner that Npc1 knockout in MEFs significantly alters normal activities of various endocytic pathways, implying significantly decreased caveolae-mediated endocytosis, slightly reduced clathrin-mediated endocytosis, and slightly upregulated macropinocytosis. However, it should be noted that cholera toxin B is not necessarily a selective marker of caveolae-mediated

endocytosis as some studies have reported its entry through alternative pathways depending on the cell type[64].

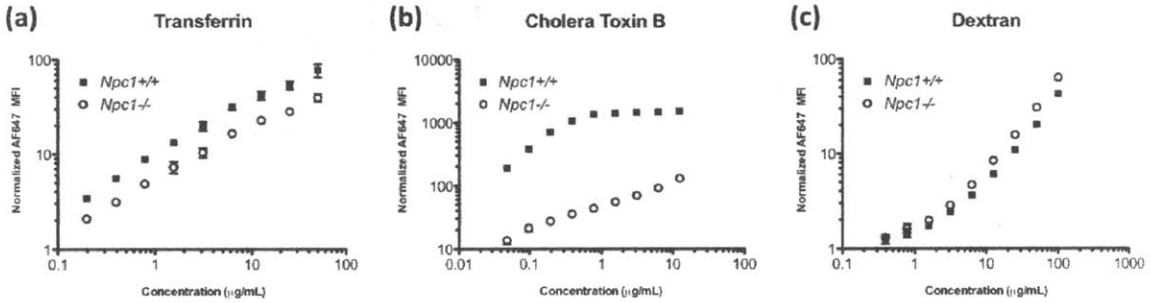

Figure 6.10 FACS analysis of relative endocytic pathway activities in *Npc1+/+* and *Npc1-/-* MEFs
MEFs were incubated for 3 h with media containing various doses of AF647-labeled **(a)** transferrin, **(b)** cholera toxin B, or **(c)** dexran. After 3 h, the cells were washed, fixed, and analyzed for AF647 signal by FACS.

To determine whether PBAE polyplexes share common uptake pathways with these markers during endocytosis, we incubated the C32-122 polyplexes containing labeled DNA in the presence of each one of these markers and used confocal microscopy to characterize the extent of co-localization in wild-type MEFs at various time points (Figure 6.11). Confirming our hypothesis that PBAEs utilize multiple endocytic pathways, we observed evidence of DNA co-localization with all three markers. However, the greatest extent of co-localization occurred with cholera toxin B. Moreover, the kinetics of PBAE/DNA uptake indicated on an intermediate time scale corresponding more closely to that of cholera toxin B uptake than to either the fast or slow kinetics of transferrin or dextran uptake, respectively (data not shown). These results suggests that PBAE polyplexes and cholera toxin B may

rely on common uptake pathways for internalization and retention in MEFs that are dramatically altered in cells lacking Npc1.

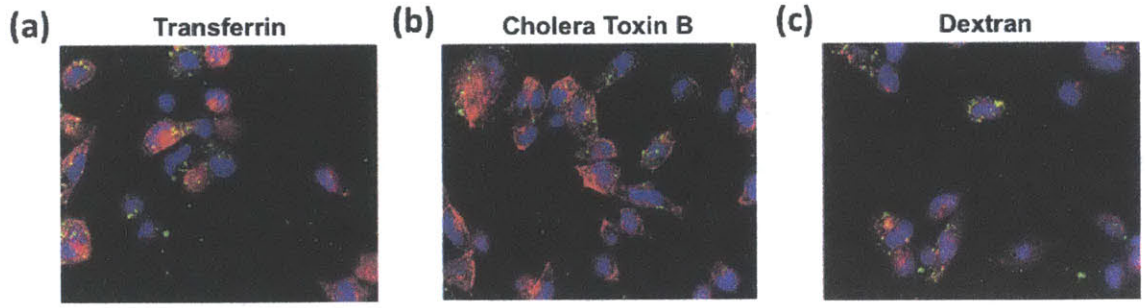

Figure 6.11 Co-localization of internalized DNA delivered by C32-122 with markers of distinct endocytic pathways in MEFs
Npc1+/+ MEFs were transfected with C32-122 polyplexes containing Cy3-labeled DNA in the presence of AF647-labeled **(a)** 50 μg/ml transferrin, **(b)** 55 ng/ml cholera toxin B, or **(c)** 100 ug/ml 10,000 MW dextran. After 3 h, the cells were washed, fixed, treated with the nuclear stain Hoescht (blue), and analyzed by high-throughput confocal microscopy for intracellular co-localization of DNA (green) with each marker (red).

Taken together, these data imply that Npc1 regulates certain uptake and trafficking pathways that markedly affect internalization and retention of PBAE/DNA polyplexes. Because Npc1 plays a key role in regulating the trafficking of cholesterol, and because cholesterol has been shown to be critically involved in both caveolin- and clathrin-mediated endocytosis[65-69], it is quite plausible that Npc1 knockout would affect these processes. To our knowledge, although Npc1 knockout has been associated with altered intracellular localization of cholera toxin B and lactosylceramide (LacCer),[59, 70] two markers of caveolin-mediated endocytosis, and with defective recycling of transferrin receptor[71], quantitative analysis of uptake for multiple endocytic markers has not yet been reported. Despite previous reports that fluid-phase uptake of horseradish peroxidase is impaired in Npc1 knockout

cells[72, 73], possibly due to abnormal localization of annexin II, our results suggest that macropinocytic internalization of dextran is slightly increased in Npc1-deficient cells.

At present, the precise molecular mechanisms by which Npc1 affects endocytic processes is unknown. One group has recently reported that perturbation of cholesterol content by U18666A can induce mislocalization of caveolin-1 from the plasma membrane to late endosomes and lysosomes[65]. However, the authors did not test whether this mislocalization also occurs in Npc1 knockout cells. Another study suggested that Npc1 deficiency is associated with deregulation of lysosomal calcium that is in turn responsible for sphingolipid accumulation as well as defects in endosomal trafficking[74]. Further studies are needed to determine whether Npc1 plays a more direct role in regulation of early endocytic pathways. Such studies would help to elucidate both the biology of endolysosomal trafficking and the pathology of glycosphingolipid storage diseases.

Finally, the novel investigation of non-viral DNA transfection of Npc1-deficient cells reported here demonstrates the importance of proper regulation of cholesterol trafficking for certain delivery reagents such as poly(β-amino ester)s. Future studies should evaluate whether Npc1 plays a similar role in cell types other than MEF and CHO cells, particularly human fibroblast and epithelial cells. In this study, one of the most striking observations was that stable overexpression of Npc1 significantly improved DNA internalization and transfection by PBAEs. These findings raise the tantalizing prospect of enhancing non-viral gene delivery through

active modulation of cellular factors known to play key roles in internalization, such as lysobisphosphatidic acid (LBPA), Rab5, and perhaps Npc1.

6.4 Conclusions

In this chapter, the uptake of PBAE/DNA nanoparticles was investigated through pharmacological inhibition and marker co-localization studies. Our results indicated that internalization of PBAE/DNA polyplexes in immortalized mouse embryonic fibroblast (MEF) cells likely proceeds through multiple pathways, with an apparent dependence on normal cholesterol trafficking. We showed that MEFs deficient in a lysosomal cholesterol transport protein, Npc1, exhibit significantly reduced PBAE gene transfection efficacy. Moreover, Npc1 knockout in MEFs greatly inhibited PBAE-mediated DNA internalization, with a slight decrease in DNA uptake mediated by PEI and no apparent effect on DNA uptake mediated by LF 2000. Strikingly, stable overexpression of human Npc1 in Chinese hamster ovary (CHO) cells was associated with enhanced gene uptake and transfection by PBAEs. We observed that retention of various endocytic markers was altered in Npc1-deficient MEFs, with significant reduction in uptake of cholera toxin B, a marker traditionally associated with caveolae-mediated endocytosis. DNA internalized by PBAEs showed the greatest extent of co-localization with the cholera toxin B marker, suggesting the involvement of shared uptake pathways that are altered in cells lacking Npc1. These studies provide additional support for the idea that Npc1 plays a critical role in the regulation of endocytic mechanisms affecting internalization and efficacy of nanoparticles.

6.5 REFERENCES

[1] Kay, M. A. State-of-the-art gene-based therapies: the road ahead. *Nat. Rev. Genet.* **12**, 316 (2011).

[2] Giacca, M., Zacchigna, S. Virus-mediated gene delivery for human gene therapy. *J Control Release* **161**, 377 (2012).

[3] Mintzer, M. A., Simanek, E. E. Nonviral vectors for gene delivery. *Chem. Rev.* **109**, 259 (2009).

[4] Edelstein, M. in J Gene Med, Vol. 2011 (Wiley, 2011).

[5] Guo, X., Huang, L. Recent advances in nonviral vectors for gene delivery. *Acc Chem Res* **45**, 971 (2012).

[6] Sahay, G., Alakhova, D. Y., Kabanov, A. V. Endocytosis of nanomedicines. *J Control Release* **145**, 182 (2010).

[7] Doherty, G. J., McMahon, H. T. Mechanisms of endocytosis. *Annu Rev Biochem* **78**, 857 (2009).

[8] Vasir, J. K., Labhasetwar, V. Quantification of the force of nanoparticle-cell membrane interactions and its influence on intracellular trafficking of nanoparticles. *Biomaterials* **29**, 4244 (2008).

[9] Panyam, J., Labhasetwar, V. Dynamics of endocytosis and exocytosis of poly(D,L-lactide-co-glycolide) nanoparticles in vascular smooth muscle cells. *Pharm Res* **20**, 212 (2003).

[10] Qaddoumi, M. G., Ueda, H., Yang, J., Davda, J., Labhasetwar, V., Lee, V. H. The characteristics and mechanisms of uptake of PLGA nanoparticles in rabbit conjunctival epithelial cell layers. *Pharm Res* **21**, 641 (2004).

[11] Sahay, G., Kim, J. O., Kabanov, A. V., Bronich, T. K. The exploitation of differential endocytic pathways in normal and tumor cells in the selective targeting of nanoparticulate chemotherapeutic agents. *Biomaterials* **31**, 923 (2010).

[12] Miele, E., Spinelli, G. P., Tomao, F., Tomao, S. Albumin-bound formulation of paclitaxel (Abraxane ABI-007) in the treatment of breast cancer. *Int J Nanomedicine* **4**, 99 (2009).

[13] Love, K. T., Mahon, K. P., Levins, C. G., Whitehead, K. A., Querbes, W., Dorkin, J. R., Qin, J., Cantley, W., Qin, L. L., Racie, T., Frank-Kamenetsky, M., Yip, K. N., Alvarez, R., Sah, D. W., de Fougerolles, A., Fitzgerald, K., Koteliansky, V., Akinc, A., Langer, R., Anderson, D. G. Lipid-like materials for low-dose, in vivo gene silencing. *Proceedings of the National Academy of Sciences* **107**, 1864 (2010).

[14] Rejman, J., Bragonzi, A., Conese, M. Role of clathrin- and caveolae-mediated endocytosis in gene transfer mediated by lipo- and polyplexes. *Mol Ther* **12**, 468 (2005).

[15] Luhmann, T., Rimann, M., Bittermann, A. G., Hall, H. Cellular uptake and intracellular pathways of PLL-g-PEG-DNA nanoparticles. *Bioconjug Chem* **19**, 1907 (2008).

[16] van der Aa, M. A., Huth, U. S., Hafele, S. Y., Schubert, R., Oosting, R. S., Mastrobattista, E., Hennink, W. E., Peschka-Suss, R., Koning, G. A., Crommelin, D. J. Cellular uptake of cationic polymer-DNA complexes via caveolae plays a pivotal role in gene transfection in COS-7 cells. *Pharm Res* **24**, 1590 (2007).
[17] von Gersdorff, K., Sanders, N. N., Vandenbroucke, R., De Smedt, S. C., Wagner, E., Ogris, M. The internalization route resulting in successful gene expression depends on both cell line and polyethylenimine polyplex type. *Mol Ther* **14**, 745 (2006).
[18] Wong, A. W., Scales, S. J., Reilly, D. E. DNA internalized via caveolae requires microtubule-dependent, Rab7-independent transport to the late endocytic pathway for delivery to the nucleus. *J Biol Chem* **282**, 22953 (2007).
[19] Grosse, S., Aron, Y., Thévenot, G., François, D., Monsigny, M., Fajac, I. Potocytosis and cellular exit of complexes as cellular pathways for gene delivery by polycations. *The Journal of Gene Medicine* **7**, 1275 (2005).
[20] Rejman, J., Conese, M., Hoekstra, D. Gene transfer by means of lipo- and polyplexes: role of clathrin and caveolae-mediated endocytosis. *J Liposome Res* **16**, 237 (2006).
[21] Khalil, I. A., Kogure, K., Futaki, S., Harashima, H. High density of octaarginine stimulates macropinocytosis leading to efficient intracellular trafficking for gene expression. *J Biol Chem* **281**, 3544 (2006).
[22] Anderson, D. G., Peng, W., Akinc, A., Hossain, N., Kohn, A., Padera, R., Langer, R., Sawicki, J. A. A polymer library approach to suicide gene therapy for cancer. *Proc. Natl. Acad. Sci. USA* **101**, 16028 (2004).
[23] Peng, W., Anderson, D. G., Bao, Y., Padera, R. F., Jr., Langer, R., Sawicki, J. A. Nanoparticulate delivery of suicide DNA to murine prostate and prostate tumors. *Prostate* **67**, 855 (2007).
[24] Huang, Y. H., Zugates, G. T., Peng, W., Holtz, D., Dunton, C., Green, J. J., Hossain, N., Chernick, M. R., Padera, R. F., Jr., Langer, R., Anderson, D. G., Sawicki, J. A. Nanoparticle-delivered suicide gene therapy effectively reduces ovarian tumor burden in mice. *Cancer Res* **69**, 6184 (2009).
[25] Yang, F., Cho, S. W., Son, S. M., Bogatyrev, S. R., Singh, D., Green, J., Mei, Y., Park, S., Bhang, S. H., Kim, B. S., Langer, R., Anderson, D. Genetic engineering of human stem cells for enhanced angiogenesis using biodegradable polymeric nanoparticles. *Proc. Natl. Acad. Sci. USA* **107**, 3317 (2010).
[26] Green, J., Shi, J., Chiu, E., Leshchiner, E., Langer, R., Anderson, D. Biodegradable Polymeric Vectors for Gene Delivery to Human Endothelial Cells. *Bioconjugate Chem.* **17**, 1162 (2006).
[27] Green, J., Zhou, B., Mitalipova, M., Beard, C., Langer, R., Jaenisch, R., Anderson, D. Nanoparticles for Gene Transfer to Human Embryonic Stem Cell Colonies. *Nano Lett.* **8**, 3126 (2008).
[28] Yang, F., Green, J. J., Dinio, T., Keung, L., Cho, S. W., Park, H., Langer, R., Anderson, D. G. Gene delivery to human adult and embryonic cell-derived stem cells using biodegradable nanoparticulate polymeric vectors. *Gene Ther* **16**, 533 (2009).
[29] Lynn, D. M., Langer, R. Degradable Poly ([beta]-amino esters): Synthesis, Characterization, and Self-Assembly with Plasmid DNA. *J. Am. Chem. Soc* **122**, 10761 (2000).

[30] Lynn, D., Anderson, D., Putnam, D., Langer, R. Accelerated Discovery of Synthetic Transfection Vectors: Parallel Synthesis and Screening of a Degradable Polymer Library. *J. Am. Chem. Soc.* **123**, 8155 (2001).
[31] Akinc, A., Lynn, D., Anderson, D., Langer, R. Parallel Synthesis and Biophysical Characterization of a Degradable Polymer Library for Gene Delivery. *J. Am. Chem. Soc.* **125**, 5316 (2003).
[32] Anderson, D. G., Lynn, D. M., Langer, R. Semi-Automated Synthesis and Screening of a Large Library of Degradable Cationic Polymers for Gene Delivery. *Angew. Chem. Int. Ed.* **42**, 3153 (2003).
[33] Akinc, A., Anderson, D. G., Lynn, D. M., Langer, R. Synthesis of Poly(β-amino ester)s Optimized for Highly Effective Gene Delivery. *Bioconjugate Chem.* **14**, 979 (2003).
[34] Anderson, D., Akinc, A., Hossain, N., Langer, R. Structure/property studies of polymeric gene delivery using a library of poly(beta-amino esters). *Mol Ther* **11**, 426 (2005).
[35] Eltoukhy, A. A., Siegwart, D. J., Alabi, C. A., Rajan, J. S., Langer, R., Anderson, D. G. Effect of molecular weight of amine end-modified poly(beta-amino ester)s on gene delivery efficiency and toxicity. *Biomaterials* **33**, 3594 (2012).
[36] Eltoukhy, A. A., Chen, D., Alabi, C. A., Langer, R., Anderson, D. G. Degradable terpolymers with alkyl side chains demonstrate enhanced gene delivery potency and nanoparticle stability. *Adv Mater* **25**, 1487 (2013).
[37] Green, J. J., Zugates, G. T., Tedford, N. C., Huang, Y., Griffith, L. G., Lauffenburger, D. A., Sawicki, J. A., Langer, R., Anderson, D. G. Combinatorial modification of degradable polymers enables transfection of human cells comparable to adenovirus. *Adv. Mater.* **19**, 2836 (2007).
[38] Zugates, G. T., Peng, W., Zumbuehl, A., Jhunjhunwala, S., Huang, Y. H., Langer, R., Sawicki, J. A., Anderson, D. G. Rapid optimization of gene delivery by parallel end-modification of poly(beta-amino ester)s. *Mol. Ther.* **15**, 1306 (2007).
[39] Zugates, G., Tedford, N., Zumbuehl, A., Jhunjhunwala, S., Kang, C., Griffith, L., Lauffenburger, D., Langer, R., Anderson, D. Gene Delivery Properties of End-Modified Poly(β-amino ester)s. *Bioconjugate Chem.* **18**, 1887 (2007).
[40] Sunshine, J., Green, J. J., Mahon, K. P., Yang, F., Eltoukhy, A. A., Nguyen, D. N., Langer, R., Anderson, D. G. Small-Molecule End-Groups of Linear Polymer Determine Cell-type Gene-Delivery Efficacy. *Adv. Mater.* **21**, 4947 (2009).
[41] Scott, C., Ioannou, Y. A. The NPC1 protein: structure implies function. *Biochim Biophys Acta* **1685**, 8 (2004).
[42] Cote, M., Misasi, J., Ren, T., Bruchez, A., Lee, K., Filone, C. M., Hensley, L., Li, Q., Ory, D., Chandran, K., Cunningham, J. Small molecule inhibitors reveal Niemann-Pick C1 is essential for Ebola virus infection. *Nature* **477**, 344 (2011).
[43] Carette, J. E., Raaben, M., Wong, A. C., Herbert, A. S., Obernosterer, G., Mulherkar, N., Kuehne, A. I., Kranzusch, P. J., Griffin, A. M., Ruthel, G., Dal Cin, P., Dye, J. M., Whelan, S. P., Chandran, K., Brummelkamp, T. R. Ebola virus entry requires the cholesterol transporter Niemann-Pick C1. *Nature* **477**, 340 (2011).
[44] Miller, E. H., Obernosterer, G., Raaben, M., Herbert, A. S., Deffieu, M. S., Krishnan, A., Ndungo, E., Sandesara, R. G., Carette, J. E., Kuehne, A. I., Ruthel, G., Pfeffer, S. R., Dye, J. M., Whelan, S. P., Brummelkamp, T. R., Chandran, K. Ebola virus

entry requires the host-programmed recognition of an intracellular receptor. *EMBO J* **31**, 1947 (2012).
[45] Hussain, K. M., Leong, K. L., Ng, M. M., Chu, J. J. The essential role of clathrin-mediated endocytosis in the infectious entry of human enterovirus 71. *J Biol Chem* **286**, 309 (2011).
[46] Hufnagel, H., Hakim, P., Lima, A., Hollfelder, F. Fluid phase endocytosis contributes to transfection of DNA by PEI-25. *Mol Ther* **17**, 1411 (2009).
[47] Duchardt, F., Fotin-Mleczek, M., Schwarz, H., Fischer, R., Brock, R. A comprehensive model for the cellular uptake of cationic cell-penetrating peptides. *Traffic* **8**, 848 (2007).
[48] Damke, H., Baba, T., van der Bliek, A. M., Schmid, S. L. Clathrin-independent pinocytosis is induced in cells overexpressing a temperature-sensitive mutant of dynamin. *J Cell Biol* **131**, 69 (1995).
[49] Phillips, W. A., Avigan, J. Inhibition of cholesterol biosynthesis in the rat by 3 beta-(2-diethylaminoethoxy) androst5-en-17-one hydrochloride. *Proc Soc Exp Biol Med* **112**, 233 (1963).
[50] Cenedella, R. J. Concentration-dependent effects of AY-9944 and U18666A on sterol synthesis in brain. Variable sensitivities of metabolic steps. *Biochem Pharmacol* **29**, 2751 (1980).
[51] Sexton, R. C., Panini, S. R., Azran, F., Rudney, H. Effects of 3 beta-[2-(diethylamino)ethoxy]androst-5-en-17-one on the synthesis of cholesterol and ubiquinone in rat intestinal epithelial cell cultures. *Biochemistry* **22**, 5687 (1983).
[52] Panini, S. R., Sexton, R. C., Rudney, H. Regulation of 3-hydroxy-3-methylglutaryl coenzyme A reductase by oxysterol by-products of cholesterol biosynthesis. Possible mediators of low density lipoprotein action. *J Biol Chem* **259**, 7767 (1984).
[53] Liscum, L., Faust, J. R. The intracellular transport of low density lipoprotein-derived cholesterol is inhibited in Chinese hamster ovary cells cultured with 3-beta-[2-(diethylamino)ethoxy]androst-5-en-17-one. *J Biol Chem* **264**, 11796 (1989).
[54] Liscum, L. Pharmacological inhibition of the intracellular transport of low-density lipoprotein-derived cholesterol in Chinese hamster ovary cells. *Biochim Biophys Acta* **1045**, 40 (1990).
[55] Liscum, L., Collins, G. J. Characterization of Chinese hamster ovary cells that are resistant to 3-beta-[2-(diethylamino)ethoxy]androst-5-en-17-one inhibition of low density lipoprotein-derived cholesterol metabolism. *J Biol Chem* **266**, 16599 (1991).
[56] Liscum, L., Klansek, J. J. Niemann-Pick disease type C. *Curr Opin Lipidol* **9**, 131 (1998).
[57] Lange, Y., Ye, J., Rigney, M., Steck, T. Cholesterol movement in Niemann-Pick type C cells and in cells treated with amphiphiles. *J Biol Chem* **275**, 17468 (2000).
[58] Ko, D. C., Gordon, M. D., Jin, J. Y., Scott, M. P. Dynamic movements of organelles containing Niemann-Pick C1 protein: NPC1 involvement in late endocytic events. *Mol Biol Cell* **12**, 601 (2001).
[59] Sugimoto, Y., Ninomiya, H., Ohsaki, Y., Higaki, K., Davies, J. P., Ioannou, Y. A., Ohno, K. Accumulation of cholera toxin and GM1 ganglioside in the early endosome of Niemann-Pick C1-deficient cells. *Proc Natl Acad Sci U S A* **98**, 12391 (2001).

[60] Liu, R., Lu, P., Chu, J. W., Sharom, F. J. Characterization of fluorescent sterol binding to purified human NPC1. *J Biol Chem* **284**, 1840 (2009).
[61] Eltoukhy, A. A., Chen, D., Alabi, C. A., Langer, R., Anderson, D. G. Degradable terpolymers with alkyl side chains demonstrate enhanced gene delivery potency and nanoparticle stability. *Adv. Mater.*, Forthcoming (2013).
[62] Millard, E. E., Gale, S. E., Dudley, N., Zhang, J., Schaffer, J. E., Ory, D. S. The sterol-sensing domain of the Niemann-Pick C1 (NPC1) protein regulates trafficking of low density lipoprotein cholesterol. *Journal of Biological Chemistry* **280**, 28581 (2005).
[63] Millard, E. E., Srivastava, K., Traub, L. M., Schaffer, J. E., Ory, D. S. Niemann-pick type C1 (NPC1) overexpression alters cellular cholesterol homeostasis. *Journal of Biological Chemistry* **275**, 38445 (2000).
[64] Wernick, N. L. B., Chinnapen, D. J. F., Cho, J. A., Lencer, W. I. Cholera Toxin: An Intracellular Journey into the Cytosol by Way of the Endoplasmic Reticulum. *Toxins* **2**, 310 (2010).
[65] Mundy, D. I., Li, W. P., Luby-Phelps, K., Anderson, R. G. Caveolin targeting to late endosome/lysosomal membranes is induced by perturbations of lysosomal pH and cholesterol content. *Mol Biol Cell* **23**, 864 (2012).
[66] Subtil, A., Gaidarov, I., Kobylarz, K., Lampson, M. A., Keen, J. H., McGraw, T. E. Acute cholesterol depletion inhibits clathrin-coated pit budding. *Proc Natl Acad Sci U S A* **96**, 6775 (1999).
[67] Rodal, S. K., Skretting, G., Garred, O., Vilhardt, F., van Deurs, B., Sandvig, K. Extraction of cholesterol with methyl-beta-cyclodextrin perturbs formation of clathrin-coated endocytic vesicles. *Mol Biol Cell* **10**, 961 (1999).
[68] Cheng, Z. J., Singh, R. D., Sharma, D. K., Holicky, E. L., Hanada, K., Marks, D. L., Pagano, R. E. Distinct mechanisms of clathrin-independent endocytosis have unique sphingolipid requirements. *Mol Biol Cell* **17**, 3197 (2006).
[69] Hooper, N. M. Detergent-insoluble glycosphingolipid/cholesterol-rich membrane domains, lipid rafts and caveolae (review). *Mol Membr Biol* **16**, 145 (1999).
[70] Sun, X., Marks, D. L., Park, W. D., Wheatley, C. L., Puri, V., O'Brien, J. F., Kraft, D. L., Lundquist, P. A., Patterson, M. C., Pagano, R. E., Snow, K. Niemann-Pick C variant detection by altered sphingolipid trafficking and correlation with mutations within a specific domain of NPC1. *Am J Hum Genet* **68**, 1361 (2001).
[71] Pipalia, N. H., Hao, M., Mukherjee, S., Maxfield, F. R. Sterol, protein and lipid trafficking in Chinese hamster ovary cells with Niemann-Pick type C1 defect. *Traffic* **8**, 130 (2007).
[72] Mayran, N., Parton, R. G., Gruenberg, J. Annexin II regulates multivesicular endosome biogenesis in the degradation pathway of animal cells. *EMBO J* **22**, 3242 (2003).
[73] te Vruchte, D., Lloyd-Evans, E., Veldman, R. J., Neville, D. C., Dwek, R. A., Platt, F. M., van Blitterswijk, W. J., Sillence, D. J. Accumulation of glycosphingolipids in Niemann-Pick C disease disrupts endosomal transport. *J Biol Chem* **279**, 26167 (2004).
[74] Lloyd-Evans, E., Morgan, A. J., He, X., Smith, D. A., Elliot-Smith, E., Sillence, D. J., Churchill, G. C., Schuchman, E. H., Galione, A., Platt, F. M. Niemann-Pick disease type

C1 is a sphingosine storage disease that causes deregulation of lysosomal calcium. *Nat Med* **14**, 1247 (2008).

7 NUCLEIC ACID CONJUGATION ENABLES EFFICIENT INTRACELLULAR PROTEIN DELIVERY BY LIPID-BASED NANOPARTICLES

7.1 INTRODUCTION

Since the approval of recombinant human insulin for diabetes treatment nearly three decades ago, protein therapeutics now comprise a major class of pharmaceuticals with a range of functions and applications, including enzyme replacement, monoclonal antibodies, hormones, and protein-based vaccines[1]. However, most protein therapeutics act extracellularly or at the cell surface, or if endocytosed, carry out their function within lysosomes. Effective intracellular protein delivery remains an enormous technical challenge[2, 3], yet offers the potential to broaden the scope of diseases amenable to this class of drugs and circumvent the inherent risks of gene therapeutics[4].

Cell-penetrating peptides[5] represent one widely studied approach to achieving intracellular delivery through covalent or non-covalent attachment of protein transduction domains, which include TAT-derived peptides[6-8], arginine-rich peptides[9, 10], Antennapedia-derived penetratin peptides[11], and amphiphilic peptide carriers such as Pep-1[12]. A related approach involves fusion of a protein known or engineered to achieve intracellular localization, such as herpes simplex virus protein VP22[13, 14], or more recently, a supercharged variant of GFP[15]. Limitations with these methods include the lack of protection from proteases and the absence of an active mechanism to achieve endosomal escape[16, 17].

A number of materials have been described for encapsulation and intracellular delivery of proteins, including lipids and liposomes[18, 19], charge-conversional polyionic micelles[20], cationic amphiphiles[21], and various polymers[22-24]. Nonetheless, because protein loading depends on the strength of non-covalent interactions between the protein cargo and the material, these techniques may be useful only for a subset of proteins with suitable physicochemical properties. A more promising approach involves synthesis of a biodegradable polymeric shell directly from the protein itself, so that the protein core is encapsulated within a nanocarrier that facilitates intracellular delivery[25]. In general, most of these materials have not yet achieved clinical or even preclinical demonstration of their safety and efficacy for systemic delivery.

By comparison, a much wider array of materials has been developed for non-viral delivery of nucleic acids[26]. In particular, a group of lipid-like molecules termed lipidoids has demonstrated safe, effective, and potent delivery of RNAi therapeutics in preclinical studies involving mice, rats, and nonhuman primates[27, 28]. We hypothesized that these lipid-based nanoparticle (LNP) formulations might also mediate effective protein encapsulation and intracellular delivery if the protein cargo were conjugated to one or more oligonucleotides (Figure 7.1). To our knowledge, this simple idea has not yet been tested with other delivery reagents.

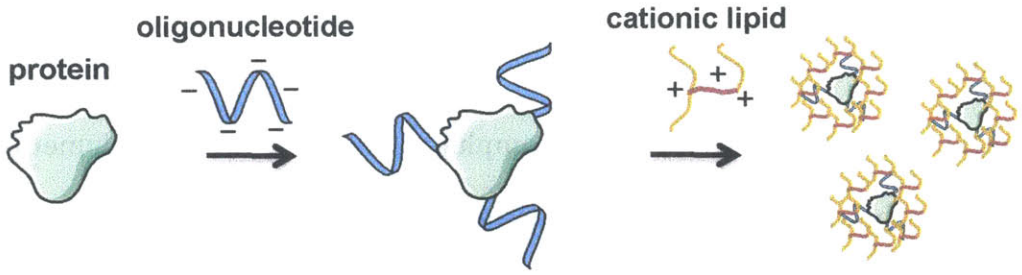

Figure 7.1 Scheme for delivery of proteins by lipid-based nanoparticles via oligonucleotide conjugation

In this chapter, we develop LNP formulations for intracellular delivery of protein-oligonucleotide conjugates. Working with horseradish peroxidase (HRP) as a model protein, we show that one particular lipidoid, C14-113, mediates effective intracellular delivery of HRP-oligonucleotide conjugates to HeLa cells, that the enzyme retains activity after delivery, and that delivery depends on HRP-oligonucleotide conjugation. Similarly, with NeutrAvidin, a variant of avidin, we show that oligonucleotide conjugation significantly improves intracellular protein delivery by C14-113 in HeLa cells, likely owing to a threefold enhancement in NeutrAvidin loading. When we formulated C14-113 LNPs with either free NeutrAvidin or with NeutrAvidin-oligonucleotide conjugates and injected them intravenously in mice, we observed that oligonucleotide conjugation significantly enhanced intracellular protein uptake in macrophages and dendritic cells within the spleen, suggesting delivery of protein-based vaccines as a potential application of this approach.

7.2 MATERIALS AND METHODS

7.2.1 Materials

Lipidoids were synthesized as previously described[27]. Horseradish peroxidase (type VI, 250-330 units/mg), copper (II) sulfate, tris(2-carboxyethyl)phosphine hydrochloride (TCEP), tris[(1-benzyl-1H-1,2,3-triazol-4-yl)methyl]amine (TBTA), cholesterol, and O-phenylenediamine were purchased from Sigma-Aldrich (St. Louis, MO, USA). Unlabeled NeutrAvidin, Oregon Green 488-labeled NeutrAvidin, and AlexaFluor 488 carboxylic acid, succinimidyl ester, were purchased from Invitrogen (Carlsbad, CA, USA). Cy5.5 mono-reactive NHS ester was acquired from GE Healthcare (Pittsburgh, PA, USA). Three oligonucleotide variants (unmodified, 5'-hexynyl, and 5'-biotin-PEG_4-modified) with the following sequence were custom synthesized and desalted by Integrated DNA Technologies (Coralville, IA, USA): 5'-CGGGCGCGACTAGTGTGAAATCTGAATAATTTTGTGTTACTC-3'. NHS-PEG_4-Azide crosslinker, Slide-A-Lyzer G2 dialysis cassettes (20K MWCO), and Zeba Spin desalting columns (40K MWCO) were acquired from Pierce Biotechnology (Rockford, IL). mPEG2000-DMG was synthesized by Alnylam (Cambridge, MA, USA) as described[28]. 1,2-distearoyl-sn-glycero-3-phosphocholine (DSPC) and 1,2-dioleoyl-sn-glycero-3-phosphoethanolamine (DOPE) were obtained from Avanti Polar Lipids (Alabaster, AL, USA). HeLa cells (ATCC, Manassas, VA, USA) were cultured in DMEM (Invitrogen) supplemented with 10% fetal bovine serum (Invitrogen).

7.2.2 Protein-oligonucleotide conjugation

For DNA oligonucleotide conjugation to horseradish peroxidase (HRP), HRP was first azide-functionalized using NHS-PEG_4-Azide crosslinker according to the manufacturer's directions. Briefly, NHS-PEG_4-Azide (2.27 mM, MW = 388.37 Da) in anhydrous DMSO was added to HRP (0.176 mM, MW = 44 kDa) in a total volume of 2.425 mL PBS (20 mM sodium phosphate, 0.15 M sodium chloride, pH 7.2) and then incubated for 30 min at RT. To quench the reaction, 1 M Tris-HCl (pH 8.0) was added to achieve a final Tris-HCl concentration of 0.1 M. The reaction was incubated for an additional 5 min at RT and then dialyzed against 3 L PBS overnight at 4°C using a Slide-A-Lyzer G2 cassette (20 K MWCO) with two buffer exchanges. Azide-functionalized HRP (72.5 μM) was then incubated with 5'-alkyne-modified oligonucleotide (109 μM, MW = 13.14 kDa), $CuSO_4$ (1 mM), TCEP (4 mM), and TBTA (100 μM) in a final volume of 3.9 mL for 5 h at RT, with minor modification from a previous report[29]. The reaction was then purified by dialysis against 3 L PBS overnight at 4°C using a Slide-A-Lyzer G2 cassette (20 K MWCO) with two buffer exchanges. The HRP-oligo conjugate concentration was determined in two ways with roughly equivalent results: absorbance measurement at 403 nm ($\varepsilon_{HRP,\,403\,nm}$ = 102 $mM^{-1}\,cm^{-1}$) using a NanoDrop 1000 spectrophotometer (Thermo Scientific, Waltham, MA, USA), and a BCA Protein assay (Thermo Scientific).

For oligo conjugation to NeutrAvidin (nAv), 5'-biotin-PEG_4-functionalized oligo (37.2 μM, MW = 13.46 kDa) was incubated with fluorescently labeled nAv (18.6 μM, MW = 60 kDa) in a final volume of 0.75 ml PBS for 1 h at RT and used without purification. nAv was pre-labeled with either Cy5.5 mono-reactive NHS

ester (GE Healthcare) or AF 488 carboxylic acid, succinimidyl ester, (Invitrogen) using the manufacturers' instructions and was purified prior to conjugation using a Zeba Spin desalting column (40 K MWCO) equilibrated with PBS. For both labeling reactions, the final fluorophore:protein labeling molar ratio was approximately 1:1 as determined with a spectrophotometer. The conjugate concentration was determined by using the absorbance measurement at 280 nm ($\varepsilon_{nAv,\ 280\ nm}$ = 99.6 $mM^{-1}\ cm^{-1}$).

7.2.3 Microfluidic device formulation of lipid nanoparticles (LNPs)

Stock solutions of lipidoid, cholesterol (MW = 387 Da), DSPC (MW = 790 Da), and mPEG2000-DMG (MW = 2660 Da) were prepared in ethanol at concentrations of 100, 20, 20, and 20 mg/mL, respectively. In most experiments, the components were combined to yield molar fractions of 50:38.5:10:1.5; however, in one experiment, DSPC was substituted with DOPE (MW =744 Da) at the same molar fraction.

The HRP-DNA conjugate, or the free HRP control, was diluted in 10 mM citrate buffer (pH 3.0) at a concentration of 0.5 mg/mL DNA, corresponding to an HRP concentration of 1.13 mg/mL. Due to differences in stabilities between the free nAv protein and the nAv-DNA conjugate, the nAv-DNA conjugate was diluted in 25 mM citrate buffer (pH 5.2) at a concentration of 0.375 mg/mL DNA (equivalent protein concentration of 0.845 mg/mL), while the free nAv was diluted to 0.845 mg/mL in 10 mM citrate buffer (pH 3.0). The lipid solution was diluted as necessary to yield a lipidoid:DNA weight ratio of 10:1.

Microfluidic devices were synthesized as described previously[30]. To prepare LNPs, the protein solution and the lipid solution were injected into the microfluidic device at a relative volumetric flow rate of 3:1 (0.9 mL/min : 0.3 mL/min) using two syringes (Gastight syringes, Hamilton Company, NV, USA) that were controlled by two syringe pumps (PHD 2000, Harvard Apparatus, MA, USA). To remove ethanol, the freshly prepared LNPs were dialyzed for 2 h against 3 L PBS using Slide-A-Lyzer G2 cassettes (20K MWCO).

7.2.4 In vitro protein transfection

One day before transfection, HeLa cells (100 µL) were seeded in a clear 96-well tissue culture plate at 15,000 cells per well. LNPs and naked protein/conjugate control treatments were diluted in freshly warmed growth medium as necessary to achieve the desired protein dose (generally 100 ng – 1 µg per 150 µL per well). The conditioned medium was aspirated just before transfection and replaced with the LNPs/proteins diluted in fresh medium. The nanoparticles were incubated with the cells for 3 h at 37°C.

7.2.5 HRP activity assay

After incubation with the nanoparticles, the cells were washed 3 times with PBS (200 µL) and treated with 0.25% w/v trypsin-EDTA (25 µL) for 5 min at 37°C to detach cells as well as to digest any remaining membrane-bound HRP. Upon addition of growth medium (50 µL), the cells were pipet-mixed, transferred to a clear 96-well assay plate, pelleted using a centrifuge, re-suspended in 100 µL of

substrate solution, and repeatedly pipet-mixed. Substrate solution was prepared by dissolving a 15 mg tablet of o-phenylenediamine in 12.5 mL 100 mM sodium citrate, pH 4.5, and adding 3.5 µL of hydrogen peroxide solution (30% w/v) immediately before use. The assay plate was incubated for 10 min at RT with orbital shaking prior to addition of 50 µL 2.5 M H_2SO_4. The absorbance at 490 nm was then immediately measured using a SpectraMax 190 microplate reader (Molecular Devices, Sunnyvale, CA, USA). The activity assay was performed in an analogous manner on a series of dilutions of the free HRP protein and the conjugate to generate a standard curve for each.

7.2.6 FACS analysis

After aspirating conditioned medium and washing cells three times with PBS, cells were detached using 25 µl per well of 0.25% trypsin-EDTA (Invitrogen). Following a 5 min incubation at 37°C, fresh medium (50 µl) was added to the cells, which were mixed thoroughly and then transferred to a 96-well round-bottom plate. Cells were then pelleted, re-suspended in fixation buffer (4% v/v formaldehyde in PBS), incubated for 10 min at RT, pelleted again, and finally re-suspended in ice-cold FACS running buffer (2% v/v FBS in PBS) containing 1:200 v/v propidium iodide (Invitrogen). The cells were kept at 4°C until FACS analysis using a BD LSR II (Becton Dickinson, San Jose, CA, USA). Gating and analysis were performed using FlowJo v8.8 software (TreeStar, Ashland, OR, USA).

7.2.7 Gel electrophoresis

Oligos and protein-oligo conjugates were run on a pre-cast 4-20% polyacrylamide-TBE gel (Bio-Rad, Hercules, CA, USA) for 1 h at 100 V. The gel was then stained for 30 min with SYBR Gold (Invitrogen) and visualized with a Bio-Rad GelDoc XR+ imager.

LNPs formulated with nAv or nAv-oligo conjugates were run on a pre-cast Any kD mini-Protean TGX gel (Bio-Rad) for 30 min at 100 V. The gel was stained for 1 h with Bio-Safe Coomassie Stain (Bio-Rad), destained overnight, and visualized using a Bio-Rad GelDoc XR+ imager. The entrapment efficiency was determined as: $(S_{free} - S_{LNP})/S_{free}$, where S_{free} is the total signal per lane for the free protein or conjugate and S_{LNP} that for the LNP-encapsulated protein or conjugate.

7.2.8 Animal experiments

Animal experiments were performed using 6-8 wk old, female C57BL/6 mice (Charles River, Wilmington, MA) in accordance with protocols approved by MIT's Committee on Animal Care (CAC). Mice were injected intravenously via the tail-vein with 0.2 mL of LNP formulations, unformulated controls, or PBS at a nAv protein dose of 2.5 mg/kg. After 2 h, the animals were euthanized, and the livers, spleens, kidneys, lungs and heart were dissected and analyzed for fluorescence (ex = 675 nm, em = 720 nm) using an IVIS imaging system (Xenogen, Alameda, CA). Xenogen Living Image v. 4.2 acquisition and analysis software was used to quantify fluorescent radiant efficiency of each organ from the optical images. The livers and spleens were then frozen on dry ice using Tissue-Tek OCT (Sakura, Torrance, CA, USA) and sectioned with a cryotome. Some frozen sections were scanned for Cy5.5

fluorescence using a Li-COR Odyssey imager (Lincoln, NE, USA). The other frozen sections were fixed and stained for analysis of Cy5.5-nAv uptake by confocal microscopy.

For analysis of splenocyte uptake, spleens were harvested 2 h post-injection, and the spleen cell suspension was analyzed for different immune cell populations and for AF488-labeled nAv uptake by flow cytometry (CD11b+: cells of the macrophage/monocyte lineage; CD11b+GR1+: neutrophils; CD11c+: dendritic cells; GR1+: granulocytes; CD19+: B-cells; TCRb+: T cells).

7.3 Results and Discussion

7.3.1 Intracellular delivery of horseradish peroxidase

Horseradish peroxidase (HRP), a 44 kDa enzyme with an isoelectric point of approximately 8.0-9.0, was initially selected as a model protein for intracellular delivery, since the enzymatic activity of the delivered protein could be readily assayed. We prepared HRP-oligonucleotide conjugates via an azide-alkyne click reaction. Briefly, HRP was azide-functionalized using an NHS-ester crosslinker with a short PEG spacer. The azide-modified HRP was then conjugated to a 42 base 5'-hexynyl-functionalized DNA oligonucleotide (oligo) with reaction conditions as reported previously[29] using a molar ratio of 1.5:1.0 oligo:HRP.

A gel shift assay confirmed the presence of HRP-DNA conjugates bearing one or more oligonucleotides (Figure 7.2a). To determine whether these HRP-DNA conjugates still retained their activity, we compared the enzymatic activity of the HRP-oligonucleotide conjugates to that of the free HRP protein (Figure 7.2b) using

o-phenylenediamine (OPD). Surprisingly, the HRP-oligo conjugates displayed greater apparent activity than unmodified HRP, a result that we initially attributed to an underestimation of the conjugate protein concentration as determined by the absorbance at 403 nm. However, an independent measurement of the conjugate protein concentration using a bicinchoninic acid (BCA) assay yielded essentially the same result to within 10% as that of UV/vis spectroscopy, so we relied on these concentrations as measured for the ensuing transfection experiments.

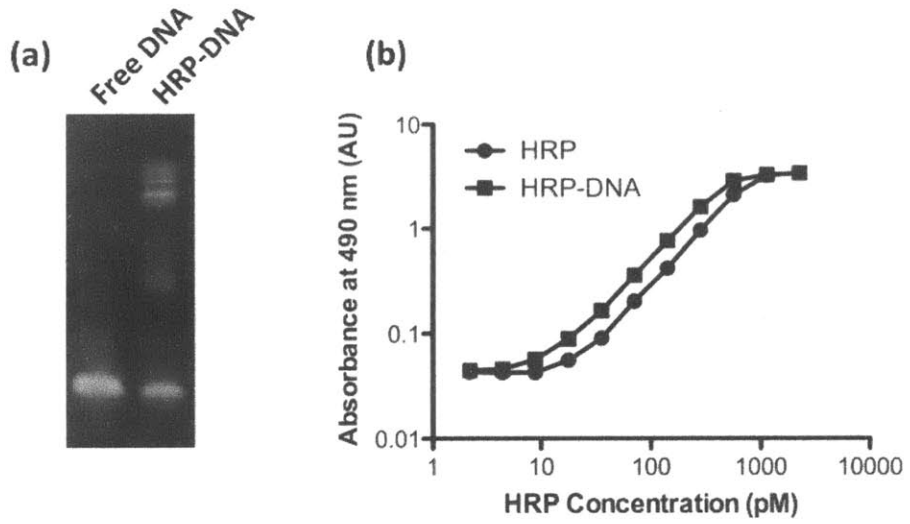

Figure 7.2 Characterization of HRP-DNA oligonucleotide conjugates. **(a)** Polyacrylamide gel electrophoresis of free DNA oligonucleotide (42 nt) and HRP-DNA oligo conjugates. **(b)** OPD-based assay of peroxidase activity for free HRP and HRP-oligo conjugates.

We first screened a panel of lipidoid formulations for *in vitro* delivery of the HRP-oligo conjugates. Sixteen lipidoids varying in their amine cores and alkyl tails as described[27] were mixed with DSPC, PEG-DMG, and cholesterol and then formulated with HRP-oligonucleotide conjugates. The resulting nanoparticle formulations were incubated with HeLa cells for 4 h, after which the cells were

washed 3 times with PBS and treated with trypsin to digest any remaining membrane-bound HRP. Subsequently, the cells were transferred to an assay plate, pelleted, and re-suspended in OPD substrate buffer for an HRP activity assay. As shown in Figure 7.3, lipidoids bearing longer alkyl tails (C14) generally displayed more effective delivery of active HRP-oligo conjugates. Using the top four lipidoids from this screen, further optimization of formulation conditions indicated that formulations including DSPC and cholesterol delivered HRP conjugates more effectively than those containing DOPE (Figure 7.4). In particular, the lipidoid C14-113 appeared to outperform the other lipidoids with respect to delivery activity.

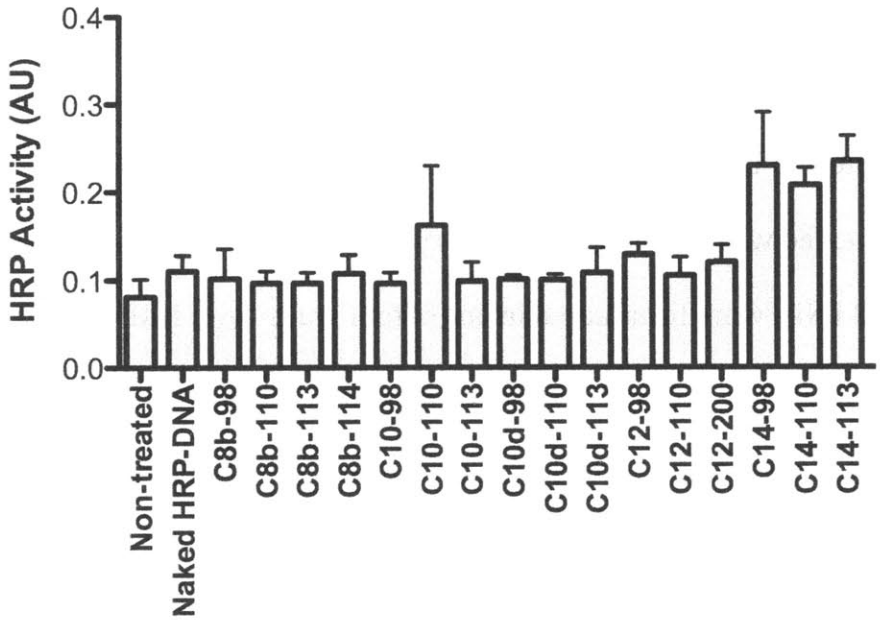

Figure 7.3 Screen of various lipidoids for delivery of active HRP-oligo conjugates
The indicated lipidoids were formulated with HRP-oligo conjugates (250 ng HRP/well; 96-well plate) and incubated for 4 h with HeLa cells, which were then washed, trypsinized, and subjected to an HRP activity assay.

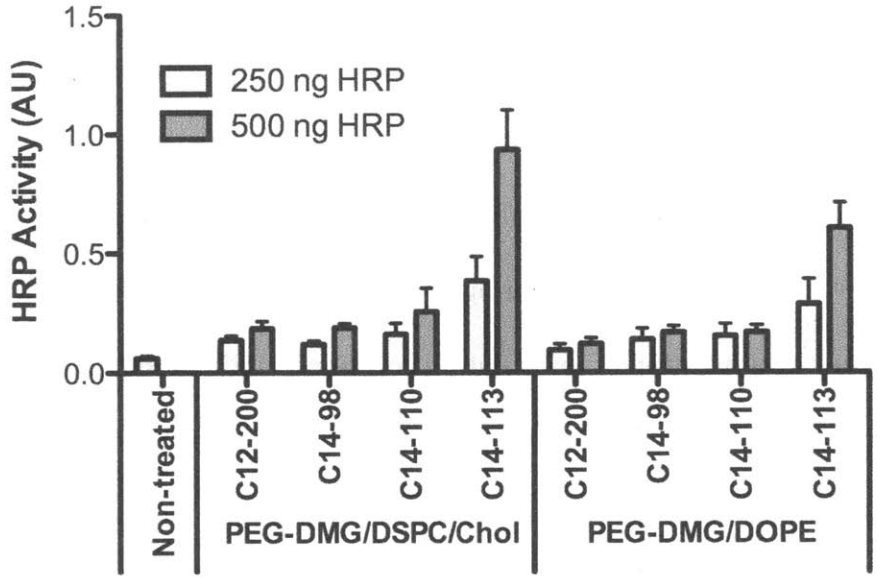

Figure 7.4 Optimization of LNP formulations for delivery of HRP-oligo conjugates
Four lipidoids were formulated with HRP-oligo conjugates as indicated and incubated for 4 h with HeLa cells, which were then washed, trypsinized, and subjected to an HRP activity assay.

Having identified an LNP formulation mediating delivery of HRP-DNA conjugates, we then tested whether effective delivery depends on oligonucleotide conjugation. C14-113 LNPs were formulated in one of four ways: with HRP protein alone; with a mixture of HRP protein and unconjugated, unmodified oligonucleotide; with a mixture of free HRP protein and unconjugated, 5'-hexynyl-modified oligonucleotide; or with the HRP-oligonucleotide conjugates prepared by click chemistry. In addition to naked HRP protein and naked HRP-oligo conjugates as control treatments, the formulations were incubated for 4 h with HeLa cells. As shown in Figure 7.5, only the C14-113 LNPs formulated with HRP-oligo conjugates yielded significant HRP activity after washing and trypsinizing the cells. This result suggests that HRP-oligonucleotide conjugation is required to achieve significant intracellular HRP delivery with these LNPs.

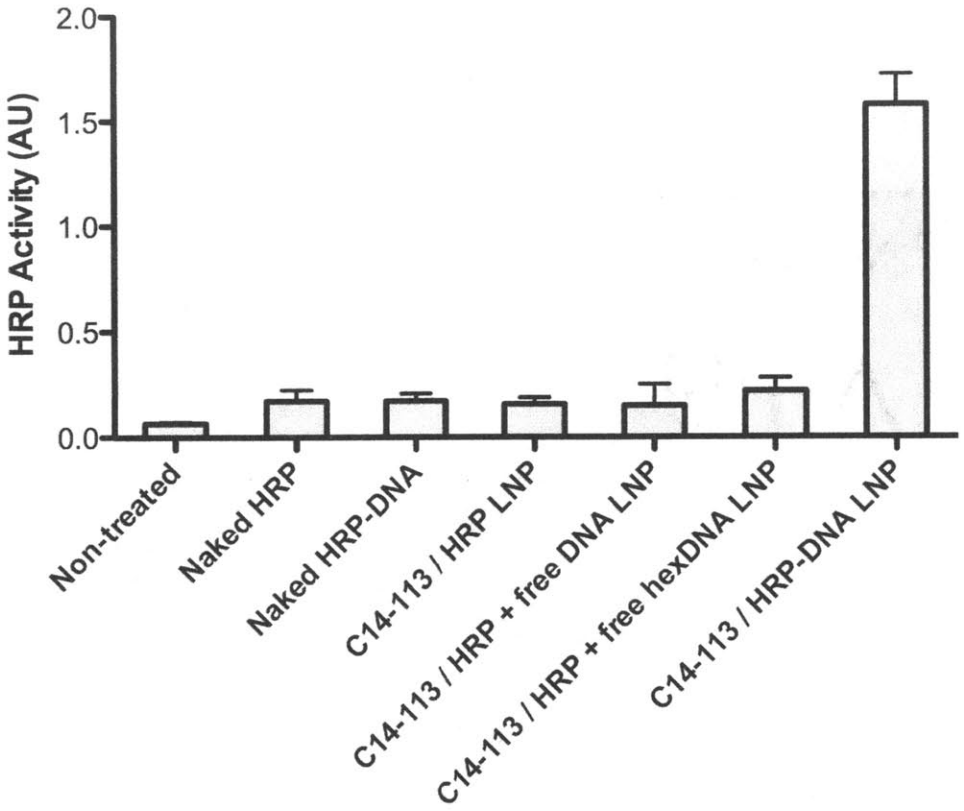

Figure 7.5 Oligonucleotide conjugation is required for effective delivery of HRP by LNPs
HeLa cells were incubated for 4 h with C14-113 LNPs formulated with HRP; with HRP and free unmodified DNA oligo; with HRP and free hexynl-modified DNA oligo; or with HRP-DNA oligo conjugates (500 ng HRP/well; 96-well plate). Controls included naked HRP protein and naked HRP-DNA conjugates. The cells were then washed, trypsinized, and subjected to an HRP activity assay.

To confirm that the HRP-oligonucleotide conjugates localized within the cells, we performed immunocytochemistry (ICC) and confocal microscopy. The imaging data revealed significant intracellular HRP staining within cells treated with LNPs containing HRP-oligo conjugates, but no such staining in cells treated with naked HRP-oligo conjugates (Figure 7.6). These results substantiate the conclusions from

the enzymatic activity assay that the C14-113 LNP mediates intracellular transfection of horseradish peroxidase-oligonucleotide conjugates.

(a)

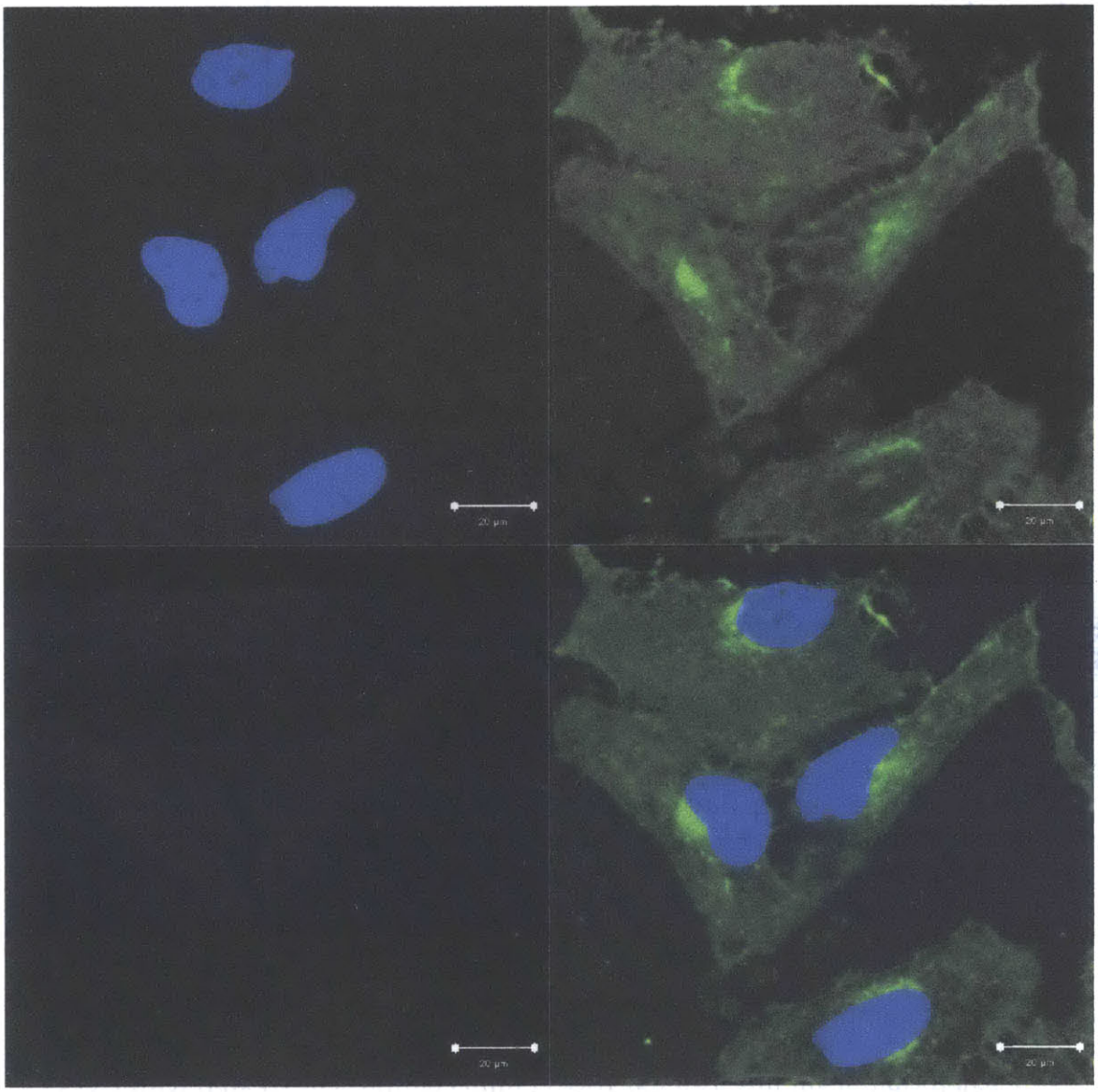

(b)

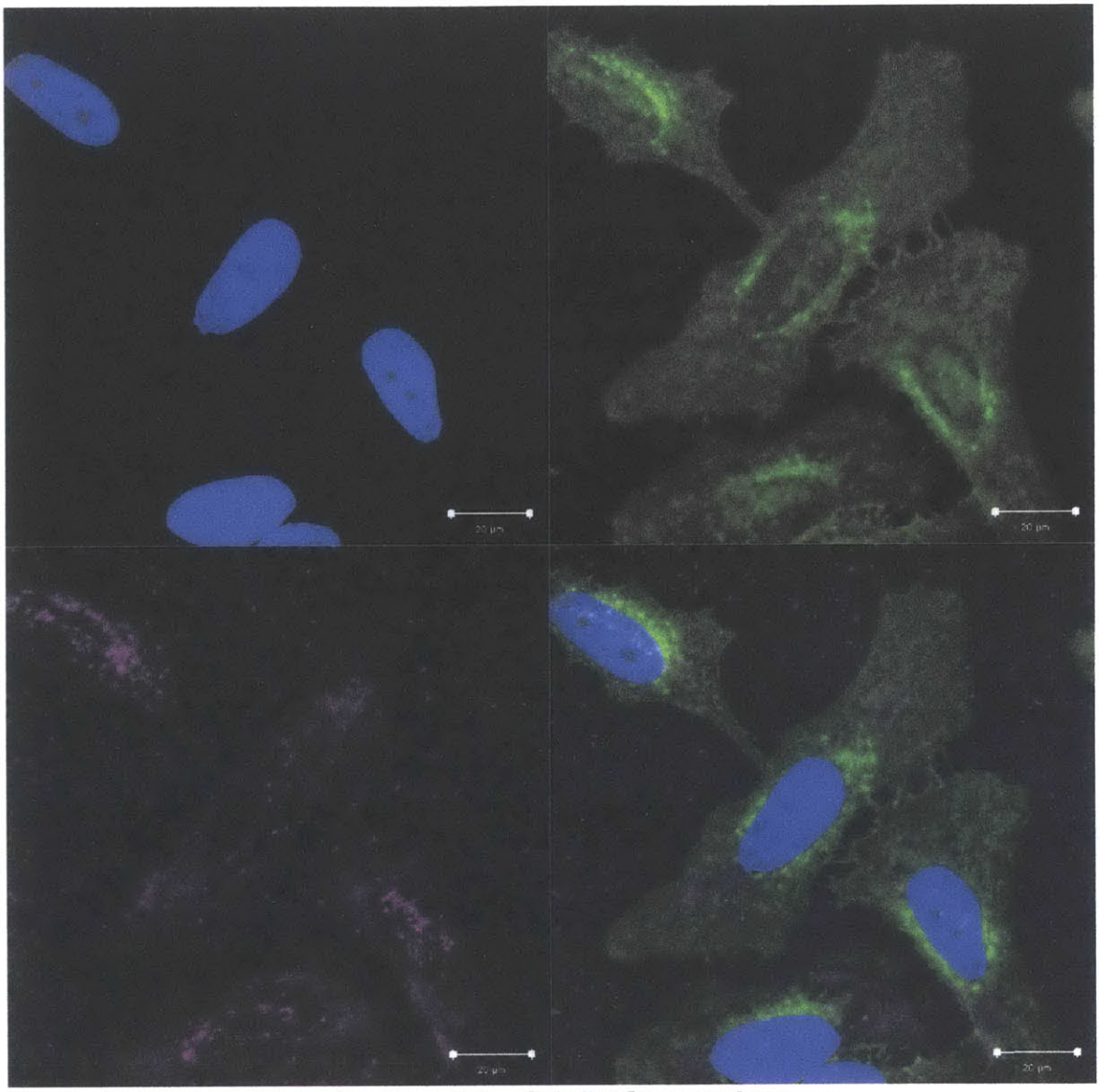

Figure 7.6 Intracellular localization of HRP-oligo conjugates
HeLa cells were treated in 6-well plates with **(a)** naked HRP-oligo conjugates or **(b)** C14-113 LNPs formulated with HRP-oligo conjugates (10 ug HRP per well). The cells were then washed, fixed, stained for various markers including HRP, and analyzed by confocal microscopy. *Blue*: nuclei (DAPI), *green*: membrane (AF488-labeled wheat germ agglutinin), *purple*: HRP (AF647-labeled anti-HRP).

7.3.2 Intracellular delivery of NeutrAvidin

The same principle was illustrated for intracellular delivery of another model protein, NeutrAvidin, a deglycosylated variant of avidin with a molecular weight of 60 kDa and an isoelectric point of 6.3. Fluorescently labeled NeutrAvidin-oligonucleotide conjugates were prepared by incubating Oregon Green 488-labeled NeutrAvidin (nAv), which has four biotin binding sites, with various stoichiometric ratios of 5'-biotinylated oligonucleotides. The resulting conjugates were analyzed with a gel shift assay, which showed efficient conjugation at the 1:1 and 2:1 molar ratios of oligo:nAv (Figure 7.7a). Excess free oligo was detected in the mixture prepared at a 4:1 oligo:nAv ratio, most likely due to interference of the fluorescent label with one or more of NeutrAvidin's four potential biotin-binding sites. For ensuing experiments, the oligo:nAv ratio was maintained at 2:1.

To determine whether oligonucleotide conjugation affected the encapsulation efficiency of nAv within LNPs, C14-113 LNPs were formulated either with free nAv or with nAv-oligo conjugates and characterized by SDS-PAGE alongside naked nAv and naked nAv-oligo conjugates (Figure 7.7b). Quantification of the gel results indicated that the encapsulation efficiency of nAv alone within C14-113 LNPs was ~11.0%, in comparison with ~30.8% for nAv-oligo conjugates. These data suggest that oligonucleotide conjugation enhances the encapsulation efficiency of nAv within C14-113 LNPs by approximately threefold.

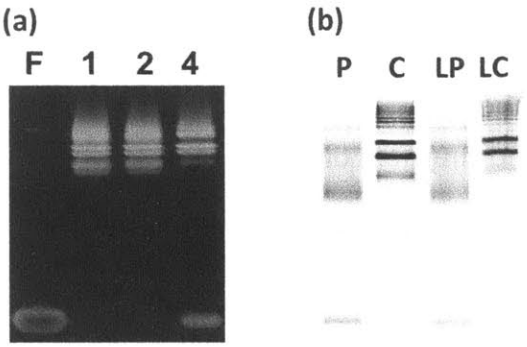

Figure 7.7 Characterization of NeutrAvidin-oligonucleotide conjugates and LNPs by gel electrophoresis
(a) Polyacrylamide gel electrophoresis (PAGE) of free (F) biotinylated DNA oligonucleotide (42 nt) and NeutrAvidin-DNA oligo conjugates prepared at various molar ratios of oligo:DNA (1:1, 2:1, and 4:1). **(b)** SDS-PAGE of naked nAv protein (P), naked nAv-oligo conjugate (C), C14-113 LNPs encapsulating nAv protein (LP), and C14-113 LNPs encapsulating nAv-oligo conjugates (LC).

To characterize the effect of oligo conjugation on intracellular nAv delivery *in vitro*, HeLa cells were incubated with one of three C14-113 LNP formulations: those encapsulating nAv protein alone, those encapsulating a mixture of nAv protein and unconjugated, unmodified oligo; and those encapsulating the nAv-oligo conjugates. HeLa cells were treated for 4 h with these formulations, along with the naked protein and the naked conjugate treatments. The cells were then washed several times, trypsinized, and analyzed by fluorescence-activating cell sorting (FACS) for Oregon Green 488 signal. As displayed in Figure 7.8, neither the naked nAv nor the naked nAv-oligo conjugates yielded significant cellular internalization. At the same nAv dose, the C14-113 LNPs encapsulating nAv-oligo conjugates transfected ~65% of HeLa cells, in comparison with ~19% transfection efficiency for LNPs encapsulating the nAv protein alone, and ~5% transfection efficiency for LNPs encapsulating a mixture of nAv and unconjugated oligo. These results demonstrate that oligo conjugation significantly improves intracellular delivery of nAv mediated

by C14-113 LNPs. Meanwhile, the reduction in transfection observed for LNPs formulated with a mixture of nAv and unconjugated oligo compared with those formulated with nAv alone suggests that the unconjugated oligo may compete with nAv for loading into the C14-113 LNPs. The extent of protein uptake for these treatments was also evaluated by microscopy, which confirmed that only the HeLa cells treated with C14-113 LNPs encapsulating nAv-oligo conjugates showed significant uptake (Figure 7.9).

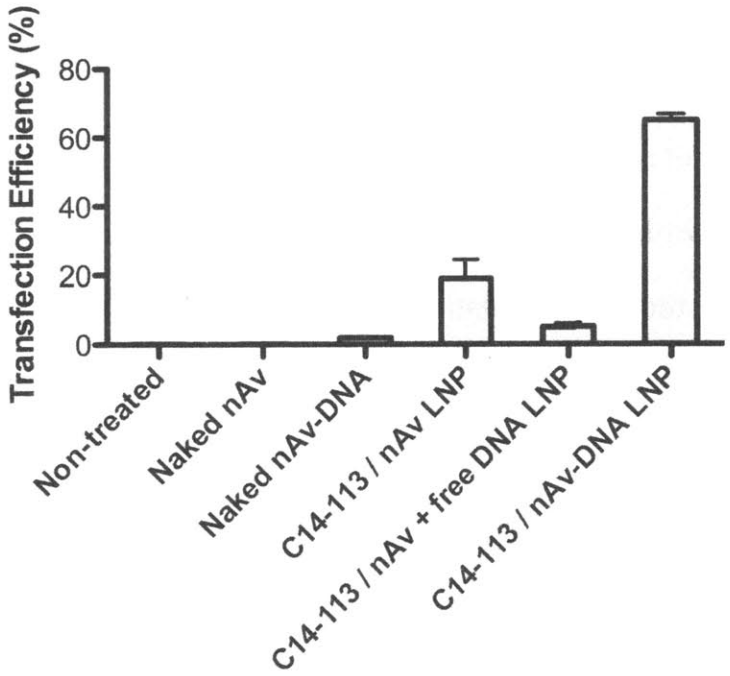

Figure 7.8 Oligonucleotide conjugation is required for efficient delivery of nAv by LNPs
HeLa cells were incubated for 4 h with C14-113 LNPs formulated with nAv; with nAv and free unmodified DNA oligo; or with nAv-DNA oligo conjugates (100 ng nAv/well; 96-well plate). Controls included naked nAv protein and naked nAv-DNA conjugates. For all treatments, nAv was labeled with OregonGreen 488. The cells were then washed, trypsinized, and analyzed by FACS for uptake of nAv.

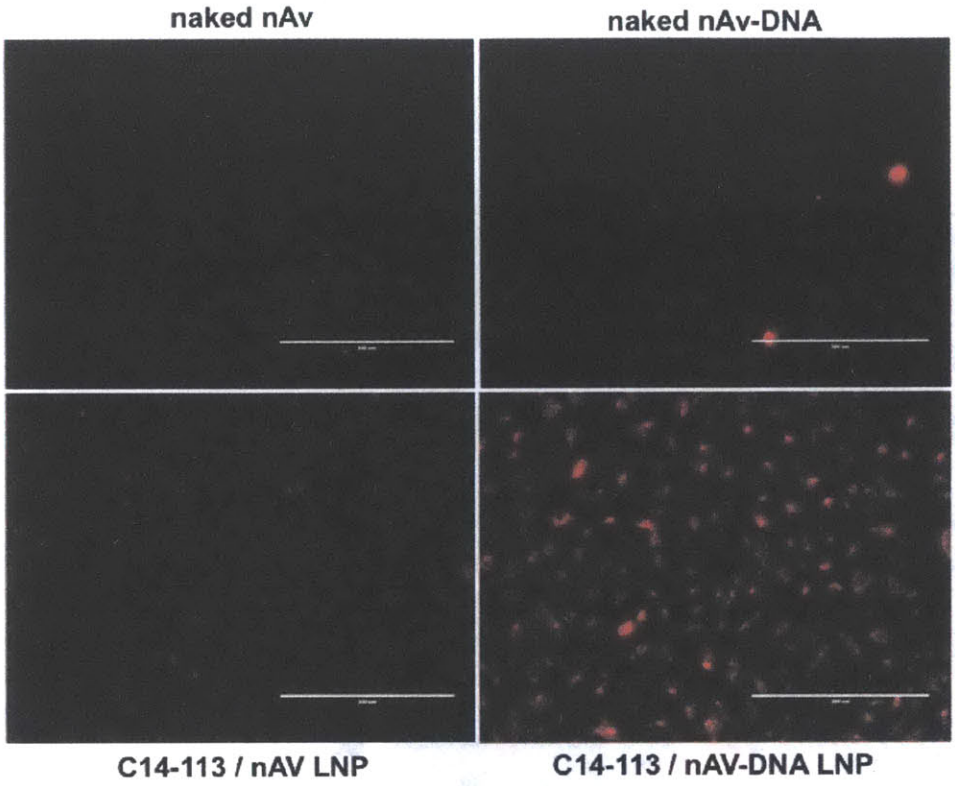

Figure 7.9 Uptake of nAv-oligo conjugates in HeLa cells
HeLa cells were treated with naked nAv, with naked nAv-DNA oligo conjugates, with C14-113 LNPs formulated with free nAv, or with C14-113 LNPs formulated with nAv-DNA conjugates (100 ng nAv/well; 96-well plate). The cells were then washed, trypsinized, and fixed. *Red*: Cy5.5-nAv.

To examine whether oligo conjugation also affects LNP-mediated protein uptake *in vivo*, we investigated the biodistribution of these LNPs 2 h after intravenous (IV) administration to mice. As displayed by fluorescence imaging of the dissected organs, both the LNPs encapsulating the nAv-oligo conjugates (C14-113/nAv-DNA LNPs) and the LNPs encapsulating the free nAv protein (C14-113/nAv) were associated with greatly increased nAv-associated Cy5.5 signal in the liver as compared with naked nAv-oligo conjugates (Figure 7.10). However, the C14-113/nAv-DNA LNP-treated mice showed higher Cy5.5 signal within the spleens and lower signal within the kidneys than those that were treated with C14-113 / nAv

LNPs, suggesting altered biodistribution of the LNPs as a result of protein-oligo conjugation.

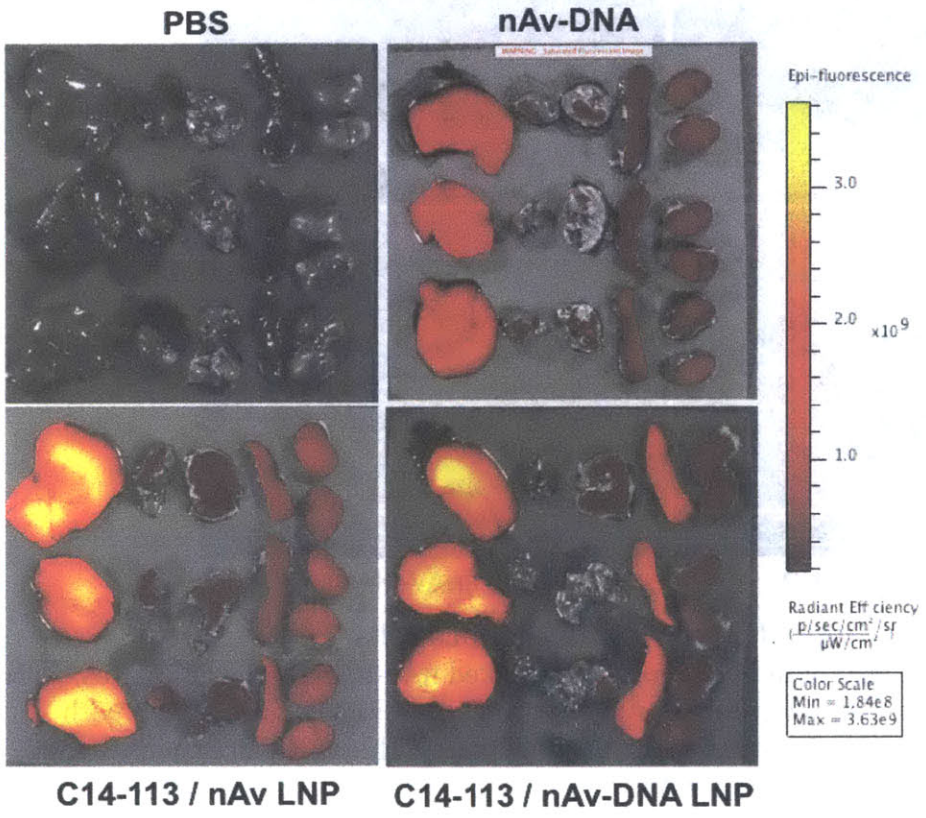

Figure 7.10 Biodistribution of nAv-oligo conjugates in mice
Optical images of Cy5.5 fluorescence in dissected mouse organs 2 h after intravenous injection of the indicated Cy5.5-labeled nAv treatments (2.5 mg/kg nAv dose). Radiant efficiency (photons/s/sr/ µW) is indicated in the color scale bar at left. *L to R*: liver, heart, lungs, spleen, kidneys.

To quantify the difference in protein localization observed in the spleens, we imaged the organ sections using a Li-COR Odyssey near-infrared fluorescence scanner (Figure 7.11). The results indicated approximately 2.5-fold higher uptake of nAv in the spleens of mice treated with LNPs encapsulating the nAv-oligo conjugates compared with those treated with LNPs containing the nAv protein alone. Furthermore, comparing treatment with C14-113/nAv-DNA LNPs and treatment

with naked nAv-DNA conjugates, encapsulation within LNPs increased spleen protein uptake approximately 3.5-fold.

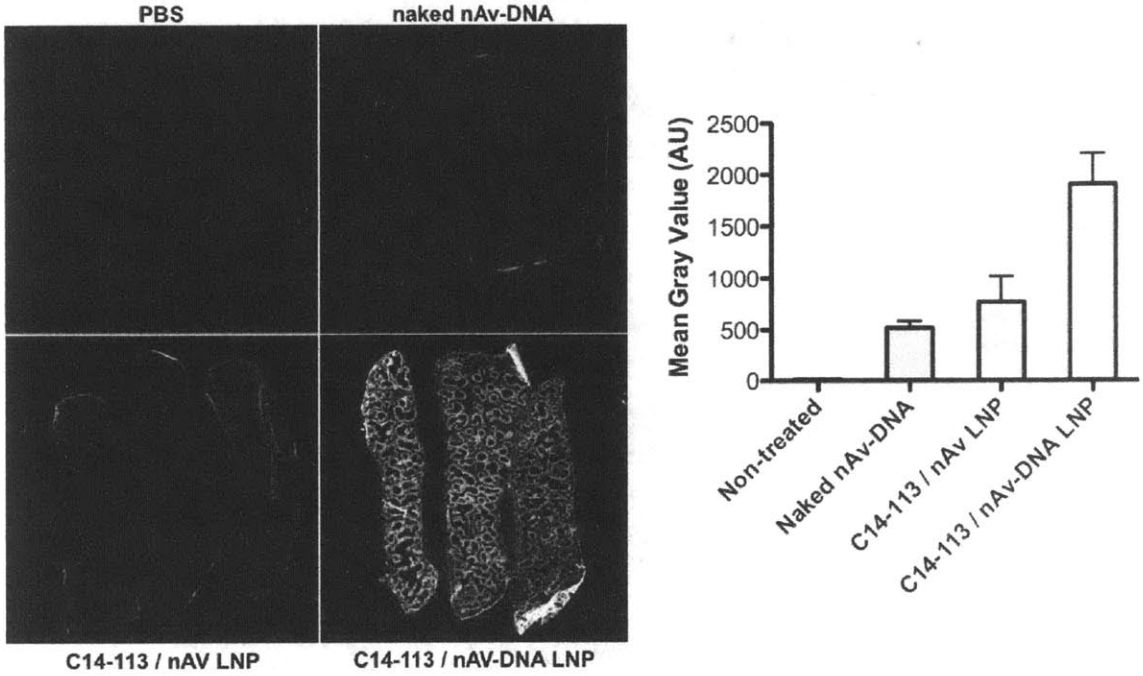

Figure 7.11 Quantification of nAv-oligo localization in mouse spleens
Left: Near-infrared fluorescence scans of Cy5.5 signal in spleen sections harvested from mice 2 h after IV injection of the indicated Cy5.5-labeled nAv treatments (2.5 mg/kg nAv dose). *Right:* Quantification of mean gray values of spleens for each group (n = 3).

Immunohistochemical staining and confocal microscopy confirmed increased accumulation of Cy5.5-labeled nAv in those mice treated with C14-113/nAv-DNA LNPs (Figure 7.12). By comparison, much less accumulation was observed for those mice treated with either naked nAv-DNA conjugates or with C14-113/nAv LNPs. Moreover, in the spleens of mice treated with C14-113 / nAv-DNA LNPs, the nAv signal was quite diffuse within the tissue, contrasting sharply with the punctate nAv signal observed in the spleens of mice treated with the naked conjugates. This

observation suggests the possibility of enhanced endosomal escape and cytosolic localization of nAv-DNA conjugates mediated by the C14-113 LNPs.

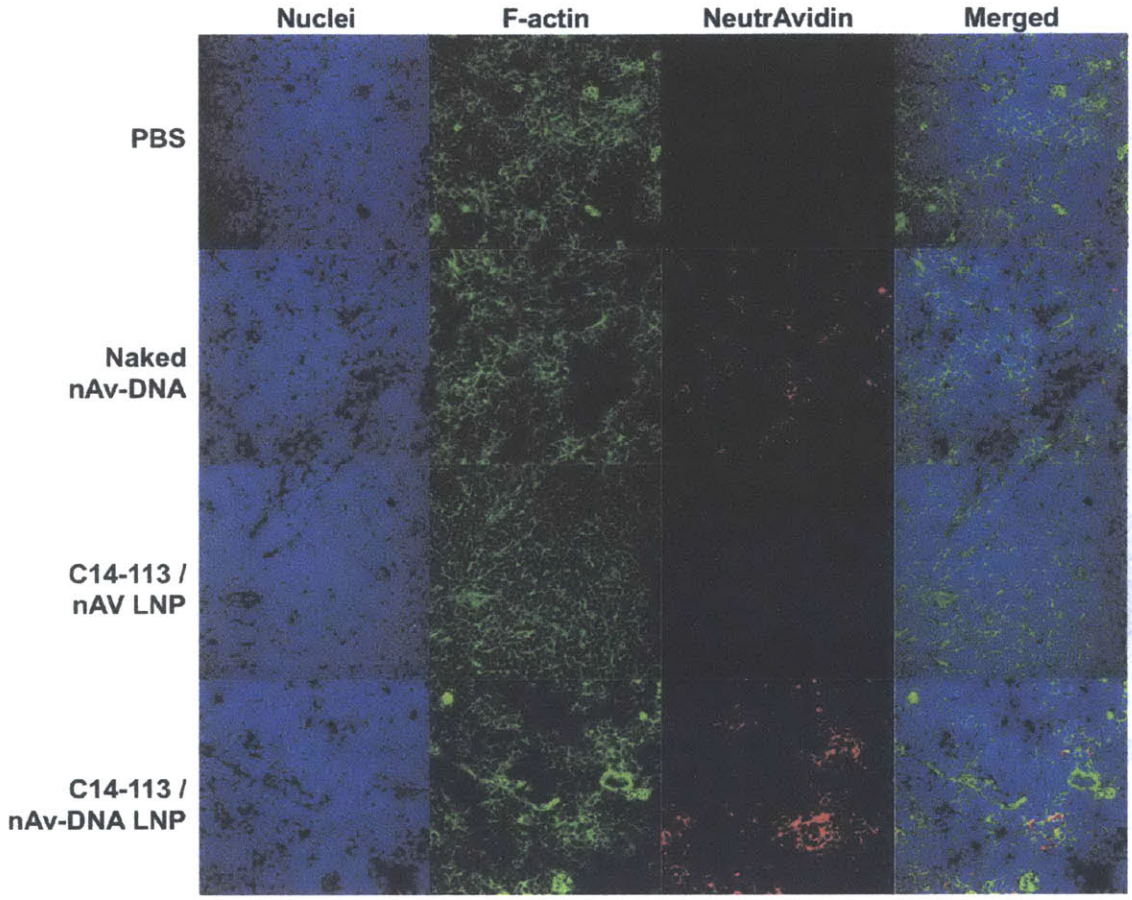

Figure 7.12 Immunohistochemical analysis of mouse spleen sections following nAv-oligo delivery
Immunohistochemical staining revealed increased accumulation of Cy5.5-labeled nAv in spleen sections harvested from mice 2 h after IV injection of C14-113 / nAv-DNA LNPs.

To determine more quantitatively which immune cell populations within the spleen were transfected, mice were injected IV with LNPs encapsulating AF488-labeled nAv protein or nAv-oligo conjugates, along with their naked counterparts. Two hours after injection, the spleens were harvested and the spleen cell suspension was analyzed by FACS for various immune cell markers as well as for

AF488-labeled NAv uptake (Figure 7.13). Both LNP treatments showed increased nAv transfection efficiency in splenic dendritic cells and cells of the macrophage/monocyte lineage relative to naked nAv or nAv-DNA conjugates (Figure 7.13a). Interestingly, comparing the two LNP treatments, the FACS data showed only slightly higher or equivalent nAv uptake efficiency within macrophages/monocytes (CD11b+) and dendritic cells (CD11c+) for the LNPs encapsulating nAv-oligo conjugates. For example, the C14-113/nAv-DNA LNPs transfected ~37% of splenic dendritic cells, compared with ~29% uptake efficiency for C14-113/nAv LNPs, a statistically significant but relatively narrow difference. However, analysis of the AF488 geometric mean fluorescent intensity (GMFI) of transfected macrophages/monocytes and dendritic cells indicated 2-to-3-fold enhancement in nAv uptake for the LNPs encapsulating the nAv-oligo conjugates (Figure 7.13b). This enhancement is especially noteworthy considering that there were no major differences in the uptake levels of transfected macrophages or dendritic cells among the naked control treatment groups and the group treated with LNPs encapsulating free nAv. These results suggest that protein-oligo conjugation significantly increases the level of protein uptake in those immune cells within the spleen susceptible to transfection by LNPs.

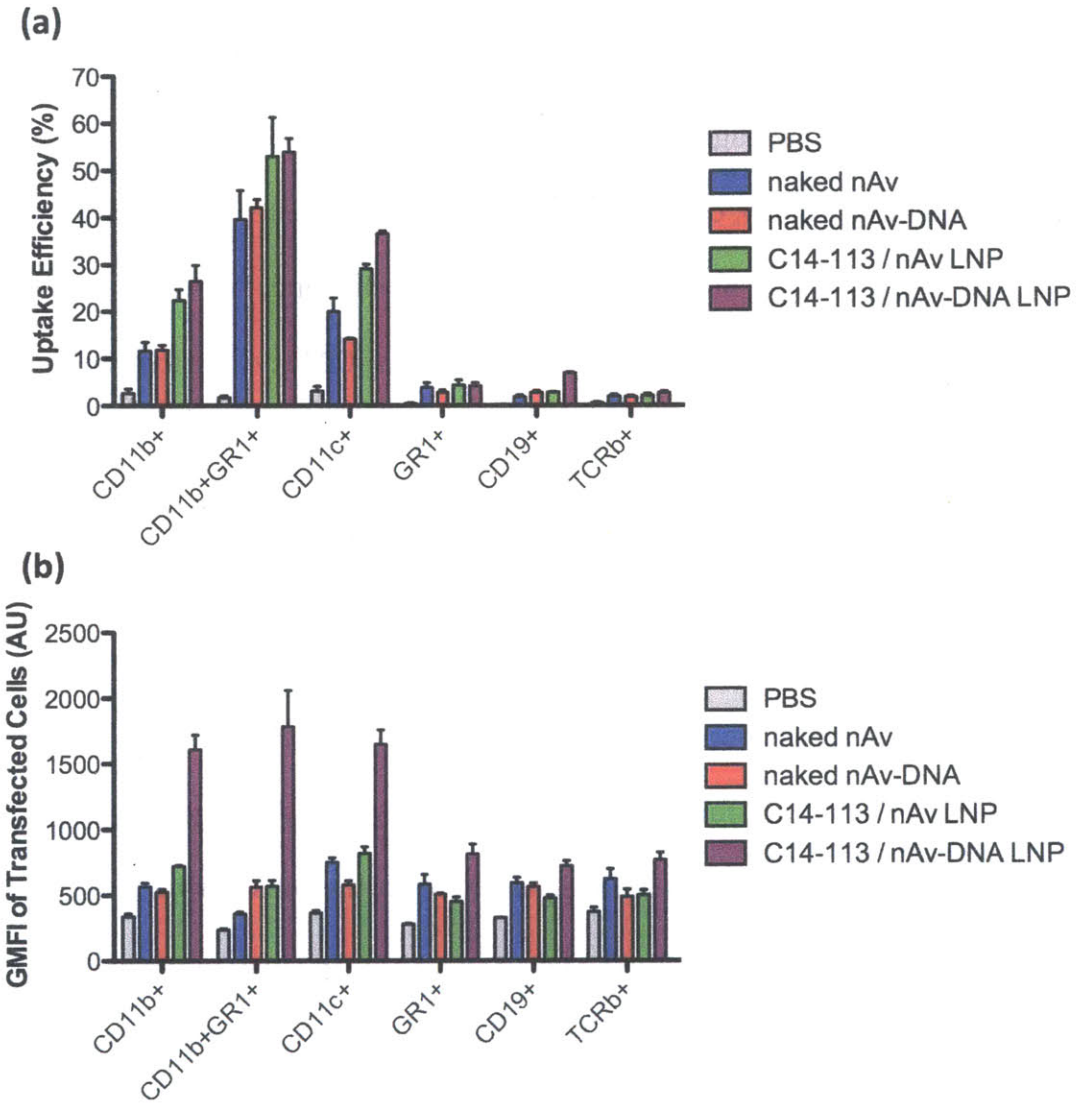

Figure 7.13 Quantification of nAv-oligo uptake in distinct immune cell populations within the spleen

Mice were injected IV with the indicated AF488-labeled nAv treatments, and the spleens were harvested 2 h post-injection. The spleen cell suspension was analyzed by FACS for different immune cell populations as well as for **(a)** nAv uptake efficiency (% AF488+) and **(b)** geometric mean fluorescent intensity (GMFI) of AF488+ cells. *CD11b+*: macrophages/monocytes; *CD11b+GR1+*: neutrophils; *CD11c+*: dendritic cells; *GR1+*: granulocytes; *CD19+*: B-cells; *TCRb+*: T cells.

Recombinant protein-based vaccines are considered less toxic and easier to produce than traditional vaccines based on whole organisms; however, the

comparatively lower immunogenicity of protein-based vaccines requires the development of methods for improved delivery to and activation of antigen-presenting cells including dendritic cells and macrophages[31, 32]. In this regard, our observation that oligonucleotide conjugation results in enhanced LNP-mediated protein uptake within splenic dendritic cells and macrophages/monocytes represents a promising preliminary finding. Further experiments are necessary to determine whether this enhanced protein uptake is also associated with the induction of a more robust immune response characterized by increases in relevant cytokine levels and stimulation of specific T-cell and B-cell responses. Because immunostimulatory oligos such as those enriched in unmethylated CpG motifs are known to be potent vaccine adjuvants[33-35], the approach outlined here could be well suited for the delivery of a vaccine comprising a protein antigen conjugated to a functional, immunostimulatory oligo adjuvant[36]. Moreover, since many vaccines are delivered intramuscularly or subcutaneously, future studies should evaluate whether these administration routes similarly yield enhanced uptake of conjugates in antigen-presenting cells not only within the spleen, but also within the lymph nodes and the peritoneal cavity.

More broadly, the delivery studies with HRP and nAv offer potential for the use of this oligonucleotide conjugation approach for LNP-mediated delivery of other protein cargo. In many cases, the protein-oligonucleotide conjugation will likely require optimization in terms of the number of attached oligos, their length, and their cleavability in order to conserve protein function and achieve delivery. Further study is needed to determine whether the properties of these nanoparticles can be

tailored in terms of size and charge to achieve intracellular protein delivery to specific organs and tissues other than the spleen. Successfully tuning both the conjugation strategy and the properties of the lipid nanoparticles may permit realization of a range of applications, such as the introduction of reprogramming factors to generate induced pluripotent stem cells, enzyme replacement for inherited liver diseases, and the transfection of engineered nucleases for genome editing.

7.4 CONCLUSIONS

In this chapter, using two distinct model proteins, we demonstrated that intracellular protein delivery with LNPs is significantly enhanced through conjugation of oligonucleotides to the protein cargo. Using click chemistry, we synthesized conjugates of horseradish peroxidase (HRP) and a DNA oligonucleotide, and we show that one particular lipidoid, C14-113, mediates effective intracellular delivery to HeLa cells of HRP-oligo conjugates but not free HRP protein. Similarly, with NeutrAvidin (nAv), a variant of avidin, we show that binding to a biotinylated oligo significantly enhances intracellular nAv delivery by C14-113 in HeLa cells. When mice were injected intravenously with C14-113 LNPs encapsulating either free nAv or nAv-oligo conjugates, we observed that oligonucleotide conjugation significantly improved intracellular nAv uptake in macrophage/monocytes and dendritic cells within the spleen. These preliminary *in vivo* results suggest that this approach may be suitable for improved delivery of protein-based vaccines by LNPs.

7.5 REFERENCES

[1] Leader, B., Baca, Q. J., Golan, D. E. Protein therapeutics: a summary and pharmacological classification. *Nat Rev Drug Discov* **7**, 21 (2008).

[2] Gu, Z., Biswas, A., Zhao, M., Tang, Y. Tailoring nanocarriers for intracellular protein delivery. *Chem Soc Rev* **40**, 3638 (2011).

[3] Torchilin, V. Intracellular delivery of protein and peptide therapeutics. *Drug Discovery Today: Technologies* **5**, e95 (2008).

[4] Ford, K. G., Souberbielle, B. E., Darling, D., Farzaneh, F. Protein transduction: an alternative to genetic intervention? *Gene Ther* **8**, 1 (2001).

[5] Heitz, F., Morris, M. C., Divita, G. Twenty years of cell-penetrating peptides: from molecular mechanisms to therapeutics. *Br J Pharmacol* **157**, 195 (2009).

[6] Rapoport, M., Lorberboum-Galski, H. TAT-based drug delivery system--new directions in protein delivery for new hopes? *Expert Opin Drug Deliv* **6**, 453 (2009).

[7] Fawell, S., Seery, J., Daikh, Y., Moore, C., Chen, L. L., Pepinsky, B., Barsoum, J. Tat-mediated delivery of heterologous proteins into cells. *Proc Natl Acad Sci U S A* **91**, 664 (1994).

[8] Schwarze, S. R., Ho, A., Vocero-Akbani, A., Dowdy, S. F. In vivo protein transduction: delivery of a biologically active protein into the mouse. *Science* **285**, 1569 (1999).

[9] Wender, P. A., Mitchell, D. J., Pattabiraman, K., Pelkey, E. T., Steinman, L., Rothbard, J. B. The design, synthesis, and evaluation of molecules that enable or enhance cellular uptake: peptoid molecular transporters. *Proc Natl Acad Sci U S A* **97**, 13003 (2000).

[10] Futaki, S., Suzuki, T., Ohashi, W., Yagami, T., Tanaka, S., Ueda, K., Sugiura, Y. Arginine-rich peptides. An abundant source of membrane-permeable peptides having potential as carriers for intracellular protein delivery. *J Biol Chem* **276**, 5836 (2001).

[11] Derossi, D., Joliot, A. H., Chassaing, G., Prochiantz, A. The third helix of the Antennapedia homeodomain translocates through biological membranes. *J Biol Chem* **269**, 10444 (1994).

[12] Morris, M. C., Depollier, J., Mery, J., Heitz, F., Divita, G. A peptide carrier for the delivery of biologically active proteins into mammalian cells. *Nat Biotechnol* **19**, 1173 (2001).

[13] Elliott, G., O'Hare, P. Intercellular Trafficking and Protein Delivery by a Herpesvirus Structural Protein. *Cell* **88**, 223 (1997).

[14] Phelan, A., Elliott, G., O'Hare, P. Intercellular delivery of functional p53 by the herpesvirus protein VP22. *Nat Biotechnol* **16**, 440 (1998).

[15] Cronican, J. J., Thompson, D. B., Beier, K. T., McNaughton, B. R., Cepko, C. L., Liu, D. R. Potent delivery of functional proteins into Mammalian cells in vitro and in vivo using a supercharged protein. *ACS Chem Biol* **5**, 747 (2010).

[16] El-Sayed, A., Futaki, S., Harashima, H. Delivery of macromolecules using arginine-rich cell-penetrating peptides: ways to overcome endosomal entrapment. *AAPS J* **11**, 13 (2009).
[17] Patel, L. N., Zaro, J. L., Shen, W. C. Cell penetrating peptides: intracellular pathways and pharmaceutical perspectives. *Pharm Res* **24**, 1977 (2007).
[18] Debs, R. J., Freedman, L. P., Edmunds, S., Gaensler, K. L., Duzgunes, N., Yamamoto, K. R. Regulation of gene expression in vivo by liposome-mediated delivery of a purified transcription factor. *J Biol Chem* **265**, 10189 (1990).
[19] Zelphati, O., Wang, Y., Kitada, S., Reed, J. C., Felgner, P. L., Corbeil, J. Intracellular delivery of proteins with a new lipid-mediated delivery system. *J Biol Chem* **276**, 35103 (2001).
[20] Lee, Y., Ishii, T., Cabral, H., Kim, H. J., Seo, J. H., Nishiyama, N., Oshima, H., Osada, K., Kataoka, K. Charge-conversional polyionic complex micelles-efficient nanocarriers for protein delivery into cytoplasm. *Angew Chem Int Ed Engl* **48**, 5309 (2009).
[21] Weill, C. O., Biri, S., Adib, A., Erbacher, P. A practical approach for intracellular protein delivery. *Cytotechnology* **56**, 41 (2008).
[22] Tinsley, J. H., Hawker, J., Yuan, Y. Efficient protein transfection of cultured coronary venular endothelial cells. *Am J Physiol* **275**, H1873 (1998).
[23] Futami, J., Kitazoe, M., Maeda, T., Nukui, E., Sakaguchi, M., Kosaka, J., Miyazaki, M., Kosaka, M., Tada, H., Seno, M., Sasaki, J., Huh, N. H., Namba, M., Yamada, H. Intracellular delivery of proteins into mammalian living cells by polyethylenimine-cationization. *J Biosci Bioeng* **99**, 95 (2005).
[24] Coue, G., Engbersen, J. F. Functionalized linear poly(amidoamine)s are efficient vectors for intracellular protein delivery. *J Control Release* **152**, 90 (2011).
[25] Yan, M., Du, J., Gu, Z., Liang, M., Hu, Y., Zhang, W., Priceman, S., Wu, L., Zhou, Z. H., Liu, Z., Segura, T., Tang, Y., Lu, Y. A novel intracellular protein delivery platform based on single-protein nanocapsules. *Nat Nanotechnol* **5**, 48 (2010).
[26] Mintzer, M. A., Simanek, E. E. Nonviral vectors for gene delivery. *Chem. Rev.* **109**, 259 (2009).
[27] Love, K. T., Mahon, K. P., Levins, C. G., Whitehead, K. A., Querbes, W., Dorkin, J. R., Qin, J., Cantley, W., Qin, L. L., Racie, T., Frank-Kamenetsky, M., Yip, K. N., Alvarez, R., Sah, D. W., de Fougerolles, A., Fitzgerald, K., Koteliansky, V., Akinc, A., Langer, R., Anderson, D. G. Lipid-like materials for low-dose, in vivo gene silencing. *Proceedings of the National Academy of Sciences* **107**, 1864 (2010).
[28] Akinc, A., Zumbuehl, A., Goldberg, M., Leshchiner, E. S., Busini, V., Hossain, N., Bacallado, S. A., Nguyen, D. N., Fuller, J., Alvarez, R., Borodovsky, A., Borland, T., Constien, R., de Fougerolles, A., Dorkin, J. R., Narayanannair Jayaprakash, K., Jayaraman, M., John, M., Koteliansky, V., Manoharan, M., Nechev, L., Qin, J., Racie, T., Raitcheva, D., Rajeev, K. G., Sah, D. W., Soutschek, J., Toudjarska, I., Vornlocher, H. P., Zimmermann, T. S., Langer, R., Anderson, D. G. A combinatorial library of lipid-like materials for delivery of RNAi therapeutics. *Nat Biotechnol* **26**, 561 (2008).
[29] Duckworth, B. P., Chen, Y., Wollack, J. W., Sham, Y., Mueller, J. D., Taton, T. A., Distefano, M. D. A universal method for the preparation of covalent protein-DNA conjugates for use in creating protein nanostructures. *Angew Chem Int Ed Engl* **46**, 8819 (2007).

[30] Chen, D., Love, K. T., Chen, Y., Eltoukhy, A. A., Kastrup, C., Sahay, G., Jeon, A., Dong, Y., Whitehead, K. A., Anderson, D. G. Rapid Discovery of Potent siRNA-Containing Lipid Nanoparticles Enabled by Controlled Microfluidic Formulation. *J. Am. Chem. Soc.* **134**, 6948 (2012).
[31] Peek, L. J., Middaugh, C. R., Berkland, C. Nanotechnology in vaccine delivery. *Adv Drug Deliv Rev* **60**, 915 (2008).
[32] Singh, M., Chakrapani, A., O'Hagan, D. Nanoparticles and microparticles as vaccine-delivery systems. *Expert Review of Vaccines* **6**, 797 (2007).
[33] Klinman, D. M. CpG DNA as a vaccine adjuvant. *Expert Review of Vaccines* **2**, 305 (2003).
[34] Chu, R. S., Targoni, O. S., Krieg, A. M., Lehmann, P. V., Harding, C. V. CpG oligodeoxynucleotides act as adjuvants that switch on T helper 1 (Th1) immunity. *J Exp Med* **186**, 1623 (1997).
[35] Weeratna, R. D., McCluskie, M. J., Xu, Y., Davis, H. L. CpG DNA induces stronger immune responses with less toxicity than other adjuvants. *Vaccine* **18**, 1755 (2000).
[36] Datta, S. K., Cho, H. J., Takabayashi, K., Horner, A. A., Raz, E. Antigen–immunostimulatory oligonucleotide conjugates: mechanisms and applications. *Immunological Reviews* **199**, 217 (2004).

8 CONCLUSIONS

8.1 MAIN CONTRIBUTIONS

The overarching aim of this thesis was to develop polymer and lipid-based materials for safe, effective intracellular delivery of gene and protein therapeutics. This objective was specifically motivated by a set of unaddressed challenges and questions relating to two groups of materials, poly(β-amino ester)s (PBAEs) and lipidoids. For the promising PBAE gene delivery polymers, these issues included the poor stability of polymer/DNA polyplexes under physiological conditions, polymer batch-to-batch variability, and a lack of knowledge regarding polyplex cellular uptake and trafficking mechanisms. For lipidoids, the question was whether these materials, which have demonstrated exceptional potency for delivery of oligonucleotides, could also be applied toward effective intracellular delivery of proteins.

To address the issue of PBAE polyplex stability, we developed novel, degradable PBAE polymers displaying enhanced gene delivery potency and nanoparticle aggregation resistance. We hypothesized that the inclusion of alkyl side chains within PBAE polymers would render them sufficiently hydrophobic to interact with PEG-lipid conjugates, and upon association with DNA, result in the formation of ternary complexes with improved stability. Using a combinatorial library approach to synthesize and screen over 120 structurally distinct hydrophobic PBAE terpolymers, we identified several polymers that displayed

transfection activities in HeLa cells significantly greater than that of the popular commercially available transfection reagent Lipofectamine 2000. The most effective PBAE terpolymers were characterized by transfection potencies in HeLa cells approximately 10 to 20-fold that of C32-122, one of the top-performing amine end-modified polymers from the previous generation of PBAEs. We observed that increasing polymer hydrophobicity, as defined by either increasing the feed ratio of alkylamine monomer or increasing its chain length, was associated with increasing transfection activity, an observation which we attribute to tighter binding and encapsulation of DNA. Furthermore, increasing polymer hydrophobicity was correlated with greater polyplex stability at low DNA concentration. In a confirmation of our hypothesis, at high DNA concentrations under conditions of physiological pH and ionic strength, these hydrophobic PBAE terpolymers facilitated interaction with PEG-lipid and DNA to yield stable, well-defined nanoparticles capable of transfecting cultured cells *in vitro*.

Through a series of additional experiments, hydrophobic PBAE terpolymers, including DD24-C12-122 and LL24-C12-122, were found to mediate superior transfection of HUVECs, porcine MSCs, and neonatal rat cardiomyocytes relative to C32-122 and to Lipofectamine 2000. Formulation development with the terpolymer D60-C12-122 suggested that the identity of the PEG-lipid conjugate strongly affects the stability of the nanoparticle formulations and their corresponding transfection efficacies. Following IP or IV administration, D60-C12-122 and D90-C12-122 terpolymer formulations yielded transgene expression in mice persisting for at least three days. Taken together, these findings suggest that modulation of

hydrophobicity is a simple yet powerful approach to improving the gene transfection potency and formulation stability of degradable cationic polymers.

Regarding PBAE batch-to-batch variability, we hypothesized that this issue was related to subtle differences in the molecular weight distribution (MWD) of the polymers. Therefore, we investigated the effect of PBAE MW on the transfection activity, toxicity, and biophysical properties of the resulting polymer-DNA nanoparticles. In spite of the tendency of these polymers to lose transfection activity upon work-up, we developed a method based on size-exclusion chromatography (SEC) that allowed isolation of well-defined, monodisperse PBAE fractions still retaining transfection efficacy. We found that the transfection activities of size-fractionated PBAEs generally increased with MW, a trend that was weakly associated with more efficient DNA binding. We also observed a relatively steep drop-off in transfection performance below a threshold polymer length, lending support to our hypothesis that minor variation in the MW and MWD could in fact account for the inconsistency in batch-to-batch performance. However, because this method enabled the preparative isolation of monodisperse polymer fractions with higher transfection potency than the starting material, it potentially represents a robust solution to this issue.

To address the issue of limited mechanistic knowledge regarding PBAE internalization, uptake of PBAE/DNA nanoparticles was investigated through pharmacological inhibition and marker co-localization studies. Our results indicated that internalization of PBAE/DNA polyplexes in immortalized mouse embryonic fibroblast (MEF) cells likely proceeds through multiple pathways, with a potential

dependence on cholesterol trafficking. Treatment with the cholesterol synthesis and transport inhibitor U18666A resulted in reduced uptake and transfection efficacy. Moreover, significantly decreased uptake and transfection efficacy were observed in MEFs deficient in an endosomal/lysosomal cholesterol transport protein, Niemann-Pick C1 (Npc1). In contrast, Npc1 knockout was only associated with a marginal decrease in DNA uptake mediated by polyethylenimine (PEI) and no apparent effect on DNA uptake mediated by Lipofectamine 2000, suggesting that this cholesterol trafficking dependence is relatively specific to PBAE polyplex uptake. To identify a potential mechanism, we quantified internalization of various endocytic markers in Npc1-deficient MEFs and observed significant reduction in uptake of cholera toxin B (CTB), a marker traditionally associated with caveolae-mediated endocytosis. DNA internalized by PBAEs showed the greatest extent of co-localization with the CTB marker, indicating the possibility of shared uptake pathways that are reduced in cells lacking Npc1. Combined with data indicating improved silencing potency for lipidoid/siRNA nanoparticles in MEF deficient cells, these studies bolster the hypothesis that Npc1 plays a key role in the regulation of endocytic mechanisms affecting uptake and efficacy of nanoparticles.

Finally, to develop lipidoids for protein delivery, we applied a simple strategy showing that effective intracellular protein delivery could be achieved through conjugation of nucleic acids to the protein cargo. For the model enzyme horseradish peroxidase (HRP), we demonstrated that one particular lipidoid, C14-113, mediates effective intracellular delivery to HeLa cells of active HRP-DNA oligonucleotide conjugates but not free HRP protein. Analogously, with NeutrAvidin (nAv), a variant

of avidin, we showed that binding to a biotinylated oligo significantly enhanced intracellular nAv delivery by C14-113 in HeLa cells, most likely due to improved protein entrapment. When mice were injected intravenously with C14-113 lipid-based nanoparticles (LNPs) encapsulating either free nAv or nAv-oligo conjugates, we found that oligonucleotide conjugation improved intracellular nAv uptake in macrophages and dendritic cells within the spleen 2-3-fold. These preliminary *in vivo* results indicate the potential utility of this nucleic acid conjugation approach toward improved LNP-mediated delivery of protein-based vaccines.

8.2 FUTURE OUTLOOK

With a number of promising gene therapeutics currently under advanced clinical development, the gene therapy field finally appears to be coming of age after a notoriously turbulent history. Viral vectors remain the preferred delivery vehicle in most active clinical studies, with considerations of efficacy outweighing concerns regarding their safety risks. However, non-viral vectors are being employed in a growing proportion of clinical trials, a trend that will likely persist with the continued development of improved synthetic gene carriers.

A large focus of this thesis represents an attempt to advance that development for one class of promising degradable gene vectors, PBAEs. The development of novel hydrophobic PBAE terpolymers with dramatic enhancements in gene delivery potency and nanoparticle stability should heighten their prospects for clinical translation. Poor nanoparticle stability is an issue not only for the PBAEs, but also for many gene delivery materials. The solution presented in this thesis,

which involved the incorporation of alkyl side chains into the terpolymers and formulation with PEG-lipid conjugates to produce stable nanoparticles, may therefore be applicable to other polymers as well. Although preliminary experiments suggested that these terpolymers are capable of mediating effective gene delivery *in vivo* following intraperitoneal administration without obvious toxicity, future studies are required to determine their potential for gene delivery through other injection routes, their dose-response and toxicity profiles, and the biodistribution and duration of gene expression. These experiments would lay the groundwork for preclinical studies evaluating their suitability as gene delivery reagents for therapeutic applications in animal models of disease. Furthermore, the development of a robust, preparative technique based on size-exclusion chromatography to isolate homogeneous, well-defined PBAE fractions should reduce issues of molecular weight (MW) heterogeneity and batch-to-batch variability that have been frequently encountered.

On a more fundamental level, while the data presented here elucidate some important structure-activity relationships for these PBAEs, particularly with respect to polymer hydrophobicity and molecular weight, future studies should investigate in more detail potential explanations for the trends that were observed. For example, for the PBAE terpolymers, optimal gene delivery activity was associated with an intermediate degree of polymer hydrophobicity. One hypothesis is that this optimum represents a balance between the rates or extents of DNA binding and unpacking. This hypothesis could be tested experimentally by measuring the DNA binding affinities of terpolymers of varying hydrophobicities by surface plasmon

resonance (SPR). Similarly, as it was observed that the surface charge of the polyplexes became more positive as the terpolymer hydrophobicity increased, a variety of techniques including cryo-transmission electron micrscopy (TEM), atomic force microscopy (AFM), sum frequency generation (SFG) spectroscopy, and molecular dynamics simulations could shed light on the surface characteristics and morphology of the nanoparticles.

The discovery of a critical role for cholesterol trafficking and regulation for gene transfection by PBAEs should enable the identification of potential targets, including Npc1, which might be selectively leveraged to further improve delivery efficacy. As was observed, stable overexpression of Npc1 was associated with increased gene uptake and transfection by PBAEs. High-throughput screening of small molecules or bioactive lipids may reveal compounds that enhance polymeric gene delivery through modulation of critical cellular factors including Npc1. Given the contradictory role of Npc1 in PBAE/DNA and lipid/siRNA transfection, respectively, future studies should elucidate the mechanisms responsible for this discrepancy. One possibility is that in the case of lipid/siRNA transfection of Npc1-deficient cells, the nanoparticles enter through a pathway that is uninhibited by impaired cholesterol trafficking (such as macropinocytosis) and accumulate within late endosomes due to a block in exosomal recycling. In contrast, internalization of PBAE/DNA nanoparticles proceeds through alternate pathways (perhaps caveolae and clathrin-mediated endocytosis) that are blocked due to a critical lack of cholesterol at the plasma membrane, which may impair the formation of caveolae and clathrin-coated vesicles.

In some ways, intracellular delivery of protein-based therapeutics represents a hedge against the risks inherent in gene therapy and therefore also merits suitable research effort. Unfortunately, in contrast to nucleic acids, the wide range of physicochemical properties that proteins possess impedes the development of a generalized protein delivery platform. We have shown the utility of a simple approach in which nucleic acids serve as a handle for encapsulation of proteins by lipidoids, and the resulting LNPs are able to mediate effective intracellular delivery of model proteins *in vitro* and *in vivo*. Future studies should determine the generality of this approach for the delivery of protein-based vaccines as well as other protein cargo of interest, such as enzymes for inherited liver diseases and engineered nucleases for genome editing.

APPENDIX: LIST OF PUBLICATIONS

Published or in press:

1. **Eltoukhy AA**, Chen D, Alabi CA, Langer R, Anderson DG (2013). Degradable terpolymers with alkyl side chains demonstrate enhanced gene delivery and nanoparticle stability. *Adv. Mater.* 25(10), 1487-1493.
2. Jiang S, **Eltoukhy AA**, Love KT, Langer R, Anderson DG (2013). Lipidoid-coated Iron Oxide Nanoparticles for Efficient DNA and siRNA delivery. *Nano Lett.* 13(3), 1059-64.
3. Sahay G, Querbes W, Alabi CA, **Eltoukhy AA**, Sarkar S, Karagiannis E, Love KT, Chen D, Buganim Y, Schroeder A, Langer R, Anderson DG (2013). Disruption of endocytic recycling enhances cellular retention and efficacy of lipid based nanoparticles for siRNA delivery. *Nat. Biotechnol.* Accepted.
4. **Eltoukhy AA**, Siegwart DJ, Alabi CA, Rajan JS, Langer R, Anderson DG (2012). Effect of molecular weight of amine end-modified poly(β-amino ester)s on gene delivery efficiency and toxicity. *Biomaterials* 33(13), 3594-3603.
5. Chen D, Love KT, Chen Y, **Eltoukhy AA**, Sahay G, Kastrup C, Jeon A, Dong Y, Whitehead KA, Anderson DG (2012). Rapid Discovery of Potent siRNA-Containing Lipid Nanoparticles Enabled by Controlled Microfluidic Formulation. *J. Am. Chem. Soc.* 134(16), 6948-6951.
6. Schroeder A, Dahlman JE, Sahay G, Love KT, Jiang S, **Eltoukhy AA**, Levins CG, Wang Y, Anderson DG (2012). Alkane-modified short polyethyleneimine for siRNA delivery. *J. Controlled Release* 160(2), 172-176.
7. Huang YH, Cozzitorto JA, Richards NG, **Eltoukhy AA**, Yeo CJ, Langer R, Anderson DG, Brody JR, Sawicki JA (2010). CanScript, an 18-Base pair DNA sequence, boosts tumor cell-specific promoter activity: implications for targeted gene therapy. *Cancer Biol. Ther.* 10(9), 878-884.
8. Sunshine J, Green JJ, Mahon KP, Yang F, **Eltoukhy AA**, Nguyen DN, Langer R, Anderson DG (2009). Small-Molecule End Group of Linear Polymer Determines Cell-type Gene Delivery Efficacy. *Adv. Mater.* 21(48), 4947-4951.

Manuscripts in preparation:

1. **Eltoukhy AA**, Sahay G, Anderson DG (2013).
2. **Eltoukhy AA**, Chen D, Veiseh O, Pelet J, Yin H, Dong Y, Anderson DG (2013).
3. Dong Y, **Eltoukhy AA**, et al. (2013).
4. Kontorovich AR, **Eltoukhy AA**, Turnbull IC, Cashman TJ, Langer R, Rao SK, Anderson DG, Hajjar RJ, Costa KD (2013).
5. Hong CA, **Eltoukhy AA**, et al. (2013).
6. Ishikawa K, Yaniz-Galende E, Aguero J, Tilemann L, Jeong D, Liang L, Fish K, Costa KD, **Eltoukhy AA**, Anderson DG, Hajjar RJ (2013).